Distribution and Abundances of Diazotrophs and Microbial Nutrient Limitations in the North Atlantic Ocean

Dissertation
zur Erlangung des Doktorgrades
IFM-GEOMAR,
Leibniz-Institut für Meereswissenschaften
an der Mathematisch-Naturwissenschaftlichen Fakultät der
Christian-Albrechts Universität zu Kiel

Vorgelegt von

Rebecca Judith Langlois-Warnat

Kiel, 2008

Table of Contents:

List of Figures and Tables III

Summary V

Zusamenfassung VII

I. Introduction

A. Global Marine Nitrogen Cycle 1

B. Dinitrogen Fixation 5

C. The Nitrogenase Enzyme 6

D. Diazotrophic Organisms 9

E. Methods for Studying Marine Dinitrogen Fixation 12

F. Aim of Thesis 14

II. Procedure for *nifH* Gene Analysis

A. Sample Collection and Genetic Material Extraction 21

B. nifH *Amplification* 23

C. Determining Abundances of nifH *Genes Using qPCR* 24

1. Selection of Primers and Probes 26
2. Construction of Plasmid Standards and qPCR Assays 27
3. Testing Primer Efficiency and Specificity 28
4. Eliminating Environmental Sample Inhibition with BSA 31
5. Considerations for Interpreting qPCR Data 35

III. Major Results

A. *Diazotrophic Diversity and Distribution in the Tropical and Subtropical Atlantic Ocean* 41

B. *Abundances and Distribution of the Dominant* nifH *Phylotypes in the Northern Atlantic Ocean* 53

C. *Iron limits primary productivity during spring bloom development in the central North Atlantic* 65

D. *Relative influence of nitrogen and phosphorus availability on phytoplankton physiology and productivity in the oligotrophic sub-tropical North Atlantic Ocean* 75

E. *Nitrogen and phosphorus co-limitation of bacterial productivity and growth in the oligotrophic subtropical North Atlantic* 93

F. *Effects of Dust and Nutrient Additions on Diazotrophic Communities (in prep)* 107

G. *Impacts of Atmospheric Anthropogenic Nitrogen on the Open Ocean* 131

IV. Discussion

A. *Nutrient Limitation in the North Atlantic Ocean* 139

B. *Changes in Nitrogen Fixation Paradigms* 141

C. *Potential Consequences of Anthropogenic Perturbations on the Marine Nitrogen Cycle* 144

V. Conclusions and Outlook 151

VI. Acknowledgements 157

List of Figures and Tables:

I. Introduction:

Figure I-1: The Marine Nitrogen Cycle 2

Table I-1: Summary of Nitrogen Transformations and Responsible Genes 3

Table I-2: Inventory of Oceanic Nitrogen Pools 3

Table I-3: Examples of Marine Nitrogen Budgets for the Present 4

Table I-4: Element Requirements of the Nitrogenase Complex 7

Table I-5: Nitrogenase Genes and Functions 8

Figure I-2: Distribution of Sampling Sites for Diazotrophs in the Atlantic Ocean up to 2004 15

II. Procedure for *nifH* Gene analysis:

Table II-1: Regions Sampled for *nifH* Gene Analysis 22

Table II-2: Degenerate Primers for Nested *nifH* PCR 24

Table II-3: qPCR Primers and Probes 27

Figure II-1: Average Standard Curves 29

Table II-4: Atlantic Primer and Probe Specificity 30

Table II-5: Mediterranean Primer and Probe Specificity 31

Figure II-2: Performance of Standards with Varying Amounts of Similar DNA 32

Table II-6: Effect of BSA on Four Environmental Samples with Different Degrees of Inhibition 33

Figure II-3: BSA Additions to a Standard and an Environmental DNA Sample 34

IV. Discussion:

Figure IV-1: Correlation of Group C with Dim Synechococcus Abundances 140

V. Conclusions:

Figure V-1: Global Distribution of Sites Where Diazotroph Abundances Were Determined by qPCR 150
Boxed Text 1: Major Findings 152
Figure V-2: Results of a Bioassay Experiment in the Sargasso Sea 153
Boxed Text 2: Future Research Directions 154

Summary

The diazotrophic community of the North Atlantic Ocean was investigated using a combination of molecular techniques. Samples were collected from a series of research cruises to the North Atlantic Ocean and total DNA was extracted. Diazotrophic organisms were characterized by amplifying the *nifH* gene, which codes for the iron protein of the nitrogenase enzyme, using a nested-PCR technique. The amplified *nifH* products were cloned and sequenced. The results of this study showed that the diazotrophic community of the North Atlantic is more diverse than previously described. *Trichodesmium spp. nifH* sequences were recovered and two new uncultured diazotrophic phylotypes were identified; a *Cyanothece*-like cyanobacterial (later called unicellular Group C) and a γ–proteobacterial sequence called Gamma A. This study was the first to report an uncultured Cluster III diazotroph in the Atlantic Ocean. The presence of seven diazotrophic phylotypes was observed repeatedly in clone libraries from sampling sites across the North Atlantic Ocean indicating dominance of these groups. Abundances and distributions of these phylotypes were quantified by designing a qPCR assay using TaqMan MGB® probes and primers which specifically targeted the seven phylotypes. The distribution and abundances of filamentous cyanobacterial, unicellular cyanobacterial Groups A, B and C, two γ–proteobacterial, and a Cluster III phylotype(s) were estimated in 145 samples from the Atlantic Ocean covering an area of 0-42°N and 67-13°W. Phylotype abundances showed a relationship with estimated annual Saharan dust deposition. This study provided information about several diazotrophic organisms in the North Atlantic Ocean on an unprecedented scale.

In addition to characterization of the diazotrophic community, nutrient addition bioassay experiments were conducted to investigate nutrient limitations in the North Atlantic microbial community. Many parameters, including chlorophyll a analysis, analytical flow cytometry, $^{15}N_2$ determination of dinitrogen fixation, ^{14}C carbon fixation, and molecular analyses were measured. Results showed that primary production was generally nitrogen limited and heterotrophic bacterial growth was nitrogen and phosphorus co-limited. Iron limitation of primary production was shown in one bioassay experiment conducted during the spring bloom. In contrast to the phytoplankton and

heterotrophic bacteria, dinitrogen fixation was co-limited by phosphorus and iron. Saharan dust, which supplies the North Atlantic Ocean with iron and phosphorus, also stimulated dinitrogen fixation and induced large increases in diazotrophic phylotype abundances. A laboratory culture experiment with *Trichodesmium erythraeum* ISM101 demonstrated that this organism can utilize iron from Saharan dust. The results of the bioassay experiments indicate diazotrophic organisms have an important role in the Atlantic Ocean by providing fixed nitrogen to the nitrogen limited phytoplankton and heterotrophic bacteria. They also indicate that Saharan dust could potentially have a key function in determining the distribution of diazotrophs and dinitrogen fixation in the Atlantic Ocean.

Zusammenfassung

Durch die Kombination mehrerer molekularer Techniken wurde die diazotrophe Gemeinschaft des Nordatlantischen Ozeans untersucht. Während einer Reihe von Expeditionen in den Nordatlantik wurden Seewasserproben genommen, aus denen später die gesamte DNS extrahiert wurde. Die diazotrophen Organismen wurden anhand ihres *nifH*-Gens charakterisiert, welches mit Hilfe einer nested-PCR Methode amplifiziert wurde.
Die erhaltenen *nifH*-Amplifikate wurden kloniert und sequenziert. Die diazotrophe Gemeinschaft des Nordatlantik zeigte eine höhere Diversität als zuvor beschrieben. Zusätzlich zur Entdeckung vieler DNS-Sequenzen von *Trichodesmium spec.* wurden auch zwei neue, nicht kultivierte, diazotrophe Phylotypen identifiziert: eine cyanobakterielle Sequenz ähnlich der von *Cyanothece* (später unizelluläre Gruppe C genannt) und eine γ–proteobakterielle Sequenz, genannt Gamma A. In dieser Studie wurde zum ersten Mal von einem nicht-kultivierten Cluster III Diazotroph im Atlantischen Ozean berichtet. Wiederholt wurden sieben diazotrophe Phylotypen in Klon-Bibliotheken verschiedener Probennahmegebiete des Nordatlantischen Ozeans gefunden, was auf eine Dominanz dieser Gruppen hinweist. Die Abundanz und Verteilung dieser Phylotypen wurde durch die Entwicklung einer qPCR-Methode quantifiziert, wobei TaqMan MGB® Sonden und Primer benutzt wurden, die speziell für die sieben Phylotypen erstellt wurden. Die Verteilung und Abundanz von filamentösen cyanobakteriellen Phylotypen, von unizellulären Gruppen A, B und C cyanobakteriellen Phylotypen, von zwei γ–proteobakteriellen Phylotypen, sowie eines Cluster III-Phylotyps wurde an 145 Probenahmegebieten im Atlantik berechnet, wobei ein Gebiet zwischen 0° bis 42°N und 67° bis 13°W abgedeckt wurde. Die Phylotypen-Abundanz korrelierte mit dem geschätzten jährlichen Eintrag von Saharastaub. In dieser Studie wurden Informationen über mehrere diazotrophe Organismen gewonnen wie sie zuvor noch nicht erzielt wurden.

Zusätzlich zur Charakterisierung der diazotrophen Gemeinschaft wurden Bioassay-Experimente mit Nährstoffzugaben durchgeführt, um Nährstofflimitierungen innerhalb der nordatlantischen mikrobiellen Gemeinschaft zu untersuchen. Dafür wurden zahlreiche Parameter gemessen, einschließlich Chlorophyll a Analyse, analytischer Durchfluss-zytometrie, $^{15}N_2$ Bestimmung der Distickstoff-Fixierung, ^{14}C Messung der Kohlenstoff-Fixierung und molekularbiologischer Analysen. Die Ergebnisse zeigten, dass die Primärproduktion hauptsächlich stickstofflimitiert war, das Wachstum heterotrophischer Bakterien war dagegen durch Stickstoff und Phosphor co-limitiert. Während eines Experiments zur Zeit der Frühjahrsblüte wurde die Primärproduktion jedoch durch Eisen

limitiert. Im Gegensatz zu Phytoplankton und heterotrophen Bakterien war die Distickstoff-Fixierung durch Phosphor und Eisen co-limitiert. Zugaben von Saharastaub, der den Nordatlantik mit Eisen und Phosphor versorgt, stimulierte die Distickstoff-Fixierung und führte zu großen Zunahmen in diazotropher Phylotypen-Abundanz. Ein Laborexperiment mit *Trichodesmium erythraeum* ISM101 zeigte, dass dieser Organismus Eisen des Saharastaubes nutzen kann. Die Ergebnisse der Bioassay-Experimente deuten darauf hin, dass diazotrophe Organismen eine bedeutende Funktion im atlantischen Ozean übernehmen, in dem sie fixierten Stickstoff an stickstofflimitiertes Phytoplankton und heterotrophe Bakterien liefern. Sie zeigen auch, dass Saharastaub eventuell eine Schlüsselrolle in der geographischen Verteilung von Diazotrophen und in der Distickstoff-Fixierung im atlantischen Ozean spielt.

I. Introduction

The element nitrogen is a critical nutrient for all organisms. Nitrogen is incorporated into cells for building essential genetic material, amino acids, and proteins, without which cells could not function. Primary productivity appears to be nitrogen limited throughout much of the world's surface open oceans [*Karl et al.*, 2002]. In many oligotrophic oceans, including the North Atlantic, concentrations of the biologically useable forms of nitrogen, NH_3, NO_3^- and NO_2^-, are very low to undetectable. N_2 gas is the most abundant form of nitrogen in the ocean, but is not readily available to most organisms. Therefore organisms with the ability to utilize N_2 occupy an important niche in the oceans by providing a source of biologically useable nitrogen. These organisms, diazotrophs, contain the nitrogenase enzyme, which is the enzyme responsible for converting N_2 to NH_3. Nitrogenase has relatively high trace metal and energy requirements, making diazotrophs susceptible to nutrient limitations different to those of primary producers. Interest in the marine nitrogen cycle has increased substantially over the past 20 years [*Capone et al.*, 2008], especially the topic of biological dinitrogen fixation. Despite their importance diazotrophs were largely overlooked in nitrogen cycle studies until relatively recently (reviewed in [*Mahaffey et al.*, 2005]). The development of molecular techniques has led to an explosion in the identification of diazotrophs in a variety of environments [*Brown et al.*, 2003; *Hewson et al.*, 2007; *Langlois et al.*, 2008; *Mehta et al.*, 2003]; however the factors that control their distribution and ability to fix nitrogen still remain poorly described.

Global Marine Nitrogen Cycle

The marine nitrogen cycle is one of the most complex biogeochemical cycles. Nitrogen exists in many forms in the oceans (Figure I-1) and biological organisms are responsible for changes in the redox state of nitrogen. Nitrogen enters the marine nitrogen cycle through the process of biological dinitrogen fixation. Only bacteria and

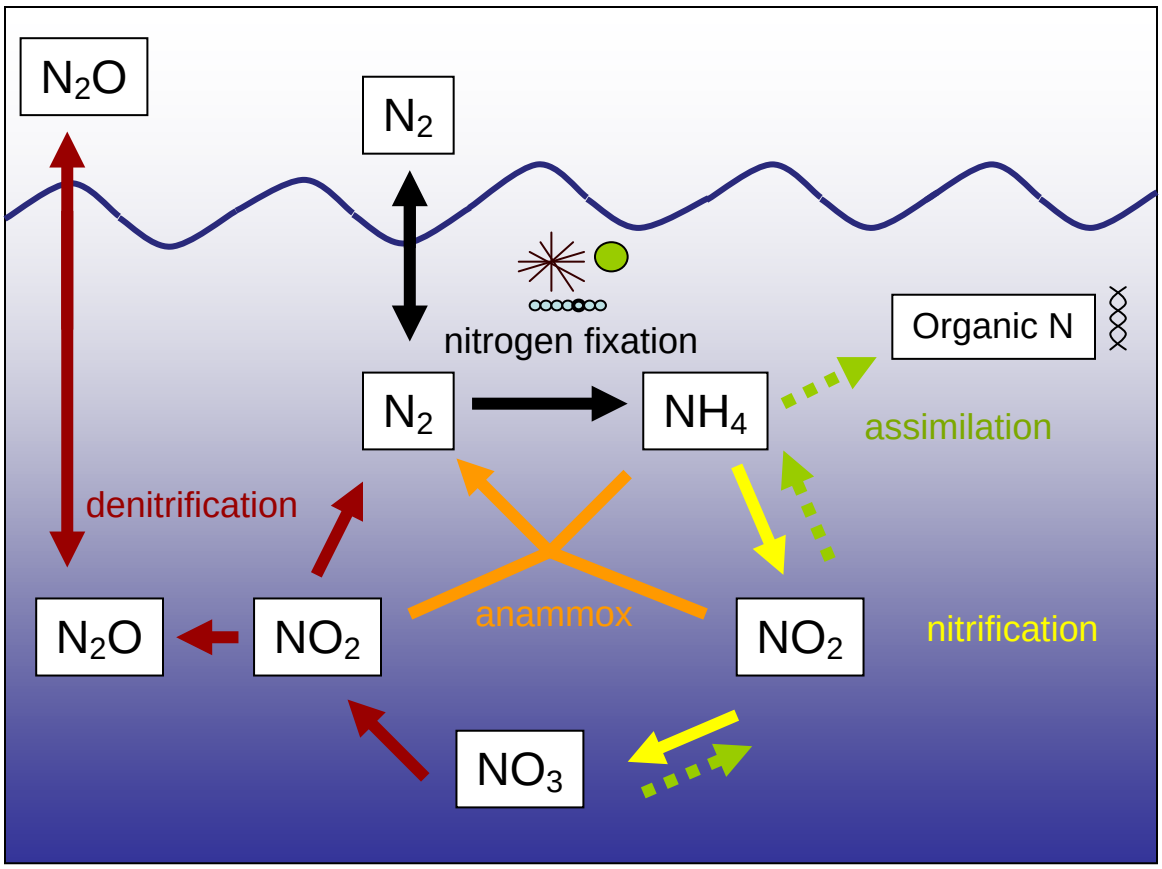

Figure I-1: The Marine Nitrogen Cycle Pools of nitrogen are shown in the white boxes. Possible nitrogen transformations are depicted by arrows and the major redox processes are color coded to the arrows. N_2 and N_2O gases equilibrate with the atmosphere and can thus enter or leave the oceans.

archaea which contain the nitrogenase enzyme are capable of dinitrogen fixation (Table I-1). These organisms are able convert N_2 into ammonia, or "fixed" nitrogen. N_2 gas is the largest pool of nitrogen in the ocean (Table I-2) and due to this large abundance, diazotrophs are not considered to be limited by nitrogen. The fixed nitrogen produced by diazotrophs is either used directly by the organism or can be released to the water column by the organism or through viral lysis. Dissolved organic nitrogen (DON) is the third largest pool of nitrogen (Table I-2) in the marine environment, but is very poorly classified.

Nitrification is the process where ammonium is transformed to nitrate. This is a two step process performed by specialized bacteria. Ammonium oxidizing bacteria and archaea, use ammonia oxygenase to catalyze the oxidation of ammonia to nitrite (Table

Table I-1: Summary of Nitrogen Transformations and Responsible Genes

Protein	Gene(s) used in Environmental Studies	Transformation Catalyzed
Nitrogen Fixation		
Nitrogenase	*nifH, nifD*	N_2 to NH_3
Nitrogen assimilation		
Assimilatory nitrate reductase	*nas, nar*	NO_3^- to NO_2^-
Glutamine synthetase	*Gln*	NH_3 to $_L$-glutamine
Nitrification		
Ammonia monooxygenase	*amoA*	NH_4^+ to NH_2OH
Hydroxylamine oxidoreductase	*hao*	NH_2OH to NO_2^-
Canonical Denitrification		
Dissimilatory nitrate reductase	*napA, narG*	NO_3^- to NO_2^-
Nitrite reductase	*nirK, nirS*	NO_2^- to NO
Nitric oxide reductase	*norB*	NO to N_2O
Nitrous oxide reductase	*nosZ*	N_2O to N_2
Anammox		
Hydrazine dehydrogenase	*hao*	N_2H_4 to N_2

Data summarized from Table 30.1 in [*Jenkins and Zehr*, 2008].

Table I-2: Inventory of Oceanic Nitrogen Pools

Pool	Oceanic Pool Size (Tg N)
N_2	$1 \times 10^7 \pm 10\%$
Fixed Nitrogen	
NO_3^-	$5.8 \times 10^5 \pm 5\%$
NO_2^-	$160 \pm 20\%$
NH_4^+	$340 \pm 20\%$
DON	$7.7 \times 10^4 \pm 30\%$
PON	$400 \pm 50\%$
N_2O	$750 \pm 20\%$

Data source: [*Gruber*, 2008]

I-1). The produced nitrite can then be converted to nitrate by nitrite oxidizing bacteria using the nitrite oxidoreductase enzyme (Table I-1). These nitrifiying bacteria and archaea use nitrification as a source of energy, however little energy is gained from these transformations resulting in slow doubling times of the organisms. Nitrification requires oxygen but the organisms are inhibited by light. It is not yet clear why nitrifiying bacteria

are inhibited by light, but it may have to do with photodamage to the electron transport system [*Ward*, 2008]. Most nitrification occurs at the base of the euphotic zone and in oxygenated marine sediments. Nitrate and nitrite are both bio-available nitrogen sources to marine microorganisms, though the respective pools of both are vastly different (Table I-2). Nitrate is the thermodynamically stable form of nitrogen in the marine environment and is the second largest pool. The nitrite pool is estimated to be about 3 orders of magnitude less. This may be because nitrite is an intermediate product of two processes, nitrification and denitrification.

Table I-3: Examples of Marine Nitrogen Budgets for the Present

Process	Codispoti et al 2001[a]	Gruber 2008[b]
Sources (Tg N yr^{-1})		
N_2 Fixation		
Pelagic	110	120
Benthic	15	15
Rivers		
DN	34	35
PON	42	45
Atmospheric Deposition		50
Net	30	
DON	56	
Total Sources	287	265
Sinks (Tg N yr^{-1})		
Organic N export	1	1
Denitrification		
Benthic	300	180
Water Column	150	65
Sedimentation	25	25
N_2O loss	6	4
Total Sinks	482	275

[a][*Codispoti et al.*, 2001]
[b][*Gruber*, 2008]

Denitrification is the loss of fixed nitrogen from the nitrogen cycle. There are two processes by which nitrogen is lost from the oceanic inventory, canonical denitrification

and anammox, both of which are mediated by bacteria and archaea. The bacteria responsible for canonical denitrification are mostly proteobacterial, facultative anaerobes which contain reductase enzymes that reduce NO_3^- to either N_2O or N_2, with NO_2^- and NO^- being produced as intermediates (Table I-1). Anaerobic ammonium oxidation (anammox) bacteria are chemoautotrophs that combine NO_2^- and NH_4^+ and produce N_2. Only one of the three known genera of anammox bacteria, *Scalindua*, has been described in the marine environment [*Devol*, 2008]. Low (2.5 μm O_2) to anoxic environments are a pre-requisite for denitrification to occur, thus the oxygen minimum zones of the eastern tropical North and South Pacific Ocean and Arabian Sea and shallow coastal sediments are considered to be the locations of denitrification.

The marine nitrogen cycle is balanced by the processes of biological dinitrogen fixation and denitrification, as the major sources and sinks, respectively. However rate estimates of these processes are difficult to extrapolate from field measurements to ocean basins, resulting in a large variation in nitrogen budgets (Table I-3). The various nitrogen budgets indicate that the oceans are either losing large amounts of fixed nitrogen or that the two processes are almost balanced. This discrepancy is most likely due to uncertainties in the estimates of denitrification and biological dinitrogen fixation. Better estimates of dinitrogen fixation and identification of new diazotrophic organisms has increased the estimated value of fixed nitrogen entering the marine nitrogen cycle from early nitrogen budgets and most present budgets agree on a value of about 100-150 Tg N yr^{-1} [*Mahaffey et al.*, 2005]. Benthic and water column denitrification rates remain quite variable [*Gruber*, 2008].

Dinitrogen Fixation

A N_2 molecule contains two triple bonded nitrogen atoms. The energy required to break the strong triple bonds is 945 kJ mol^{-1}. Abiotic dinitrogen fixation can occur by lightning or through a chemical process called the Haber-Bosch process (see below). Biologically nitrogenase is the only enzyme known to catalyze this reaction. Diazotrophic organisms are, thus, key components in both terrestrial and aquatic systems as they are the only organisms capable of converting dinitrogen gas to ammonia. A total

of 16 ATP molecules are required to convert one molecule of dinitrogen to two molecules of ammonia in biological dinitrogen fixation. The overall reaction is:

$$N_2 + 8H^+ + 16ATP \xrightarrow{8^e} 2NH_3 + H_2 + 16ADP$$

As nitrogen is a limiting nutrient in terrestrial systems, the Haber-Bosch process was developed in order to produce nitrogenous fertilizers. The Haber-Bosch process uses temperatures of 400-500°C and a pressure of 200 bar to combine hydrogen and nitrogen gas and produces ammonium. The Haber-Bosch reaction is:

$$N_2 + 3H_2 \longleftrightarrow 2NH_3$$

and requires a ΔH of -92.3 kJ mol^{-1} [*Latscha and Klein*, 2007]. The efficiency of the Haber-Bosch process is only 21%. It is not known exactly how nitrogenase functions, as diazotrophs are able to fix dinitrogen at ambient temperatures and pressure. There are significant research efforts directed to understanding how the nitrogenase enzyme functions, because this knowledge could improve the efficiency of nitrogenous fertilizer production.

The Nitrogenase Enzyme

Nitrogenase (Nif) is the name given to a family of very similar enzymes which enable bacteria and archaea to fix nitrogen. There are three types of nitrogenase enzymes, but there is a set of conserved properties [*Postgate*, 1998]. One of the more important properties of the nitrogenase enzyme is that it is very oxygen sensitive; it is irreversibly inactivated in the presence of oxygen. This is an important consideration as anoxic conditions are not a prerequisite for diazotrophy. Two separate proteins, dinitrogenase and dinitrogenase reductase, comprise the nitrogenase enzyme. These proteins contain iron, sulfur, molybdenum, and phosphorus (Table I-4). Lastly, nitrogenase does not bind specifically to N_2 gas, as it is also capable of reducing other small triple bonded molecules such as acetylene. This fact has been taken advantage of in the development of methods for measuring biological dinitrogen fixation.

Table I-4: Element Requirements of the Nitrogenase Complex

		Number of Atoms[a]			
Protein	Cofactors	Fe	P	S	Mo
Diitrogenase reductase	Fe protein	4		4	
Dinitrogenase	P cluster	8	1	7	
	FeMoCo	7		9	1
Total Atoms in Nitrogenase Complex		19	1	20	1

[a]Number of atoms per monomer based on values given in [*Shi et al.*, 2007].

Dinitrogenase reductase is the smaller of the two nitrogenase complex proteins. Its role is to provide electrons to the larger dinitrogenase protein [*Berges and Mulholland*, 2008] and is particularly sensitive to O_2. Dinitrogenase reductase is a γ_2 homodimer coded for by NifH. Dinitrogenase has two subunits including the active binding site for dinitrogen, FeMoCo. The enzyme is an $\alpha_2\beta_2$ heterotetramer, with NifD and NifK coding for the α and β peptides, respectively. The α subunit is the site of N_2 reduction [*Raymond et al.*, 2004]. NifE and NifN are very similar to NifD and NifK, respectively, however their role in nitrogenase is not certain. They could possibly be the result of duplication of NifD and NifK [*Raymond et al.*, 2004] or they may form a scaffold for FeMoCo [*Postgate*, 1998]. The genes which code for the various components of the nitrogenase complex have been identified and are summarized in Table I-5. The proteins NifH, NifD, NifK, NifE, and NifN are universal and very highly conserved among diazotrophs [*Raymond et al.*, 2004].

Alternative nitrogenases exist which contain variations in the FeMoCo subunit. In these nitrogenases the Mo center is replaced by either vanadium (Vnf) or iron (Anf). The alternative nitrogenases are only expressed when Mo is limiting [*Raymond et al.*, 2004]. Very few organisms have alternative nitrogenases and so far all that have been described also contain Nif [*Raymond et al.*, 2004]. Of the three nitrogenases, Nif is the most efficient followed by Vnf. Anf is the least efficient nitrogenase [*Raymond et al.*, 2004]. Alternative nitrogenases have been proposed to be either primitive nitrogenases [*Berman-Frank et al.*, 2008] or paralogs of Nif [*Raymond et al.*, 2004].

Table I-5: Nitrogenase Genes and Functions

Gene	Product Type	Product Function
FeMoCo		
nifD	Peptide molecule	Two combine to form α_2
nifK	Peptide molecule	Two combine to form β_2
nifV	Peptide	Two combine to form homocitrate
nifB	Protein	Synthesis
nifQ	Protein	Uptake of molybdenum
nifZ	Protein	Insertion of FeMoCo into dinitrogenase
Putative FeMoCo Template		
nifE	Peptide molecule	Two combine to form NifE
nifN	Peptide molecule	Two combine to form NifN
Dinitrogenase Reductase		
nifH	Peptide molecule	Two combine to form dinitrogenase reductase
nifJ	Pyruvate oxido-reductase	Generates electrons
nifF	Flavodoxin	Moves electrons from pyruvate to dinitrogenase
nifU	Protein	Possible iron-sulphur center
nifS	Protein	Possible iron-sulphur center
Regulation		
nifA	Protein	Initiates *nif*
nifX	Protein	
nifM	Protein	Activates dinitrogenase
nifL	Protein	Deactivates *nif*
Unknown		
nifW	Protein	Necessary for nitrogenase activity
nifT	Protein	
nifY	Protein	

Source: [*Postgate*, 1998]

Biological dinitrogen fixation is an ancient biochemical pathway that is thought to have originated in the Archean Ocean [*Shi et al.*, 2007]. The basis for this theory is that the ancient oceans were not oxygenated and N_2 was very abundant, whereas fixed nitrogen was probably not. Iron was most likely not limiting as the Archean Ocean was an oxidizing environment [*Shi and Falkowski*, 2008]. Anoxic environments, abundant N_2 and iron and low fixed nitrogen availability should select for diazotrophic organisms. Additionally, these factors could also explain the oxygen sensitivity and high iron

requirement of nitrogenase. It has also been proposed that the original function of nitrogenase was to rid organisms of poisonous triple bonded molecules, such as cyanide, which were also present in early oceans due to the ability of nitrogenase to bind to other triple bonded molecules [*Postgate*, 1998]. This theory, however, has not been given much consideration.

Another line of evidence that points to nitrogenase being a very old enzyme is the diversity of diazotrophic organisms. Phylogenetic trees of *nifH* genes show diazotrophic representatives throughout the bacteria and archaea [*Zehr et al.*, 2003]. The *nifH* gene, which codes for the iron protein of dinitrogenase reductase, is highly conserved and therefore useful for phylogenetic studies. The high conservation of a gene across a wide range of organisms can be an indication of horizontal (lateral) gene transfer, but this does not seem to be the case with nitrogenase. Horizontal gene transfers of nitrogenase undoubtedly occurred during the course of time, but it will probably be impossible to tell exactly how often and when they occurred [*Raymond et al.*, 2004]. There is much evidence that points to a common ancestor containing nitrogenase. Horizontal gene transfer does not occur equally among all genes. Some genes, such as those for photosynthesis, the Calvin cycle and ribosomal proteins, are seldom transferred [*Shi and Falkowski*, 2008]. One indication of horizontal gene transfer is that the distribution of organisms in phylogenetic trees from a functional gene differ from a 16S rRNA tree [*Shi and Falkowski*, 2008]. This is not seen with nitrogenase genes, as there is a high congruency between phylogenetic trees of *nifH* and 16S rRNA [*Zehr et al.*, 2003]. It should also be considered that the nitrogenase family may be highly conserved because slight variations in the amino acid sequence may change the functionality of the enzyme drastically [*Berman-Frank et al.*, 2008].

Diazotrophic Organisms

Diazotrophic organisms are very diverse and can inhabit a wide variety of environments. For instance, terrestrial diazotrophs are commonly associated in plant root nodules, but can also be free-living. Aquatic diazotrophs, including those described only from *nifH* genes, have been described in sediments [*Burns et al.*, 2002], seagrasses

[*Brown et al.*, 2003], salt marshes [*Lovell et al.*, 2001], cyanobacterial mats [*Omoregie et al.*, 2004], coral [*Lesser et al.*, 2004], surface oceans [*Langlois et al.*, 2005; *Zehr et al.*, 2001], deep in the water column [*Hewson et al.*, 2007] and deep sea vents [*Mehta et al.*, 2003]. Marine diazotrophs are also known to form symbioses with diatoms [*Foster et al.*, 2007] and dinoflagellates [*Kneip et al.*, 2008]. Copepods have been reported to have symbionts in their guts [*Proctor*, 1997]. It is important to note that many diazotrophic organisms are described only by a *nifH* gene sequence and are not in culture. Despite the wide diversity of diazotrophic organisms, they group into well defined clades based on phylogenetic analyses of the *nifH* gene.

There are five clades, or clusters, of nitrogenase containing organisms. The grouping of diazotrophs based on NifH and NifD phylogenies according to [*Raymond et al.*, 2004] follows. Cluster I is the largest clade and contains the well described molybdenum-iron nitrogenases. Cyanobacterial and proteobacterial diazotrophs are located in this clade. Organisms with anaerobic molybdenum-iron nitrogenases, such as *Clostridium* and methanogens are found in Cluster II. The alternative nitrogenases Anf and Vnf group in Cluster III. Some VnfH, however, are more similar to NifH than to AnfH. Cluster IV is composed of uncharacterized nif homologs, methanogens, and some anoxygenic photosynthetic bacteria. Cluster V contains bacteriochlorophyll and chlorophyll biosynthesis genes, which belong to the nitrogenase protein family although they have a different function. Archaeal sequences group in Clusters II and IV. The majority of marine diazotrophs located throughout oceanic environments [*Church et al.*, 2005; *Langlois et al.*, 2008; *Man-Aharonovich et al.*, 2007; *Mazard et al.*, 2004], are Cluster I cyanobacteria and proteobacteria. Much research on marine nitrogen fixation has focused on diazotrophic cyanobacteria, especially the large filamentous cyanobacterium, *Trichodesmium spp*. [*Capone et al.*, 2005; *Mahaffey et al.*, 2005]. Cyanobacterial diazotrophs are important contributors of fixed nitrogen to the marine nitrogen cycle [*Capone et al.*, 2005; *Montoya et al.*, 2004; *Montoya et al.*, 2006] and very little is known about the marine proteobacterial diazotrophs, therefore the focus of the following will be placed on the cyanobacteria.

The cyanobacteria are one of the largest and most diverse groups of bacteria [*Shi and Falkowski*, 2008] and there are many diazotrophic representatives. Oxygen

concentrations rose due to the development of photosynthesis by cyanobacteria about 3.5 Gyr [*Berman-Frank et al.*, 2008]. The resulting oxygenation of the atmosphere and oceans circa 2.4 Gyr created a problem for the diazotrophs, as the nitrogenase enzyme is very sensitive to oxygen. Oxygen is especially problematic for diazotrophic cyanobacteria because they both produce oxygen through photosynthesis and need to fix nitrogen. Diazotrophic cyanobacteria use a variety of strategies for dealing with this issue.

Some filamentous cyanobacteria separate photosynthesis from nitrogen fixation spatially. These organisms, such as *Anabaena*, create special cells called heterocysts. Nitrogen fixation occurs in heterocyst cells and photosynthesis is carried out in the other cells along the filament. Filamentous heterocystous diazotrophs are found mainly in fresh and brackish waters. The thick cell wall of the heterocyst cell provides extra protection against oxygen fluxes from the cool fresh and brackish waters. In contrast, most marine filamentous diazotrophic cyanobacteria do not possess heterocysts. The lack of heterocysts in marine diazotrophs found in well oxygenated tropical oceanic surface waters is puzzling but has been explained by the decrease in dissolved oxygen in salty warm water. Additionally, gas diffuses more readily across membranes at higher temperatures, making heterocysts less effective in tropical areas [*Staal et al.*, 2003].

Unicellular diazotrophs can not produce heterocyst cells and have therefore developed a strategy to protect nitrogenase by separating photosynthesis and nitrogen fixation processes temporally. The diel cycle of nitrogen fixation and photosynthesis in the unicellular cyanobacterium *Cyanothece* has been well described [*Colon-Lopez and Sherman*, 1998]. This organism photosynthesizes during daylight and fixes nitrogen in the dark, thus separating the oxygen producing process from oxygen sensitive nitrogen fixation. *Crocosphaera watsonii*, as close relative of *Cyanothece*, uses the same strategy [*Zehr et al.*, 2007]. Spatial and temporal separation of nitrogen fixation and photosynthesis are common ways that diazotrophs overcome the problem of using both of the seemingly incompatible processes of nitrogen fixation and photosynthesis, however at least one unicellular organism exists that does not use this strategy [*Zehr et al.*, 2008; *Zehr et al.*, 2007].

The filamentous non-heterocystous diazotroph *Trichodesmium* is present throughout surface tropical oceans. Similar to unicellular diazotrophs, *Trichodesmium* fixes nitrogen on a diel cycle; however *Trichodesmium* fixes nitrogen during the middle of the light cycle instead of during the dark. Immunological studies have shown that all cells along a *Trichodesmium* filament are capable of photosynthesis, however only certain cells, termed diazocytes, actively fix nitrogen [*Berman-Frank et al.*, 2001; *El-Shehawy et al.*, 2003]. *Trichodesmium* has a further nitrogenase protection measure in that oxygen is efficiently cycled by the Mehler reaction [*Berman-Frank et al.*, 2001]. In the Mehler reaction, or pseudocyclic phosphorylation, chloroplasts use oxygen as an electron acceptor and oxygen produced by photosynthesis is consumed, thus reducing the concentration of oxygen in a cell [*Berman-Frank et al.*, 2008].

An uncultured unicellular diazotroph, termed unicellular Group A, identified through *nifH* gene analysis also fixes nitrogen during the day [*Zehr et al.*, 2007]. This organism is widespread in both the Atlantic and Pacific Oceans [*Church et al.*, 2008; *Langlois et al.*, 2008] and is capable of high rates of nitrogen fixation [*Montoya et al.*, 2004]. Despite the fact that this organism is not in culture, the genome has recently been partially sequenced by collecting size sorted cells during analytical flow cytometry. Genome analysis revealed that although this organism is a cyanobacterium, it does not contain any genes for photosystem II [*Zehr et al.*, 2008]. In other words, the unicellular Group A cyanobacterium is not capable of producing oxygen. Biogeochemically, this is very significant because in this organism, unlike other cyanobacterial diazotrophs, dinitrogen fixation and carbon fixation are uncoupled [*Zehr et al.*, 2008].

Methods for Studying Marine Dinitrogen Fixation

New methods have been employed making it easier to study dinitrogen fixation, including improvements for direct measurements of dinitrogen fixation, the use of molecular analyses, and analyses of ratios of nitrogen and phosphorus to predict areas of nitrogen fixation. Data obtained from these studies has changed the way nitrogen fixation is viewed.

Dinitrogen fixation can be measured by using either the acetylene reduction method or the $^{15}N_2$ stable isotope. The acetylene reduction method is possible due to the fact that nitrogenase can reduce small triple bonded molecules. Briefly, an amount of acetylene is injected into a sample containing diazotrophs and incubated. During this time nitrogenase reduces acetylene to ethylene. The amount of ethylene produced is then measured in a gas chromatograph. This method works well for samples with high concentrations of diazotrophs. In contrast, the $^{15}N_2$ stable isotope method can be applied to samples with very low concentrations diazotrophs [*Montoya et al.*, 1996]. In this method a water sample is injected with $^{15}N_2$ gas and incubated. At the end of the incubation, the water sample is filtered. The filter is then measured by mass spectrometry and the amount of ^{15}N assimilated can be used to calculate a dinitrogen fixation rate. The ^{15}N method is much more sensitive than the acetylene reduction method and can therefore be used on bulk water samples [*Montoya et al.*, 1996]. Since the innovation of the ^{15}N stable isotope method for measuring dinitrogen fixation, the number of field measurements of dinitrogen fixation has increased [*Mahaffey et al.*, 2005].

Molecular biological techniques have also changed rapidly in the past 20 years and there are now a whole range of tools available for detecting and quantifying diazotrophs in the marine environment. Polymerase chain reaction (PCR) of the *nifH* gene from water samples and subsequent cloning [*Zani et al.*, 2000] has been used quite effectively to identify new diazotrophic organisms in a variety of environments (see previous section). Macro- and micro-arrays of *nifH* genes have been used to show semi-quantitative distribution patterns of diazotrophs in an environment [*Hewson et al.*, 2007; *Jenkins et al.*, 2004]. Basin wide estimations of diazotroph abundances have been made using real-time quantitative PCR (qPCR) [*Church et al.*, 2008; *Church et al.*, 2005; *Langlois et al.*, 2008]. Molecular methods allow for a more in-depth look at dinitrogen fixing organisms that was not possible previously [*Mahaffey et al.*, 2005].

Analysis of the ratios of nitrogen to phosphorus in a water mass can also be used to predict dinitrogen fixing capabilities. The Redfield ratio of 106C:16N:1P is the average ratio of nutrients assimilated into organic matter [*Redfield*, 1958]. N* and P* describe variations from the Redfield ratio of 16N:P and ascribe these variations to the processes of either dinitrogen fixation or denitrification . The principle of N* and P* is

that P is not gained or lost during either dinitrogen fixation or denitrification, only the ratio of nitrate to phosphate is changed [*Mahaffey et al.*, 2005]. A positive N* value indicates that nitrate is in excess of phosphate, which can happen in areas of nitrogen fixation. A negative N* value is an indication of denitrification, or of a low N:P ratio. Positive N* values are found in the North Atlantic Ocean and eastern equatorial Pacific and the major denitrification areas have negative N* signals [*Gruber*, 2008]. P* takes into consideration that when dinitrogen fixation is present, phosphate is depleted relative to nitrate therefore producing a lower P*. In contrast to N*, P* identifies the Pacific Ocean as the area of highest dinitrogen fixation due to the increase in phosphate from denitrification [*Deutsch et al.*, 2007].

Aim of Thesis

As work began on this thesis, *Trichodesmium* was considered to be the main diazotrophic organism in tropical oceans with diatom-diazotroph associations being credited as the second most important [*Capone et al.*, 2005]. The marine nitrogen budget was estimated to be grossly out of balance, with nitrogen loss processes greatly exceeding inputs [*Codispoti et al.*, 2001] and the paucity of marine diazotrophic organisms was theorized to be one of the causes [*Zehr et al.*, 2000]. Shortly before work began the unicellular Group A diazotroph was identified in both the Pacific [*Zehr et al.*, 2001] and Atlantic Oceans [*Falcon et al.*, 2002], supporting this suspicion. Research on diazotrophs in Atlantic Ocean was focused on abundances and nitrogen fixation rates of *Trichodesmium* [*Carpenter et al.*, 2004; *Tyrrell et al.*, 2003] and only one study had been published that looked at other diazotrophic cyanbacteria [*Falcon et al.*, 2002]. *Trichodesmium* abundances were determined throughout the Atlantic Ocean, but virtually no information about other diazotrophs was known at the start of this work, especially in the eastern Atlantic Ocean (Figure I-2).

The focus of this thesis was to first identify diazotrophs in the Atlantic Ocean using a nested PCR method (Paper A [*Langlois et al.*, 2005]). Samples from three cruises covering both the western and eastern subtropical Atlantic Ocean were analyzed and *nifH* genes were characterized. For the first time, new diazotrophic phylotypes were identified

and distributions of diazotrophic organisms in addition to *Trichodesmium* were presented across a wide section of the Atlantic Ocean.

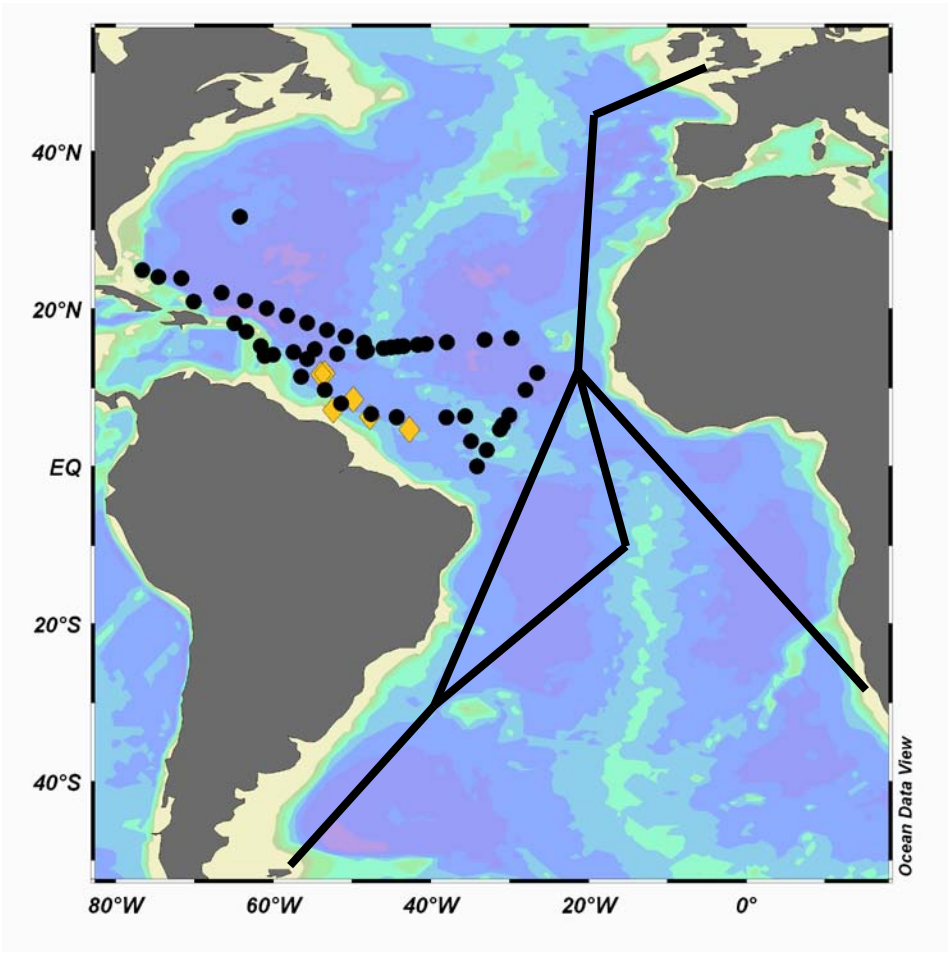

Figure I-2: Distribution of Sampling Sites for Diazotrophs in the Atlantic Ocean up to 2004 Black dots indicate stations where *Trichodesmium* abundances and fixation rates were estimated. The black lines are the cruise tracks of the AMT 1-6 cruises where *Trichodesmium* abundances were determined. The yellow diamonds designate stations where *nifH* gene analysis was performed.

After having assessed the phylogenetic diversity of diazotrophs in the North Atlantic, the focus of this thesis then shifted to determining the abundances of diazotrophic organisms across the Atlantic Ocean. For the second part of the study a real-time PCR (qPCR) method for quantifying diazotrophic phylotypes was developed and used to describe the distributions of seven diazotrophic phylotypes in the Atlantic Ocean (Paper B [*Langlois et al.*, 2008]). Samples from the first study were re-analyzed by qPCR. Additional samples from a new cruise in the northern Atlantic Ocean were

also analyzed, further expanding the area of the Atlantic Ocean sampled for diazotrophs. The results of the second study revealed insights into factors that may potentially influence the distribution of diazotrophs in the environment, especially the influence of Saharan Dust.

During the cruises, nutrient addition bioassay experiments were performed in addition to collecting samples for *nifH* gene analyses. These large scale bottle incubation experiments were used to determine nutrient limitations of the marine microbial community. In Paper C, evidence of iron limitation of primary productivity during the spring bloom was given [*Moore et al.*, 2006]. Other than this one sampling site, the picophytoplankton community of the sampling area was determined to be nitrogen limited (Paper D [*Moore et al.*, 2008]) and bacterial growth and productivity were nitrogen and phosphorus co-limited (Paper E [*Mills et al.*, 2008]). The results of these experiments showed that generally the phytoplankton and bacterial communities in the Atlantic Ocean are limited by fixed nitrogen.

Samples collected during nutrient addition bioassay experiments were analyzed using the qPCR method described in Paper B to identify nutrient limitations of and effects of Saharan dust additions on diazotrophic phylotypes (Paper F [Langlois et al. in prep.]). In contrast to the phytoplankton and heterotrophic bacteria, nitrogen fixation was co-limited by phosphorus and iron. Saharan dust additions, however, caused the greatest increases in all diazotrophic *nifH* abundances.

In addition to the field work, Paper G presents data on the effects of atmospheric anthropogenic nitrogen on the open ocean. This paper is the result of discussions held during a workshop on atmospheric anthropogenic nitrogen.

The overall aim of this thesis was to characterize the diazotrophic community in the North Atlantic Ocean, to gain a better understanding of the distributions and abundances of these diazotrophs, to identify factors which determine their distributions, and to qualify the importance of biological dinitrogen fixation by looking at nutrient limitations of the co-existing phytoplanktonic and bacterial communities.

References:

Berges, J.A., and M.R. Mulholland, Enzymes and Nitrogen Cycling, in *Nitrogen in the Marine Environment*, pp. 1385-1444, Elsevier, Burlington, 2008.

Berman-Frank, I., Y.-B. Chen, Y. Gao, K. Fennel, M.J. Follows, A.J. Milligan, and P. Falkowski, Feedbacks Between the Nitrogen, Carbon and Oxygen Cycles, in *Nitrogen in the Marine Environment*, pp. 1537-1564, Elsevier, Burlington, 2008.

Berman-Frank, I., P. Lundgren, Y.-B. Chen, H. Kupper, Z. Kolber, B. Bergman, and P. Falkowski, Segregation of Nitrogen Fixation and Oxygenic Photosynthesis in the Marine Cyanobacterium Trichodesmium, *Science*, *294* (5546), 1534-1537, 2001.

Brown, M.M., M.J. Friez, and C.R. Lovell, Expression of nifH genes by diazotrophic bacteria in the rhizosphere of short form Spartina alterniflora, *Fems Microbiology Ecology*, *43* (3), 411-417, 2003.

Burns, J.A., J.P. Zehr, and D.G. Capone, Nitrogen-fixing phylotypes of Chesapeake Bay and Neuse River Estuary sediments, *Microbial Ecology*, *44* (4), 336-343, 2002.

Capone, D., D.A. Bronk, M.R. Mulholland, and E.J. Carpenter, *Nitrogen in the Marine Environment*, 1758 pp., Elsevier, Burlington, 2008.

Capone, D., J. Burns, J.P. Montoya, A. Subramaniam, C. Mahaffey, T. Gunderson, A.F. Michaels, and E.J. Carpenter, Nitrogen fixation by Trichodesmium spp.: An important source of new nitrogen to the tropical and subtropical North Atlantic Ocean, *Global Biogeochemical Cycles*, *19* (GB2024), doi:10.1029/2004GB002331, 2005.

Carpenter, E.J., A. Subramaniam, and D. Capone, Biomass and primary productivity of the cyanobacterium Trichodesmium spp. in the tropical N Atlantic ocean, *Deep-Sea Research Part I-Oceanographic Research Papers*, *51*, 173-203, 2004.

Church, M.J., K.M. Bjoerkman, D.M. Karl, M.A. Saito, and J.P. Zehr, Regional distribution of nitrogen-fixing bacteria in the Pacific Ocean, *Limnol. Oceanogr.*, *53* (1), 63-77, 2008.

Church, M.J., B.D. Jenkins, D.M. Karl, and J.P. Zehr, Vertical distributions of nitrogen-fixing phylotypes at Stn ALOHA in the oligotrophic North Pacific Ocean, *Aquatic Microbial Ecology*, *38*, 3-14, 2005.

Codispoti, L.A., J.A. Brandes, J.P. Christensen, A.H. Devol, S.W.A. Naqvi, H.W. Paerl, and T. Yoshinari, The oceanic fixed nitrogen and nitrous oxide budgets: Moving targets as we enter the anthropocene?, *Sci. Mar.*, *62*, 85-105, 2001.

Colon-Lopez, M.S., and L.A. Sherman, Transcriptional and Translational Regulation of Photosystem I and II Genes in Light-Dark- and Continuous-Light-Grown Cultures of the Unicellular Cyanobacterium Cyanothece sp. Strain ATCC 51142, *J. Bacteriol.*, *180* (3), 519-526, 1998.

Deutsch, C., J. Sarmiento, D.M. Sigman, N. Gruber, and J.P. Dunne, Spatial coupling of nitrogen inputs and losses in the ocean, *Nature*, *445*, 163-167, 2007.

Devol, A.H., Denitrification Including Anammox, in *Nitrogen in the Marine Environment*, pp. 263-302, Elsevier, Burlington, 2008.

El-Shehawy, R., C. Lugomela, A. Ernst, and B. Bergman, Diurnal expression of hetR and diazocyte development in the filamentous non-heterocystous cyanobacterium Trichodesmium erythraeum, *Microbiology*, *149* (5), 1139-1146, 2003.

Falcon, L.I., F. Cipriano, A.Y. Chistoserdov, and E.J. Carpenter, Diversity of diazotrophic unicellular cyanobacteria in the tropical North Atlantic Ocean, *Appl. Envir. Microbiol.*, *68* (11), 5760-5764, 2002.

Foster, R.A., A. Subramaniam, C. Mahaffey, E.J. Carpenter, D. Capone, and J.P. Zehr, Influence of the Amazon River plume on distributions of free-living and symbiotic cyanobacteria in the western tropical north Atlantic Ocean, *Limnology and Oceanography*, *52* (2), 517-532, 2007.

Gruber, N., The Marine Nitrogen Cycle: Overview and Challenges, in *Nitrogen in the Marine Environment*, pp. 1-50, Elsevier, Burlington, 2008.

Hewson, I., P.H. Moisander, K.M. Achilles, C.A. Carlson, B.D. Jenkins, E. Mondragon, A.E. Morrison, and J.P. Zehr, Characteristics of diazotrophs in surface to abyssopelagic waters of the Sargasso Sea, *Aquatic Microbial Ecology*, *46*, 15-30, 2007.

Jenkins, B.D., G.F. Steward, S.M. Short, B.B. Ward, and J.P. Zehr, Fingerprinting Diazotroph Communities in the Chesapeake Bay by Using a DNA Macroarray, *Appl. Environ. Microbiol.*, *70* (3), 1767-1776, 2004.

Jenkins, B.D., and J.P. Zehr, Molecular Approaches to the Nitrogen Cycle, in *Nitrogen in the Marine Environment*, pp. 1303-1344, Elsevier, Burlington, 2008.

Karl, D., A. Michaels, B. Bergman, D. Capone, E. Carpenter, R. Letelier, F. Lipschultz, H. Paerl, D. Sigman, and L. Stal, Dinitrogen fixation in the world's oceans, *Biogeochemistry*, *57*, 47-98, 2002.

Kneip, C., C. Voss, P.J. Lockhart, and U.G. Maier, The cyanobacterial endosymbiont of the unicellular algae *Rhopalodia gibba* shows reductive genome evolution, *BMC Evolutionary Biology*, *8* (30), 2008.

Langlois, R.J., D. Huemmer, and J. La Roche, Abundances and Distributions of the Dominant *nifH* Phylotypes in the Northern Atlantic Ocean, *Appl. Envir. Microbiol.*, *74* (6), 1922-1931, 2008.

Langlois, R.J., J. La Roche, and P.A. Raab, Diazotrophic Diversity and Distribution in the Tropical and Subtropical Atlantic Ocean, *Appl. Envir. Microbiol.*, *71* (12), 7910-7919, 2005.

Latscha, H.P., and H.A. Klein, *Anorganische Chemie*, Springer, Berlin, 2007.

Lesser, M.P., C. Mazel, M.Y. Gorbunov, and P. Falkowski, Discovery of Symbiotic Nitrogen-Fixing Cyanobacteria in Corals, *Nature*, *305*, 997-1000, 2004.

Lovell, C.R., M.J. Friez, J.W. Longshore, and C.E. Bagwell, Recovery and phylogenetic analysis of nifH sequences from diazotrophic bacteria associated with dead aboveground biomass of Spartina alterniflora, *Appl. Envir. Microbiol.*, *67* (11), 5308-5314, 2001.

Mahaffey, C., A.F. Michaels, and D. Capone, The Conundrum of Marine N_2 Fixation, *American Journal of Science*, *305*, 546-595, 2005.

Man-Aharonovich, D., N. Kress, E.B. Zeev, I. Berman-Frank, and O. Beja, Molecular ecology of *nifH* genes and transcripts in the eastern Mediterranean Sea, *Environmental Microbiology*, *In press*, 2007.

Mazard, S.L., N.J. Fuller, K.M. Orcutt, O. Bridle, and D.J. Scanlan, PCR Analysis of the Distribution of Unicellular Cyanobacterial Diazotrophs in the Arabian Sea, *Appl. Envir. Microbiol.*, *70* (12), 7355-7364, 2004.

Mehta, M.P., D.A. Butterfield, and J.A. Baross, Phylogenetic diversity of nitrogenase (nifH) genes in deep-sea and hydrothermal vent environments of the Juan de Fuca ridge, *Appl. Envir. Microbiol.*, *69* (2), 960-970, 2003.

Mills, M.M., C.M. Moore, R.J. Langlois, A. Milne, E.P. Achterberg, K. Nachtigall, K. Lochte, R. Geider, and J. La Roche, Nitrogen and phosphorus co-limitation of bacterial productivity and growth in the oligotrophic subtropical North Atlantic, *Limnology and Oceanography*, *53* (2), 824-834, 2008.

Montoya, J.P., C.M. Holl, J.P. Zehr, A. Hansen, T.A. Villareal, and D. Capone, High rates of N2 fixation by unicellular diazotrohps in the oligotrophic Pacific Ocean, *Nature*, *430*, 1027-1031, 2004.

Montoya, J.P., M. Voss, and D. Capone, Spatial variation in N_2-fixation rate and diazotroph activity in the Tropical Atlantic, *Biogeosciences Discussions*, *3*, 1739-1761, 2006.

Montoya, J.P., M. Voss, P. Kähler, and D.G. Capone, A simple, high-precision, high-sensitivity tracer assay for N_2 fixation, *Applied and Environmental Microbiology*, *62* (3), 986-993, 1996.

Moore, C.M., M. Mills, R.J. Langlois, A. Milne, E.P. Achterberg, J. La Roche, and R. Geider, Relative influence of nitrogen and phosphorus availability on phytoplankton physiology and productivity in the oligotrphic sub-tropical North Atlantic Ocean, *Limnology and Oceanography*, *53* (1), 291-305, 2008.

Moore, C.M., M. Mills, A. Milne, R.J. Langlois, E.P. Achterberg, K. Lochte, R. Geider, and J. La Roche, Iron limits primary productivity during spring bloom development in the central North Atlantic, *Global Change Biology*, *12*, 626-634, 2006.

Omoregie, E.O., L.L. Crumbliss, B.M. Bebout, and J.P. Zehr, Determination of Nitrogen-Fixing Phylotypes in Lyngbya sp. and Microcoleus chthonoplastes Cyanobacterial Mats from Guerrero Negro, Baja California, Mexico, *Appl. Environ. Microbiol.*, *70* (4), 2119-2128, 2004.

Postgate, J., *Nitrogen Fixation*, Cambridge University Press, Boston, 1998.

Proctor, L., Nitrogen-fixing, photosynthetic, anaerobic bacteria associated with pelagic copepods, *Aquatic Microbial Ecology*, *12*, 105-113, 1997.

Raymond, J., J.L. Siefert, C.R. Staples, and R.E. Blankenship, The Natural History of Nitrogen Fixation, *Molecular Biology and Evolution*, *21* (3), 541-554, 2004.

Redfield, A.C., The biological control of chemical factors in the environment, *American Scientist*, *46*, 205-221, 1958.

Shi, T., and P. Falkowski, Genome evolution in cyanobacteria: The stable core and the variable shell, *PNAS*, *105* (7), 2510-2515, 2008.

Shi, T., Y. Sun, and P. Falkowski, Effects of iron limitation on the expression of metabolic genes in the marine cyanobacterium *Trichodesmium erythraeum* IMS101, *Environ Microbiol*, *9* (12), 2945-2956, 2007.

Staal, M., F.J.R. Meysman, and L.J. Stal, Temperature excludes N2-fixing heterocystous cyanobacteria in the tropical oceans, *Nature*, *425* (6957), 504-507, 2003.

Tyrrell, T., E. Maranon, A.J. Poulton, A.R. Bowie, D.S. Harbour, and E.M.S. Woodward, Large-scale latitudinal distribution of Trichodesmium spp. in the Atlantic Ocean, *Journal of Plankton Research*, *25* (4), 405-416, 2003.

Ward, B.B., Nitrification in Marine Systems, in *Nitrogen in the Marine Environment*, pp. 199-262, Elsevier, Burlington, 2008.

Zani, S., M.T. Mellon, J.L. Collier, and J.P. Zehr, Expression of nifH Genes in Natural Microbial Assemblages in Lake George, New York, Detected by Reverse Transcriptase PCR, *Appl. Envir. Microbiol.*, *66*, 3119-3124, 2000.

Zehr, J.P., S.R. Bench, B.J. Carter, I. Hewson, F. Niazi, T. Shi, H.J. Tripp, and J.P. Affourtit, Globally Distributed Uncultivated Oceanic N_2-fixing Cyanobacteria Lack Oxygenic Photosystem II, *Science*, *322*, 1110-1112, 2008.

Zehr, J.P., E.J. Carpenter, and T. Villareal, New perspectives on nitrogen-fixing microorganisms in tropical and subtropical oceans, *Trends in Microbiology*, *8* (2), 68-73, 2000.

Zehr, J.P., B.D. Jenkins, S.M. Short, and G.F. Steward, Nitrogenase gene diversity and microbial community structure: a cross-system comparison, *Environmental Microbiology*, *5* (7), 539-554, 2003.

Zehr, J.P., J.P. Montoya, B.D. Jenkins, I. Hewson, E. Mondragon, C.M. Short, M.J. Church, A. Hansen, and D.M. Karl, Experiments linking nitrogenase gene expression to nitrogen fixation in the North Pacific subtropical gyre, *Limnol. Oceanogr.*, *52* (1), 169-183, 2007.

Zehr, J.P., J. Waterbury, P.J. Turner, J.P. Montoya, E. Omoregie, G. Steward, A. Hansen, and D.M. Karl, Unicellular cyanobacteria fix N2 in the subtropical North Pacific Ocean, *Nature*, *412* (9 August), 635-638, 2001.

II. Procedure for *nifH* Gene Analysis

The majority of this thesis is based on three manuscripts that explore diazotroph diversity, distribution and abundance through analysis of the *nifH* gene of the nitrogenase enzyme complex. This section describes only the methods which were adapted or developed for *nifH* gene analysis during work on this thesis. Details on all methods used can be found in the following section. This section also includes information on samples that were collected and partially analyzed during the thesis work, but are not completed data sets. Special care was taken for the development of the quantitative PCR method and will be the subject of an additional peer-reviewed manuscript to be submitted to Limnology and Oceanography Methods.

Sample Collection and Nucleic Acid Extraction

Samples for *nifH* gene analysis were collected during several cruises to the Atlantic and Pacific Oceans and the Mediterranean, North and Baltic Seas (Table II-1). Seawater was collected either in Niskin bottles attached to a CTD rosette from different depths or from surface waters with an overboard trace metal clean diaphragm pump. 300 ml to 2 l of water were filtered through a 0.2 µm Millipore Durapore filter. Samples for the S152, P284 and M55 cruises were filtered onto 25 mm diameter filters, but filtration times were very long. In order to reduce the amount of time required for filtration and to preserve RNA integrity, samples were subsequently filtered onto 47 mm diameter filters. Immediately after filtration samples were frozen and stored at -80°C until extraction in the laboratory.

Several DNA and RNA extraction kits were tested during the course of the thesis work. All kits produced comparable results with respect to amounts of genetic material extracted, quality of down-stream procedures and quantities of *nifH*, provided that filters were properly crushed to small fragments. A series of tests demonstrated that chilling the cryo-tube containing the filter in liquid nitrogen for at least 30 sec and then grinding the filter with a large pipette tip was the only way to break up the filter into small fragments. A bead homogenizer was also tested and failed to break apart the filter. Durapore filters

become very brittle when frozen in liquid nitrogen and the homogenizer was not able to chill the filter.

Table II-1: Regions Sampled for *nifH* Gene Analysis

Cruise Name	Dates	No. Samples	State of Analysis
North Atlantic			
S152	Dec. 2000	20	Published[4,5]
P254	March 2002	12	Published[4,5]
M55[1,3]	Oct./Nov 2002	61	Published[4,5,6]
M60[1,3]	March 2004	47	Published[4,5,6,7,8,9]
P332	Jan./Feb 2006	40	qPCR analysis finished
M68[2,3]	July 2006	125	qPCR and ^{15}N rate analysis
P348	Feb. 2007	12	Phylogenetic analysis
North and South Atlantic			
AMT	Oct./Nov. 2005	61	Phylogenetic and qPCR analysis
North Pacific			
KH0502	Aug./Sept. 2005	39	Sample extraction
South Pacific			
KH0405	Dec. 2004/March 2005	53	Sample extraction
Cost	Feb. 2005	42	qPCR analysis
N-Cycle	March/Apr. 2006	12	qPCR analysis
Mediterranean Sea			
M71[2,3]	Jan. 2007	53	qPCR optimization and ^{15}N rate analysis
Baltic and North Seas			
Innofond	Jan. 2007-present	32	Phylogenetic analysis
China Sea			
KT0524	Oct. 2005	23	Sample extraction

[1.] Cruise participant.
[2.] Cruise participant and responsible for all planning, preparation and execution of experiments.
[3.] Bioassay experiments performed in parallel. Samples collected for ^{15}Nitrogen fixation rates, chlorophyll a and analytical flow cytometry.
[4.] Paper A [*Langlois et al.*, 2005]
[5.] Paper B [*Langlois et al.*, 2008]
[6.] Paper C (in prep)
[7.] Paper D [*Moore et al.*, 2006]
[8.] Paper E [*Moore et al.*, 2008]
[9.] Paper F [*Mills et al.*, 2008]

A combination of liquid nitrogen to break up the filter and beads to homogenize the samples resulted in DNA shearing. In order to avoid this, samples were instead homogenized by vortexing vigorously for 30 sec which did not shear the DNA. All

samples from one data set were extracted using the same method and kit (from Qiagen) in order to prevent any possible variations in the composition of the extracted genetic material due to the extraction. Manufacturers' protocols were used except that elution volumes were reduced to 50 µl due to the low biomass in oligotrophic waters. Extracted DNA was always run on an agarose gel to verify integrity.

DNA and RNA concentrations were measured by several methods. Originally an Eppendorf Biophotometer was used. However, in order to have enough volume for a measurement, samples needed to be diluted. The Biophotometer was not sensitive enough to measure the diluted samples. Reproducible DNA and RNA concentrations in environmental samples could also not be obtained using a NanoDrop ND-1000 Spectrophotometer. Fluorometric determination of DNA and RNA concentrations using the PicoGreen and RiboGreen quantitation reagents (Molecular Probes), respectively, produced highly reproducible results and all samples were measured using this method. While the quantitation reagents bind only to double and single stranded genetic material, respectively, giving accurate DNA and RNA concentrations, this method unfortunately does not provide any information on the purity of the DNA or RNA.

nifH Amplification

A nested PCR technique was used to amplify a 359 bp segment of the *nifH* gene [*Langlois et al.*, 2005]. The *nifH* nested PCR consists of two rounds of PCR using two sets of degenerate primers, the second set targeting a section of DNA just inside the first set. This method increases the sensitivity of the PCR [*Zani et al.*, 2000]. A high sensitivity is needed for amplifying *nifH* genes as diazotrophic organisms make up only a small part of the entire marine microbial community. The first round of PCR is done by mixing (final concentrations) 1.6 mM nifH3 and nifH4 primers (Table II-2), 4 mM $MgCl_2$, 0.2 mM each dNTPs, 10x AmpliTaq Buffer II, 1.25 U AmpliTaq Gold polymerase (Applied Biosystems), and 1 µl DNA in a 50 µl reaction. The first round thermal cycler program consists of a 10 min. activation step at 95°C, followed by 35 cycles of a 1 min. denaturation step at 95°C, 1 min. annealing at 45°C, and 1 min. elongation at 72°C. The program ends with a final 10 min. elongation at 72°C. The PCR

reagent mix for the second round is the same except that nifH1 and nifH2 primers (Table II-2) are used, the $MgCl_2$ concentration is lowered to 3 mM and 1 µl PCR product from the first round is used instead of DNA. The number of cycles for the second round PCR program is lowered to 28 and the annealing temperature is raised to 54°C. The nested *nifH* PCR method is unusual in that high magnesium chloride and primer concentrations are used and the annealing temperatures are considerably low. Attempts to raise the annealing temperatures, lower the primer concentrations and reduce the reaction volume to 25 µl resulted in losses of the *nifH* PCR product.

Table II-2: Degenerate Primers for Nested *nifH* PCR

Primer	Sequence (5'→ 3')	Position in *Azotobacter vinelandii*	Melting Temperature
NifH$_1$	TGYGAYCCNAARGCNGA	639-655	54°C
NifH$_2$	ANDGCCATCATYTCNCC	1000-984	52.4°C
NifH$_3$	ATRTTRTTNGCNGCRTA	1018-1002	46.7°C
NifH$_4$	TTYTAYGGNAARGGNGG	546-562	51.6°C

Y= T or C; R= A or G; D= A,G, or T; N= A, C, G, or T

Determining Abundances of *nifH* Genes Using qPCR

There are several advantages to using qPCR over traditional PCR methods. For instance, qPCR gives results more quickly, is considerably more sensitive than PCR and many biases of the standard PCR method are avoided. Methods which use an end point PCR product are sensitive to multiple target gene copies which can lead to biases during amplification and replication. Amplification biases can also result from preferential primer binding. Even the use of different types of Taq-polymerases can lead to differing results [*Osborn et al.*, 2000]. Since qPCR primers and probes are designed to target only a specific phylogenetic group, there is no preferential amplification. By using different primer and probe sets, one can select for as many (or few) phylogenetic groups as required for a given environment. Most importantly, qPCR data is not based on an end-point PCR product.

In traditional PCR, a DNA fragment is amplified so that the target sequence, or amplicon, is concentrated enough that it can be further studied using other techniques,

such as gel electrophoresis or cloning. However, this method gives little indication as to the initial amount of target sequence which makes quantitative comparisons of samples very difficult. In qPCR, one calculates the initial amount of target sequence based on the start of exponential amplification of the product above a set threshold, called the threshold cycle (Ct). This method functions by adding a dye to the PCR reaction that fluoresces whenever a PCR product is amplified. The sample is run in a real-time thermocycler which measures and graphically displays the increase in a sample's fluorescence. Very short segments (up to 150 b) are amplified by qPCR primers; which reduces the time required for the elongation step.

There are two methods for detecting product accumulation in qPCR, SYBRgreen and TaqMan probes. SYBRgreen is a fluorescent dye which is added to the PCR master mix and fluoresces whenever a double-strand of DNA is joined, including when primer-dimers are formed or unspecific product amplification occurs. In TaqMan qPCR, specific fluorescent probes, which contain a fluorescent dye at the 5' prime end and a quencher dye at the 3' end, are designed. TaqMan MGB® probes contain a minor groove binder which gives extra reliability in the fluorescent signal by stabilizing the bond between the non-fluorescent quencher and the probe. Since qPCR primers and TaqMan probes are all about 20 bp in length, very few regions of the targeted sequence are left uncovered which greatly increases the specificity of and confidence in the reported signal. Because there are many uncharacterized sequences in the environment, TaqMan MGB® probes were used in order to obtain the highest specificity possible and reduce the chance of false positives.

Absolute quantification is achieved by amplifying a serially diluted standard and creating a graph of log (gene copy number) versus Ct. The resulting linear regression is then used to convert the sample Ct values to initial gene copy numbers. The theoretical standard curve is $y = -3.33 + 40$, $R^2 = 0.999$. The theoretical detection limit of qPCR assays is one gene copy.

Selection of Primers and Probes

TaqMan MGB® probes and primers were designed for seven diazotrophic phylotypes due to the occurrence of these phylotypes in several *nifH* clone libraries constructed from samples collected throughout the Atlantic Ocean [*Langlois et al.*, 2008] using Primer Express (v. 2.0, Applied Biosystems) (Table II-3). The guidelines set forth by Applied Biosystems for real-time PCR primer and probe design were followed. Four cyanobacterial (filamentous, Group A, B, and C unicellular), two γ–proteobacterial (Gamma A and Gamma P), and one Cluster III phylotype(s) were targeted. There is a high similarity (>98%) between the various *Trichodesmium spp*. and *Katagnymene spiralis nifH* sequences [*Langlois et al.*, 2005]. It was not possible to design a primer and probe set that selected only for one *Trichodesmium* or one *Katagnymene nifH*, therefore the filamentous primer set was designed to target as many *Trichodesmium*-type filamentous cyanobacterial *nifH* sequences as possible. Phylogenetic analysis of the unicellular Group A sequences revealed a relatively large diversity (Figure 5 in [*Langlois et al.*, 2005]). The Group A primer set was designed to target the larger clade including the first described Group A sequence. Primer and probe sequences were checked for possible similarities to sequences from non-target organisms using the NCBI database and none were found.

The filamentous, unicellular Groups A and C, and Gamma A phylotypes were also the most common or, in some cases, the only phylotypes recovered in clone libraries from the P332, M68, Cost, and N-cycle cruises. The Mediterranean (M71) cruise appeared to have a slightly different diazotroph composition than found in the open ocean clone libraries and new primers and probes needed to be designed (Table II-3). The filamentous and Group B phylotypes were recovered. Group A and γ–proteobacterial phylotypes were also recovered, but varied considerably from the open ocean phylotypes, so much that the originally designed primers and probes amplified these groups very poorly and new primer/probe sets needed to be constructed. The clone libraries from the Mediterranean were also the first data sets where we recovered the diatom-diazotroph associations (DDAs). DDAs have been hypothesized to be correlated with high salinity

waters [*Foster et al.*, 2007] which may explain why this phylotype was found only in the Mediterranean clone libraries.

Table II-3: qPCR Primers and Probes

Type	Primer (position[1])		Probe (position[1])	Reference Sequence
	Reverse	Forward		
Atlantic				
Filamentous	GCAAATCCACCGCAAACAAC (275-256)	TGGCCGTGGTATTATTACTGCTATC (165-189)	AAGGAGCTTATACAGATCTA (206-225)	AY896367.1
Group A	TCAGGACCACCGGACTCAAC (146-127)	TAGCTGCAGAAAGAGGAACTGTAGAAG (50-76)	TAATTCCTGGCTATAACAAC (98-117)	AF059627.1
Group B	TCAGGACCACCAGATTCTACACACT (146-122)	TGCTGAAATGGGTTCTGTTGAA (54-75)	CGAAGACGTAATGCTC (87-102)	AY896454.1
Group C	GGTATCCTTCAAGTAGTACTTCGTCTAGCT (112-83)	TCTACCCGTTTGATGCTACACACTAA (1-26)	AAACTACCATTCTTCACTTAGCAG (32-55)	AY896461.1
Gamma A	AACAATGTAGATTTCCTGAGCCTTATTC (321-294)	TTATGATGTTCTAGGTGATGTG (240-266)	TTGCAATGCCTATTCG (275-290)	AY896371.1
Gamma P	CATCGCGAAACCACCACATAC (282-262)	TTGTGCAGGTCGTGGTGTAATC (159-180)	CCTATGACGAAGACCTAGAC (212-231)	AY896428.1
CIII	GCAGACCACGTCACCCAGTAC (267-247)	ACCTCGATCAACATGCTCGAA (175-195)	CCTGGACTACGCGTTC (225-240)	AY896461.1
Mediterranean				
MedGrp A	CCACGACCAGCACATCCA (173-156)	CCTGGTTACAACAACGTTTTATGTGT (103-128)	AATCTGGTGGTCCTGAGC (131-148)	cSK01Contig_1
Richelia	CACGACCCGCACAACCA (172-156)	CCGTGAAGTACGTTGTGTGGAA (111-132)	TGGTCCTGAGCCTGGT (138-153)	cH04Contig_2
MedGam1	TTCGTATGCGCCTTCTTCTTC (219-199)	GTTGTGCAGGTCGTGGTGTT (158-177)	ACAGCGATTAACTTCTT (181-197)	H01_80mContig_1
MedGam2	CTTCGTAAGCGCCTTCCTCTT (220-200)	GTTGTGCAGGTCGTGGTGTT (158-177)	ACTGCAATTAACTTCCT (181-197)	Her03_80Contig_1

[1.] Sequences given 5'-3' and all positions refer to the 354 bp *nifH* product.

Construction of Plasmid Standards and qPCR Assays

Representative cloned *nifH* sequences for each primer and probe set (Table II-3) were re-cloned into the Topo vector and subsequently transformed into Top10 cells according to the manufacturer's instructions (Invitrogen). In addition, a clone similar to Group A (A2) and a *Katagnymene spiralis* clone were also re-cloned in order to test the specificity of the primer and probe sets with nearly identical sequences. Plasmid extractions were performed for each representative sequence using the Qiagen Plasmid Purification Kit and the manufacturer's instructions. The DNA concentrations of the purified plasmids were determined using a NanoDrop ND-1000 Spectrophotometer. The molecular weight of one plasmid plus *nifH* insert was calculated and the plasmids were

accordingly diluted to 10^8 *nifH* copies μl^{-1}. Standards for qPCR analyses consisted of serial dilutions from 10^7 to 10^1 *nifH* copies μl^{-1} of the purified plasmids. Primer and probe concentrations in qPCR assays were optimized before testing primer specificity and efficiency according to the guidelines recommended by Applied Biosystems. Standards were then used in qPCR assays.

All qPCR assays were performed in duplicate using an ABI Prism 7000 (Applied Biosystems) and 25 µl reactions containing: 1x TaqMan PCR buffer (Applied Biosystems), 100 nM TaqMan probe, 5 pmol μl^{-1} each of the forward and reverse primers, PCR water and 5 µl DNA. The default program was used, only the number of cycles was increased to 45. No template controls (NTCs) were always run in duplicate for each master mix and were undetectable after 45 cycles. The qPCR results were analyzed using the ABI 7000 system SDS software (version 1.2.3) with RQ study application (Applied Biosystesms).

Testing Primer Efficiency and Specificity

Standards for each Atlantic primer and probe set were diluted and run many times over several weeks to determine the stability of the standards. The average of all standard dilutions (n=14-39) measured are shown in Figure II-1. The standards varied by an average of only 1.14 Ct, indicating a high reproducibility in diluting and/or storage of the standards over time. The formula $E = 10^{-1/slope} - 1$ was applied to the average slope of these standard curves in order to calculate the primer amplification efficiency [*Atallah et al.*, 2007]. High primer efficiencies for all but one of the Atlantic primer sets were obtained. The Atlantic set primer efficiencies are as follows: 96.5% ± 2% (n =37) for filamentous, 94.9% ± 1% (n =39) for Group A, 96.1% ± 2% (n =22) for Group B, 89.1% ± 6% (n = 24) for Group C, 95.3% ± 2% (n =24) for Gamma A, 100% ± 2% (n = 14) for Gamma P, and 100% ± 1% (n =22) for Cluster III. Preliminary results show that the Mediterranean primers also have high amplification efficiencies except for the Richelia primer set. These primer efficiencies are: 98% +/- 3% (n=6) for Med Group A, 85% ± 3% (n=2) for Med Gam1, 86% ± 3% (n=2) for Med Gam2 and 73% ± 4% (n=4) for

Richelia. Due to the poor performance of the Richelia primers new primers were designed, but have not yet been tested.

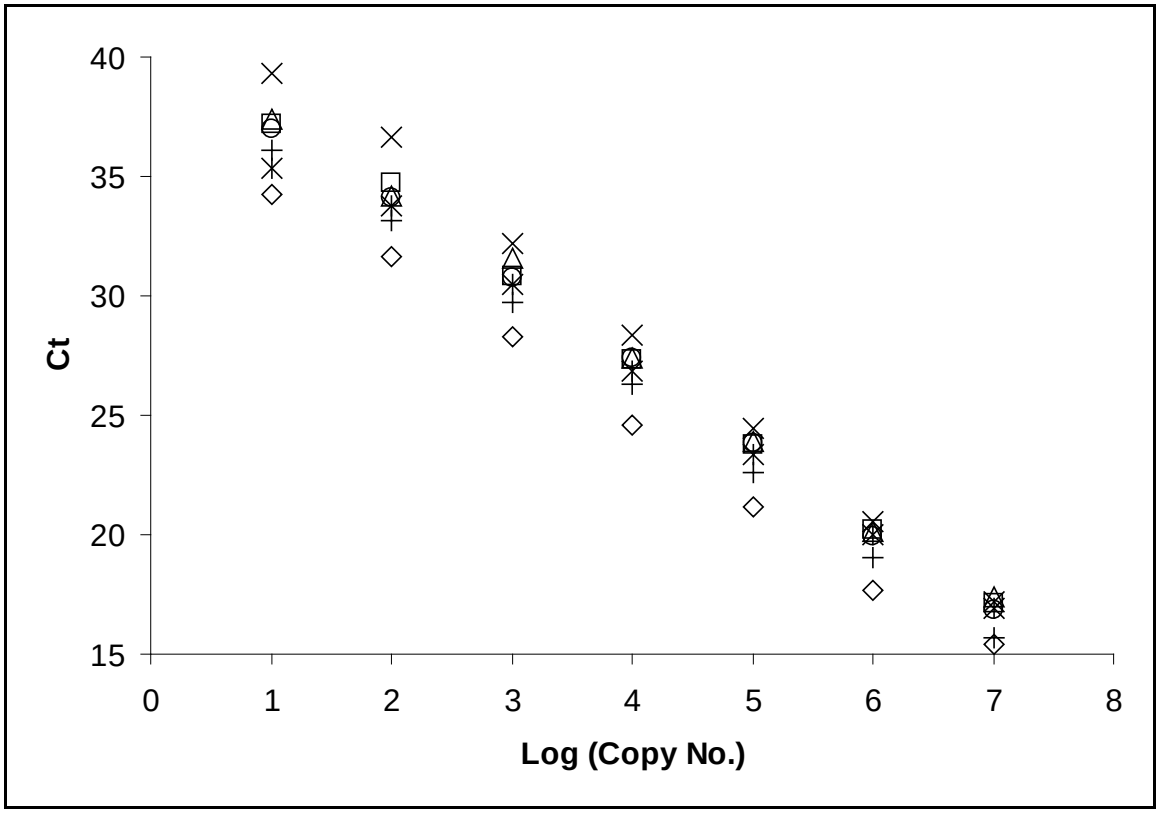

Figure II-1: Average Standard Curves Standard curves for the filamentous ('○', y=-3.47x + 40.8, R^2=0.999), Group A ('+', y=-3.45x + 39.9, R^2=0.999), Group B ('Δ', y=-3.42x + 41, R^2=0.998), Group C ('x', y=-3.8x + 43.6, R^2=0.998), Gamma A ('□', y=-3.43x + 41, R^2=0.998), Gamma P ('◊', y=-3.27x + 37.7, R^2=0.997), and CIII ('*', y=-3.21x + 39.5, R^2=0.994) plasmids are shown. Error bars have been omitted to improve visualization.

As concentrations of various diazotrophic phylotypes are unknown in environmental samples, it is important to determine how the specificity of the qPCR assay could change under various conditions. Specificity of the primer and probe sets was determined by testing each primer set for amplification of each purified plasmid diluted to 10^7 and 10^4 *nifH* copies. This test was repeated five times for the Atlantic primers and the same results were always obtained. So far the specificity of the Mediterranean primers has been tested only once. The Atlantic primers and probes are very specific and amplified only the target plasmid(s) (Table II-4). The filamentous primer set was designed to target

both *Trichodesmium* and *Katagnymene*, however amplification of *Trichodesmium* was slightly later (i.e. larger Ct) than that of *Katagnymene*. The Group A primer set also amplified a very similar sequence (A2, 99% similarity), but amplification occurred much later than for the target plasmid. The Mediterranean primers were very specific (Table II-5), however the test needs to be repeated as low primer efficiencies can affect the outcome and the 10^4 Richelia plasmid was not tested against all primer sets. The two Med Gamma primer sets cross amplified each other, but with a much larger Ct than expected. The amount (or lack) of unspecific amplification of the primer sets needs to be taken into consideration when interpreting qPCR data. For instance, if a diazotrophic community consists mostly of the *Trichodesmium* or Group A-II phylotypes, this method would underestimate the *nifH* abundances, whereas high cross-reactivity (small Ct values) between two phylotypes could result in overestimations of *nifH* abundances.

Table II-4: Atlantic Primer and Probe Specificity

10^4 Standard	Primers and Probes						
	Filamentous	Group A	Group B	Group C	Gamma A	Gamma P	CIII
TT	31	u	u	u	u	u	u
KS	27	u	u	u	u	u	u
Group A	u	29	u	u	u	u	u
Group A2	u	33	u	u	u	u	u
Group B	u	u	31	u	u	u	u
Group C	u	u	u	29	u	u	u
Gamma A	u	u	u	u	28	u	u
Gamma P	u	u	u	u	u	29	u
CIII	u	u	u	u	u	u	28

Note: Two filamentous standards, *Trichodesmium thiebautii* (TT) and *Katagnymene spiralis* (KS) were tested. Ct values are given where amplification occurred. U stands for undetected after 45 cycles.

Table II-5: Mediterranean Primer and Probe Specificity

10^7 Standard	Primers and Probes			
	Med Group A	Richelia	MedGam1	MedGam2
Med Group A	14.3	u	u	u
Richelia	u	18.3	u	u
Med Gamma 1	u	u	13	20.1
Med Gamma 2	u	u	23.8	17.1

Note: Ct values are given where amplification occurred. U stands for undetected after 45 cycles.

Primer specificity in mixes of varying concentrations of similar DNA was also investigated. In this test combinations of serially diluted plasmids were mixed at ratios of 10^7 filamentous:10^1 Group A to 10^1 filamentous:10^7 Group A and changes in the primer efficiency and standard linear regressions were noted. The linear regressions of the filamentous and Group A standard curves did not change over seven orders of magnitude, nor did the primer efficiencies (Figure II-2). The only exception to this was that the filamentous standard was undetectable below 10^3 *nifH* copies when combined with high amounts (above 10^6 *nifH* copies) of Group A. This situation is unlikely to occur in field samples. Phylotype abundances have very rarely been estimated at concentrations above 10^6 *nifH* copies l^{-1} in samples measured by qPCR.

Eliminating Environmental Sample Inhibition with BSA

Simultaneous purification of PCR inhibitors along with genetic material is often a concern when working with environmental samples. Substances such as humics, tannic acid, EDTA, ethanol, and salts (including NaCl) are either known or suspected to be inhibitory to PCR reactions [Kreader, 1996]. Inhibition of qPCR was observed in serially diluted environmental samples. A total of 17 samples from different data sets were tested for inhibition and all but one sample showed inhibition. In addition, each sample was inhibited to a varying degree. In order to avoid diluting samples [*Church et al.*, 2005a], which reduces the sensitivity of the method or the use of complicated tables to explain the level of inhibition in each sample (see [*Foster et al.*, 2007]), additions of the PCR enhancer bovine serum albumin (BSA) to qPCR reactions were tested. BSA has been shown to be effective at relieving inhibition in traditional PCR methods [*Maaroufi et al.*, 2004; *Malorny and Hoorfar*, 2005] and in qPCR using SYBRgreen chemistry

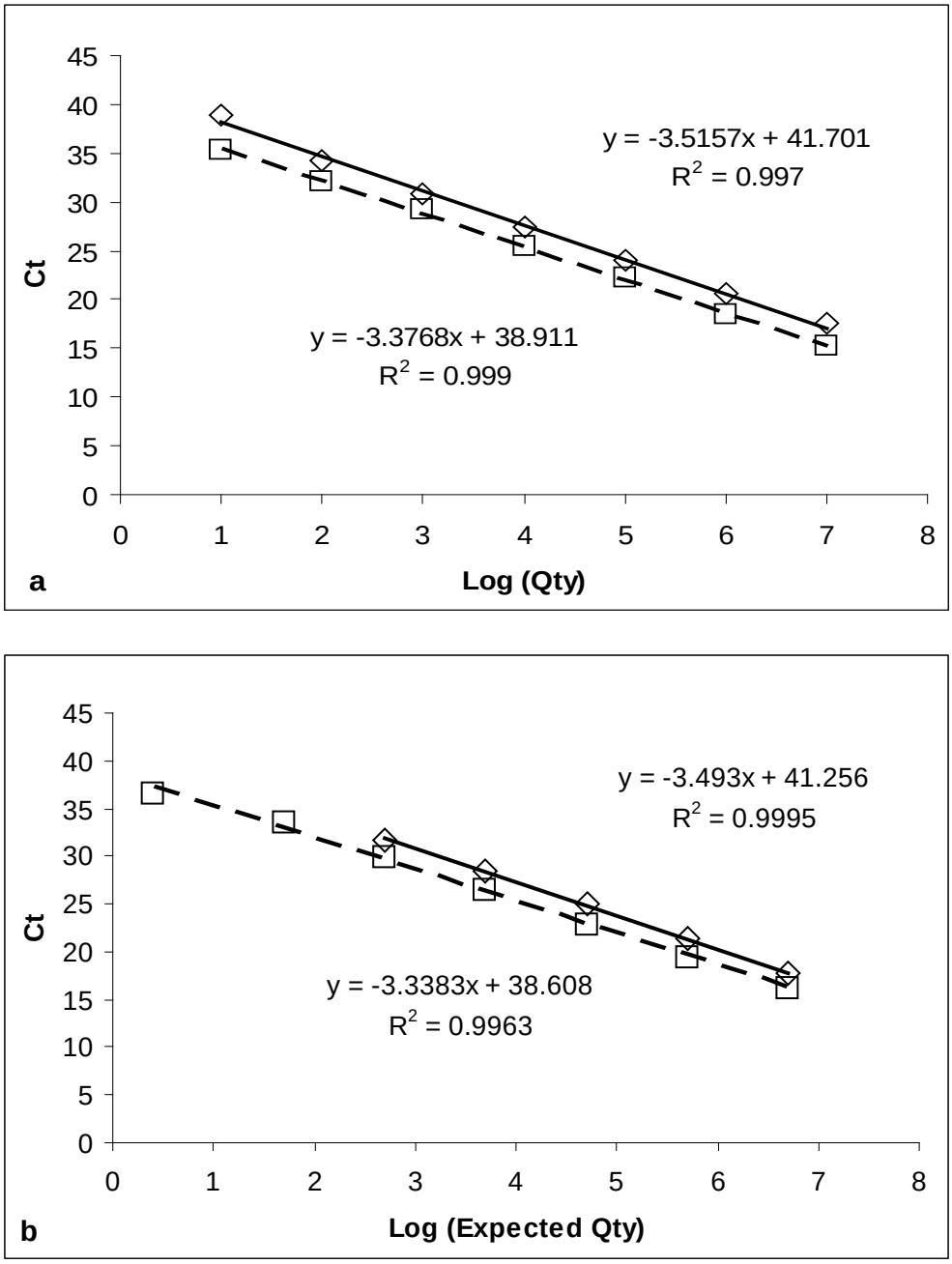

Figure II-2: Performance of Standards with Varying Amounts of Similar DNA Typical filamentous (diamond, upper linear regression) and Group A (squares, lower linear regression) standard curves are shown in a. Combinations of the same standard dilutions were combined at ratios of 10^7 filamentous:10^1 Group A to 10^1 filamentous:10^7 Group A and measured (b), resulting in minor changes to the linear regressions. Primer efficiencies for filamentous were 93% in both panels and Group A were 98% and 100% in a and b, respectively.

[*Al-Soud and Radstrom*, 2000], but how BSA would affect the TaqMan chemistry was unknown until now. Standards were run in parallel with and without additions of 40 ng μl^{-1} BSA (final concentration) to determine whether or not BSA affected primer efficiency or the qPCR chemistry. Additions of BSA to the qPCR assay did not affect the standard curve linear regression and thus the primer efficiency (Figure II-3a).

Comparisons of amplification of diluted environmental samples with and without BSA additions were also made to determine the effectiveness of BSA in relieving sample inhibition. BSA additions were very effective at eliminating inhibition in environmental samples (Figure II-3b). Some samples that were undetectable without BSA were detectable after BSA additions (Table II-6), indicating that BSA is a good tool for eliminating, or at the very least, greatly reducing environmental sample inhibition without lowering the detection limit of the method. BSA is now routinely added to qPCR assays of environmental samples in our laboratory.

Table II-6: Effect of BSA on Four Environmental Samples with Different Degrees of Inhibition

Dilutions	-BSA	+BSA
Pos144		
0.2	4.3×10^1	1.9×10^5
0.1	8.2×10^4	2.0×10^5
0.02	1.1×10^5	1.7×10^5
0.01	1.9×10^5	1.7×10^5
Pos148		
0.2	1.3×10^3	1.9×10^5
0.1	9.9×10^5	1.7×10^5
0.02	2.3×10^5	2.0×10^5
0.01	1.6×10^5	2.6×10^5
102294		
0.2	u	2.2×10^2
0.1	u	3.2×10^2
0.02	u	u
0.01	u	1.5×10^2
100064		
0.2	2.5×10^3	2.4×10^3
0.1	1.8×10^3	2.3×10^3
0.02	2.4×10^3	4.0×10^3
0.01	7.4×10^3	2.7×10^3

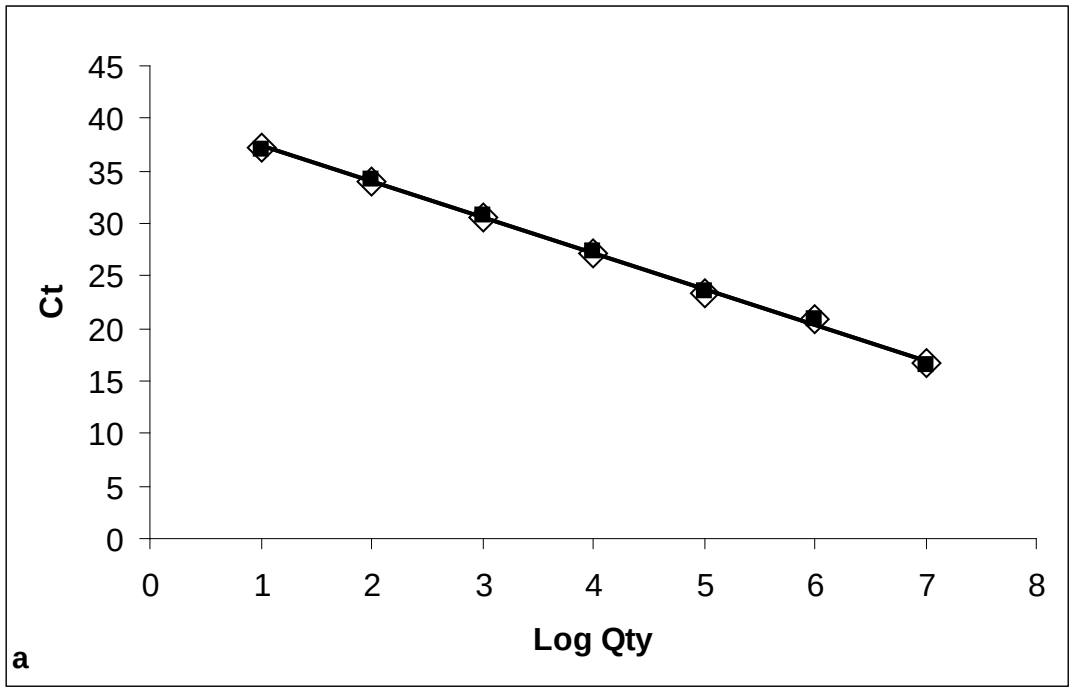

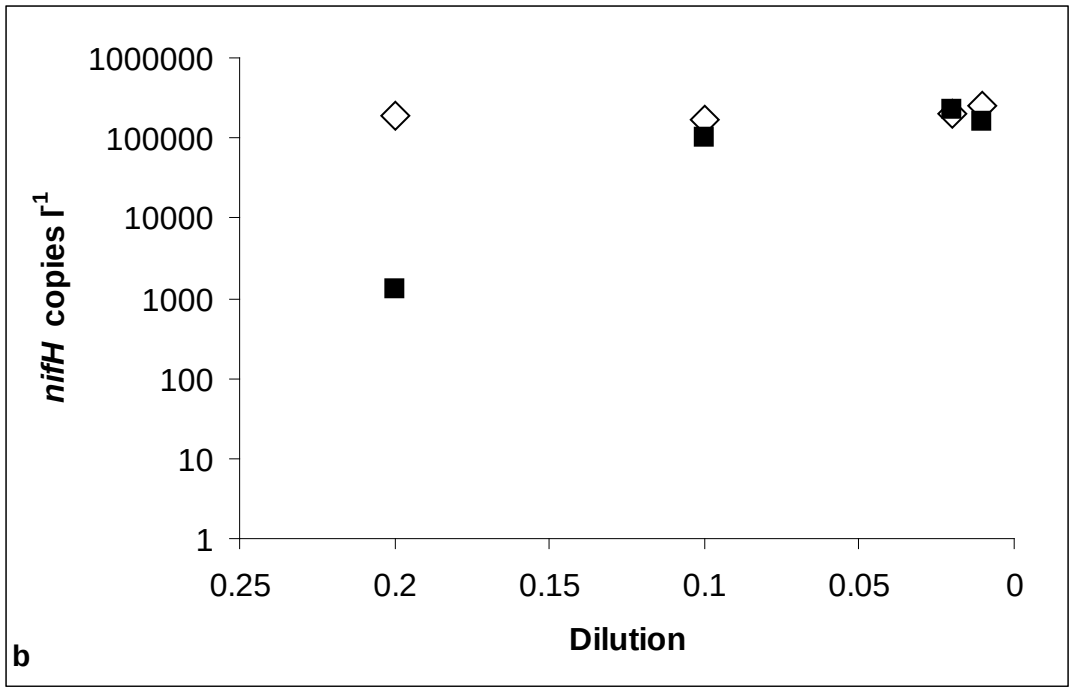

Figure II-3: BSA Additions to a Standard (a) an Environmental DNA Sample (b) Reactions with BSA added are marked with (◊) and samples without BSA are labeled (■). The linear regressions for a are: + BSA: $y = -3.4x + 40.8$; $R^2 = 0.998$ and - BSA added: $y = -3.4x + 40.7$; $R^2 = 0.998$.

Considerations for Interpreting qPCR Data

Depending on the efficiency of the primers and quality of the run, the theorectical detection limit of a qPCR assay is one copy per volume of sample loaded. The realized detection limit is actually higher. When determining the detection limit, the first consideration is the no template controls (NTCs). Amplification in NTCs indicates contamination in the qPCR reagents and thus the detection limit can not be set lower than any observed NTC amplification. There should be no amplification in NTCs, but this value can be high and is often not reported in publications (see [*Smith et al.*, 2005]). We usually detect no amplification in NTCs and re-run the qPCR analysis when amplification is detected.

Another concern is that there is sometimes a larger variability in duplicate Ct values of the standard as the amount of DNA loaded reaches one copy per volume of sample loaded. Standards that amplify with high primer efficiency generally produce highly replicable data, even down to one copy. Those with a lower efficiency usually are more variable, especially at lower copy numbers and the R^2 value reflects this (Figure II-1). One reason for this is that pipetting errors increase as DNA amounts get smaller. This variability is even larger when measuring environmental samples. Due to this several studies have used a cut off of Ct =37 instead of 40 for collecting quantitative data [*Church et al.*, 2005a; *Church et al.*, 2005b; *Foster et al.*, 2007; *Langlois et al.*, 2008]. Samples which amplify with a Ct of 37 or greater are considered detectable, but not quantifiable. This raises the absolute detection limit of the qPCR assay to 10 gene copies. However, since only a fraction of the eluted DNA sample is loaded into the qPCR reaction there is also a sample dilution to consider, which again raises the detection limit of the method. As gene abundances are often reported as concentrations (gene copies l^{-1}), the amount of water filtered for a sample needs to be factored in as well. The amount of water filtered determined the detection limits for the samples measured during this thesis, because the elution volumes and amount of sample loaded into a reaction were kept constant. The actual detection limits of the qPCR method described in this thesis ranged from 20 (S154) to 75 (M60) *nifH* copies l^{-1} [*Langlois et al.*, 2008].

The calculation for the detection limit described above assumes a 100% extraction efficiency of all phylotypes being quantified. Lysis of cells varies from organism to organism. Some, such as *Trichodesmium*, break apart very easily while others, such as diatoms and *Crocosphaera*, require more effort. As the composition of environmental samples is unknown, it is hard to determine whether or not all cellular material is being lysed effectively. The genetic material extraction itself also introduces an error that is not addressed in the method above. This is one of the major complications of interpreting qPCR data. Other studies have addressed this problem by adding a known number of cells to the sample as an internal standard for simultaneous extraction [*Brinkman et al.*, 2003]. This not only gives information on extraction efficiencies, but also information on PCR inhibition. This method, however, relies on the assumption that the internal standard cells and the target cells can be lysed and extracted with the same efficiency. Ct values for the internal standard could also be biased if the qPCR primers co-amplify uncharacterized environmental sequences [*Coyne et al.*, 2005]. One way to avoid this is to add exogenous DNA (i.e. a plasmid) instead of cells to the samples before extraction [*Coyne et al.*, 2005]. The qPCR method described in this thesis could be improved by using exogenous DNA to describe differences in sample extraction; but the problem of cells with different lysis efficiencies would remain.

A comparative Ct method has been described for estimating abundances of harmful algal bloom species [*Coyne et al.*, 2005]. In this method, an environmental water sample was used instead of a plasmid standard. Target cells in the water standard were counted by microscopy and the standard was diluted appropriately. Ct values of the water standard and environmental samples were compared. This method shows promise for enumeration of large, easily identifiable and countable cells. It is not currently adaptable to the study of open ocean diazotrophs. Most open ocean diazotrophs studied by qPCR are identified only by a *nifH* sequence. They are not in culture and very little information is known about their cellular characterization and appearance. In addition the described species are either very hard to accurately count by microscopy, such as *Trichodesmium,* or are small, unicellular and, therefore, nearly impossible to distinguish from the rest of the picoplankton community.

Many precautions were taken in developing this qPCR method to reduce unspecific amplification. The more specific TaqMan probes were used instead of SYBRgreen. Primers and probes were checked against known sequences for possible similarities and primer specificity was thoroughly tested. Despite this, anomalous amplification with the filamentous primer and probe set was observed in a bottle incubation experiment at 42°N during the spring bloom. Stations sampled around the incubation experiment site did not contain the filamentous phylotype, as shown by qPCR [*Langlois et al.*, 2008]. A nested *nifH* PCR was performed on the incubation samples several times and no *nifH* genes were recovered. A product was finally obtained by modifying the nested *nifH* PCR; the filamentous reverse primer was substituted for the nifH3 primer in the second round. This short product (200 bp) was sequenced and the resulting sequence translated into an amino acid sequence. A BlastN search revealed that it was not closely related to any sequences in the databases. The sequence was eventually determined to be distantly similar to a protochlorophyllide reductase gene through a BlastX search. Although protochlorophyllide reductase belongs to the *nifH* protein family, it is surprising that the primers and probe specific for the filamentous phylotypes amplified this gene. Such a result was not foreseeable and emphasizes that qPCR data must be scrutinized and products should be checked by sequencing, even when the method was carefully tested and designed. Clone libraries from a data set to be measured by qPCR should also always be constructed in order to ensure that all phylotypes to be quantified are targeted by the primers and probes. Despite the concerns addressed here, qPCR is an extremely useful tool for characterizing and estimating abundances of organisms in the environment. It allows for sampling a large number of samples in a relatively short amount of time and provides quantitative data.

References:

Al-Soud, W.A., and P. Radstrom, Purification and Characterization of PCR-Inhibitory Components in Blood Cells, *Journal of Clinical Microbiology*, *39* (2), 485-493, 2000.

Atallah, Z.K., J. Bae, S.H. Jansky, D.I. Rouse, and W.R. Stevenson, Multiplex Real-Time Quantitative PCR to Detect and Quantify *Verticillium dahliae* Colonization in Potato Lines that Differ in Response to Verticillium Wilt, *The American Phytopathological Society*, *97* (7), 865-872, 2007.

Brinkman, N.E., R.A. Haugland, L.J. Wymer, M. Byappanahalli, R.L. Whitman, and S.J. Vesper, Evaluation of a rapid quantitative real-time PCR method for enumeration of pathogenic *Candida* cells in water, *Appl. Envir. Microbiol.*, *69*, 1775-1782, 2003.

Church, M.J., B.D. Jenkins, D.M. Karl, and J.P. Zehr, Vertical distributions of nitrogen-fixing phylotypes at Stn ALOHA in the oligotrophic North Pacific Ocean, *Aquatic Microbial Ecology*, *38*, 3-14, 2005a.

Church, M.J., C.M. Short, B.D. Jenkins, D.M. Karl, and J.P. Zehr, Temporal Patterns of Nitrogenase (nifH) Gene Expression in the Oligotrophic North Pacific Ocean, *Appl. Envir. Microbiol.*, *71* (9), 2005b.

Coyne, K., S.M. Handy, E. Demir, E.B. Whereat, D.A. Hutchins, K.J. Portune, M.A. Doblin, and S.C. Cary, Improved quantitative real-time PCR assays for enumeration of harmful algal species in field samples using an exogenous DNA reference standard, *Limnol. Oceanogr.: Methods*, *3*, 381-391, 2005.

Foster, R.A., A. Subramaniam, C. Mahaffey, E.J. Carpenter, D. Capone, and J.P. Zehr, Influence of the Amazon River plume on distributions of free-living and symbiotic cyanobacteria in the western tropical north Atlantic Ocean, *Limnology and Oceanography*, *52* (2), 517-532, 2007.

Kreader, C.A., Relief of Amplification Inhibition in PCR with Bovine Serum Albumin or T4 Gene 32 Protein, *Applied and Environmental Microbiology*, *62* (3), 1102-1106, 1996.

Langlois, R.J., D. Huemmer, and J. La Roche, Abundances and Distributions of the Dominant *nifH* Phylotypes in the Northern Atlantic Ocean, *Appl. Envir. Microbiol.*, *74* (6), 1922-1931, 2008.

Langlois, R.J., J. La Roche, and P.A. Raab, Diazotrophic Diversity and Distribution in the Tropical and Subtropical Atlantic Ocean, *Appl. Envir. Microbiol.*, *71* (12), 7910-7919, 2005.

Maaroufi, Y., J.-M. De Bruyne, V. Duchateau, A. Georgala, and F. Crokaert, Early Detection and Identification of Commonly Encountered Candida Species from Simulated Blood Cultures by Using a Real-Time PCR-Based Assay, *Journal of Molecular Diagnostics*, *6* (2), 108-114, 2004.

Malorny, B., and J. Hoorfar, Toward Standardization of Diagnostic PCR Testing of Fecal Samples: Lessons from the Detection of Salmonellae in Pigs, *Journal of Clinical Microbiology*, *43* (7), 3033-3037, 2005.

Mills, M.M., C.M. Moore, R.J. Langlois, A. Milne, E.P. Achterberg, K. Nachtigall, K. Lochte, R. Geider, and J. La Roche, Nitrogen and phosphorus co-limitation of

bacterial productivity and growth in the oligotrophic subtropical North Atlantic, *Limnology and Oceanography*, *53* (2), 824-834, 2008.

Moore, C.M., M. Mills, R.J. Langlois, A. Milne, E.P. Achterberg, J. La Roche, and R. Geider, Relative influence of nitrogen and phosphorus availability on phytoplankton physiology and productivity in the oligotrphic sub-tropical North Atlantic Ocean, *Limnology and Oceanography*, *53* (1), 291-305, 2008.

Moore, C.M., M. Mills, A. Milne, R.J. Langlois, E.P. Achterberg, K. Lochte, R. Geider, and J. La Roche, Iron limits primary productivity during spring bloom development in the central North Atlantic, *Global Change Biology*, *12*, 626-634, 2006.

Osborn, A.M., E.R.B. Moore, and K.N. Timmis, An evaluation of terminal-restriction fragment length polymorphism (T-RFLP) analysis for the study of microbial community structure and dynamics, *Environ Microbiol*, *2* (1), 39-50, 2000.

Smith, C.J., D.B. Nedwell, L.F. Dong, and A.M. Osborn, Evaluation of quantitative polymerase chain reaction-based approaches for determining gene copy and gene transcript numbers in environmental samples, *Environ Microbiol*, 2005.

Zani, S., M.T. Mellon, J.L. Collier, and J.P. Zehr, Expression of nifH Genes in Natural Microbial Assemblages in Lake George, New York, Detected by Reverse Transcriptase PCR, *Appl. Envir. Microbiol.*, *66*, 3119-3124, 2000.

Paper A: *Diazotrophic Diversity and Distribution in the Tropical and Subtropical Atlantic Ocean*

Synopsis

The diversity of dinitrogen fixing organisms in the sub-tropical Atlantic Ocean was determined by analyzing *nifH* sequences amplified by nested PCR from samples collected during three separate cruises. Data from this study showed that *Trichodesmium* and diatom-diazotroph symbionts are not the only diazotrophs in the Atlantic Ocean. Filamentous cyanobacterial sequences similar to *T. erythraeum*, *T. thiebautii*, and *Katagnymene spiralis* were indeed recovered, as were unicellular cyanobacterial, γ-proteobacterial, and CIII *nifH* sequences. The other cyanobacterial sequences had high similarities to *nifH* from *Crocosphaera watsonii*, *Cyanothece*-like (later identified as unicellular Groups B and C, respectively) and unicellular Group A. The γ-proteobacterial sequences were similar to *nifH* sequences previously described from the Atlantic and Pacific Oceans and to *Klebsiella pneumoniae*. Langlois et al. 2005 was the first study to identify the Group C unicellular group and to describe the CIII group in the Atlantic Ocean. Many *nifH* sequences recovered in this study had high similarity (100%) to sequences originating from the Pacific Ocean indicating that some diazotrophs have a widespread distribution. Some *nifH* sequences were recovered from water with high nitrate concentrations which indicates that presence of nitrate should not always be equated with an absence of diazotrophic organisms. All *nifH* sequences were found in samples above 4°N and no *nifH* products were obtained from samples collected along the equator, thus identifying a band where nitrogen fixation potentially occurs in the Atlantic Ocean.

Contribution

Samples from the Poseidon 284 and Sonne 152 cruises were collected prior to the beginning of this thesis work. Samples from the Meteor 55 cruise were collected by me during my time as a Fulbright scholar. The five clone libraries from the Sonne 152 cruise were prepared by P. Raab as part of his Diploma Thesis, but sequences were re-analyzed by me for the preparation of the peer-reviewed manuscript. PCR reactions, construction of clone libraries, and phylogenetic analyses from the remaining samples as well as analysis of cruise metadata were completed by me. I prepared the figures and wrote the manuscript.

APPLIED AND ENVIRONMENTAL MICROBIOLOGY, Dec. 2005, p. 7910–7919 Vol. 71, No. 12
0099-2240/05/$08.00+0 doi:10.1128/AEM.71.12.7910–7919.2005

Diazotrophic Diversity and Distribution in the Tropical and Subtropical Atlantic Ocean

Rebecca J. Langlois, Julie LaRoche,* and Philipp A. Raab†

IFM-GEOMAR, Leibniz-Institut fuer Meereswissenschaften, Duesternbrooker Weg 20, 24105 Kiel, Germany

Received 16 March 2005/Accepted 22 August 2005

To understand the structure of marine diazotrophic communities in the tropical and subtropical Atlantic Ocean, the molecular diversity of the *nifH* gene was studied by nested PCR amplification using degenerate primers, followed by cloning and sequencing. Sequences of *nifH* genes were amplified from environmental DNA samples collected during three cruises (November-December 2000, March 2002, and October-November 2002) covering an area between 0 to 28.3°N and 56.6 to 18.5°W. A total of 170 unique sequences were recovered from 18 stations and 23 depths. Samples from the November-December 2000 cruise contained both unicellular and filamentous cyanobacterial *nifH* phylotypes, as well as γ-proteobacterial and cluster III sequences, so far only reported in the Pacific Ocean. In contrast, samples from the March 2002 cruise contained only phylotypes related to the uncultured group A unicellular cyanobacteria. The October-November 2002 cruise contained both filamentous and unicellular cyanobacterial and γ-proteobacterial sequences. Several sequences were identical at the nucleotide level to previously described environmental sequences from the Pacific Ocean, including group A sequences. The data suggest a community shift from filamentous cyanobacteria in surface waters to unicellular cyanobacteria and/or heterotrophic bacteria in deeper waters. With one exception, filamentous cyanobacterial *nifH* sequences were present within temperatures ranging between 26.5 and 30°C and where nitrate was undetectable. In contrast, nonfilamentous *nifH* sequences were found throughout a broader temperature range, 15 to 30°C, more often in waters with temperature of <26°C, and were sometimes recovered from waters with detectable nitrate concentrations.

Dinitrogen (N_2) fixation is a biological process carried out by prokaryotic organisms, known as diazotrophs. These organisms are particularly important in environments where nitrogen limits primary production, as they are the only organisms capable of converting molecular N_2 into NH_4, a more readily assimilated form of dissolved nitrogen (18). Oligotrophic oceans, chronically deficient in dissolved inorganic nitrogen, should be important niches for diazotrophs (13, 18). Early work on N_2 fixation focused on the easily identifiable, abundant, filamentous cyanobacterium *Trichodesmium*, considered until recently the most important marine diazotroph (13). Imbalances in the oceanic nitrogen budget (15) prompted a reassessment of the contribution of marine diazotrophs to the oceanic nitrogen cycle (2, 5, 9, 18). Discrepancies between geochemical estimates of N_2 fixation and measured N_2 fixation rates from field populations of *Trichodesmium*, accompanied by the known biases in isolating and culturing bacteria from natural environments (25), led to the realization that the diversity and abundance of oceanic diazotrophs may have been underestimated (41).

The development of molecular methods to amplify, clone, and sequence the *nifH* gene from environmental DNA samples (40) has recently led to the discovery of new types of marine diazotrophs. The *nifH* gene, which encodes the iron protein of nitrogenase, is a highly conserved functional gene (13, 41) useful in phylogenetic studies (42). The assessment of diazotroph diversity by this approach has been performed in various environments including soils (28), freshwater and saltwater lakes (33, 39), salt marshes (4, 20), stromatolites and microbial mats (26, 31), and deep-sea vents (22). This method has yielded evidence of new, unicellular diazotrophs in both the open Atlantic and Pacific oceans (11, 12, 44, 45).

The spatial and temporal distributions of the new diazotroph phylotypes in open oceans are poorly characterized, and there is a need to assess the importance of these new groups quantitatively. Although *nifH* sequences from environmental samples are available in public databases, the success of quantitative methods such as quantitative PCR (7) and micro- or macroarrays (17, 32) is largely dependent on a good initial characterization of the diversity of the *nifH* genes in a specific study area (8).

The purpose of this study was to characterize the diversity of *nifH* in the tropical and subtropical Northern Atlantic Ocean, as well as to look for environmental factors that may influence the distribution of the various *nifH* phylotypes. Samples from surface, 1% light, and <1% light depths were analyzed and show a possible depth segregation between filamentous and unicellular cyanobacterial phylotypes. Phylogenetic relationships between *nifH* sequences recovered as part of this study and those available in GenBank were also investigated (1, 27). Several of our Atlantic *nifH* sequences were identical to environmental *nifH* sequences, which until now had only been recovered from the Pacific Ocean. This indicates that some diazotrophic phylotypes, specifically unicellular group A, may be common between the Pacific and Atlantic Oceans.

* Corresponding author. Mailing address: IFM-GEOMAR, Leibniz-Institut fuer Meereswissenschaften, Duesternbrooker Weg 20, 24105 Kiel, Germany. Phone: 49 431 600 4212. Fax: 49 431 600 1515. E-mail: jlaroche@ifm-geomar.de.

† Present address: Institute of Botany, University of Basel, Hebelstrasse 1, 4056 Basel, Switzerland.

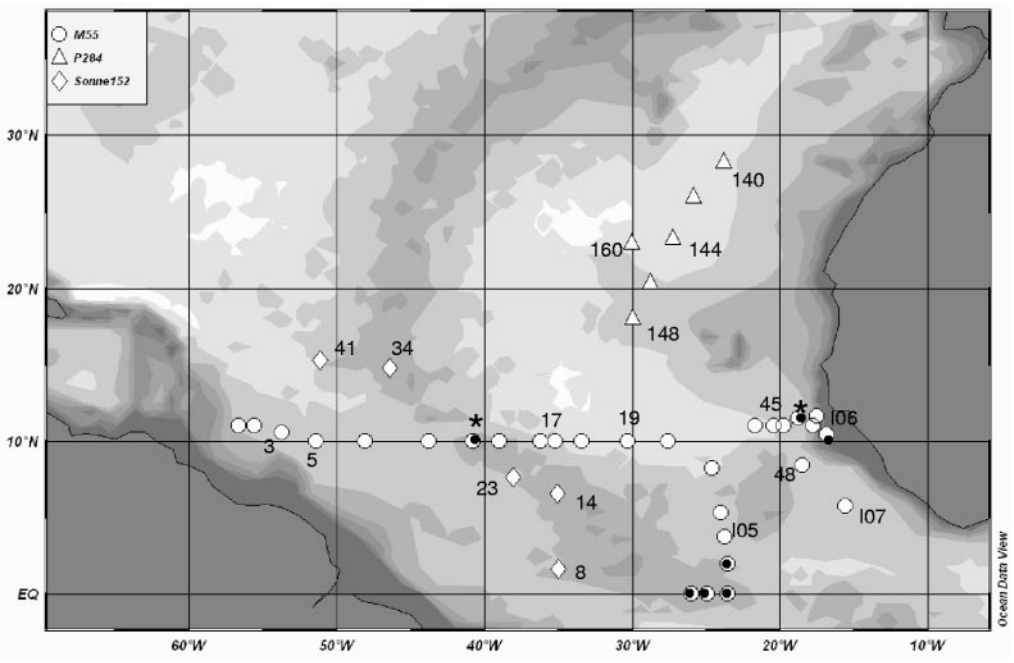

FIG. 1. Cruise tracks and stations analyzed. Stations which produced a negative *nifH* signal are indicated by a black circle within the station mark. Surface samples for stations marked with ∗ were unavailable for analysis and deepwater samples were negative. The numbered stations indicate stations from which the *nifH* amplicons were cloned and sequenced, and the numbers correspond to those listed in Table 2 and Fig. 2.

MATERIALS AND METHODS

Sample collection. Samples were collected during three cruises in the tropical and subtropical Atlantic Ocean (Fig. 1). Sonne 152 (1.7°N 35°W to 15.3°N 51.1°W) occurred during late fall 2000, where water was collected with an overboard pump from a depth of 8 m. Water from station 14 was taken from a depth of 100 m using a CTD rosette. Poseidon 284 (28.3°N 23.8°W south to 18°N 30°W north to 23°N 30°W) took place during spring 2002, and Meteor 55 (west-to-east transect along 10°N with south transect along 30°W, west along the equator, and a north transect around 23°W back to 10°N) during fall 2002. During both of these cruises, water samples were collected using a CTD rosette sampler. Three samples (I05, I06, and I07) from the Meteor 55 cruise were collected using an underway trace metal-clean diaphragm pump (1- to 3-m depth) and were used to characterize the initial diazotroph community for bioassay nutrient addition experiments (23). Water was pumped into trace metal-cleaned 60-liter carboys and siphoned into filtration bottles. All other Meteor 55 stations were sampled at three depths. A total of 28 samples from the surface (≤10 m), 26 samples from the 1% light zone, and 6 samples from depths below the 1% light level were analyzed. Samples from the Poseidon 284 cruise were collected at depths between 10 to 30 m. Seawater volumes ranging from 1.5 to 8 liters were vacuum filtered (20 to 30 kPa) through a 0.22-μm Durapore filter (Poseidon and Meteor) or through a 0.2-μm Isopore filter (Sonne 152). All filters were stored at −80°C in cryovials until nucleic acid extraction in the laboratory. Samples for nucleic acid extraction were not prescreened to remove net plankton to study the entire diazotrophic community. Samples for nutrient analysis were collected using the CTD rosette sampler and analyzed on board (14). Nutrient data were available for all three cruises; however, the data for the Sonne 152 cruise had very low resolution in the upper 500 m and could not be used for our study. Cruise track coordinates were graphed with Ocean Data View (29).

DNA amplification and sequence analysis. DNA was extracted using the QIAGEN DNeasy Plant mini kit. All extracted DNA samples were checked for integrity by agarose gel electrophoresis. In all cases, bands of large sizes were obtained, which indicated that the DNA was of high quality and not degraded. *nifH* sequences were amplified from environmental DNA (1 to 20 ng/μl) using Taq-Gold polymerase (Applied Biosystems); the primers and nested PCR method are described in reference 39, with the following modifications. The first round of PCR (10× buffer II, $MgCl_2$ [final concentration, 4 mM], 10 mM deoxynucleoside triphosphates, 80 pmol of each primer [nifH3 and nifH4]), consisted of 10 min at 95°C; 35 cycles, each consisting of 1 min at 95°C, 1 min at 45°C, and 1 min at 72°C; and finally 10 min at 72°C. The second round (10× buffer II, $MgCl_2$ [final concentration, 6 mM], 10 mM deoxynucleoside triphosphates, 80 pmol of each primer [nifH1 and nifH2]) used a similar thermocycler program but with an annealing temperature of 54°C and only 28 cycles. Amplicons of the predicted 359-bp size, as proven by gel electrophoresis, were cloned using the TOPO TA cloning kit (Invitrogen) according to the manufacturer's instructions. Randomly picked clones were sequenced in the reverse direction using the T7 primer. Sequences were placed in the correct reading frame and trimmed to an approximately 345-bp segment corresponding to bases 639 to 984 in *Azotobacter vinelandii* with BioEdit Sequence Alignment Editor (16). Alignments were performed with ClustalX, version 1.6 (34). Sequence names were indicated as follows: TA, tropical Atlantic; P, S, or M, first letter of the ship on which the sample was collected; sample number; and clone number.

A *nifH* sequence database for phylogenetic analysis was assembled by combining the recovered sequences with *nifH* sequences (11, 42) from GenBank. This included sequences that had the highest similarity to the recovered sequences, as determined through BLASTx and BLASTn searches, and sequences obtained from other environmental *nifH* studies. This database, used for all phylogenetic analyses, contained >300 sequences, trimmed to the same segment and length as our recovered sequences. Our sequences and those from the database were analyzed for frameshifts by translation into amino acid sequences in all six frames. Sequences containing frameshifts were excluded from the analysis. Groups of identical sequences were represented by only one sequence.

TABLE 1. Temperature and nutrient concentrations for the three North Atlantic cruises[a]

Cruise	Date (mo yr)	Temperature (°C)		NO_3 (μM)	
		Mean	SD	Mean	SD
Sonne 152	Oct. 2000	26.7	1.0	NA	NA
Poseidon 284	Apr. 2002	23.0*	1.3	0.01	0.01
Meteor 55-surface	Nov. 2002	28.5	0.6	0.09	0.18
Meteor 55-deep	Nov. 2002	19.9*	3.1	9.02	9.85

[a] All temperatures were significantly different from one another except for the two sample sets indicated by asterisks. NA, not available.

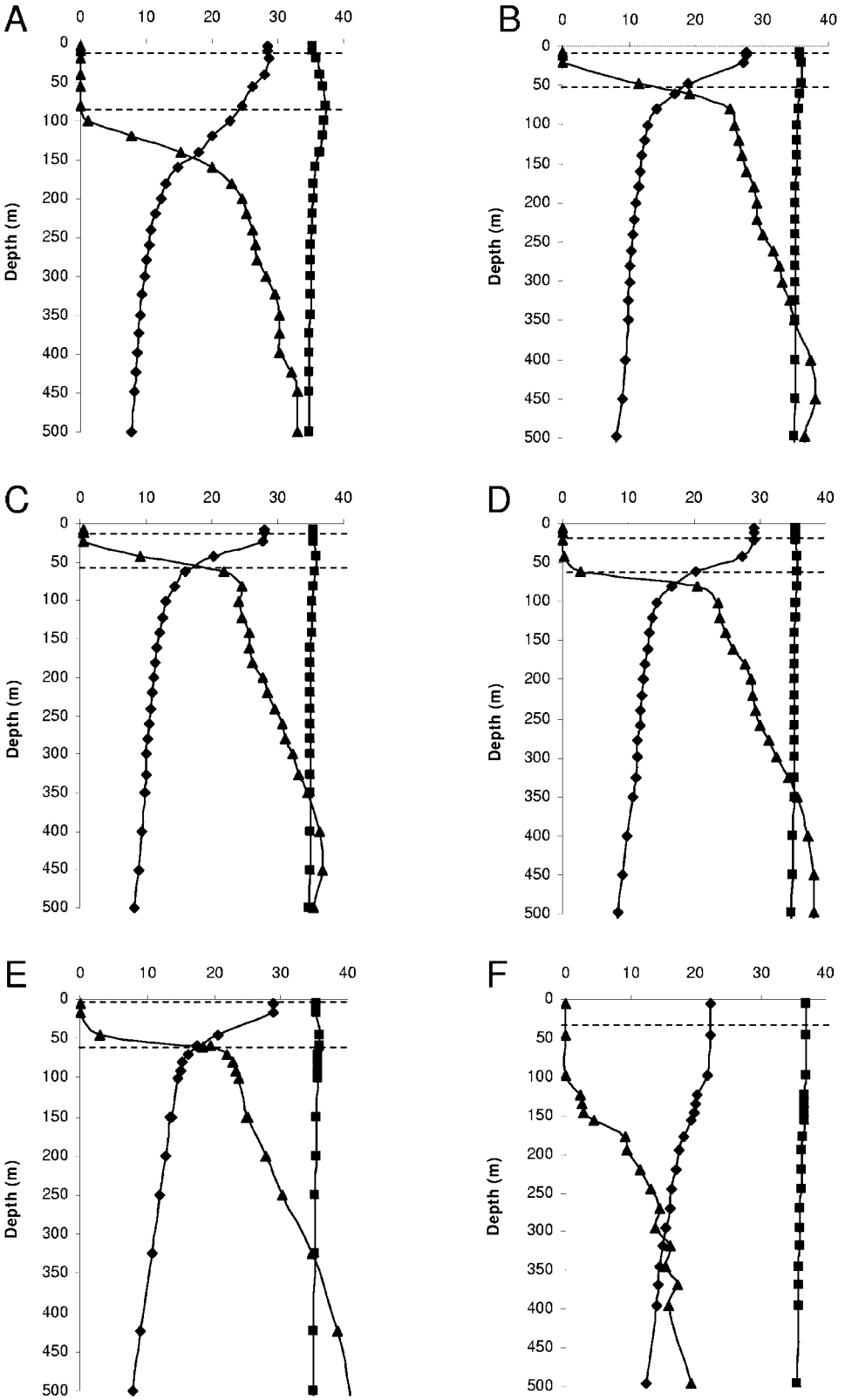

FIG. 2. Representative vertical profiles for temperature, salinity, and nitrate during the Meteor 55 and Poseidon cruises. All profiles show depth (in meters) on the *y* axis. The following variables are plotted on the same scale on the *x* axis as follows: ◆, temperature in degrees Celsius; ■, salinity in parts per thousand; and ▲, NO_3 in micromoles per liter. The dashed lines mark the depths from which samples were collected. Station numbers correspond to those given in Table 2 and Fig. 1: Meteor station 3, which is influenced by the Amazon Plume (A), Meteor station 17 (B), Meteor station 19 (C), Meteor station 45 (D), Meteor station 48 (E), and Poseidon station 144 (F) (representative of all Poseidon stations).

TABLE 2. Summary of station and cloning information[a]

Sta	Pos	Depth (m)	Sample no.	No. of clones	Cluster I									Cluster III
					Unicellular cyanobacterium			Filamentous cyanobacterium			γ-Proteobacterium			
					Cy	Cr	UA	Tt	Te	Ks	Kl	AO	PO	
8	1.7°N, 35.0°W	8	TAS8**	10									100	
14	6.6°N, 35.1°W	100	TAS14**	11	9.1			45.5						45.5
23	7.6°N, 38.0°W	8	TAS23**	24				66.7		33.3				
34	14.8°N, 46.4°W	8	TAS34**	14			100							
41	15.3°N, 51.1°W	8	TAS41**	9		44		33.3			11.1			11.1
140	28.3°N, 23.8°W	10	TAP140**	11			100							
144	23.13°N, 27.3°W	30	TAP144**	8			100							
148	18.0°N, 30.0°W	20	TAP148**	11			100							
160	23.0°N, 30.0°W	20	TAP160**	11			100							
3	10.6°N, 53.7°W	5	TAM0128	11				81.8	9.1	9.1				
3	10.6°N, 53.7°W	80	TAM0123**	15			100							
5	10.0°N, 51.4°W	4	TAM0228**	14				50		28.6		21.4		
17	10.0°N, 33.4°W	8	TAM0797**	11				36.4		63.6				
17	10.0°N, 33.4°W	47	TAM0794**	25				48	4		20	28		
19	10.0°N, 30.3°W	8	TAM0902**	19				68.4		31.8				
19	10.0°N, 30.3°W	62	TAM0898**	12	100									
I05	3.7°N, 23.7°W	<5	TAM105**	39		2.6		30.8		66.7				
I06	11°N, 17.8°W	<5	TAM106**	26			3.8	11.5	3.8	80.8				
45	11°N, 20.4°W	6	TAM2179**	13				84.6		15.4				
45	11°N, 20.4°W	61	TAM2175**	24			100							
I07	5.8°N, 15.6°W	<5	TAM107**	25				52		48				
48	8.4°N, 18.5°W	7	TAM2305**	8					100					
48	8.4°N, 18.5°W	62	TAM2294**	6							16.7	83.3		
Total no. of recovered sequences				354	13	5	95	108	11	87	6	15	111	6
Total no. of unique sequences				170	5	2	34	58	8	38	6	10	6	2

[a] The station numbers and positions correspond to those in Fig 1. Sequences are grouped by station (Sta) and cruise (TAS-Sonne, TAP-Poseidon, and TAM-Meteor). The sample collection depths in meters (Depth m) and station positions (Pos) are given. **, clone number. No. of clones, number of clones used for phylogenetic analyses from each station. The columns following correspond to the percentage of the recovered sequences with high similarity to cluster I *nifH Cyanothece* (Cy), *Crocosphaera/Synechocystis* (Cr), unicellular group A (UA), *T. thiebautii* (Tt), *T. erythraeum* (Te), *K. spiralis* (Ks), *Klebsiella pneumoniae* (Kl), an environmental clone from the Atlantic Ocean (AO), an environmental clone from the Pacific Ocean (PO), or cluster III *nifH*.

Phylogenetic analysis was performed using TREECON (36). Distances were estimated by the Kimura method ($P/Q = 2$ for nucleotide analyses), and the neighbor-joining method was utilized for inferring tree topologies. Both nucleotide and protein trees were constructed several times as in reference 43 with the *nifH* database, changing the outgroup organisms and bootstrap calculations. Sequences for a protochlorophyllide reductase enzyme from *Leptolyngbya boryana* (gi:441179), a nitrogenase subunit *NifH* ATPase from *Trichodesmium erythraeum* ISM101 (gi:23042334), and *Methanobrevibacter arboriphilicus* (gi:780707) were tried as outgroups for the protein tree without causing major changes to the clades. The *nifH* sequence from *Archea* member *Methanosarcina barkerii* (AB019139.1) was used as the outgroup as previously described (11).

Nucleotide sequence accession numbers. The environmental sequences recovered from this study have been placed in the GenBank database with accession numbers AY896295 through AY896469.

RESULTS

Diazotrophic distribution and environmental conditions. As indicated by near detection limit or undetectable surface water nutrient concentrations, all samples were collected in oligotrophic waters (38), with the exception of three samples from below the mixed layer, in which NO_3 concentrations were elevated, reaching values as high as 21.9 μM (Table 1). In contrast, water temperatures differed significantly during the three cruises. Warmest temperatures were observed in surface waters during the Meteor 55 west-east transect (Table 1). The coldest temperatures were recorded in surface waters during the Poseidon cruise at latitudes between 18 and 28°N, as well as in deepwater samples. Mixed layer depths during the Meteor 55 cruise ranged between 20 and 30 m for the east-west transect and around 50 m at the equator (Fig. 2A to E) (10). Deep mixed layer depths (50 to 70 m), in addition to poor thermal stratification, were characteristic throughout all Poseidon stations, which may explain the lower surface water temperature there (Fig. 2F).

The target *nifH* segment was recovered nearly everywhere throughout the area studied, except for along the equator and at a few stations near the African coast (Fig. 1). The distribution of phylotypes found at selected stations is presented in Table 2. In cloned samples, *nifH* sequences from *Trichodesmium* spp. were present throughout much of the Atlantic Ocean surface waters at latitudes ranging from 4 to 16°N, as previously reported for this area (15). However, a shift to *nifH* sequences clustering with unicellular cyanobacteria and γ-proteobacterial phylotypes was detected in water samples collected below a depth of 10 m (Table 2). Group A *nifH* sequences were the only types recovered during the Poseidon cruise (18 to 28°N). In addition, this phylotype was only recovered once from samples where *Trichodesmium* sequences were dominant. γ-Proteobacterial sequences were not as common as cyanobacterial *nifH* sequences and had a scattered distribution throughout the sample area. Cluster III *nifH* sequences were

uncommon in our sample set and found only twice in samples collected from the western and central tropical Atlantic Ocean.

***nifH* Diversity and phylogenetic analysis.** Overal, 354 *nifH* sequences were recovered from 19 stations and 23 depths during the three cruises. Of these recovered sequences, 170 were unique and fell into clusters I and III of the previously described *nifH* gene clusters (Fig. 3) (22, 42). Only 2% of the recovered *nifH* sequences grouped within cluster III; a group containing phototrophic, anaerobic bacteria, and sulfate reducers such as chlorobi, δ-proteobacteria, and spirochaetes. The two unique *nifH* nucleic acid sequences recovered in our study showed 99% similarity to another cluster III environmental *nifH* sequence (Fig. 4) previously isolated from the Hawaii ocean time series station in the Pacific Ocean (7). Sequences within this clade are all derived from uncultured marine bacteria that have approximately 83% similarity to the *nifH* sequence from *Chlorobium tepidum*, the closest identified bacterium.

The rest of the *nifH* sequences clustered either with the cyanobacterial (Fig. 5) or γ-proteobacterial (Fig. 6) clades of cluster I. Thirty-two percent of the recovered sequences had high similarities to unicellular cyanobacterial phylotypes and grouped with other environmental sequences to form three distinct clades (Fig. 5): the unicellular group A clade, consisting of uncultured environmental sequences distantly related to *Cyanothece*; the *Cyanothece*-like clade, with environmental sequences closely related to the genus *Cyanothece*; and the unicellular group B, represented by *Crocosphaera watsonii.* Almost all (84%) of our unicellular sequences clustered with group A phylotypes. The group A *nifH* sequence was originally characterized in samples collected at the HOT station. In our analysis, the group A cluster was interspersed with sequences from both the Pacific and Atlantic Oceans. Furthermore, nucleic acid sequences, which were recovered several times from seven of our Atlantic sites, were identical to the Pacific clones HT1150 (AF059627.1) and HT1205 (AF059642.1), suggesting that some unicellular cyanobacterial phylotypes may be cosmopolitan in tropical oceans. Similar results were obtained for the group B clade.

Filamentous cyanobacterial *nifH* phylotypes were abundant in our clone libraries and appeared to be less divergent than unicellular cyanobacterial sequences. The known species, *Trichodesmium thiebautii*, *T. erythraeum*, and *Katagnymene spiralis*, did not form three separate clades but clustered into two clades, with *T. erythraeum* forming a clade alone. Sequences from *K. spiralis* and *T. erythraeum* are identical at the amino acid level, but at the nucleotide level, *K. spiralis* and *T. thiebautii* appear to be more closely related.

The remaining cluster I sequences (9%) had the highest similarity to γ-proteobacteria (Fig. 6). These sequences separated into two distantly related clades, which were <80% homologous to each other. These clades were composed solely of environmental sequences from uncharacterized, uncultured organisms but were distantly related to *Vibrio diazotrophicus*. Sequences within the first clade were >97% similar to an environmentally recovered clone, AO1113 (AAC36068.1), originally described in the Atlantic Ocean but with representatives in the Pacific Ocean. The second clade was only distantly related (87 to 90% similarity) to the previously isolated Pacific Ocean clone PO3137 (AF059647.1).

Overall, 11 different *nifH* phylotypes were recovered from our study of the tropical Atlantic. Graphs of phylotype occurrence as a function of temperature and depth or nitrate concentration suggest that the pattern of species distribution may be highly influenced by temperature (Fig. 7). With one exception, filamentous cyanobacteria and *Crocosphaera* sequences were found at a temperature range of 27 to 30°C and in waters with undetectable nitrate concentrations. In contrast, group A and *Cyanothece*-like phylotypes were present over a wide temperature range, from 16 to 29°C. Similarly, most *nifH* phylotypes were detected in nitrate-depleted waters, but some group

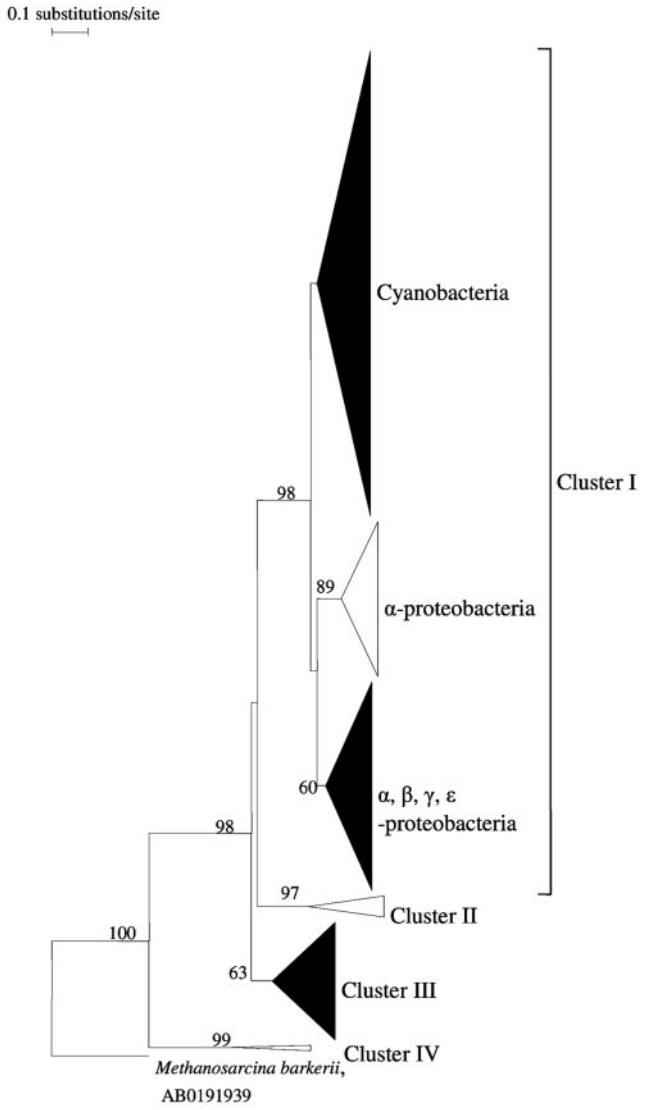

FIG. 3. Phylogenetic tree of global NifH protein sequences. To better visualize the relationship between the groups, only the major clusters and clades with significant bootstrap values (>60) were shown. Sizes of the triangles reflect the number of sequences in that clade. Clades that contained sequences from our study are shown in black. Cluster I includes cyanobacteria, α-proteobacteria, β-proteobacteria, γ-proteobacteria, and ε-proteobacteria. Cluster II consists of δ-proteobacteria, spirochaetes, and members of the *Archeaea*. Members of the *Firmicutes*, *Spirochaeta*, δ-proteobacteria, chlorobi, and *Archaea* comprise cluster III. Cluster IV is formed by archaeal sequences. The tree was bootstrapped 100 times with *Methanosarcina barkerii* AB0191939 as the outgroup.

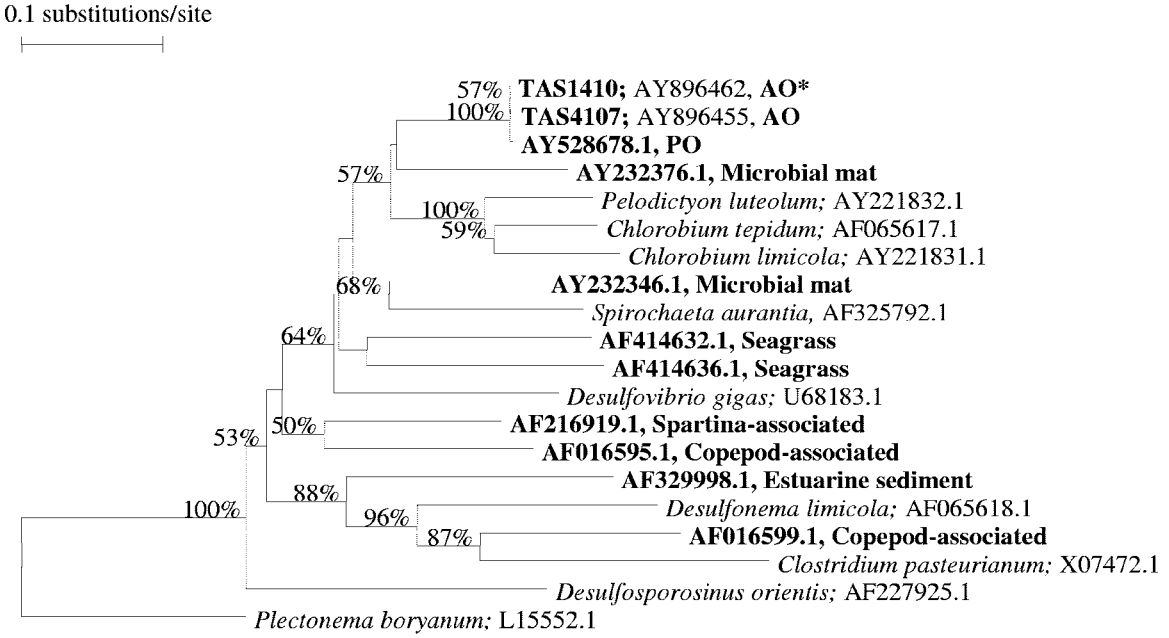

FIG. 4. Phylogenetic tree of cluster III *nifH*. Environmental sequences are shown in boldface type, followed by the environment from where they were collected. AO, Atlantic Ocean; PO, Pacific Ocean. AY896462, marked with an asterisk, represents five sequences of 100% similarity at the nucleotide level. Relationships were bootstrapped 1,000 times, and values above 50% are shown. This tree is based on Fig. 3b in reference 8.

A phylotypes were also observed where nitrate concentrations were high. The depth segregation of phylotypes is noticeable in the data shown in Table 2. In all four stations where surface and deep samples were analyzed, filamentous cyanobacterial *nifH* sequences were restricted to surface waters, and unicellular cyanobacterial or γ-proteobacterial sequences dominated deepwater clone libraries.

DISCUSSION

The results from our study document the presence and diversity of *nifH* phylotypes in the tropical and subtropical Atlantic. As expected, *nifH* sequences were found throughout the surface water samples of the tropical Atlantic, except for samples collected at the equator and at some upwelling stations near the African coast (6, 35). Parallel measurements of depth-integrated N_2 fixation rates during the Meteor 55 cruise varied from 3.7 to 255 μmol N m^{-2} day^{-1}, with the lowest rates at the equator (37). This supports the observed absence of *nifH* sequences in our nucleic acid samples from equatorial stations.

Filamentous cyanobacterial *nifH* phylotypes were recovered mainly from warm surface waters, and many features of the ecophysiology of *Trichodesmium* may explain this distribution pattern (for a review, see reference 19). The distribution of *Trichodesmium* is mostly limited to seawater temperatures of >20°C, but other factors correlated with high temperature, such as high levels of light and low levels of nutrients, may also be partly responsible for the observed temperature dependence (18). Laboratory experiments have corroborated that the optimal growth temperature range for pure cultures of *Trichodesmium* is between 25 and 30°C (3) and that high water temperatures may be required for effective nitrogenase activity in this nonheterocystous cyanobacteria (30). Input of iron through atmospheric dust deposition is another possible determinant of *Trichodesmium* distribution. The equatorial stations had low levels of dissolved iron (10) at the time of sampling; this may explain why filamentous diazotrophs, considered to have a high iron requirement (19), were not recovered in samples from this oligotrophic, upwelling region. Two complementary studies on Meteor 55 concluded that iron was an important factor affecting the activity of diazotrophs in the tropical Atlantic (23, 37). Voss et al. (37) found a significant correlation between depth-integrated total dissolved iron and depth-integrated N_2 fixation levels. Mills et al. (23) determined that even at the easternmost stations, addition of dissolved iron or of iron-rich Saharan dust stimulated N_2 fixation relative to control incubations.

The relative abundance of *nifH* phylotypes in our clone libraries suggests a segregation of filamentous sequences at the surface and unicellular cyanobacterial and heterotrophic bacterial sequences in deeper water. However, the abundance of specific phylotypes in a clone library is semiquantitative at best and must be interpreted with caution. The results we obtained from the clone libraries will need to be confirmed by more quantitative methods that account for possible PCR and cloning biases. Nevertheless, the predominance of *Trichodesmium* phylotypes in surface waters and lack thereof in deeper waters fit well with the autecology of *Trichodesmium.* Deepwater samples were collected at temperatures below the optimal growth range (25 to 30°C) of filamentous cyanobacteria, which may be one explanation for this observation. In addition, the presence of intracellular gas vacuoles, which give buoyancy to *Trichodesmium* (18), could also contribute to the apparent dominance of the filamentous phylotypes in surface waters. The dominance of *Trichodesmium* in surface waters of the tropical North Atlantic (35) and the observed dominance of unicellular cya-

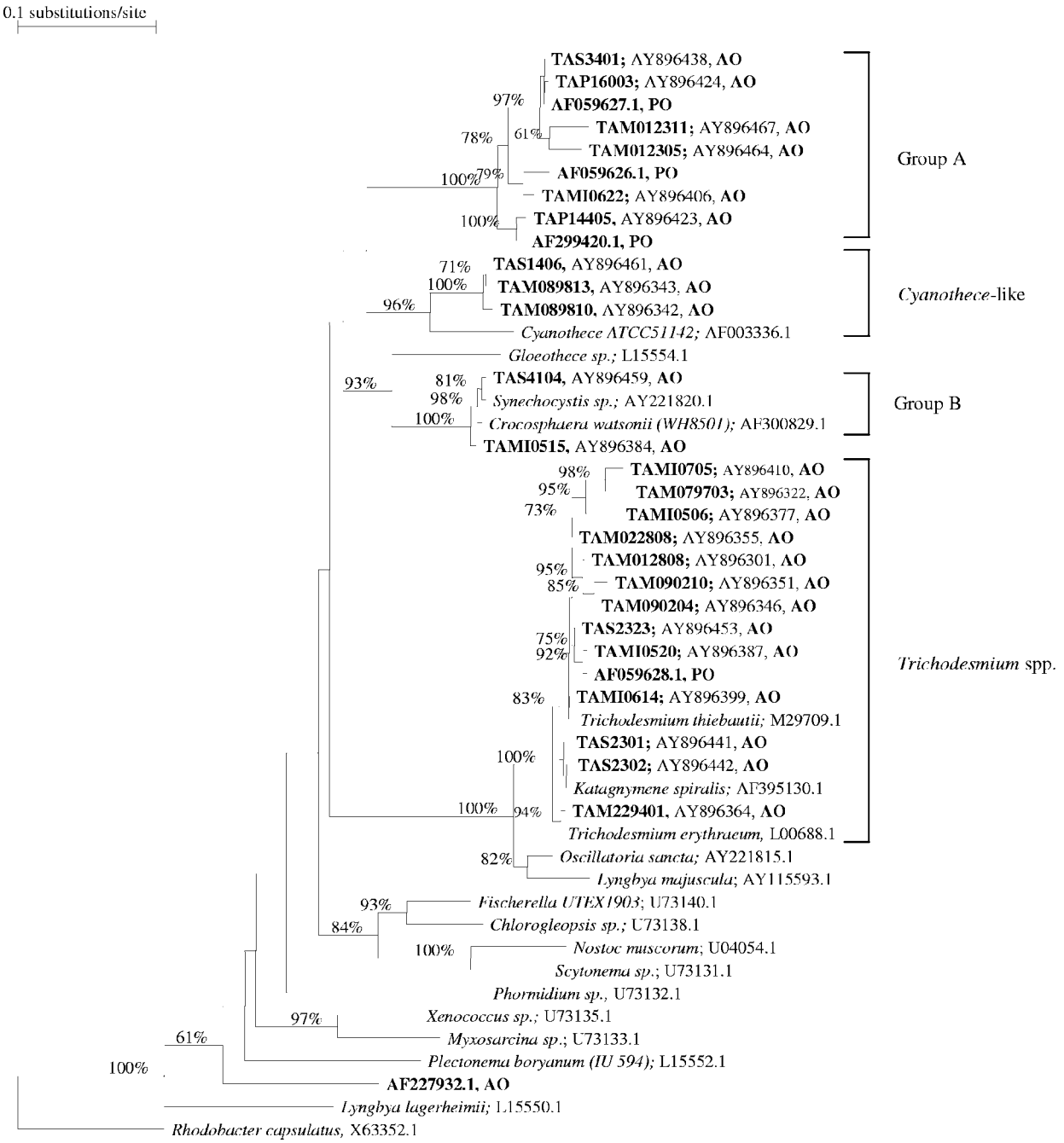

FIG. 5. Phylogenetic relationships of *nifH* cyanobacterial sequences. Environmental sequences are shown in boldface type, followed by the environment from where they were collected. AO, Atlantic Ocean; PO, Pacific Ocean. Relationships were bootstrapped 1,000 times, and values over 50% were shown, except for those in the *Trichodesmium* spp. group where values above 70% are shown. For visual purposes, only environmental sequences which had bootstrap values above 70% are shown.

nobacterial *nifH* phylotypes throughout the mixed layer in the Pacific Ocean (24) also support our observations.

Although the occurrence of *Crocosphaera nifH* phylotypes was restricted to a temperature range comparable to that of *Trichodesmium*, two other unicellular cyanobacterial phylotypes were found at temperatures as low as 15°C. Group A sequences were the only phylotypes recovered from several stations located between 18 and 28°N, where the mean surface water temperature was 23°C. In contrast, Mazard et al. (21) found that unicellular cyanobacterial diazotrophs were restricted to temperatures above 25°C, similar to filamentous cyanobacteria distributions. This discrepancy may be due to the fact that their study did not include the uncultured group A phylotype, which is uncharacterized by a 16S rRNA sequence. Whether or not the organisms present at these low temperatures and depths actively fix nitrogen can only be resolved with further studies by methods, such as reverse

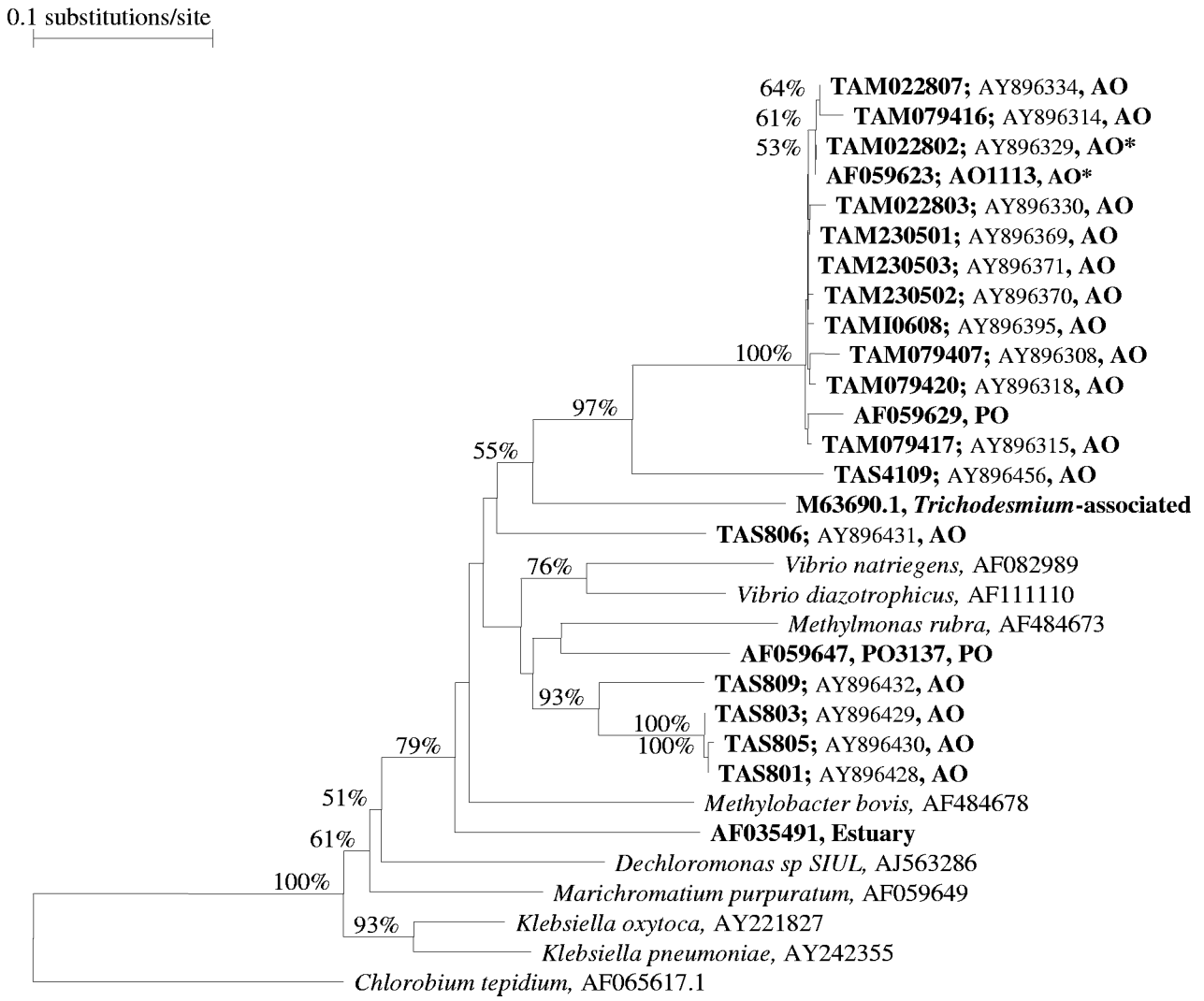

FIG. 6. Phylogenetic relationships between γ-proteobacteria *nifH* nucleotide sequences. Sequence names in boldface type indicate environmental sequences and are marked according to recovery from the Pacific Ocean (PO) or the Atlantic Ocean (AO). Sequence names beginning with "TA" were obtained in this study. AY896329 and AF059623, indicated by asterisks, represent several sequences which were identical. The tree was bootstrapped 1,000 times, and values over 50% are shown.

transcription-PCR, that allow the monitoring of RNA expression. However, Voss et al. (37) observed a trend of high N_2 fixation at the surface, which rapidly decreased with depth. One exception was at eastern stations, where rates of 3.1 nmol N liter^{-1} h^{-1} at the surface were comparable to rates of 2.2 nmol N liter^{-1} h^{-1} from below the mixed layer and where high nitrate concentrations prevailed. Since both the group A and the γ-proteobacteria phylotypes were recovered in this area, they are potential candidates for diazotrophic activity in the deeper waters.

It has been suggested that unicellular cyanobacteria populations from the Atlantic and Pacific Oceans are divergent (11). In contrast, this study found several phylotypes, especially group A, which had 100% homology at the nucleic acid level with sequences found in the Pacific, indicating that some diazotroph phylotypes are common to both oceans. A total of 66 sequences were found to be identical at the nucleotide level with sequences isolated from the Pacific Ocean, and many others with 99% similarity formed clades with Pacific Ocean sequences. Furthermore, our results also demonstrated a very high degree of similarity (99%) between two cluster III *nifH* sequences from the Pacific Ocean and ours from the Atlantic. This is the first time that this cluster III sequence has been reported for Atlantic samples. As we have not collected samples in the Pacific Ocean, potential DNA contamination of the samples can be ruled out. The high conservation between Pacific and Atlantic phylotypes will be useful when designing nucleic acid primers and probes for the enumeration of *nifH* phylotypes. N_2 fixation in the Atlantic Ocean appears to be potentially performed by a few species that have widespread distribution, based on *nifH* gene DNA analyses.

This study has presented data on the potential for N_2 fixation through the analysis of *nifH* gene diversity across the Atlantic Ocean. Our data suggest a potential community shift from filamentous cyanobacterial phylotypes to unicellular cyanobacterial or heterotrophic bacterial phylotypes with depth, and we hypothesize that growth temperature preferences of

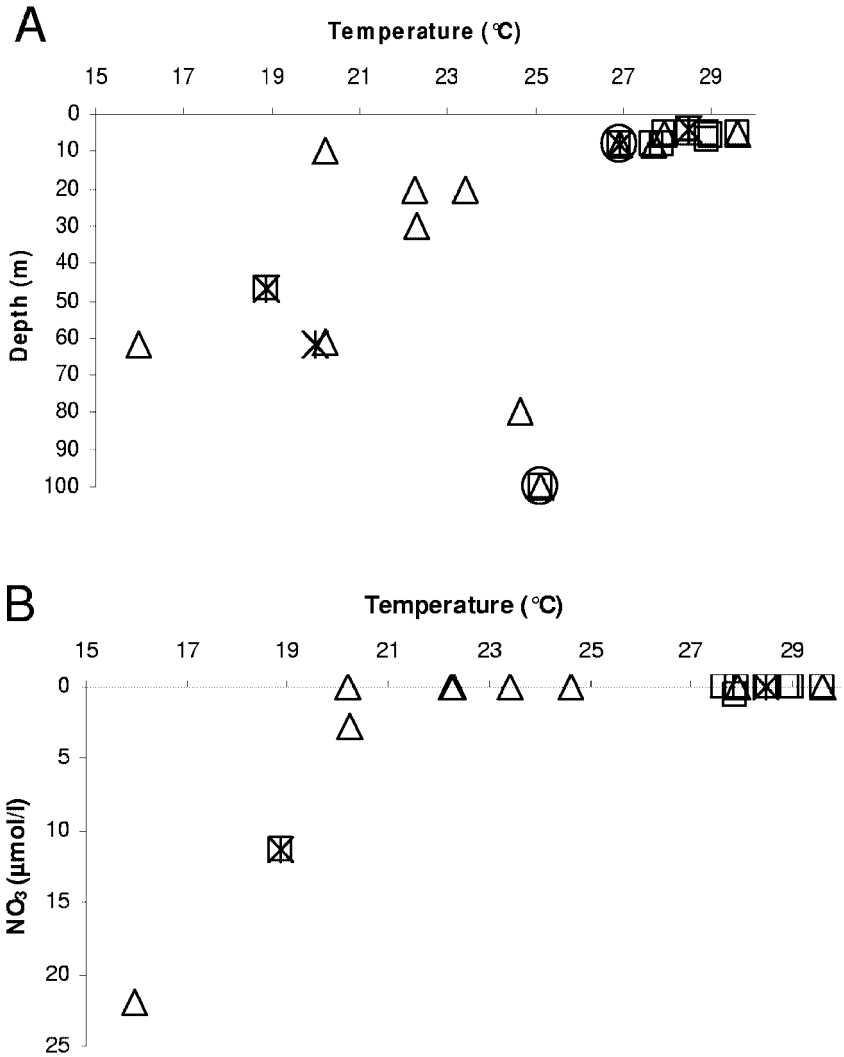

FIG. 7. Phylotype occurrence. □, filamentous cyanobacteria; Δ, unicellular cyanobacteria; ∗, γ-proteobacteria; ○, cluster III bacteria graphed as a function of sample temperature versus sample depth (in meters) (A) or nitrate concentration (in micromoles per liter) (B). There are fewer points in panel B because nutrient data were not available from the Sonne cruise (see Materials and Methods).

the various diazotrophs may explain the observed differences. While group A diazotrophs have already been shown to be important and widespread in the Pacific Ocean, this study revealed that they are also widely distributed throughout the Atlantic Ocean.

ACKNOWLEDGMENTS

We thank the captains and crews of the FS Meteor, FS Poseidon, and FS Sonne and head scientists D. Wallace, H. Bange, A. Oschlies, P. Kähler, and M. Rhein. We also thank T. Kluever, S. Nissen, and N. Winter for technical assistance. We thank three anonymous reviewers for helpful suggestions.

This work was supported by a Fulbright Scholarship to R.J.L., a DFG grant to J.L.R. (RO2138/4-1), and a grant to D. Wallace for the Meteor 55 ship time.

REFERENCES

1. **Allen, A. E., M. G. Booth, M. E. Frischer, P. G. Verity, J. P. Zehr, and S. Zani.** 2001. Diversity and detection of nitrate assimilation genes in marine bacteria. Appl. Environ. Microbiol. **67:**5343–5348.
2. **Berman-Frank, I., P. Lundgren, and P. Falkowski.** 2003. Nitrogen fixation and photosynthetic oxygen evolution in cyanobacteria. Res. Microbiol. **154:** 157–164.
3. **Breitbarth, E.** 2005. Ecophysiology of the cyanobacterium *Trichodesmium*. Ph.D. thesis. Christian Albrechts University of Kiel, Kiel, Germany.
4. **Brown, M. M., M. J. Friez, and C. R. Lovell.** 2003. Expression of nifH genes by diazotrophic bacteria in the rhizosphere of short form Spartina alterniflora. FEMS Microbiol. Ecol. **43:**411–417.
5. **Capone, D. G., J. P. Zehr, H. W. Paerl, B. Bergman, and E. J. Carpenter.** 1997. *Trichodesmium*, a globally significant marine cyanobacterium. Science **276:**1221–1229.
6. **Carpenter, E. J., A. Subramaniam, and D. G. Capone.** 2004. Biomass and primary productivity of the cyanobacterium *Trichodesmium* spp. in the tropical N Atlantic ocean. Deep Sea Res. I Oceanogr. Res. Pap. **51:**173–203.
7. **Church, M. J., B. D. Jenkins, D. M. Karl, and J. P. Zehr.** 2005. Vertical distributions of nitrogen-fixing phylotypes at Stn ALOHA in the oligotrophic North Pacific Ocean. Aquat. Microb. Ecol. **38:**3–14.
8. **Church, M. J., C. M. Short, B. D. Jenkins, D. M. Karl, and J. P. Zehr.** 2005. Temporal patterns of nitrogenase (*nifH*) gene expression in the oligotrophic North Pacific Ocean. Appl. Environ. Microbiol. **71:**5362–5370.
9. **Codispoti, L. A.** 1997. The limits to growth. Nature **387:**237–238.
10. **Croot, P. L., P. Streu, and A. R. Baker.** 2004. Short residence time for iron in surface seawater impacted by atmospheric dry deposition from Saharan dust events. Geophys. Res. Lett. **31**. [Online.] doi:10.1029/2004GL020153.
11. **Falcon, L. I., E. J. Carpenter, F. Cipriano, B. Bergman, and D. Capone.** 2004.

N2 fixation by unicellular bacterioplankton from the Atlantic and Pacific Oceans: phylogeny and in situ rates. Appl. Environ. Microbiol. **70:**765–770.

12. **Falcon, L. I., F. Cipriano, A. Y. Chistoserdov, and E. J. Carpenter.** 2002. Diversity of diazotrophic unicellular cyanobacteria in the tropical North Atlantic Ocean. Appl. Environ. Microbiol. **68:**5760–5764.
13. **Falkowski, P. G.** 1997. Evolution of the nitrogen cycle and its influence on the biological sequestration of CO_2 in the ocean. Nature **387:**272–275.
14. **Grasshoff, K., M. Ehrhardt, and K. Kremling.** 1983. Methods of seawater analysis. Springer-Verlag, New York, N.Y.
15. **Gruber, N., and J. L. Sarmiento.** 1997. Global patterns of marine nitrogen fixation and denitrification. Global Biogeochem. Cycles **11:**235–266.
16. **Hall, T.** 2004. BioEdit, version 6.0.7. Ibis Therapeutics, Carlsbad, Calif.
17. **Jenkins, B. D., G. F. Steward, S. M. Short, B. B. Ward, and J. P. Zehr.** 2004. Fingerprinting diazotroph communities in the Chesapeake Bay by using a DNA macroarray. Appl. Environ. Microbiol. **70:**1767–1776.
18. **Karl, D., A. Michaels, B. Bergman, D. Capone, E. Carpenter, R. Letelier, F. Lipschultz, H. Paerl, D. Sigman, and L. Stal.** 2002. Dinitrogen fixation in the world's oceans. Biogeochemistry **57:**47–98.
19. **La Roche, J., and E. Breitbarth.** 2005. Importance of the diazotrophs as a source of new nitrogen in the ocean. J. Sea Res. **53:**67–91.
20. **Lovell, C. R., M. J. Friez, J. W. Longshore, and C. E. Bagwell.** 2001. Recovery and phylogenetic analysis of *nifH* sequences from diazotrophic bacteria associated with dead aboveground biomass of *Spartina alterniflora*. Appl. Environ. Microbiol. **67:**5308–5314.
21. **Mazard, S. L., N. J. Fuller, K. M. Orcutt, O. Bridle, and D. J. Scanlan.** 2004. PCR analysis of the distribution of unicellular cyanobacterial diazotrophs in the Arabian Sea. Appl. Environ. Microbiol. **70:**7355–7364.
22. **Mehta, M. P., D. A. Butterfield, and J. A. Baross.** 2003. Phylogenetic diversity of nitrogenase (*nifH*) genes in deep-sea and hydrothermal vent environments of the Juan de Fuca Ridge. Appl. Environ. Microbiol. **69:**960–970.
23. **Mills, M. M., C. Ridame, M. Davey, J. La Roche, and R. J. Geider.** 2004. Iron and phosphorus co-limit nitrogen fixation in the eastern tropical North Atlantic. Nature **429:**292–294.
24. **Montoya, J. P., C. M. Holl, J. P. Zehr, A. Hansen, T. A. Villareal, and D. Capone.** 2004. High rates of N_2 fixation by unicellular diazotrohps in the oligotrophic Pacific Ocean. Nature **430:**1027–1032.
25. **Nuebel, U., F. Garcia-Pichel, M. Kuehl, and G. Muyzer.** 1999. Quantifying microbial diversity; morphotypes, 16S rRNA genes, and carotenoids of oxygenic phototrophs in microbial mats. Appl. Environ. Microbiol. **65:**422–430.
26. **Omoregie, E. O., L. L. Crumbliss, B. M. Bebout, and J. P. Zehr.** 2004. Determination of nitrogen-fixing phylotypes in *Lyngbya* sp. and *Microcoleus chthonoplastes* cyanobacterial mats from Guerrero Negro, Baja California, Mexico. Appl. Environ. Microbiol. **70:**2119–2128.
27. **Prieme, A., G. Braker, and J. M. Tiedje.** 2002. Diversity of nitrite reductase (*nirK* and *nirS*) gene fragments in forested upland and wetland soils. Appl. Environ. Microbiol. **68:**1893–1900.
28. **Rosado, A. S., G. F. Duarte, L. Seldin, and J. D. Van Elsas.** 1998. Genetic diversity of *nifH* gene sequences in *Paenibacillus azotofixans* strains and soil samples analyzed by denaturing gradient gel electrophoresis of PCR-amplified gene fragments. Appl. Environ. Microbiol. **64:**2770–2779.
29. **Schlitzer, R.** 2004. Ocean Data View, 2.0 ed. Alfred Wegener Institute, Bremerhaven, Germany.
30. **Staal, M., F. J. R. Meysman, and L. J. Stal.** 2003. Temperature excludes N2-fixing heterocystous cyanobacteria in the tropical oceans. Nature **425:**504–507.
31. **Steppe, T. F., J. L. Pinckney, J. Dyble, and H. W. Paerl.** 2001. Diazotrophy in modern marine Bahamian stromatolites. Microb. Ecol. **41:**36–44.
32. **Steward, G. F., B. D. Jenkins, B. B. Ward, and J. P. Zehr.** 2004. Development and testing of a DNA macroarray to assess nitrogenase (*nifH*) gene diversity. Appl. Environ. Microbiol. **70:**1455–1465.
33. **Steward, G. F., J. P. Zehr, R. Jellison, J. P. Montoya, and J. T. Hollibaugh.** 2004. Vertical distribution of nitrogen-fixing phylotypes in a meromictic, hypersaline lake. Microb. Ecol. **47:**30–40.
34. **Thompson, J. D., T. J. Gibson, F. Plewniak, F. Jeanmougin, and D. G. Higgins.** 1997. The ClustalX windows interface: flexible strategies for multiple sequence alignment aided by quality analysis tools. Nucleic Acids Res. **24:**4876–4882.
35. **Tyrrell, T., E. Maranon, A. J. Poulton, A. R. Bowie, D. S. Harbour, and E. M. S. Woodward.** 2003. Large-scale latitudinal distribution of Trichodesmium spp. in the Atlantic Ocean. J. Plankton Res. **25:**405–416.
36. **Van de Peer, Y.** 2001. TREECON for Windows, version 1.3b. Department of Biology, University of Konstanz, Konstanz, Germany.
37. **Voss, M., P. Croot, K. Lochte, M. Mills, and I. Peeken.** 2004. Patterns of nitrogen fixation along 10°N in the tropical Atlantic. Geophys. Res. Lett. **31**. [Online.] doi:10.1029/2004GL020127.
38. **Wallace, D. W. R., and H. W. Bange.** 2004. Introduction. Results of the Meteor 55: tropical SOLAS expedition. Geophys. Res. Lett. **31.** doi:1029/2004GL021014.
39. **Zani, S., M. T. Mellon, J. L. Collier, and J. P. Zehr.** 2000. Expression of *nifH* genes in natural microbial assemblages in Lake George, New York, detected by reverse transcriptase PCR. Appl. Environ. Microbiol. **66:**3119–3124.
40. **Zehr, J. P.** 1991. Molecular biology of nitrogen fixation in natural populations of marine cyanobacteria, p. 249–264. *In* E. J. Carpenter, D. G. Capone, and J. G. Rueter (ed.), Marine pelagic cyanobacteria: *Trichodesmium* and other diazotrophs, vol. 362. Kluwer Academic Publishers, Dordrecht, The Netherlands.
41. **Zehr, J. P., E. J. Carpenter, and T. Villareal.** 2000. New perspectives on nitrogen-fixing microorganisms in tropical and subtropical oceans. Trends Microbiol. **8:**68–73.
42. **Zehr, J. P., B. D. Jenkins, S. M. Short, and G. F. Steward.** 2003. Nitrogenase gene diversity and microbial community structure: a cross-system comparison. Environ. Microbiol. **5:**539–554.
43. **Zehr, J. P., M. T. Mellon, and W. D. Hiorns.** 1997. Phylogeny of cyanobacterial *nifH* genes: evolutionary implications and potential applications to natural assemblages. Microbiology **143:**1443–1450.
44. **Zehr, J. P., M. T. Mellon, and S. Zani.** 1998. New nitrogen-fixing microorganisms detected in oligotrophic oceans by amplification of nitrogenase (*nifH*) genes. Appl. Environ. Microbiol. **64:**3444–3450.
45. **Zehr, J. P., J. Waterbury, P. J. Turner, J. P. Montoya, E. Omoregie, G. Steward, A. Hansen, and D. M. Karl.** 2001. Unicellular cyanobacteria fix N2 in the subtropical North Pacific Ocean. Nature **412:**635–638.

Paper B: *Abundances and Distributions of the Dominant* nifH *Phylotypes in the Northern Atlantic Ocean*

Synopsis

An in-depth look at the distribution of diazotrophs across the northern Atlantic Ocean was made for this manuscript. In addition to information on the abundances of different phylotypes, factors that could potentially influence the distribution of diazotrophs were identified. A qPCR method was developed and used to estimate abundances of seven *nifH* phylotypes in 141 samples collected during four cruises. The seven phylotypes, filamentous, Groups A, B and C unicellular, Gammas A and P and Cluster III, were selected based on re-analysis of the clone libraries from Paper A. This study showed that cyanobacterial *nifH* phylotypes were by far the most dominant diazotrophic phylotypes, especially filamentous and Group A. The filamentous phylotype alone accounted for 51% of total *nifH* copies detected. The gamma A phylotype was detected in nearly all samples, but only at low concentrations. This indicates that the often overlooked Gamma A may be an important contributor to marine nitrogen fixation given the wide distribution of this phylotype. The Cluster III phylotype may also be important in some areas. This phylotype was more commonly detected at low light levels and concentrations of nitrate greater than 0.5 μM. Phylotype abundances correlated well with water temperature and showed a relationship with estimated annual atmospheric dust deposition. Dust deposition may determine the phylotype abundances while water temperature may determine phylotype niches. This study investigated the abundances and distributions of diazotrophs in the Atlantic Ocean on a scale that had not been previously undertaken. This paper has been cited by the Faculty 1000.

Contribution

Samples from the Meteor 55 and Meteor 60 cruise were collected by me. Poseidon 284 and Sonne 154 samples were collected before my arrival. DNA extractions, with the exception of five Sonne 152 samples, were done by me. I planned the experimental work and the development of the qPCR method. D. Huemmer assisted with plasmid preparations for the qPCR standards for a semester project. She also helped with testing the specificity of the qPCR primers and probes and in preparation of the qPCR plates. All data analysis, figure and manuscript preparation was done by me.

APPLIED AND ENVIRONMENTAL MICROBIOLOGY, Mar. 2008, p. 1922–1931 Vol. 74, No. 6
0099-2240/08/$08.00+0 doi:10.1128/AEM.01720-07

Abundances and Distributions of the Dominant *nifH* Phylotypes in the Northern Atlantic Ocean▽†

Rebecca J. Langlois, Diana Hümmer, and Julie LaRoche*

Leibniz Institute for Marine Sciences, Duesternbrooker Weg 20, 24105 Kiel, Germany

Received 26 July 2007/Accepted 22 January 2008

Understanding the factors that influence the distribution and abundance of marine diazotrophs is important in order to assess their role in the oceanic nitrogen cycle. Environmental DNA samples from four cruises to the North Atlantic Ocean, covering a sampling area of 0°N to 42°N and 67°W to 13°W, were analyzed for the presence and amount of seven *nifH* phylotypes using real-time quantitative PCR and TaqMan probes. The cyanobacterial phylotypes dominated in abundance (94% of all *nifH* copies detected) and were the most widely distributed. The filamentous cyanobacterial type, which included both *Trichodesmium* and *Katagnymene*, was the most abundant (51%), followed by group A, an uncultured unicellular cyanobacterium (33%), and gamma A, an uncultured gammaproteobacterium (6%). Group B, unicellular cyanobacterium *Crocosphaera*, and group C *Cyanothece*-like phylotypes were not often detected (6.9% and 2.3%, respectively), but where present, could reach high concentrations. Gamma P, another uncultured gammaproteobacterium, was seldom detected (0.5%). Water temperature appeared to influence the distribution of many *nifH* phylotypes. Very high (up to 1×10^6 copies liter^{-1}) *nifH* concentrations of group A were detected in the eastern basin (25 to 17°N, 27 to 30°W), where the temperature ranged from 20 to 23°C. The highest concentrations of filamentous phylotypes were measured between 25 and 30°C. The uncultured cluster III phylotype was uncommon (0.4%) and was associated with mean water temperatures of 18°C. Diazotroph abundance was highest in regions where modeled average dust deposition was between 1 and 2 g/m^2/year.

Input and removal of fixed nitrogen in the ocean are largely controlled by the microbial processes of dinitrogen fixation and anaerobic ammonia oxidation and denitrification, respectively (23). Global rate estimates of both input and removal processes do not balance and suggest a net loss of fixed nitrogen from oceanic systems (11, 16). One reason for the imbalance of the marine nitrogen budget may be due to the paucity of data for marine diazotrophs. Until recently, the filamentous, nonheterocystous cyanobacterium *Trichodesmium* and the diatom endosymbiont *Richelia* were considered the major diazotrophs in the world's oceans (28, 49). However, field measurements and geochemical estimates indicate that these two species together do not fix enough nitrogen to balance the global marine nitrogen budget (3, 20). Methodological advances have led to the discovery of many new marine diazotrophs, and it is now possible to detect diverse diazotrophs by PCR analysis of the *nifH* gene, which encodes the highly conserved iron-protein subunit of the nitrogenase enzyme (22, 25, 26, 45, 47).

Although our knowledge of *nifH* sequence diversity from the marine environment has been rapidly expanding (46, 48), the temporal and spatial distributions of the various *nifH* phylotypes remain poorly characterized (22) and estimates of *nifH* abundances are rare. Real-time quantitative PCR (qPCR) was successfully used to determine the abundances of two *nifH* sequences at three stations in the Chesapeake Bay (39) and five *nifH* phylotypes at Station ALOHA in the Pacific Ocean (9, 10, 38). Diazotrophs in the Sargasso Sea and Amazon River plume have also been investigated using the qPCR technique (13, 17). Although the geographical coverage was limited in each of these studies, patterns in the vertical, temporal, and seasonal distributions of *nifH* phylotypes could be identified.

The goal of this study was to determine the abundances and distributions of seven different *nifH* phylotypes over a wide geographical area of the North Atlantic ranging from the equator to 42°N. Gene copy numbers of four cyanobacterial (one filamentous and three unicellular) and two gammaproteobacterial phylotypes and one cluster III *nifH* phylotype were quantified using qPCR and TaqMan MGB probes, providing estimates of the relative distributions and abundances of these unique diazotroph groups. Our results and those of others (14, 17, 24) suggest that diazotrophy may not be as tightly constrained by geographic location as previously thought.

MATERIALS AND METHODS

Sample collection, nucleic acid extraction, and *nifH* amplification. Samples for this study were collected and analyzed from four cruises in the northern Atlantic Ocean. Samples were collected in the spring during the F/S *Meteor* 60/5 Transient Tracers Revisited cruise (March and April 2004) to the North Atlantic Ocean and the F/S *Poseidon* 284 cruise (March 2002) to the eastern subtropical Atlantic Ocean. Samples along a transect at 10°N with a second transect to the equator and back were collected during the F/S *Meteor* 55 cruise (October to November 2002). Samples were collected from the F/S *Sonne* 152 cruise (November to December 2000) in the western tropical Atlantic basin. All samples were collected using a CTD rosette except for samples from the *Sonne* 152 cruise and three samples from *Meteor* 55, which were collected using an overboard pump from a depth of 8 m and a trace-metal clean diaphragm pump, respectively. *Poseidon* 284 samples were collected from depths ranging from 10 to 30 m. Samples from both *Meteor* cruises were collected at the surface (5 m) and from one to two depths ranging from 20 to 120 m. After collection, water was filtered onto 0.22-μm Durapore (Millipore) filters under low (2 mbar) vacuum pressure

* Corresponding author. Mailing address: Leibniz Institute for Marine Sciences, Duesternbrooker Weg 20, 24105 Kiel, Germany. Phone: 49-431-600 4212. Fax: 11-49-431 600 4202. E-mail: jlaroche@ifm-geomar.de.

† Supplemental material for this article may be found at http://aem.asm.org/.

▽ Published ahead of print on 1 February 2008.

TABLE 1. qPCR primers and TaqMan probes designed for this study

Type	Sequence (position) of[a]:			Reference sequence
	Primer		Probe	
	Reverse	Forward		
Group A	TCAGGACCACCGGACTCAAC (146–127)	TAGCTGCAGAAAGAGGAACT GTAGAAG (50–76)	TAATTCCTGGCTATAA CAAC (98–117)	AF059627.1
Filamentous	GCAAATCCACCGCAAACAAC (275–256)	TGGCCGTGGTATTATTACTG CTATC (165–189)	AAGGAGCTTATACAGA TCTA (206–225)	AY896367.1
Group B	TCAGGACCACCAGATTCTAC ACACT (146–122)	TGCTGAAATGGGTTCTGT TGAA (54–75)	CGAAGACGTAATGCTC (87–102)	AY896454.1
Group C	GGTATCCTTCAAGTAGTACTT CGTCTAGCT (112–83)	TCTACCCGTTTGATGCTACAC ACTAA (1–26)	AAACTACCATTCTTCACT TAGCAG (32–55)	AY896461.1
Gamma A	AACAATGTAGATTTCCTGAG CCTTATTC 321–294	TTATGATGTTCTAGGTGA TGTG (240–266)	TTGCAATGCCTATTCG (275–290)	AY896371.1
Gamma P	CATCGCGAAACCACCAC ATAC (282–262)	TTGTGCAGGTCGTGGTGT AATC (159–180)	CCTATGACGAAGACCT AGAC (212–231)	AY896428.1
Cluster III	GCAGACCACGTCACCCA GTAC (267–247)	ACCTCGATCAACATGCT CGAA (175–195)	CCTGGACTACGCGTTC (225–240)	AY896461.1

[a] All positions and sequences relate to the 324-base *nifH* segment length (5′→3′).

without prescreening to remove large particles. One to two liters of seawater was filtered per sample during the two *Meteor* and *Poseidon* cruises. Two to seven liters of seawater was filtered during the *Sonne* cruise. After filtration, filters were frozen at −80°C until extraction in the lab. Detailed information on some of the *Sonne* 152, *Poseidon* 284, and *Meteor* 55 stations can be found in reference 22. Nutrient samples from the *Meteor* 55 and 60 and the *Poseidon* 284 cruises were measured onboard using the methods described in reference 15.

All samples were extracted using the Qiagen DNeasy mini plant kit according to the manufacturer's protocol, except that the DNA was eluted two times with 50 μl of prewarmed PCR-grade water. DNA concentrations were measured using the PicoGreen double-stranded DNA quantitation reagent (Molecular Probes) and a Fluoroscan Ascent microplate reader (Laborsystems) following the manufacturer's protocol. Amplicons of the *nifH* gene were produced using the previously described primers (45), amplified, and cloned (22).

Primer selection. Based on *nifH* sequence information from a subset of the samples (22), primers and TaqMan MGB probes (6-carboxyfluorescein reporter) were selected to target seven diazotroph phylotypes using Primer Express (version 2.0; Applied Biosystems) (Table 1). All primers and probes were checked against the NCBI database with a BLAST search to ensure that they did not contain any near perfect sequence matches, other than the selected phylotypes. Standards for the different phylotypes were obtained by cloning the environmental sequences for each phylotype into Top10 cells. Plasmid extraction and purification was done using the Qiagen plasmid purification kit according to the manufacturer's instructions. Plasmid DNA concentrations were measured with NanoDrop ND-1000 (PeqLab) and diluted to 4 pg μl^{-1}, which corresponds to 10^7 target sequence copies in a 5-μl volume. Serially diluted plasmid standards for filamentous, unicellular group A, unicellular group B, *Cyanothece*-like (group C), gammaproteobacterium AO (gamma A), gammaproteobacterium PO (gamma P), and cluster III phylotypes were used to calculate copy numbers in the qPCR assays. The group B and gammaproteobacterial primers and TaqMan probes from our study were very different from those previously reported (10), while the filamentous and group A primers and probes from reference 10 detected a segment of the *nifH* gene similar to that detected in our study. Although independently designed, the reverse primer and probe for cluster III in our study were almost identical to those described in references 9 and 10. The group C primer and probe set designed for this study selected for a different part of the group C sequence than the set described in Foster et al. (13).

qPCR assays and detection limits. All qPCRs were run on an ABI Prism 7000 (Applied Biosystems) using the default cycling program, but increasing the number of cycles to 45. The program's cycling conditions were 2 min at 50°C, 10 min at 95°C, and 45 cycles of 95°C for 15 s, followed by 1 min at 60°C. The specificity of the qPCR primer and probe sets was confirmed by testing for cross-reactivity and sensitivity against each standard diluted to 10^4 and 10^5 *nifH* copies. DNA amplification signals were detected only for the homologous phylotype. It is important to note that the filamentous primer and probe set was designed for *Trichodesmium*, but due to the high similarity in the filamentous *nifH* sequences it amplified *Katagnymene* equally well. Additionally, the sensitivity of the primers and probes in a mixed-DNA sample was tested in combinations of serially diluted standards mixed in ratios ranging from 10^7:10^1 to 10^1:10^7 copies of the specific and unspecific standard. There were no significant changes in the linear regressions, indicating that the presence of various amounts of closely related DNA sequences does not affect the quantification of a specific phylotype. However, the detection limit of the filamentous primer and probe set was 100 filamentous *nifH* copies when mixed with 10^7 group A *nifH* copies, a situation that was not observed in any samples.

qPCR mixtures contained 1× TaqMan PCR buffer (Applied Biosystems), 100 nM TaqMan probe, 5 pmol/μl each of the forward and reverse primers, 400 ng/μl bovine serum albumin (BSA), 3 μl PCR water, and 5 μl of either standard or environmental sample (which corresponded to 1 to 6 ng environmental DNA, with an average of 2 ng). To test environmental samples for PCR inhibition, serial dilutions of several samples from each cruise were run. The results indicated different levels of inhibition in almost all samples tested. Also, additions of environmental DNA to standards resulted in an underestimation of the true copy number. Dilution of the samples partially reduced PCR inhibition but affected the detection limit. Inhibition of PCR is a common problem with environmental samples and has been reported before in other studies, which estimated the degree of the inhibition from qPCR efficiency without relieving the inhibition (13). Addition of BSA to the reaction consistently relieved the inhibition without affecting the standard curves or detection limit (data not shown). We therefore routinely added BSA to all qPCR mixtures. Environmental DNA samples were run in triplicate. The coefficient of variation for the cycle threshold (C_T) value of all samples was 1.77% ($n = 251$). Standards were serially diluted (10^7 to 10^1 copies) and run in duplicate. The prepared serial dilutions were stored at 4°C and were stable for about 1 month. Standard curves from stored standard serial dilutions were highly reproducible and varied daily by an average C_T of 0.7. In contrast, freeze-thaw cycles of samples and standards resulted in 10-fold decrease in copy numbers (results not shown). To avoid this, extracted DNA was frozen in aliquots and thawed only once for qPCR determination.

No-template controls were run in duplicate for each primer and probe set and were undetectable after 45 cycles, thus setting the theoretical detection limit of our assay mixture to one *nifH* copy. However, the realized detection limit depends on the amount of seawater filtered per sample, elution volume after extraction, and the amount of sample loaded. In this study, the amount of seawater filtered determined the detection limits and these are 20, 50, and 75 copies $liter^{-1}$ of seawater for *Sonne*, *Poseidon*, *Meteor* 55, and *Meteor* 60 samples, respectively. Thus, in our assays, samples with a C_T value below 36, which corresponded to <100 copies $liter^{-1}$, were considered detectable but not quantifiable. To minimize potential differences between qPCRs run on different days, a sample was quantified with all primer and probe sets on 1 day and the same standard serial dilutions were used for all samples. The ABI 7000 system SDS software (version 1.2.3) with RQ study application was used to calculate linear regressions of C_T versus $\log_{10}$ *nifH* standard copy numbers. PCR efficiencies were calculated using the formula $E = 10^{-1/\text{slope}} - 1$ (1). Average PCR efficiencies were 96.5% ± 2% ($n = 37$; $R^2 = 0.999$) for filamentous, 94.9% ± 1% ($n = 39$; $R^2 = 0.999$) for group A, 96.1% ± 2% ($n = 22$; $R^2 = 0.997$) for group B, 89.1% ± 6% ($n = 24$; $R^2 = 0.998$) for group C, 95.3% ± 2% ($n = 24$; $R^2 = 0.998$) for

TABLE 2. Comparison of clone libraries and qPCR data given as percentages of each phylotype from the total number of either clones or phylotypes detected

Phylotype	% of clones recovered[a]	% of *nifH* copies detected from:	
		Samples with clone libraries[b]	All samples[c]
Filamentous	57.4	71.1	53.1
Group A	26.9	23.9	34.1
Group B	1.4	0.3	4.3
Group C	3.6	1.2	2.3
Gamma A	5.9	2.8	5.3
Gamma P	2.5	0.7	0.6
Cluster III	2.2	0.05	0.4

[a] A total of 357 clones was obtained from 23 cloned samples.
[b] A total of 4.9×10^6 *nifH* copies liter^{-1} was detected in samples with a corresponding clone library.
[c] A total of 1.1×10^7 *nifH* copies liter^{-1} was detected in all 142 samples.

gamma A, 100% ± 2% ($n = 14$, $R^2 = 0.997$) for gamma P, and 100% ± 1% ($n = 22$; $R^2 = 0.994$) for cluster III. Statistical analyses (Kruskal-Wallis and Mann-Whitney U tests) were performed with Statistica (version 6). P values of <0.05 were considered significant. Maps of the distribution and abundance of *nifH* phylotypes in the North Atlantic were generated with Ocean Data View (37).

RESULTS

Sampling and DNA concentrations. A total of 141 DNA samples were collected from four cruises to the northern Atlantic Ocean. Sixty-four samples were collected in surface waters, 41 from depths of 20 to 80 m, and 36 from depths below 80 m. Water temperatures from all samples ranged from 15 to 30°C, with the coldest (15 to 23°C) and highest (25 to 29°C) temperatures recorded during the *Meteor* 60 and *Meteor* 55 expeditions, respectively. All samples were collected in waters with a salinity of 34.6 to 37.2 ppt, with the exception of samples from four stations located in the Amazon River plume, where surface water salinities ranged between 31.2 and 33.4 ppt. NO_3 concentrations ranged from 0 to 25 μM; however, 65% of the samples were collected from waters with 0 to 1 μM NO_3. PO_4 concentrations ranged from 0 to 1.5 μM, and 75% of the samples had concentrations of 0.25 μM PO_4 or less. DNA concentrations ranged from 16 ng liter^{-1} to 640 ng liter^{-1} (average, 132 ng liter^{-1}). The lower DNA concentrations generally came from samples collected at depth. The *Sonne* and *Meteor* 55 samples collected with an overboard pump had on average a higher DNA concentration (237 ng liter^{-1}) than samples collected with a CTD rosette (114 ng liter^{-1}). No other trends were observed between DNA concentrations and location, depth, or time of year.

Comparison of clone libraries versus qPCR. Cyanobacterial phylotypes were the most abundantly detected diazotrophs (93.8% of the total *nifH* copies detected), with the majority being the filamentous phylotype (Table 2). The group A phylotype was the next most abundant, followed by gamma A, which was lower by 1 order of magnitude. The gamma P and cluster III phylotypes made up about 1% of all *nifH* sequences detected. These results reflect the relative abundance of phylotypes in clone libraries (22), except that rare groups detected at low abundance with qPCR were overestimated in pooled clone libraries. In direct comparisons of qPCR data and clone libraries from the same station, more diazotroph phylotypes were detected with qPCR, thus demonstrating the higher sensitivity of this technique, especially for the detection of rare phylotypes. For 10 of the samples, which contained low diversity (two to three phylotypes present), the relative abundance of phylotypes from the cloned library accurately (5% difference) reflected abundances obtained with qPCR, except that groups with low copy numbers were sometimes absent from the clone libraries. However, results from qPCR and clone libraries diverged greatly for samples containing high (more than three phylotypes present) *nifH* diversity, with minor phylotypes completely absent from the clone library and large over- or underestimates of more dominant groups based on data from clone libraries. Results showed that qPCR provided a highly sensitive and quantitative estimate of phylotype abundance, in contrast with clone libraries, which can only show relative abundances at best (Table 2).

Distributions of *nifH* phylotypes. Diazotroph phylotypes were detected throughout the northern Atlantic Ocean (Fig. 1a). In general, very low to undetectable *nifH* copy numbers were observed along the equator and at latitudes higher than 30°N. The highest *nifH* copy numbers were measured in *Poseidon* samples between 18 to 30°N and 30 to 23°W; however, the lowest diversity was also observed at this location. High copy numbers and high diversity were detected in *Sonne* samples between 50 and 34°W and 2 and 15°N. The filamentous, group A, and gamma A phylotypes were the most commonly detected phylotypes and were distributed throughout the North Atlantic (Fig. 1b, e, and f). Both gammaproteobacterial and cluster III phylotypes were only detectable at low copy numbers (Fig. 1b to d). In contrast to the other phylotypes, the cluster III distribution reached as far as 40°N (Fig. 1d). This rare phylotype was detectable in *Sonne* and *Meteor* 60 samples, but only west of 33°W. Copy numbers ranged from the detection limit to 1,600 cluster III *nifH* copies liter^{-1}, with the highest copy numbers measured at northern stations where the spring bloom was in progress (29). The gamma P phylotype occurred mainly in *Sonne* samples, and occasionally in *Poseidon* samples and the *Meteor* 55 samples, which were collected using a pump. In contrast, the gamma A *nifH* phylotype was detectable in most samples from all cruises, and ranged between 10^3 (*Sonne*) and 10^4 (*Meteor* 55) *nifH* copies liter^{-1}.

Filamentous diazotroph *nifH* copy numbers were found north of the equator to about 15°N (Fig. 1e) and reached the highest abundances between 52°W and 35°W, though areas of high abundances were also present in the eastern part of the North Atlantic basin (up to 10^6 copies liter^{-1}). Others have also observed higher abundances of *Trichodesmium* in the western Atlantic basin (12) than in the eastern basin. The filamentous phylotype was found at low copy numbers between 20°N and 30°N, and it was undetectable along the northern cruise track, except at the two southernmost stations (approximately 22°N).

Unicellular cyanobacterial diazotroph copy numbers were more variable than filamentous copy numbers. Group A unicellular cyanobacterial phylotypes were present throughout the study area and reached high concentrations (up to 10^6 group A *nifH* copies liter^{-1}) (Fig. 1f). No group A *nifH* copies were detectable in the northwestern quadrant of the Atlantic Ocean (west of 30°W and north 17°N) during spring. Group A copy numbers were moderately high (9×10^3 to 2×10^4 group A

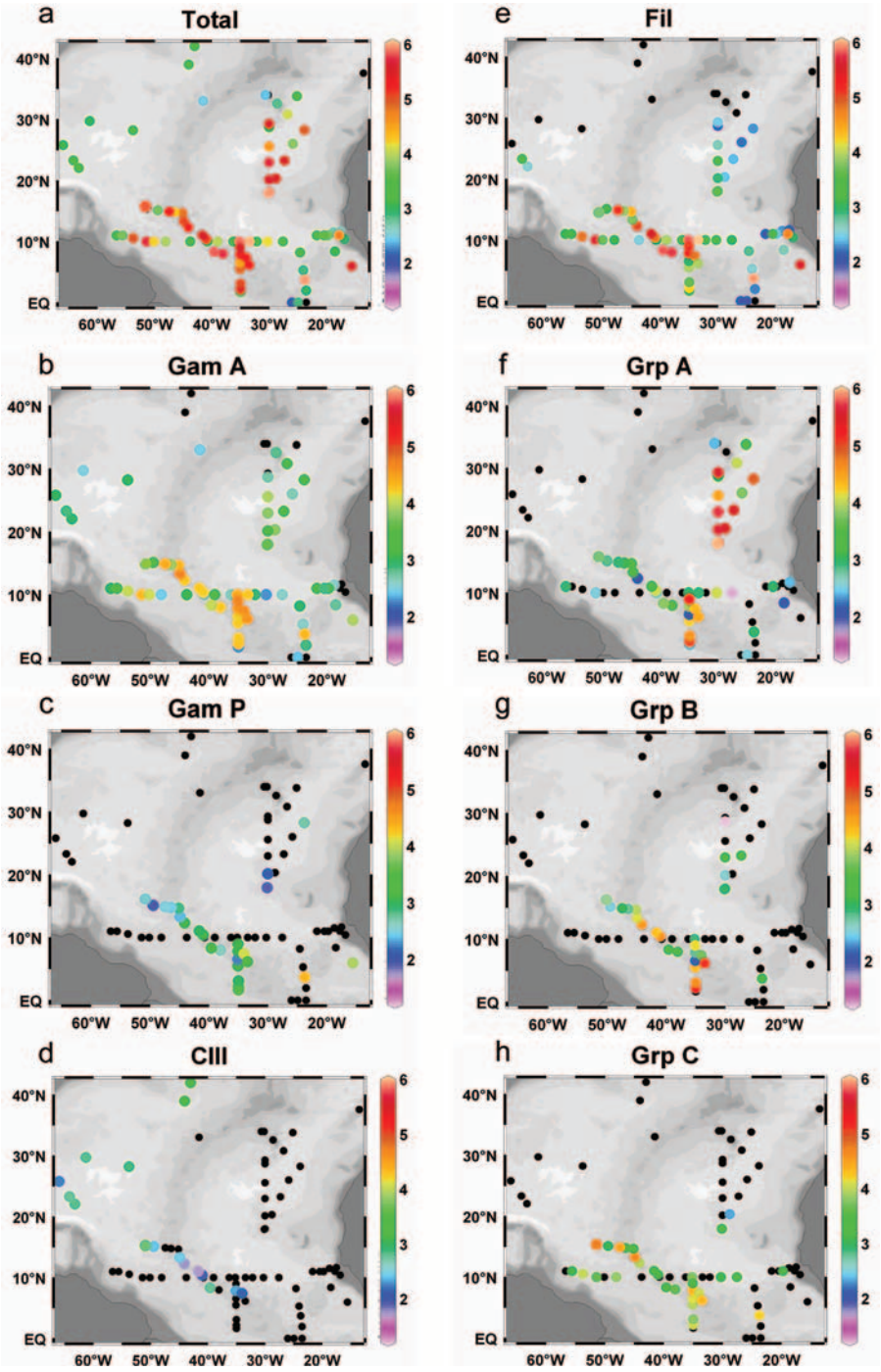

FIG. 1. Total *nifH* copies liter^{-1} detected at each station (a) and *nifH* copies liter^{-1} of each phylotype in panels b to h were plotted using Ocean Data View (37). Black dots indicate samples with concentrations below the detection limit. Note that the color scale is a log scale. Fil, filamentous; Gam, gamma; Grp, group; CIII, cluster III.

nifH copies liter^{-1}) between the equator and 15°N but reached the highest abundances between 30°W to 23°W and 30°N to 17°N (*Poseidon* cruise track), where copy numbers ranged from 4×10^5 to 10^6 copies liter^{-1}. Group C *nifH* copy numbers were low to undetectable throughout the study area, except for some *Sonne* samples. Group B unicellular phylotypes were mainly found in *Sonne* samples, as well, but at higher concentrations: 3×10^4 group B *nifH* copies liter^{-1} as opposed 1×10^4 group C *nifH* copies liter^{-1} (Fig. 1g and h). No quantifiable group B or group C phylotypes were detected north of 20°N. The group B phylotype accounted for 6.9% of the total *nifH* copies detected in our samples, despite being detected at only 27 stations.

In an attempt to identify what factors influence the distri-

TABLE 3. Effect of sampling depth and NO_3 concentration on the abundance of *nifH* phylotypes[a]

Type[b]	% of *nifH* phylotype copies detected			
	Surface samples	Depth samples	<0.5 μM NO_3	>0.5 μM NO_3
Filamentous*†	99.2	0.8	99.5	0.5
Group A†	30.7	69.3	97.5	2.5
Group C*†	90.5	9.5	96.5	3.5
Gamma A*†	89.0	11.0	95.8	4.2
Gamma P	0.0	100.0	89.8	10.2
Cluster III	24.6	75.4	40.2	59.8
Total*†	94.1	5.9	97.9	2.1

[a] Data are given as the percentage of either *nifH* phylotype copies detected in surface and depth samples (columns 1 and 2) or *nifH* phylotypes recovered in waters with less than or greater than 0.5 μM NO_3. Surface samples (up to 30 m deep) and corresponding depth samples (from 30 to 200 m) were available for 37 stations, and no group B phylotypes were detected in these samples (columns 1 and 2). NO_3 measurements were available for 112 samples.

[b] Phylotypes whose concentrations were significantly different ($P < 0.05$, Mann-Whitney U test) in samples collected at depth than in surface samples are identified by *, while those significantly affected by NO_3 concentrations are identified by †.

bution of diazotrophs, we considered sampling depth, dissolved inorganic nutrient concentrations, mixed layer depth, water temperature, geographical distribution, and Fe fertilization via mineral dust deposition. Comparison of paired surface (up to 30 m deep) and deep (30 to 200 m) samples from 37 stations indicated that overall total diazotroph abundance decreased with depth (Mann-Whitney U test; $P = 0.004$). More specifically, the filamentous, gamma A, and group C phylotype concentrations were significantly higher in the surface samples (Mann-Whitney U test; $P < 0.001$). There were a few stations where the group A phylotype was detected both at the surface and at depth; however, the majority of group A phylotypes were detected between 10 and 30 m. Cluster III and gamma P concentrations appeared to increase with depth, but this result was not statistically significant (Table 3).

Significant relationships were also observed between *nifH* distribution and residual NO_3 (Table 3) and PO_4 concentrations (results not shown), with most phylotypes being almost completely restricted to NO_3 concentrations less than 0.5 μM. One clear exception was the cluster III phylotype, which showed no significant preference for low NO_3 waters (Table 3). Mixed-layer depth showed no direct relationship with specific *nifH* phylotypes (results not shown).

The influence of temperature on the distribution of *nifH* phylotypes was investigated by calculating the mean water temperature for each phylotype in samples containing greater than 100 *nifH* copies liter^{-1}. The mean temperature for each phylotype ranged from 28°C for group C to 18°C for cluster III (Fig. 2a). We observed that most phylotypes were associated with narrow temperature ranges except for gamma P, the least abundant phylotype, which appeared to be poorly constrained by temperature. The group C phylotype was detected in very warm waters, while gamma A, gamma P, and group B were detected mainly in waters of about 24°C. Temperature means for group C, filamentous, gamma A, and cluster III were significantly different from the mean water temperature of all samples. Interestingly, cluster III was the only phylotype whose mean detection temperature was below the mean of all samples. The clearest associations between temperature and *nifH* phylotypes were for the filamentous and group A phylotypes, which were detected in significant quantities at average temperatures of 26°C and 20.9°C, respectively (Fig. 2a). Although the filamentous and group A phylotypes were detected throughout the temperature range, the highest copy numbers were detected in samples with water temperatures from 28 to 30°C and 19 to 24°C, respectively (Fig. 2b). This suggests that these two dominant groups may have different temperature optima.

Distribution by geographical areas. The large geographical coverage of our data prompted us to analyze the distributions and abundances of the *nifH* phylotypes in six regions (Fig. 3a), defined as a function of the basic water characteristics, temperature and salinity, of the surface water sample (see Fig. S1 in the supplemental material). Average *nifH* gene copy numbers for the stations within regions A, B, and C, corresponding to areas north of 35°N, the equator, and the Sargasso Sea respectively, contained very low abundances of potential diazotrophs (Fig. 3b). In contrast, the highest average surface and

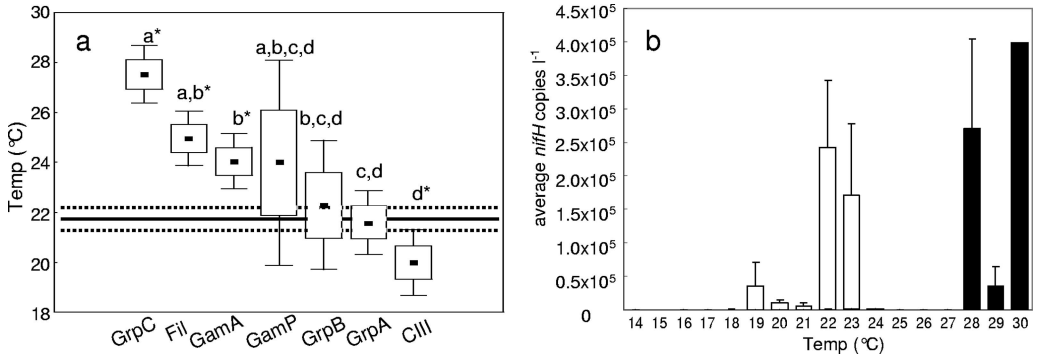

FIG. 2. Box-whisker plots (black dots, mean; boxes, standard error; bars, 95% confidence interval) show the temperatures where >100 *nifH* copies liter^{-1} were detected for all phylotypes in panel a. The mean temperature of all samples (22°C) and the associated standard error are indicated by a black line and dashed line, respectively. Phylotype temperature means which are significantly different from 22°C ($P < 0.05$, Kruskal-Wallis test) are identified by asterisks. Letters signify groups of phylotypes whose temperature means are not significantly different from another group (Mann-Whitney U test). Average filamentous and group A *nifH* copies liter^{-1} detected at sample temperatures rounded to the nearest whole degree are displayed in panel b. Error bars indicate the standard error.

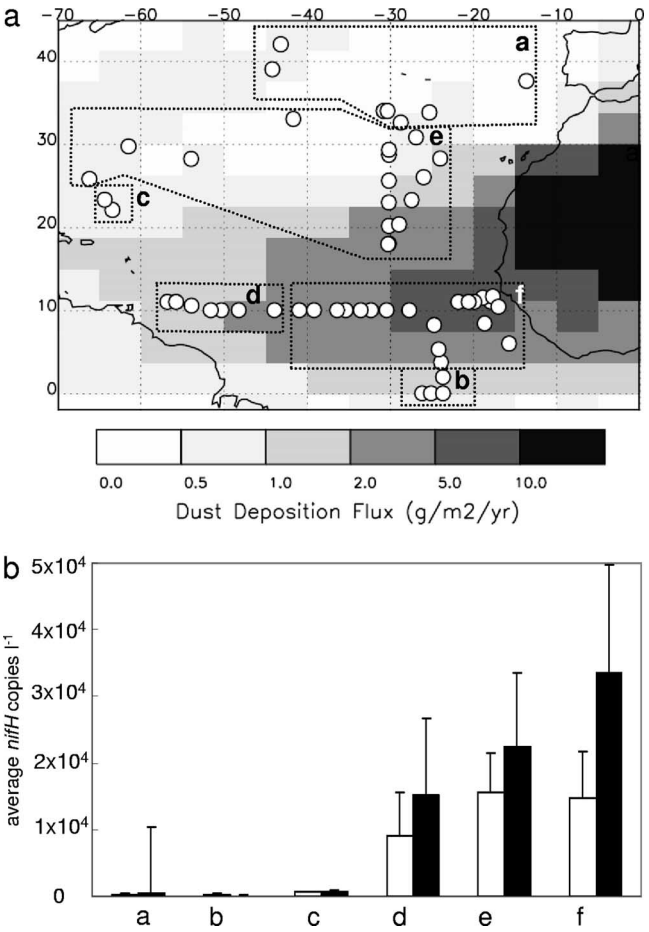

FIG. 3. Separation of stations according to geographical location (a) and physical characteristics (see the supplemental material). Station locations are overlaid on a map of predicted annual dust deposition. The average number of *nifH* copies liter^{-1} and standard error from all samples (clear bars) and only surface samples (black bars) in each region are plotted in panel b. Region letters correspond to the panels in Fig. 4. *Sonne* 152 samples were not plotted because no temperature and salinity data were available.

total *nifH* gene copy numbers were detected in regions E and F (Fig. 1a and 3b).

For each geographical area, average *nifH* concentrations of individual phylotypes were plotted versus temperature (Fig. 4). Region A (northerly stations) was characterized by low surface water temperatures (<19°C) and relatively high salinity (>36.2 ppt). This area of very low *nifH* gene copy numbers (Fig. 3 and 4a) contained only the cluster III, group A, and gamma A phylotypes. Of the eight samples measured in region B (equator), only one contained abundances well above the detection limit (Fig. 4b). Here, diversity was low and only the filamentous and a few gamma A phylotypes were detected. Stations in the Sargasso Sea were sampled in the spring time (region C, Fig. 4c), exhibited deep mixed layers, and contained low *nifH* concentrations. The three phylotypes found there consisted of the rare cluster III phylotype as well as the gamma A and filamentous phylotypes. These phylotypes were homogeneously distributed throughout the stations, even at depths up to 160 m. Region D contained samples that were influenced by the Amazon River, where surface water temperatures were greater than 28°C and diazotroph concentrations, especially the filamentous phylotype, were higher in the surface samples (Fig. 4d).

Total *nifH* concentrations were relatively similar in regions E and F (Fig. 3b), but different groups were dominant (Fig. 4e and f′). Region E samples were characterized by surface water temperatures of 20 to 23°C and salinity of 36.8 to 37 ppt. This area was dominated by the group A phylotype. The cluster III phylotype was also detected, but only in the samples from the western half of this region. In contrast, the filamentous phylotype dominated region F, where surface water temperatures were greater than 27°C and the salinity was 34.7 to 35.6 ppt.

The amount of dust deposition may play a role in determining the abundance and distribution of diazotrophs in a certain region. In Fig. 3a, the stations are plotted in relation to the annual dust deposition. Samples were then grouped according to estimated annual dust deposition (Fig. 5). The highest diazotroph concentrations were detected where the dust deposition was between 2 and 5 g m^{-2} year^{-1} (Fig. 5). The geographical regions with the lowest number of *nifH* copies detected (i.e., all of region A and most of region B samples) were located in the modeled dust deposition area with <1 g m^{-2} year^{-1}. Only the cluster III phylotype was detected more often in regions with low dust deposition (Fig. 1d and 5).

DISCUSSION

Assessing relative diversity and phylotype abundances from qPCR data. Although extensive sequencing of clone libraries generated from endpoint PCR products has the potential to uncover rare and new phylotypes, amplification biases can occur from preferential primer binding, the use of different types of *Taq* polymerases (32), nonselection by a primer set (30), and multiple target gene copies. For this reason, it is well recognized that endpoint PCR techniques are not suitable for quantitative analysis of genetically diverse phylotypes from natural microbial communities. Prior knowledge of the *nifH* gene diversity from the study area (22) allowed us to target and quantitatively estimate the abundance of the dominant phylotypes, avoiding amplification biases by using specific primer and probe sets. We found that an approach combining both sequence analyses from clone libraries and TaqMan-based qPCR assays was needed for accurately assessing both diversity and abundances of diazotrophs in a given environment.

The presence of multiple gene copies in the genome of an organism as well as multiple genome copies per cell can affect the extrapolation of qPCR results to estimates of cell abundance. It is known that some diazotrophs, such as *Clostridium pasteurianum*, have multiple copies of the *nifH* gene (35). Others, such as *Trichodesmium erythraeum* and *Crocosphaera watsonii*, have only one copy of the *nifH* gene per genome. As there is no available genome information for the uncultured phylotypes and little information on the variability of genome copies per cell for all *nifH* phylotypes, the concentrations of *nifH* genes presented in this study should be considered an upper limit of the cell density. Given the limited dissolved P and N supply in the euphotic zone of the oligotrophic North Atlantic (27, 44), the presence of multiple genome copies per cell is unlikely. In contrast, this may be a consideration for

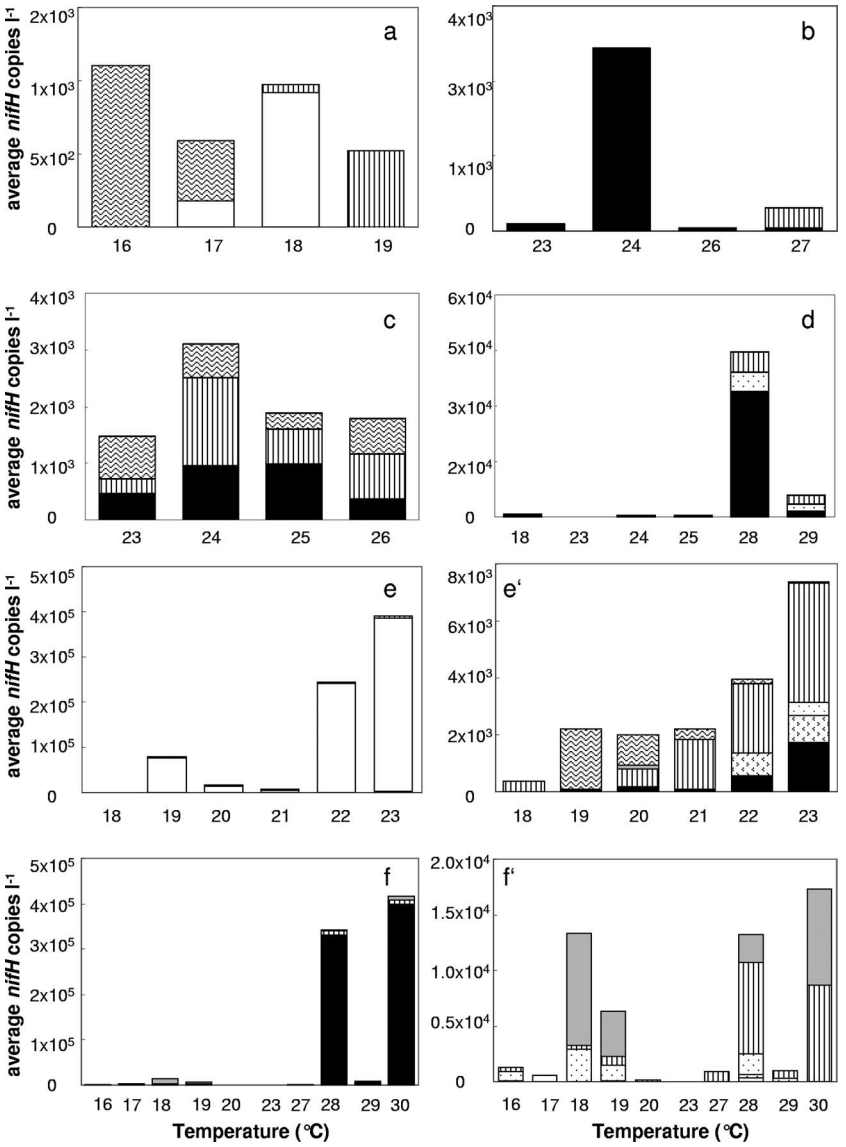

FIG. 4. Average concentrations of *nifH* copies liter^{-1} by sample temperature (rounded to the nearest whole degree) in each geographic location are shown, with panel letters corresponding to the regions in Fig. 3. ■, filamentous; □, group A, ▨ , group B; ▨ , group C; ▥, gamma A; ▩ , gamma P; and ⊙, cluster III. The numbers of samples for regions a, b, c, d, e, and f are 21, 8, 6, 40, 105, and 96, respectively. Panels e′ and f′ show the average numbers of *nifH* copies liter^{-1} from panels e and f without the dominant group A and filamentous phylotypes, respectively.

diazotrophs located below the euphotic zone, where nutrient levels are high (26).

Diazotrophic communities of the Atlantic Ocean. Our results on *nifH* phylotype distribution emphasize the importance of *Trichodesmium* in the tropical Atlantic Ocean, complementing other studies (6), as filamentous *nifH* sequences made up 51% of all detected sequences. Filamentous concentrations were similar to *Trichodesmium* cell counts (7). Although the distribution of *Trichodesmium* exhibits a latitudinal trend with increasing abundances in southerly latitudes, seasonality may also play an important role in explaining the distribution patterns of this phylotype in our study. Nitrogen fixation rates have been reported to be highest during the late summer and autumn and lowest in the winter in the area above 10°N and west of 40°W (6) The two cruises with the highest filamentous copy numbers (*Sonne* and *Meteor* 55) were during the fall. The *Meteor* 60 cruise was during the spring, the season corresponding to the lowest *Trichodesmium* abundances in this latitudinal range (31).

Although filamentous phylotypes were dominant in our study, the group A unicellular phylotype was responsible for over a third of our total *nifH* copies, suggesting that this group may periodically contribute significantly to N_2 fixation in the northern Atlantic. The gamma A phylotype, although detected at low concentrations, was found in almost all samples and may also play an important role globally due its widespread distribution. It has already been demonstrated that gammaproteobacteria are cosmopolitan (8), and an *nifH* gammapro-

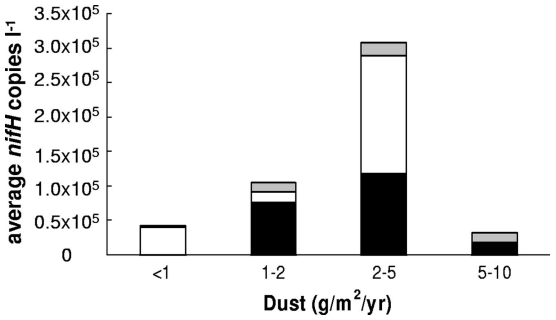

FIG. 5. Average concentrations of *nifH* copies liter^{-1} for filamentous (■), group A (□), and all other phylotypes combined (gray square) as a function of estimated annual dust deposition are shown. Average temperatures of each region were 22.3°C (5 to 10 g m^{-2} year^{-1}), 24.5°C (2 to 5 g m^{-2} year^{-1}), 26.8°C (1 to 2 g m^{-2} year^{-1}), and 19.3°C (<1 g m^{-2} year^{-1}). The dust deposition map was provided by I. Tegen, using the data from reference 42.

teobacterial sequence 99% similar to the gamma A target sequence of this study was present at all stations in an Arabian Sea study (4). Taken together, these results suggest that the widespread distribution of *nifH* phylotypes belonging to the gammaproteobacterial group warrants further study of its role in the global nitrogen cycle.

The presence of cluster III *nifH* phylotypes in oxygenated low light waters with detectable to high nitrate is puzzling. In our study, the highest concentrations of cluster III phylotypes were detected during the spring bloom at stations characterized by a deep mixed layer and high nitrate concentrations (29), suggesting that high nitrate conditions do not select against all diazotrophs (20). Even *Trichodesmium*, which in our study was abundant only in oligotrophic waters, could retain some ability to fix nitrogen when grown in cultures with high nitrate concentrations (18). Diverse cluster III *nifH* transcripts, distantly related (<60%) to the ones described here, have also been reported in well-oxygenated surface waters of the Mediterranean Sea (24). It was suggested that cluster III diazotrophs from oxygenated waters may be either facultative anaerobes or associated with zooplankton (24). Photosynthetic, diazotrophic, purple sulfur bacteria have been reported in association with copepods and have been found to fix nitrogen (34). Although prefiltered (10 μm) samples preclude zooplankton as the host of cluster III phylotypes in some studies (9), a zooplankton-cluster III association cannot be ruled out in the present study. Whether cluster III contributes significantly to global nitrogen fixation remains an open question requiring further work.

To date there have been few other studies which have looked at the distribution of oceanic diazotrophs quantitatively. Published concentrations of diazotroph phylotypes (9, 10) measured by real-time qPCR were comparable to those obtained in this study. Church et al. (9) reported the group A phylotype as being the most numerous (2×10^5 copies liter^{-1}) in upper waters and the cluster III phylotype abundant in dim waters (100 to 1,000 copies liter^{-1}). The situation was different in the Atlantic Ocean, with some stations dominated by the filamentous phylotype and cluster III often undetectable even at depth. Concentrations reported by Foster et al. (13) of the filamentous, group A, group B, and group C phylotypes were comparable to those detected in region D. We did not observe any *nifH* sequences related to the diatom-diazotroph symbiont *Richelia* in our clone libraries and therefore did not quantify these groups, although our samples were collected from waters with higher salinities and lower Si concentrations (0 to 1 μM) than those where Foster et al. (13) observed the diatom-diazotroph association. The Sargasso Sea has been considered an area where nitrogen fixation can be important (31); however, we detected low *nifH* copy numbers in this area (region C), a finding shared by others (17).

In our study, filamentous and group A were the dominant phylotypes whose distributions were well separated as a function of temperature (Fig. 2). The filamentous and group A phylotypes were dominant at stations with water temperatures ranging between 28 and 30°C and 22 and 23°C, respectively. Similarly, group A dominated at the ALOHA time series site when the water temperature ranged between 23 and 24°C (9, 22). The direct effects of temperature on the physiology of an organism can be confounded by the role temperature plays in water column stratification, light regimens, and nutrient availability. In the case of *Trichodesmium*, the association with high water temperature reflects a direct effect on nitrogen fixation and growth rates, with the optima for both physiological processes occurring between 24 and 30°C (5, 40). The physiological reasons for this high temperature preference are not completely understood (41). A combination of factors such as lower dissolved O_2 concentration and a higher respiration rate at high temperatures may favor *Trichodesmium* growth by facilitating O_2 scavenging and thereby protecting nitrogenase against irreversible O_2 damage. A change from 30°C to 20°C waters would result in a 20% increase in dissolved O_2 concentration and in a twofold reduction in respiration rates. Except for a few sparse field observations, there are currently no data for the other *nifH* phylotypes primarily because there are no culture isolates. It is therefore not possible at this stage to establish the effects of temperature on organism physiology for the other diazotrophic groups, although there is a need to carry out laboratory experiments with a group B isolate, *C. watsonii*.

The detection of *nifH* in a DNA sample gives an estimate of the potential for diazotrophy within the microbial community. Whether any of the detected diazotrophs were actively fixing dinitrogen cannot be determined from our results, as only information on *nifH* DNA copy numbers is presented here. However, dinitrogen fixation rates ranging from 3.7 to 255 μmol m^{-2} day^{-1} were measured during the same cruises (27, 43), indicating that some of the *nifH* phylotypes were actively fixing N_2.

***nifH* distribution relative to dust deposition.** Iron supply has been shown to limit diazotrohic growth (33) and, in combination with phosphate, nitrogen fixation (27). This limitation is probably because diazotrophs can have an iron requirement up to 10 times greater than that of other photoautotrophs (21, 40) which is needed for the synthesis of the nitrogenase enzyme. Iron is supplied to the Atlantic Ocean mainly through deposition of aeolian dust, originating from the Sahara (19). The concentration of *nifH* phylotypes was higher in regions which receive an estimated annual dust deposition of 2 to 5 g m^{-2} year^{-1} than in the area with 5 to 10 g m^{-2} year^{-1}. Trichomes were indeed visible in water samples and on filters in the area with 2 to 5 g m^{-2} year^{-1}. Although the western coast of Africa

receives the largest amount of dust, seasonal upwelling brings colder temperatures and higher macronutrient concentrations, which most likely favor groups other than diazotrophs, thus potentially explaining why *nifH* abundance was considerably lower in the area with dust deposition of 5 to 10 g m^{-2} $year^{-1}$. Dust particle size may also play a role in determining the bioavailability of Fe, with heavier particles deposited more quickly and sinking faster than finer particles (2). Similar to our findings, Voss et al. (43) found that nitrogen fixation rates were correlated with dissolved iron concentrations during the *Meteor* 55 cruise. In contrast, a study focused on nitrogen fixation by *Trichodesmium* in the central North Atlantic found no correlation of N_2 fixation rates with dissolved iron (36). The authors concluded that *Trichodesmium* was not iron limited in their study because of high dissolved iron concentrations observed in April, a month of high dust deposition. The cruise track from their study was mainly located within the area with a modeled annual dust deposition of 2 to 5 g/m^2/year, covering a fraction of the geographical area presented in our study. Whether temperature, geographical location, residual NO_3, or amount of dust deposition plays a larger role in determining the composition of diazotrophs requires further study.

Conclusions. Our study presents a snapshot of *nifH* phylotype distribution and abundance covering a large geographical area of the North Atlantic and expands the known distribution range of diazotrophs. The dominant phylotypes filamentous and group A had different temperature optima, indicating that these two groups may occupy different niches. Although most *nifH* phylotypes were associated with warm waters with very low NO_3 concentration, the presence of the cluster III phylotypes at relatively high latitudes and high NO_3 concentrations was unexpected. Data on nitrogenase activity or *nifH* expression will be needed to confirm that these *nifH* phylotypes actively fix dinitrogen in all of the locations where they were detected. There is currently no information on the seasonal distribution and diurnal activity of most *nifH* phylotypes, with the notable exception of *Trichodesmium* (10). Our study suggests that atmospheric mineral dust deposition and temperature are important factors determining the distribution and abundance of the various *nifH* phylotypes. However, confirmation of our observations will require a coupled seasonal analysis of the *nifH* phylotype distribution and mineral dust deposition in the North Atlantic.

ACKNOWLEDGMENTS

We thank the captains and crews of the F/S *Meteor* and *Poseidon* and chief scientists D. Wallace (*Meteor* 55 and 60 expeditions) and P. Kähler (*Poseidon* 284). We thank I. Tegen for providing the dust deposition map and F. Malien for nutrient analyses. We thank two anonymous reviewers for constructive comments.

This work was supported by DFG grants RO 2138/4–1 and RO 2138/5–1 to J.L.

REFERENCES

1. **Atallah, Z. K., J. Bae, S. H. Jansky, D. I. Rouse, and W. R. Stevenson.** 2007. Multiplex real-time quantitative PCR to detect and quantify *Verticillium dahliae* colonization in potato lines that differ in response to verticillium wilt. Am. Phytopathol. Soc. **97:**865–872.
2. **Baker, A. R., and T. D. Jickells.** 2006. Mineral particle size as a control on aerosol iron solubility. Geophys. Res. Lett. **33:**.
3. **Berman-Frank, I., P. Lundgren, and P. Falkowski.** 2003. Nitrogen fixation and photosynthetic oxygen evolution in cyanobacteria. Res. Microbiol. **154:** 157–164.
4. **Bird, C., J. Martinez Martinez, A. G. O'Donnell, and M. Wyman.** 2005. Spatial distribution and transcriptional activity of an uncultured clade of planktonic diazotrophic γ-proteobacteria in the Arabian Sea. Appl. Environ. Microbiol. **71:**2079–2085.
5. **Breitbarth, E., A. Oschlies, and J. La Roche.** 2006. Physiological constraints on the global distribution of *Trichodesmium*—effect of temperature on diazotrophy. Biogeosciences. www.biogeosciences.net/3/1/2006.
6. **Capone, D., J. Burns, J. P. Montoya, A. Subramaniam, C. Mahaffey, T. Gunderson, A. F. Michaels, and E. J. Carpenter.** 2005. Nitrogen fixation by Trichodesmium spp.: an important source of new nitrogen to the tropical and subtropical North Atlantic Ocean. Global Biogeochem. Cycles. doi:10.1029/2004GB002331.
7. **Carpenter, E. J., A. Subramaniam, and D. Capone.** 2004. Biomass and primary productivity of the cyanobacterium *Trichodesmium* spp. in the tropical N Atlantic Ocean. Deep-Sea Res. **51:**173–203.
8. **Cho, J.-C., and S. J. Giovannoni.** 2004. Cultivation and growth characteristics of a diverse group of oligotrophic marine *Gammaproteobacteria*. Appl. Environ. Microbiol. **70:**432–440.
9. **Church, M. J., B. D. Jenkins, D. M. Karl, and J. P. Zehr.** 2005. Vertical distributions of nitrogen-fixing phylotypes at Stn ALOHA in the oligotrophic North Pacific Ocean. Aquat. Microb. Ecol. **38:**3–14.
10. **Church, M. J., C. M. Short, B. D. Jenkins, D. M. Karl, and J. P. Zehr.** 2005. Temporal patterns of nitrogenase (*nifH*) gene expression in the oligotrophic North Pacific Ocean. Appl. Environ. Microbiol. **71:**5362–5370.
11. **Codispoti, L. A., J. A. Brandes, J. P. Christensen, A. H. Devol, S. W. A. Naqvi, H. W. Paerl, and T. Yoshinari.** 2001. The oceanic fixed nitrogen and nitrous oxide budgets: moving targets as we enter the anthropocene? Sci. Mar. **62:**85–105.
12. **Davis, C. S., and D. J. McGillicuddy, Jr.** 2006. Transatlantic abundance of the N_2-fixing colonial cyanobacterium *Trichodesmium*. Science **312:**1517–1520.
13. **Foster, R. A., A. Subramaniam, C. Mahaffey, E. J. Carpenter, D. Capone, and J. P. Zehr.** 2007. Influence of the Amazon River plume on distributions of free-living and symbiotic cyanobacteria in the western tropical north Atlantic Ocean. Limnol. Oceanogr. **52:**517–532.
14. **Fulweiler, R. W., S. W. Nixon, B. A. Buckley, and S. L. Granger.** 2007. Reversal of the net dinitrogen gas flux in coastal marine sediments. Nature **448:**180–182.
15. **Grasshoff, K., M. Ehrhardt, and K. Kremling.** 1983. Methods of seawater analysis. Springer-Verlag, New York, NY.
16. **Gruber, N., and J. L. Sarmiento.** 1997. Global patterns of marine nitrogen fixation and denitrification. Global Biogeochem. Cycles **11:**235–266.
17. **Hewson, I., P. H. Moisander, K. M. Achilles, C. A. Carlson, B. D. Jenkins, E. Mondragon, A. E. Morrison, and J. P. Zehr.** 2007. Characteristics of diazotrophs in surface to abyssopelagic waters of the Sargasso Sea. Aquat. Microb. Ecol. **46:**15–30.
18. **Holl, C. M., and J. P. Montoya.** 2005. Interactions between nitrate uptake and nitrogen fixation in continuous cultures of the marine diazotroph *Trichodesmium* (Cyanobacteria). J. Phycol. **41:**1178–1183.
19. **Jickells, T. D., Z. S. An, K. K. Andersen, A. Baker, G. Bergametti, N. Brooks, J. J. Cao, P. W. Boyd, R. A. Duce, K. A. Hunter, H. Kawahata, N. Kubilay, J. La Roche, P. S. Liss, N. Mahowald, J. M. Prospero, A. J. Ridgwell, I. Tegen, and O. Torres.** 2005. Global iron connections between desert dust, ocean biogeochemistry, and climate. Science **308:**67–71.
20. **Karl, D., A. Michaels, B. Bergman, D. Capone, E. Carpenter, R. Letelier, F. Lipschultz, H. Paerl, D. Sigman, and L. Stal.** 2002. Dinitrogen fixation in the world's oceans. Biogeochemistry **57:**47–98.
21. **Kustka, A., E. J. Carpenter, and S. A. Sanudo-Wilhelmy.** 2002. Iron and marine nitrogen fixation: progress and future directions. Res. Microbiol. **153:**255–262.
22. **Langlois, R. J., J. La Roche, and P. A. Raab.** 2005. Diazotrophic diversity and distribution in the tropical and subtropical Atlantic Ocean. Appl. Environ. Microbiol. **71:**7910–7919.
23. **Mahaffey, C., R. G. Williams, G. A. Wolff, N. Mahowald, W. Anderson, and M. Woodward.** 2003. Biogeochemical signatures of nitrogen fixation in the eastern North Atlantic. Geophys. Res. Lett. **30:**1300.
24. **Man-Aharonovich, D., N. Kress, E. B. Zeev, I. Berman-Frank, and O. Beja.** 2007. Molecular ecology of *nifH* genes and transcripts in the eastern Mediterranean Sea. Environ. Microbiol. **9:**2354–2363.
25. **Mazard, S. L., N. J. Fuller, K. M. Orcutt, O. Bridle, and D. J. Scanlan.** 2004. PCR analysis of the distribution of unicellular cyanobacterial diazotrophs in the Arabian Sea. Appl. Environ. Microbiol. **70:**7355–7364.
26. **Mehta, M. P., D. A. Butterfield, and J. A. Baross.** 2003. Phylogenetic diversity of nitrogenase (*nifH*) genes in deep-sea and hydrothermal vent environments of the Juan de Fuca ridge. Appl. Environ. Microbiol. **69:**960–970.
27. **Mills, M. M., C. Ridame, M. Davey, J. La Roche, and R. J. Geider.** 2004. Iron and phosphorus co-limit nitrogen fixation in the eastern tropical North Atlantic. Nature **429:**292–294.
28. **Montoya, J. P., C. M. Holl, J. P. Zehr, A. Hansen, T. A. Villareal, and D. Capone.** 2004. High rates of N_2 fixation by unicellular diazotrophs in the oligotrophic Pacific Ocean. Nature **430:**1027–1031.
29. **Moore, C. M., M. Mills, A. Milne, R. J. Langlois, E. P. Achterberg, K.**

Lochte, R. Geider, and J. La Roche. 2006. Iron limits primary productivity during spring bloom development in the central North Atlantic. Global Change Biol. **12:**626–634.

30. **Nuebel, U., F. Garcia-Pichel, M. Kühl, and G. Muyzer.** 1999. Quantifying microbial diversity: morphotypes, 16S rRNA genes, and carotenoids of oxygenic phototrophs in microbial mats. Appl. Environ. Microbiol. **65:**422–430.
31. **Orcutt, K. M., F. Lipschulz, K. Gundersen, R. Arimoto, A. F. Michaels, A. H. Knap, and J. R. Gallon.** 2001. A seasonal study of the significance of N_2 fixation by *Trichodesmium spp*. at the Bermuda Atlantic Time-series Study (BATS) site. Deep-Sea Res. Part II **48:**1583–1608.
32. **Osborn, A. M., E. R. B. Moore, and K. N. Timmis.** 2000. An evaluation of terminal-restriction fragment length polymorphism (T-RFLP) analysis for the study of microbial community structure and dynamics. Environ. Microbiol. **2:**39–50.
33. **Paerl, H. W., L. E. Prufert-Bebout, and C. Guo.** 1994. Iron-simulated N_2 fixation and growth in natural and cultured populations of the planktonic marine cyanobacterium *Trichodesmium* spp. Appl. Environ. Microbiol. **60:** 1044–1047.
34. **Proctor, L.** 1997. Nitrogen-fixing, photosynthetic, anaerobic bacteria associated with pelagic copepods. Aquat. Microb. Ecol. **12:**105–113.
35. **Rosado, A., G. F. Duarte, L. Seldin, and J. D. van Elsas.** 1998. Genetic diversity of *nifH* gene sequences in *Paenibacillus azotofixans* strains and soil samples analyzed by denaturing gradient gel electrophoresis of PCR-amplified gene fragments. Appl. Environ. Microbiol. **64:**2770–2779.
36. **Sañudo-Wilhelmy, S. A., A. B. Kustka, C. J. Gobler, D. A. Hutchins, M. Yang, K. Lwiza, J. Burns, D. G. Capone, J. A. Raven, and E. J. Carpenter.** 2001. Phosphorus limitation of nitrogen fixation by *Trichodesmium* in the central Atlantic Ocean. Nature **411:**66–69.
37. **Schlitzer, R.** 2004. Ocean Data View, 2.0 ed. AWI, Bremerhaven, Germany.
38. **Short, S. M., and J. P. Zehr.** 2005. Quantitative analysis of nifH genes and transcripts from aquatic environments. Methods Enzymol. **397:**380–394.
39. **Short, S. M., B. D. Jenkins, and J. P. Zehr.** 2004. Spatial and temporal distribution of two diazotrophic bacteria in the Chesapeake Bay. Appl. Environ. Microbiol. **70:**2186–2192.
40. **Staal, M., S. te Lintel Hekkert, P. Herman, and L. J. Stal.** 2002. Comparison of models describing light dependence of N_2 fixation in heterocystous cyanobacteria. Appl. Environ. Microbiol. **68:**4679–4683.
41. **Staal, M., F. J. R. Meysman, and L. J. Stal.** 2003. Temperature excludes N_2-fixing heterocystous cyanobacteria in the tropical oceans. Nature **425:** 504–507.
42. **Tegen, I., M. Werner, S. P. Harrison, and K. Kohfeld.** 2004. Relative importance of climate and land use in determining present and future global soil dust emission. Geophys. Res. Lett. doi:10.1029/2003GL019216.
43. **Voss, M., P. Croot, K. Lochte, M. Mills, and I. Peeken.** 2004. Patterns of nitrogen fixation along 10°N in the tropical Atlantic. Geophys. Res. Lett. do1:10.1029/2004GL020127.
44. **Wu, J., W. Sunda, E. A. Boyle, and D. M. Karl.** 2000. Phosphate depletion in the western North Atlantic Ocean. Science **289:**759–762.
45. **Zani, S., M. T. Mellon, J. L. Collier, and J. P. Zehr.** 2000. Expression of *nifH* genes in natural microbial assemblages in Lake George, New York, detected by reverse transcriptase PCR. Appl. Environ. Microbiol. **66:**3119–3124.
46. **Zehr, J. P., B. D. Jenkins, S. M. Short, and G. F. Steward.** 2003. Nitrogenase gene diversity and microbial community structure: a cross-system comparison. Environ. Microbiol. **5:**539–554.
47. **Zehr, J. P., M. T. Mellon, and S. Zani.** 1998. New nitrogen-fixing microorganisms detected in oligotrophic oceans by amplification of nitrogenase (*nifH*) genes. Appl. Environ. Microbiol. **64:**3444–3450.
48. **Zehr, J. P., J. P. Montoya, B. D. Jenkins, I. Hewson, E. Mondragon, C. M. Short, M. J. Church, A. Hansen, and D. M. Karl.** 2007. Experiments linking nitrogenase gene expression to nitrogen fixation in the North Pacific subtropical gyre. Limnol. Oceanogr. **52:**169–183.
49. **Zehr, J. P., and B. B. Ward.** 2002. Nitrogen cycling in the ocean: new perspectives on processes and paradigms. Appl. Environ. Microbiol. **68:** 1015–1024.

Paper C: *Iron limits primary productivity during spring bloom development in the central North Atlantic*

Synopsis

In this study a nutrient addition bioassay experiment conducted in the North Atlantic Ocean during the spring bloom showed that primary productivity was limited by iron. Increases in chlorophyll a concentrations and $^{14}CO_2$ incorporation occurred only with the addition of iron. The ratio of nitrate to dissolved iron was the lowest at this site compared to the other bioassay experiment sites. This is a significant finding because low iron concentrations could impede nitrate removal from freshly upwelled waters. Analysis of iron concentrations in water masses upwelled during winter mixing showed that these waters do not contain enough iron to support growth. Another iron source, such as aeolian dust deposition, is needed. Dust supplies, however, are variable and thus may affect spring bloom variability. Light levels at this spring bloom station were nearly limiting which can exacerbate iron limitation. The manuscript proposed that higher iron concentrations through increased dust deposition could therefore decrease light stress, thus changing the initiation of the spring bloom or causing a larger spring bloom. This is an important consideration for predicting changes in primary productivity of the future oceans as aeolian dust deposition is also expected to change.

Contribution

C. M. Moore, M. Mills, A. Milne, E. Achterberg and I contributed equally to the success of the eight experiments performed during the Meteor 60 cruise. I was in charge of organizing the over 100 bottles used per experiment during the experiment set-ups, ensuring that each bottle was properly filled, nutrients were added and prepared for the incubators. I also measured and analyzed the chlorophyll a data at sea. I provided comments and suggestions on the figures and manuscript that C. M. Moore prepared.

Global Change Biology (2006) **12,** 626–634, doi: 10.1111/j.1365-2486.2006.01122.x

Iron limits primary productivity during spring bloom development in the central North Atlantic

C. MARK MOORE*†, MATTHEW M. MILLS‡, ANGELA MILNE§, REBECCA LANGLOIS‡, ERIC P. ACHTERBERG§†, KARIN LOCHTE‡, RICHARD J. GEIDER* and JULIE LA ROCHE‡

*Department of Biological Sciences, University of Essex, Colchester CO4 3SQ, UK, †School of Ocean and Earth Science, Southampton Oceanography Centre, Southampton SO14 3ZH, UK, ‡Marine Biogeochemistry, Leibniz-Institut für Meereswissenschaften, D-24105 Kiel, Germany, §School of Earth, Ocean and Environmental Sciences, University of Plymouth, Plymouth PL4 8AA, UK

Abstract

We present *in situ* biophysical measurements and bioassay experiments that demonstrate iron limitation of primary productivity during the spring bloom in the central North Atlantic. Mass balance calculations indicate that nitrate drawdown is iron (Fe)-limited and that aeolian Fe supply to this region cannot support maximal phytoplankton growth during the bloom. Using a simple simulation model, we show that relief of Fe limitation during the spring bloom can increase nitrate drawdown and, hence, new primary production, by 70%. We conclude that the episodic nature of iron supplied by dust deposition is an important factor controlling the dynamics of the spring bloom. From this, we hypothesize that variability in the timing and magnitude of the spring bloom in response to aeolian Fe supply will affect carbon drawdown and food web dynamics in the central North Atlantic.

Keywords: dust, iron limitation, North Atlantic, primary production, spring bloom

Received 18 April 2005; revised version received and accepted 4 October 2005

Introduction

Iron (Fe) supply limits phytoplankton productivity in the high nitrate low chlorophyll (HNLC) regions of the Southern Ocean, Equatorial Pacific, Pacific Subpolar gyre (Martin & Fitzwater, 1988; Coale *et al*., 1996; Boyd *et al*., 2000, 2004; Tsuda *et al*., 2003) and some coastal upwelling regions (Hutchins & Bruland, 1998). In these regions the ratio of Fe to nitrate in upwelled waters is sub-optimal for phytoplankton growth (Bruland *et al*., 2001). Additional Fe sources, including atmospheric deposition (Fung *et al*., 2000), are insufficient to compensate for this deficit, resulting in depleted dissolved Fe concentrations that chronically limit phytoplankton growth and prevent the complete drawdown of macronutrients (Martin & Fitzwater, 1988; Coale *et al*., 1996, Hutchins & Bruland, 1998; Boyd *et al*., 2000).

In contrast, the North Atlantic has no permanent HNLC regions. In the permanently stratified oligotrophic subtropical and tropical North Atlantic the availability of macronutrients limits phytoplankton production year round (Graziano *et al*., 1996; Mills *et al*., 2004). Conversely, deep winter overturning injects nitrate into surface waters of the central and northern North Atlantic causing transient high nutrient conditions. These high macronutrient inputs result in the development of a marked spring bloom with accumulation of phytoplankton biomass, and significant sequestration of atmospheric CO_2 (Honjo & Manganini, 1993). The initiation of this bloom principally results from the seasonal increase in incident surface irradiance during spring which triggers the development of water column stratification and, thus, a shoaling of the mixed layer to depths less then the critical depth (Sverdrup, 1953). This transient period, during which the average light intensity of the mixed layer is increasing and nutrient concentrations are high, provides a window of opportunity for the onset of the spring bloom. However, the precise timing of the bloom is affected by interannual variability in climate (Platt *et al*., 2003). Despite the low ratios of Fe to nitrate in upwelled waters in the North Atlantic (Fung *et al*., 2000; Wu & Boyle, 2002) the spring bloom results in complete removal of nitrate from the mixed layer. The supply of Fe from mineral aerosol of African sources (Gao *et al*., 2001) is considered to be sufficient to preclude Fe limitation of phytoplankton growth in the

Correspondence: Julie La Roche, Marine Biogeochemistry, Leibniz Institute für Meereswissenschaften, D-24105 Kiel, Germany, e-mail: jlaroche@ifm-geomar.de

North Atlantic. Contrary to this paradigm, our results establish that the *in situ* phytoplankton community in certain regions of the North Atlantic is Fe limited, suggesting a significant role for aeolian Fe supply in controlling interannual variability in spring bloom progression.

Methods

The study was carried out in the central North Atlantic, a region north of the maximal dust deposition zone (Fig. 1) in March and April 2004 as part of the Meteor 60 Transient Tracers Revisited expedition. The maximum efficiency (F_v/F_m) and effective cross-section (σ_{PSII}) of photosystem II were determined by fast repetition rate fluorometry (FRRf) (Kolber *et al*., 1998) on near surface samples collected using a trace-metal clean pumping system and fish towed at $\sim$3 m and from samples collected in Niskin bottles (General Oceanics Inc. Miami, Florida, USA). Samples were dark adapted for

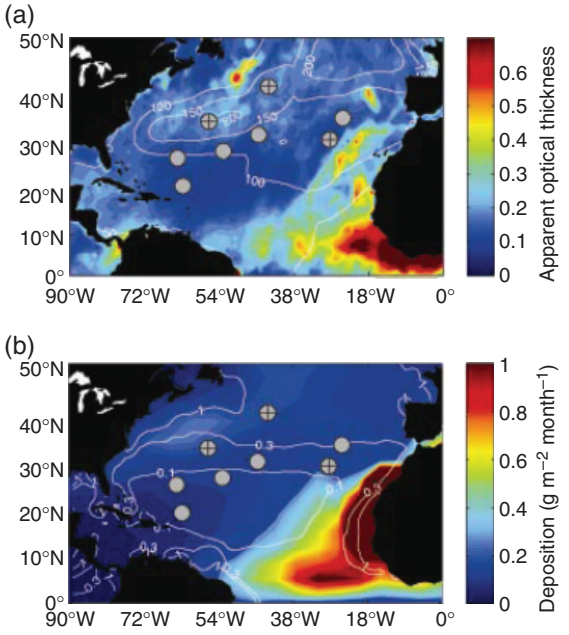

Fig. 1 Mixed layer depths, chlorophyll distribution and dust deposition to the central North Atlantic. (a) Mean apparent optical thickness derived from MODIS satellite data as a proxy of atmospheric dust load for March and April 2004 (colours) with climatological mixed layer depths (contours) superimposed. (b) Modelled mean monthly dust deposition rates for March–April (Tegen & Fung, 1995; Tegen *et al*., 2004) (colours) with mean SeaWiFS-derived chlorophyll concentration ($\mu g\,L^{-1}$) for April (contours) superimposed. Locations of nutrient enrichment bioassay experiments are indicated, crossed symbols indicate experiments presented in Fig. 2.

>30 min at *in situ* temperatures before measurement using a Chelsea Instruments FASTtracka™ FRRf (Chelsea Technologies Group, West Molesey, UK). No differences in F_v/F_m measured on trace clean samples or samples collected using Niskin bottles were observable over the short dark adaptation period. Blanks for individual samples analysed by FRRf were prepared by gentle sequential filtration through Whatman *GF/F* and 0.2 μm polycarbonate filters before measurement using identical protocols. All reported values of F_v/F_m have been corrected for blank effects (Cullen & Davis, 2003).

Vertical profiles of temperature, salinity and chlorophyll fluorescence were obtained using a CTD system from Seabird Electronic (model 911) (Sea-Bird Electronics, Bellevue, Washington, USA) mounted with a Dr Hardt fluorometer.

Nutrient addition bioassay experiments were performed using previously described methods (Mills *et al*., 2004). Nutrients were added alone and in combination to final concentrations of 1.0 μM NH_4^+, 1.0 μM NO_3^-, 0.2 μM NaH_2PO_4 and 2.0 nM $FeCl_3$. Additions of Saharan soil (Guieu *et al*., 2002) (D1) and atmospherically processed Saharan aerosol (D2), collected in Turkey using a net, were also made to final concentrations of 2 mg L^{-1} to assess the potential impact of dust deposition on ecosystem processes. Trace-metal clean techniques were used throughout, with all bottles and sampling equipment acid washed and all manipulations performed in a dedicated clean laboratory under a Class 100 laminar flow hood. Surface samples were pumped into a 60 L carboy using a PTFE diaphragm pump before siphoning into 1.18 L bottles. Incubations were performed at sea-surface temperature with light attenuated to 20% surface irradiance using blue filters (Lagoon blue, Lee filters #172) (Lee Filters, Andover, UK). All treatments were performed in triplicate. For each treatment, parallel incubations over 48 h were performed for $^{14}CO_2$ incorporation, and chlorophyll and biophysical measurements (Lohrenz *et al*., 1992; Welschmeyer, 1994; Kolber *et al*., 1998). Initial rate measurements were determined over the first 24 h on unamended samples with the final rate measurements performed over the second 24 h. Other variables were determined at the beginning and end of the experiments. $^{14}CO_2$ incorporation was measured by adding 50 μCi ^{14}C-bicarbonate to each bottle.

Total dissolved Fe (DFe) was analysed using flow-injection chemiluminescence (Bowie *et al*., 1998). Samples were filtered using 25 mm diameter Gelman™ (Pall Gelman, New York, USA) syringe filters (0.2 μm pore size, PTFE membrane). A 12 h acidification and 12 h reduction period was allowed before analysis of DFe. Along track sampling at approximately 12 h intervals indicated that differences in initial DFe concentration in the surface waters used for bioassay experiments re-

sulted from regional variation in DFe, rather then local patchiness. Fe dissolution experiments were also performed by measuring increases in ambient DFe over 8 days following the addition of various concentrations (0.1, 2 and 10 mg L^{-1}) of the dusts to 0.2 μm filtered seawater. Macronutrients were measured using the methods described in Grasshoff *et al.* (1999).

Treatment means from bioassay experiments were compared using a one-way ANOVA (all treatments including dusts) and 3-way ANOVA (N, P, Fe and all interactions) followed by a Tukey–Kramer means comparison test ($\alpha = 0.05$).

Results

Low surface chlorophyll and macronutrient concentrations indicated oligotrophic conditions at the southern stations (Table 1). Satellite and *in situ* data indicated that northern stations were sampled during the spring bloom. Bloom stations were characterized by deep surface mixed layers, higher macronutrient concentrations and higher chlorophyll concentrations (Table 1, Fig. 1). DFe concentrations ranged from 0.21 to 0.51 nM, with the highest values at the south-west stations (Table 1). Community production and biomass were limited by the availability of fixed nitrogen in oligotrophic waters (Graziano *et al.*, 1996; Mills *et al.*, 2004), and Fe addition had no effect on any measurements in these regions (Fig. 2).

As expected, for the two experiments performed at stations with high (>1 μM N) surface macronutrient concentrations, community productivity and chlorophyll increased above initial values in unamended incubations (Fig. 2). However at 42°N, 42°W, Fe addition produced a further 1.4–2-fold increase of net community production and chlorophyll concentration (Fig. 2). In contrast to systems where a lag phase precedes the alleviation of Fe limitation (Martin & Fitzwater, 1988; Hutchins & Bruland, 1998), the rapid response to Fe addition was observed despite the relatively short (48 h) experimental duration. Net growth rates calculated using chlorophyll concentrations averaged 0.28 day^{-1} in −Fe treatments compared with 0.56 day^{-1} in + Fe treatments. Independent estimates of net community growth calculated by normalizing $^{14}CO_2$ incorporation from 24–48 h to particulate organic carbon were 1.04 day^{-1} in + Fe treatments compared with 0.70 day^{-1} in −Fe treatments and 0.55 day^{-1} for the initial 24 h. In contrast chlorophyll specific carbon uptake was invariant between treatments, suggesting an increase in the chlorophyll : carbon ratio of the phytoplankton in the + Fe treatments. Analytical flow cytometry, 18S rDNA sequencing and high-performance liquid chromatography indicated that the Fe-limited station was dominated by a mixed flagellate

Table 1 Initial conditions and limiting nutrient for bioassay experiments

	21°N 62°W	28°N 64°W	29°N 53°W	31°N 27°W	32°N 44°W	36°N 24°W	35°N 56°W	42°N 42°W
SST (°C)	25.4	22.7	21.4	19.7	19.6	18.1	18.5	16.2
NO_3^- (μm)	<0.03	<0.03	<0.03	<0.03	<0.03	0.10 (0.09)	1.52 (0.06)	3.80 (0.69)
DFe (nM)	0.51 (0.05)	0.47 (0.01)	0.21 (0.02)	0.25 (0.01)	0.27 (0.03)	0.29 (0.03)	0.28 (0.04)	0.33 (0.03)
DFe : NO_3^- (mmol mol^{-1})	>17	>16	>7	>8	>12	2.9	0.18	0.09
Chl *a* (μg L^{-1})	0.067 (0.006)	0.043 (0.002)	0.045 (0.006)	0.090 (0.01)	0.081 (0.004)	0.24 (0.07)	0.57 (0.09)	0.94 (0.48)
MLD* (m)	133	67	68	122	129	144	380 (*159*)†	519 (*337*)†
Z_{CR}/MLD‡	>1	>1	>1	>1	>1	>1	0.68 (*>1*)	0.4 (*0.62*)
Limiting nutrient§	N (NP)	N (NP)	N (NP)	N (NP)	N (NP)	N (NP)	–	Fe

Mean (± standard errors) of triplicate samples: except for SST and DFe where an individual sample was analysed four times.
*Mixed layer depth (MLD) determined as 0.5 °C temperature difference from surface value from CTD profiles for comparison with climatological data (Fig. 1a).
†At these stations there were small thermoclines (~ 0.04 °C) at 159 and 337 m. Above the thermocline, chlorophyll levels were high and fairly constant. Below the thermocline, chlorophyll declined (data not shown). We conclude that the presence of structure in both biomass and temperature indicates that rigorous mixing was not penetrating throughout the surface layer. The effective mixing depth for phytoplankton growth was thus taken as the base of the surface chlorophyll layer.
‡Critical depth (Z_{CR}), as a proportion of mixed layer depth, calculated assuming compensation irradiance (I_C) = 1.3 mol photons m^{-2} day^{-1} (Siegel *et al.*, 2002). Separate calculation for effective mixing depth shown in italics.
§Nutrient resulting in significant increases in net community production and chlorophyll. (NP) indicates secondary *P* limitation.

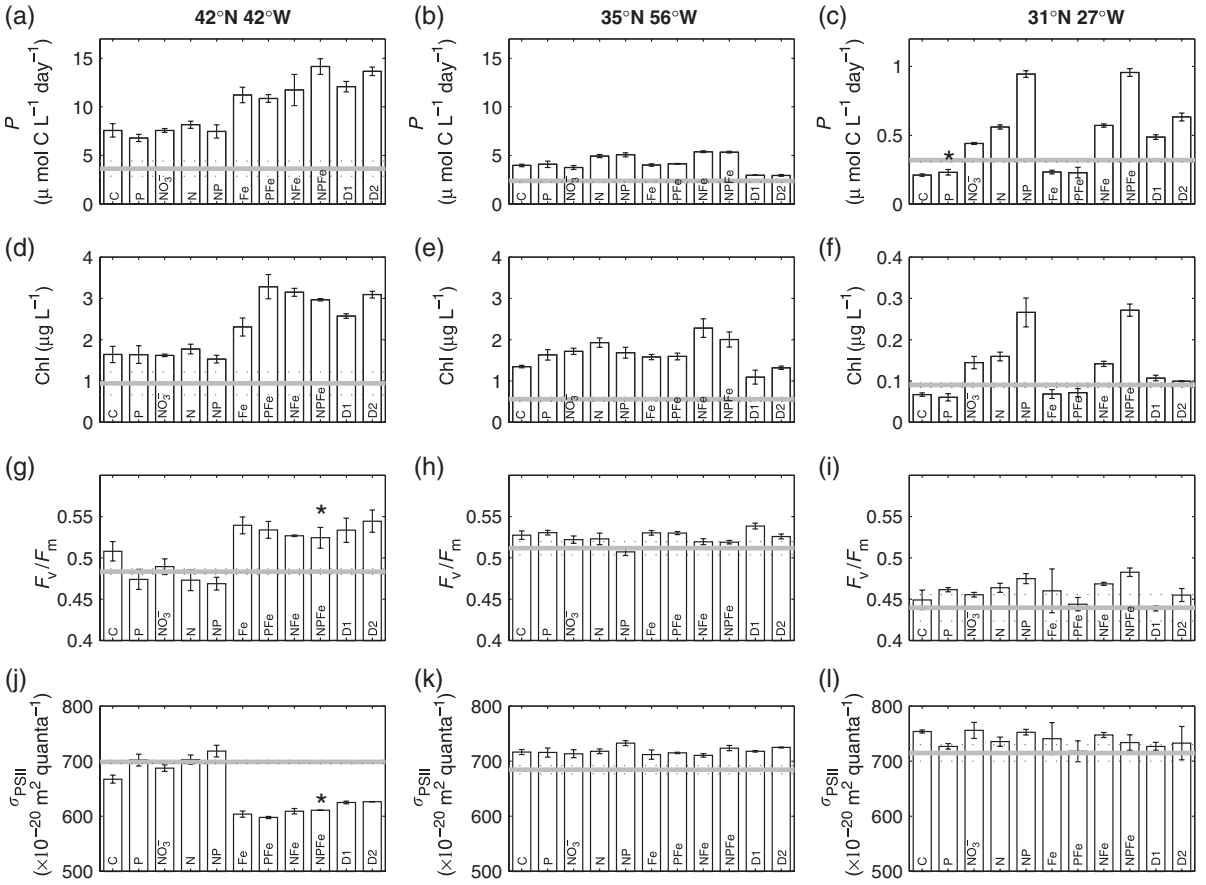

Fig. 2 Results of nutrient enrichment bioassay experiments after 48 h incubation with the indicated nutrients at three locations. (a–c) Net community production. (d–f) Chlorophyll *a* concentration. (g–i) F_v/F_m. (j–l) σ_{PSII}. Shown are means ± standard errors, $n = 3$ for all variables expect * where $n = 2$. Initial values are indicated by solid lines (dashed lines are standard error). Nitrogen was added as NH_4NO_3 except for the NO_3^- treatment.

community in contrast to macronutrient-limited stations, where prokaryotes dominated (results not shown). A 1.7-fold increase in NO_3^- utilization, was also observed on relief of Fe limitation for the station at 42°N.

DFe concentrations measured after 48 h were indistinguishable between initial values and both Fe amended and nonamended treatments at 42°N. Conversely, for stations where no biological response to Fe addition was observed, after 2 days DFe was 0.05–0.56 nM higher in treatments amended with Fe than in nonamended controls. Measured DFe is the sum of inorganic (<1–2%) and both labile and refractory dissolved organic Fe species (Rue & Bruland, 1995). As such DFe represents the maximum potentially bioavailable pool of Fe. The lack of any decrease in DFe for nonamended treatments, despite clear evidence for Fe limitation at 42°N, suggests that many of the organic species present were unavailable to the extant phytoplankton population (Hutchins *et al*., 1999).

Measurements of the maximum efficiency (F_v/F_m) and effective cross-section (σ_{PSII}) of photosystem II for initial samples and samples collected from a number of depths (0–100 m) at 42°N were equal to those from −Fe treatments (Fig. 2). Increases of F_v/F_m and declines of σ_{PSII} in response to addition of Fe indicated that Fe was a limiting nutrient *in situ* (Fig. 2). The responses that we observed in the bioassay are consistent with responses of Fe-limited phytoplankton to Fe resupply, observed in pure cultures grown under controlled laboratory conditions (Greene *et al*., 1991; Geider *et al*., 1993). Biophysical measurements, thus, confirmed *in situ* Fe stress of the phytoplankton at the time of sampling (Geider *et al*., 1993; Behrenfeld *et al*., 1996; Kolber *et al*., 1998).

At this station, addition of Saharan soils or atmospherically processed aerosols induced biological responses that were similar to + Fe treatments (Fig. 2) thus relieving the Fe limitation. Based on our dissolution experiments we calculate that 2 mg L^{-1} additions

increased DFe by ~0.05 nM for the Saharan soil and ~0.2 nM for the atmospherically processed dust. Nitrate drawdown at 42°N was ~2 and 2.3 μM greater for the two dust additions than in the −Fe treatments. Taking a range of cellular Fe:N ratios from 0.03 to 0.1 mmol mol^{-1} (Sunda & Huntsman, 1995, 1997; Ho *et al*., 2003), this drawdown requires 0.06–0.23 nM Fe.

Discussion

Fe requirements of phytoplankton and Fe supply during the spring bloom

Phytoplankton cellular Fe:N demand is governed by the relative cellular concentrations of Fe- and N-rich components, which vary between taxa and with growth conditions (Sunda & Huntsman, 1995, 1997; Ho *et al*., 2003). In particular, cellular Fe:N ratios are around an order of magnitude higher in coastal than in oceanic species (Sunda & Huntsman, 1995). Acclimation to low light intensity increases the demand for Fe-rich photosynthetic electron transfer chain components, and hence the cellular Fe demand, in many taxa (Sunda & Huntsman, 1997; Strzepek & Harrison, 2004). Assuming relatively constant cellular C:N ratios (Greene *et al*., 1991; Geider & LaRoche, 2002), we estimate that for coastal taxa, cellular Fe:N ratios <0.1 mmol mol^{-1} would significantly limit growth ($\mu < 0.6\mu_{max}$), particularly at low light (Sunda & Huntsman, 1995, 1997; Ho *et al*., 2003). For oceanic species a ratio of <0.1 mmol mol^{-1} represents the onset of Fe limitation, however even under low light conditions, reasonably high growth rates are maintained at cellular Fe:N ratios as low as 0.03 mmol mol^{-1} (Sunda & Huntsman, 1995). This range of Fe:N ratios is comparable with estimates from natural populations (Twining *et al*., 2004).

Removal of macronutrients following input to the surface ocean requires a newly available source of Fe. Hence, although recycling of Fe within surface waters may be important for prolonging bloom duration (Bowie *et al*., 2001), such regenerated Fe cannot support the initial accumulation of biomass. Fe limitation, thus, occurs in both open ocean and coastal upwelling regions when high inputs of macronutrients are not accompanied by sufficient Fe to satisfy demands for optimal phytoplankton growth (Martin & Fitzwater, 1988; Coale *et al*., 1996; Hutchins & Bruland, 1998; Boyd *et al*., 2000; Bruland *et al*., 2001). The supply of nitrate for the spring bloom in the north of the subtropical gyre in the North Atlantic results from deep winter mixing and Ekman transport (Sverdrup, 1953). These mechanisms supply DFe and nitrate at a ratio of <0.03 mmol mol^{-1} (Fig. 3). As discussed above, this ratio is suboptimal for phytoplankton growth, consistent with our observation (Fig. 2) that Fe supply does not support maximal growth rates in this region during the early spring bloom. As noted above, our results suggest that the measured DFe is likely to include forms that are unavailable to certain members of the phytoplankton community (Hutchins *et al*., 1999). The potential bioavailable Fe pool and DFe to nitrate supply ratio of <0.03 mmol mol^{-1} were, thus, both likely to be overestimates.

Efficient utilization of nitrate during the spring bloom, therefore, requires an additional supply of Fe. Aeolian deposition is the main source of DFe to the North Atlantic (Gao *et al*., 2001) (Fig. 1), although lateral inputs from nearby continental shelves may also be significant (Martin *et al*., 1993). We hypothesize that dust deposition during winter and spring can increase the rate of nitrate consumption during the bloom (Figs 3 and 4). Interannual variability in aeolian dust supply may, thus, be a significant factor contributing to variability of bloom dynamics in the North Atlantic.

Fe light colimitation of primary productivity during the spring bloom

Convergence of Ekman transports (Williams & Follows, 1998) and winter mixing, results in seasonally deep mixed layers on the northern flanks of the subtropical gyre in spring (Fig. 1a, Table 1). We assessed the degree of light limitation using the critical depth hypothesis (Sverdrup, 1953; Siegel *et al*., 2002). The critical depth (Z_{CR}) is defined as the point where integrated water column community respiration and photosynthesis are equal (Sverdrup, 1953). Net community production can, thus, occur when the mixed layer is less than Z_{CR} (Sverdrup, 1953). Z_{CR} was estimated using the incident surface daily irradiance (I_0), the diffuse attenuation coefficient (K) and the community compensation irradiance (I_C), following:

$$\frac{1}{KZ_{CR}}(1 - e^{KZ_{CR}}) = \frac{I_C}{I_0} = \frac{R_0}{P_0}, \quad (1)$$

where $R_0 = R(z)$ is the community respiration and P_0 is the photosynthetic rate at the surface (Sverdrup, 1953; Siegel *et al*., 2002). The surface chlorophyll concentration was used to calculate K from $K = 0.1211\ \mathrm{Chl}^{0.428}$ (Siegel *et al*., 2002). For typical values of I_0 Eqn (1) can therefore be simplified to

$$Z_{CR} = \frac{I_0}{0.1211\mathrm{Chl}^{0.428} I_C}. \quad (2)$$

The immediate prebloom mixed layer depth, surface irradiance and chlorophyll concentration can be used to calculate I_C by assuming that Z_{CR} is equal to the mixed layer depth at bloom initiation (Siegel *et al*., 2002). Using satellite-derived I_0 (32 mol photons m^{-2} day^{-1}) and Sea-

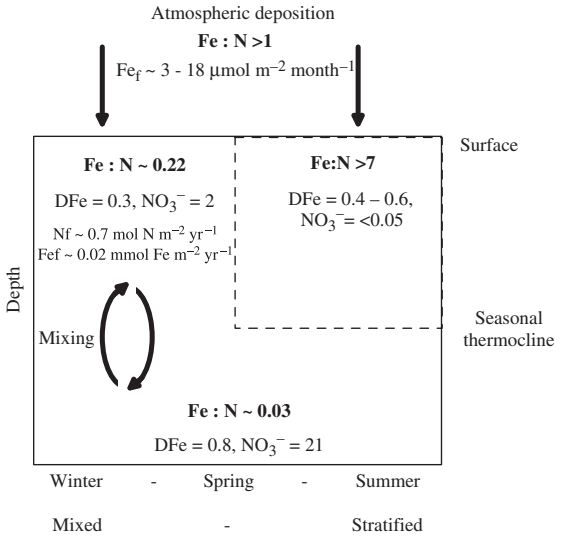

Fig. 3 Supply of N and Fe to the North Atlantic subtropical gyre. Concentrations of total dissolved Fe (DFe) (nM) and NO_3^- (µM) are from this study and others (Martin *et al.*, 1993; Wu & Luther, 1994; Wu & Boyle, 2002). Bold values are mean DFe : N (mmol mol^{-1}). The postbloom stratified period in the north of the gyre is analogous to the permanently stratified southern regions. In the winter and spring, deep mixing, the major supply mechanism of macronutrients, results in DFe : N supply ratios <0.03 mmol mol^{-1} (shown). Additional lateral Ekman transport from the subpolar gyre (Williams & Follows, 1998) would provide Fe and N in a similar ratio (Martin *et al.*, 1993). By comparing NO_3^- profiles from stratified and mixed stations we calculated nitrogen (N_f) and iron (Fe_f) mixing fluxes of 0.7 mol N m^{-2} yr^{-1} and ~ 0.02 mmol Fe m^{-2} yr^{-1}at 42°N. Taking typical phytoplankton cellular Fe : N of 0.03–0.1 mmol mol^{-1} (see text), up to an extra 0.05 mmol Fe m^{-2} is required for efficient nitrate removal. Atmospheric deposition rates in the vicinity of 42°N, 42°W of 150–190 mg m^{-2} month^{-1} (Tegen & Fung, 1995; Tegen *et al.*, 2004, personal communication) (Fig. 1) are equivalent to 0.003–0.018 mmol Fe m^{-2} month^{-1} assuming 2–10% solubility for aerosol Fe and 5% Fe by weight (Goudie & Middleton, 2001; Jickells & Spokes, 2001; Boyle *et al.*, 2005). Thus, interannual variability of atmospheric deposition in winter and spring will likely control the rate of nitrate depletion.

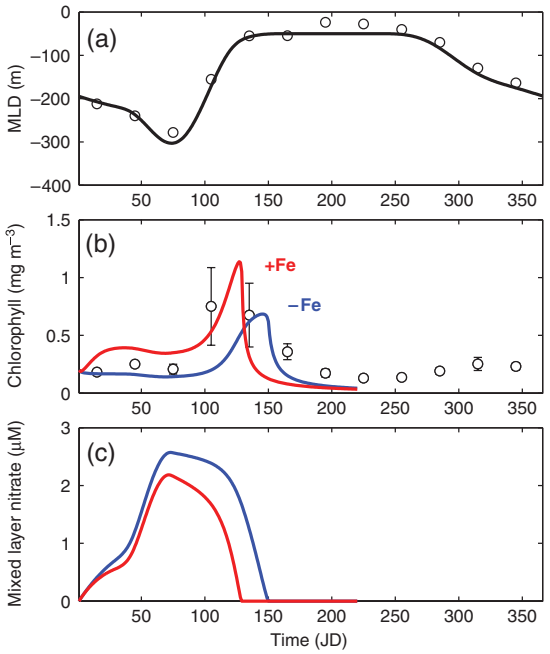

Fig. 4 Numerical model demonstrating the potential influence of iron availability on spring bloom magnitude, timing and progression at 42°N, 42°W. (a) Climatological (○) monthly mean mixed layer depths (0.5 °C difference from surface) from World Ocean Atlas 98 (http://las.pfeg.noaa.gov/las/) and model mixed layer depth. (b) SeaWiFS-derived surface chlorophyll concentrations (○ = monthly means and standard deviation for 1998–2004) compared with model output under −Fe and + Fe conditions, respectively, referring to normal and Fe-fertilized conditions in the HNLC regions modelled in Edwards *et al.* (2004). (c) Model-derived mixed layer nitrate concentrations under −Fe and + Fe conditions.

WiFS-derived prebloom chlorophyll concentrations, we calculated that $I_C = 1.2$–1.3 mol photons m^{-2} day^{-1} at 35°N and 42°N compared with estimates of 1.3 ± 0.3 throughout the North Atlantic (Siegel *et al.*, 2002). Assuming this value for I_C we calculated Z_{CR} during the bloom. Net community production was close to light limitation at both of the high macronutrient sites, although the potential for light limitation was less severe at 35°N than at 42°N (Table 1).

The critical depth hypothesis is formulated for nutrient replete conditions. Low irradiance increases cellular Fe demand (Raven, 1990; Sunda & Huntsman, 1997; Strzepek & Harrison, 2004) and deep mixed layers were, therefore, likely to have contributed to the development of Fe stress at 42°N. Colimitation by Fe and light (Sunda & Huntsman, 1997) may, therefore, significantly affect the critical depth in this region. Assuming that Fe limitation affects photosynthesis, but not respiration, the 1.6-fold increase in community production observed upon Fe addition (Fig. 2) could increase the compensation irradiance by an equivalent amount, deepening the critical depth by 60%. Such a deepening could potentially result in an earlier initiation of the bloom and/or higher accumulation of chlorophyll in the surface.

Fe limitation of spring bloom development and nitrate utilization

Shoaling of the mixed layer traps unused macronutrients below the seasonal thermocline, setting an upper limit on the total integrated biomass of the bloom. We

used a simple numerical model (Edwards *et al*., 2004) to assess the potential for alleviation of Fe limitation to increase total biomass and nutrient drawdown, as well as alter bloom timing and progression. Changes in the magnitude, and delay in the initiation and progression of the spring bloom, would likely affect the coupling of primary production to higher trophic levels and can ultimately be a critical determinant of larval fish survival (Platt *et al*., 2003).

The model of Edwards *et al*. (2004) was extended to include a nitrate limitation term, then run under the two Fe scenarios using a prescribed seasonal mixed layer based on climatological data. The −Fe and +Fe scenarios were parameterized according to Edwards *et al*. (2004), with the exception that the biomass loss term was set a factor of two lower under both conditions. In contrast to Edwards *et al*. (2004), we assumed that the C : N ratio is insensitive to Fe limitation (Greene *et al*., 1991) and hence the N : Chl ratio increases in proportion to the increase in the C : Chl ratio under conditions of Fe limitation (Greene *et al*., 1991). Nitrate limitation was parameterized as a reduction in productivity following a simple Michaelis–Menten function of mixed layer nitrate concentration with a half saturation constant of 0.5 μM. Sensitivity analysis using differing loss term parameterization and initial slopes for the *P* vs. *E* curve (Edwards *et al*., 2004) resulted in qualitatively similar results. Model output is shown for the spring–summer period only and supports the hypothesis that relief from Fe limitation can result in an earlier bloom initiation (Fig. 4). Integrated nitrate removal during spring for the +Fe scenario (0.5 mol N m^{-2}) was ~70% higher than for the −Fe scenario (0.3 mol N m^{-2}) suggesting that relief from Fe limitation also has the potential to influence the integrated new production occurring over the bloom period.

Conclusions

We interpret our results in terms of a latitudinal macronutrient gradient (Fig. 1, Table 1) and the sequence of events occurring during a bloom in a region impacted by dust deposition and deep surface mixed layers (Wu & Boyle, 2002). During the early bloom period, the deep-mixed layer imposes low mean light levels, increasing cellular Fe demand (Raven, 1990; Sunda & Huntsman, 1997), while dust deposition to surface waters produces only minor increases in DFe concentrations. As surface stratification develops, shoaling of the mixed layer results in increased light availability, decreasing the cellular Fe demand (Raven, 1990; Sunda & Huntsman, 1997). Deposition events will also result in higher DFe concentrations. Postbloom, macronutrient limitation reduces community Fe uptake (Wu & Luther, 1994; Wu & Boyle, 2002). Continued dust deposition then increases DFe concentrations in surface waters (Wu & Luther, 1994; Wu & Boyle, 2002), further increasing DFe : N (Table 1, Fig. 3). Thus, consistent with our results from oligotrophic stations and previous findings (Graziano *et al*., 1996; Mills *et al*., 2004), Fe limitation of community production in the central North Atlantic is unlikely under postbloom, or permanently stratified conditions, but likely during the early bloom period (Wu & Boyle, 2002).

Our results and others (Martin *et al*., 1993; Fung *et al*., 2000; Mills *et al*., 2004) suggest that Fe availability is a significant determinant of phytoplankton productivity in the North Atlantic. Fe supplied via dust deposition may influence the initiation, duration and magnitude of the spring bloom. Dust storms and deposition events are highly episodic and have varied in frequency over scales ranging from interannual to glacial–interglacial periods (Goudie & Middleton, 2001). These changes in aeolian Fe inputs may have influenced spring bloom dynamics over similar time scales. Predicting ocean ecosystem response to future changes in dust deposition, resulting from climate or land-use change (Goudie & Middleton, 2001; Tegen *et al*., 2004; Jickells *et al*., 2005) requires improved assessment of the extent of Fe limitation, which appears to vary both spatially and temporally in the modern ocean.

Acknowledgements

We thank the captain and crew of the F/S Meteor and the scientists aboard the Meteor 60 Transient Tracers Revisited cruise, especially D. Wallace. K. Nachtigall, P. Fritsche, F. Malien, and M. Schütt provided technical support. C. Guieu and N. Kubilay provided the dust samples, and I. Tegen provided estimates of dust deposition. The first five authors made equal contributions to the success of the experiments at sea. This work was supported by DFG grant WA1434/6-1 to D. Wallace and K. L., and RO2138/4-2 to J. L. R., and NERC grants to R. J. G. and E. P. A.

References

Behrenfeld MJ, Bale AJ, Kolber ZS *et al*. (1996) Confirmation of iron limitation of phytoplankton photosynthesis in the equatorial Pacific Ocean. *Nature*, **383**, 508–511.

Bowie AR, Achterberg EP, Mantoura RFC *et al*. (1998) Determination of sub-nanomolar levels of iron in seawater using flow injection with chemiluminescence detection. *Analytica Chimica Acta*, **361**, 189–200.

Bowie AR, Maldonado MT, Frew RD *et al*. (2001) The fate of added iron during a mesoscale fertilization experiment in the Southern Ocean. Deep-Sea Research Part II - Topical studies in oceanography, **48**, 2703–2743.

Boyd PW, Law CS, Wong CS *et al*. (2004) The decline and fate of an iron-induced subarctic phytoplankton bloom. *Nature*, **428**, 549–553.

Boyd PW, Watson AJ, Law CS *et al*. (2000) A mesoscale phytoplankton bloom in the polar Southern Ocean stimulated by iron fertilization. *Nature*, **407**, 695–702.

Boyle EA, Bergquist BA, Kayser RA *et al*. (2005) Iron, manganese, and lead at Hawaii Ocean Time-series station ALOHA: temporal variability and an intermediate water hydrothermal plume. *Geochimica et Cosmochimica Acta*, **69**, 933–952.

Bruland KW, Rue EL, Smith GJ (2001) Iron and macronutrients in California coastal upwelling regimes: implications for diatom blooms. *Limnology and Oceanography*, **46**, 1661–1674.

Coale KH, Johnson KS, Fitzwater SE *et al*. (1996) A massive phytoplankton bloom induced by an ecosystem-scale iron fertilization experiment in the equatorial Pacific Ocean. *Nature*, **383**, 495–501.

Cullen JJ, Davis RF (2003) The blank can make a big difference in oceanographic measurements. *Limnology and Oceanography Bulletin*, **12**, 29–35.

Edwards AM, Platt T, Sathyendranath S (2004) The high-nutrient, low-chlorophyll regime of the ocean: limits on biomass and nitrate before and after iron enrichment. *Ecological Modelling*, **171**, 103–125.

Fung IY, Meyn SK, Tegen I *et al*. (2000) Iron supply and demand in the upper ocean (vol 14, pg 281, 2000). *Global Biogeochemical Cycles*, **14**, 281–295.

Gao Y, Kaufman YJ, Tanre D *et al*. (2001) Seasonal distributions of aeolian iron fluxes to the global ocean. *Geophysical Research Letters*, **28**, 29–32.

Geider RJ, LaRoche J (2002) Redfield revisited: variability of C : N : P in marine microalgae and its biochemical basis. *European Journal of Phycology*, **37**, 1–17.

Geider RJ, LaRoche J, Greene RM *et al*. (1993) Response of the photosynthetic apparatus of *Phaeodactylum tricornutum* (Bacillariophyceae) to nitrate, phosphate, or iron starvation. *Journal of Phycology*, **29**, 755–766.

Goudie AS, Middleton NJ (2001) Saharan dust storms: nature and consequences. *Earth-Science Reviews*, **56**, 179–204.

Grasshoff K, Kremling K, Ehrhardt M (1999) *Methods of Seawater Analysis*. Wiley, New York.

Graziano LM, Geider RJ, Li WKW *et al*. (1996) Nitrogen limitation of North Atlantic phytoplankton: analysis of physiological condition in nutrient enrichment experiments. *Aquatic Microbial Ecology*, **11**, 53–64.

Greene RM, Geider RJ, Falkowski PG (1991) Effect of iron limitation on photosynthesis in a marine diatom. *Limnology and Oceanography*, **36**, 1772–1782.

Guieu C, Bozec Y, Blain S *et al*. (2002) Impact of high Saharan dust inputs on dissolved iron concentrations in the Mediterranean Sea. *Geophysical Research Letters*, **29**, 1911, doi: 10.1029/2001GL014454.

Ho TY, Quigg A, Finkel ZV *et al*. (2003) The elemental composition of some marine phytoplankton. *Journal of Phycology*, **39**, 1145–1159.

Honjo S, Manganini SJ (1993) Annual biogenic particle fluxe sto the interior of the North Atlantic Ocean; studied at 34°N 21°W and 48°N 21°W. *Deep-Sea Research I*, **40**, 587–607.

Hutchins DA, Bruland KW (1998) Iron-limited diatom growth and Si : N uptake ratios in a coastal upwelling regime. *Nature*, **393**, 561–564.

Hutchins DA, Witter AE, Butler A *et al*. (1999) Competition among marine phytoplankton for different chelated iron species. *Nature*, **400**, 858–861.

Jickells TD, An ZS, Andersen KK *et al*. (2005) Global iron connections between desert dust, ocean biogeochemistry, and climate. *Science*, **308**, 67–71.

Jickells TD, Spokes LJ (2001) Atmospheric iron inputs to the oceans. In: *The Biogeochemistry of Iron in Seawater* (eds. Turner DR, Hunter K), Wiley, Chichester. 85–121.

Kolber ZS, Prasil O, Falkowski PG (1998) Measurements of variable chlorophyll fluorescence using fast repetition rate techniques: defining methodology and experimental protocols. *Biochimica et Biophysica Acta. Bioenergetics*, **1367**, 88.

Lohrenz SE, Wiesenburg DA, Rein CR *et al*. (1992) A Comparison of *In situ* and Simulated *In situ* Methods for Estimating Oceanic Primary Production. *Journal of Plankton Research*, **14**, 201–221.

Martin JH, Fitzwater SE (1988) Iron deficiency limits phytoplankton growth in the north-east Pacific subarctic. *Nature*, **331**, 341–343.

Martin JH, Fitzwater SE, Gordon RM *et al*. (1993) Iron, primary production and carbon nitrogen flux studies during the JGOFS North Atlantic bloom experiment. *Deep-Sea Research Part II – Topical Studies in Oceanography*, **40**, 115–134.

Mills MM, Ridame C, Davey M *et al*. (2004) Iron and phosphorus co-limit nitrogen fixation in the eastern tropical North Atlantic. *Nature*, **429**, 292–294.

Platt T, Fuentes-Yaco C, Frank KT (2003) Spring algal bloom and larval fish survival. *Nature*, **423**, 398–399.

Raven JA (1990) Predictions of Mn and Fe use efficiencies of phototrophic growth as a function of light availability for growth and C assimilation pathway. *New Phytologist*, **116**, 1–18.

Rue EL, Bruland KW (1995) Complexation of iron(III) by natural organic-ligands in the Central North Pacific as determined by a new competitive ligand equilibration adsorptive cathodic stripping voltammetric method. *Marine Chemistry*, **50**, 117–138.

Siegel DA, Doney SC, Yoder JA (2002) The North Atlantic spring phytoplankton bloom and Sverdrup's critical depth hypothesis. *Science*, **296**, 730–733.

Strzepek RF, Harrison PJ (2004) Photosynthetic architecture differs in coastal and oceanic diatoms. *Nature*, **431**, 689–692.

Sunda WG, Huntsman SA (1995) Iron uptake and growth limitation in oceanic and coastal phytoplankton. *Marine Chemistry*, **50**, 189–206.

Sunda WG, Huntsman SA (1997) Interrelated influence of iron, light and cell size on marine phytoplankton growth. *Nature*, **390**, 389–392.

Sverdrup HU (1953) On conditions for the vernal blooming of phytoplankton. Journal du Conseil Permanent International Pour 1. Exploration de la Mer, **18**, 287–295.

Tegen I, Fung I (1995) Contribution to the Atmospheric Mineral Aerosol Load from Land-Surface Modification. *Journal of Geophysical Research – Atmospheres*, **100**, 18707–18726.

Tegen I, Werner M, Harrison SP *et al*. (2004) Relative importance of climate and land use in determining present and future

global soil dust emission. *Geophysical Research Letters*, **31**. L05105, doi: 10.1029/2003GL019216

Tsuda A, Takeda S, Saito H *et al*. (2003) A mesoscale iron enrichment in the Western subarctic Pacific induces a large centric diatom bloom. *Science*, **300**, 958–961.

Twining BS, Baines SB, Fisher NS *et al*. (2004) Cellular iron contents of plankton during the Southern Ocean Iron Experiment (SOFeX). *Deep-Sea Research Part I – Oceanographic Research Papers*, **51**, 1827–1850.

Welschmeyer NA (1994) Fluorometric analysis of chlorophyll-a in the presence of chlorophyll-b and pheopigments. *Limnology and Oceanography*, **39**, 1985–1992.

Williams RG, Follows MJ (1998) The Ekman transfer of nutrients and maintenance of new production over the North Atlantic. *Deep-Sea Research Part I – Oceanographic Research Papers*, **45**, 461–489.

Wu JF, Boyle E (2002) Iron in the Sargasso Sea: implications for the processes controlling dissolved Fe distribution in the ocean. *Global Biogeochemical Cycles*, **16**. 1086, doi: 10.1029/2001GB001453, 2002

Wu JF, Luther GW (1994) Size-fractionated iron concentrations in the water column of the Western North-Atlantic Ocean. *Limnology and Oceanography*, **39**, 1119–1129.

Paper D: *Relative influence of nitrogen and phosphorus availability on phytoplankton physiology and productivity in the oligotrophic sub-tropical North Atlantic Ocean*

Synopsis

This manuscript investigated nutrient limitations of primary productivity and phytoplankton physiology using the same nutrient addition bioassay experiments as in Papers C and E. Chlorophyll a concentrations increased with additions of N. This increase doubled with additions of N and P (NP) together. No changes in chlorophyll a concentrations with P alone or Fe additions were observed. A closer look at the different picoplankton fractions using analytical flow cytometry revealed no differences in *Prochlorococcus* and picoeukaryote chlorophyll fluorescence in N and NP treatments, while *Synechococcus* chlorophyll fluorescence increased in N treatments and increased further with NP additions. One interpretation of this result is that *Synechococcus* was pushed towards P-limitation by the N addition due to the low availability of P in oligotrophic oceans. However cellular nucleic acids increased only with NP additions indicating a possible co-limitation of nucleic acid synthesis. The Fv:Fm showed no response to alleviation of nutrient stress implying that the phytoplankton were adapted to the low nutrient levels. Evidence of N limitation in the phytoplankton community is an intriguing result because N:P ratios of the study area were in excess of the Redfield ratio 16:1, which is usually interpreted as a sign of P-limitation. One explanation put forth in this manuscript is that cellular ratios of N:P in oligotrophic phytoplankton are higher than Redfield which could give them a competitive advantage in areas where P is scarce. For instance, *Prochlorococcus* has a relatively small genome and uses sulfolipids as opposed to phospholipids. Understanding single nutrient and co-limitation should help form a better comprehension of the biogeochemical cycles.

Contribution

C. M. Moore, M. Mills, A. Milne, E. Achterberg and I contributed equally to the success of the eight bioassay experiments performed during the Meteor 60 cruise. I measured and analyzed the chlorophyll a data at sea and was in charge of organizing the bottles during the experiment set-ups. I provided comments on the manuscript that C. M. Moore prepared.

Limnol. Oceanogr., 53(1), 2008, 291–305

Relative influence of nitrogen and phosphorus availability on phytoplankton physiology and productivity in the oligotrophic sub-tropical North Atlantic Ocean

C. Mark Moore[1]
Department of Biological Sciences, University of Essex, Colchester, CO4 3SQ, United Kingdom

Matthew M. Mills
Department of Geophysics, Stanford University, Stanford, California 94305

Rebecca Langlois
Marine Biogeochemistry, Leibnitz-Institut für Meereswissenschaften, D-24105 Kiel, Germany

Angela Milne
School of Earth, Ocean and Environmental Sciences, University of Plymouth, Plymouth PL4 8AA, United Kingdom; Marine Biological Association, Citadel Hill, Plymouth PL1 2PB, United Kingdom

Eric P. Achterberg
School of Ocean and Earth Science, National Oceanography Centre, University of Southampton, Southampton SO14 3ZH, United Kingdom

Julie La Roche
Marine Biogeochemistry, Leibnitz-Institut für Meereswissenschaften, D-24105 Kiel, Germany

Richard J. Geider
Department of Biological Sciences, University of Essex, Colchester, CO4 3SQ, United Kingdom

Abstract

Nutrient addition bioassay experiments were performed in the low-nutrient, low-chlorophyll oligotrophic subtropical North Atlantic Ocean to investigate the influence of nitrogen (N), phosphorus (P), and/or iron (Fe) on phytoplankton physiology and the limitation of primary productivity or picophytoplankton biomass. Additions of N alone resulted in 1.5–2 fold increases in primary productivity and chlorophyll after 48 h, with larger (~threefold) increases observed for the addition of P in combination with N (NP). Measurements of cellular chlorophyll contents permitted evaluation of the physiological response of the photosynthetic apparatus to N and P additions in three picophytoplankton groups. In both *Prochlorococcus* and the picoeukaryotes, cellular chlorophyll increased by similar amounts in N and NP treatments relative to all other treatments, suggesting that pigment synthesis was N limited. In contrast, the increase of cellular chlorophyll was greater in NP than in N treatments in *Synechococcus*, suggestive of NP co-limitation. Relative increases in cellular nucleic acid were also only observed in *Synechococcus* for NP treatments, indicating co-limitation of net nucleic acid synthesis. A lack of response to relief of nutrient stress for the efficiency of photosystem II photochemistry, $F_v : F_m$, suggests that the low nutrient supply to this region resulted in a condition of balanced nutrient limited growth, rather than starvation. N thus appears to be the proximal (i.e. direct physiological) limiting nutrient in the oligotrophic sub-tropical North Atlantic. In addition, some major picophytoplankton groups, as well as overall autotrophic community biomass, appears to be co-limited by N and P.

[1] To whom correspondence should be addressed. Present address: School of Ocean and Earth Science, National Oceanography Centre, University of Southampton, Southampton, SO14 3ZH, United Kingdom (cmm297@noc.soton.ac.uk).

Acknowledgments

We acknowledge the captain and crew of the *F/S Meteor* and the scientists aboard the Meteor 60, especially D. Wallace, P. Fritsche, K. Nachtigal, and F. Malien. Mike Zubkov and Ross Holland assisted with the flow cytometry analysis. Comments from John Cullen and an anonymous referee considerably improved an earlier version of this manuscript.

This work was supported by Natural Environment Research Council grants to RJG and EPA (NER/A/S/2002/00791), and a Deutsche Forschungsgemeinschaft grant (RO-2138/5-1) to J.L.

Nutrient limitation can affect phytoplankton community structure and constrain the extent to which oceanic primary production influences global nutrient and carbon cycles. Establishing the limiting nutrient(s) under different oceanographic conditions, and the causes and nature of such limitation, is thus an important goal for understanding feedbacks between oceanic biota and the environment (Arrigo 2005).

The nature of phytoplankton nutrient stress has important consequences, both for understanding ecosystem functioning and for the interpretation of experimental and in situ data (Cullen et al. 1992; Arrigo 2005). In particular, a low nutrient supply can be hypothesized to

limit the yield of phytoplankton biomass (cf. Liebig's Law of the Minimum) and/or phytoplankton growth rate (Blackman's type limitation; *see* Cullen 1991). Interpretation of bioassay experiments must take account of these and other possible confounding factors, including containment effects (Graziano et al. 1996). For example, a lack of biomass accumulation may not represent the absence of growth rate limitation in a system where source and sink terms are tightly coupled by efficient grazing and nutrient recycling (Goldman 1980; Graziano et al. 1996). Conversely, biomass increases in controls may reflect a reduction in grazing pressure (Cullen et al. 1992).

Geochemical arguments suggest that phosphorus (P) should limit oceanic production because nitrogen (N) can be supplied to the biota via N_2 fixation (Redfield 1958). In contrast, N typically limits phytoplankton growth in the oligotrophic sub-tropical and tropical oceans (Ryther and Dunstan 1971; Graziano et al. 1996; Mills et al. 2004). Tyrrell (1999) attempted to reconcile these two points of view by suggesting that P-limitation of N_2 fixation leads to the N-limitation of phytoplankton growth. The modeling study of Tyrrell (1999) concluded that P was the ultimate limiting nutrient on geochemical time scales (100–1,000+ years), whereas N was the proximal (i.e., directly) limiting nutrient on physiological (day) and ecological (month to year) time scales. Alternatively, Falkowski (1997) hypothesized that oceanic primary production was N-limited because low iron (Fe) availability limits N_2 fixation.

In contrast to N, recent work has emphasized the potential role of P as the proximal limiting nutrient on physiological time scales in the sub-tropical North Atlantic (Wu et al. 2000; Ammerman et al. 2003; Lomas et al. 2004). Biological evidence for P limitation in the western sub-tropical North Atlantic comes from observations of high activities of the alkaline phosphatase (AP). AP is an enzyme that increases P availability through hydrolysis of components in the dissolved organic P pool (Ammerman et al. 2003; Lomas et al. 2004). However, interpretation of AP activity is not straightforward, and high activities may not be indicative of overall community P limitation (Moore et al. 2005*b*). Similarly, the observed expression of the inorganic P binding protein (Scanlan and Wilson 1999) and the prevalence of genes implicated in P acquisition within natural prokaryotic populations (Martiny et al. 2006) both indicate a degree of P stress resulting from low ambient concentrations in this region, but may not necessarily represent proximal sole P limitation. Indeed, up-regulation of AP activity and inorganic P acquisition mechanisms presumably serves to reduce or neutralize the effect of low dissolved inorganic P concentrations on phytoplankton growth.

Other evidence for P limitation in the sub-tropical North Atlantic is based on geochemical arguments. Specifically, high N : P ratios exceeding the Redfield ratio of 16 : 1 in both dissolved and particulate organic pools are observed in the surface waters of the Sargasso Sea (Wu et al. 2000; Ammerman et al. 2003). Ratios of nitrate (NO_3^-) to soluble reactive P (SRP) within the thermocline in this region are also high, often greater than 30 : 1 (Fanning 1992). Inputs of nutrients from below the surface layer due to winter overturning (Michaels et al. 1994), background turbulent diffusivity (Lewis et al. 1986), or vertical transport driven by mesoscale eddies (McGillicuddy et al. 1998) thus have similarly high N : P ratios.

In a classical Redfield paradigm, where 16 mol N : 1 mol P is assumed to represent the transition from N to P limitation (Falkowski 1997; Tyrrell 1999), the high N : P ratios suggest P limitation (Ammerman et al. 2003). However, it is becoming increasingly clear that phytoplankton cellular N : P ratios and the critical ratio marking the transition between N and P limitation vary greatly between taxa and with growth conditions (Geider and La Roche 2002; Quigg et al. 2003). In particular it is possible that the optimum N : P ratio in a resource-limited environment is well in excess of 16 : 1 (Klausmeier et al. 2004). The implications of this variable biological N : P stoichiometry for global nutrient cycling remain to be fully elucidated (Arrigo 2005).

In contrast to the suggestion of proximal P limitation in the Sargasso Sea near Bermuda, experimental work in other regions of the low and mid-latitude North Atlantic has indicated proximal N limitation of CO_2 fixation and net chlorophyll synthesis (Graziano et al. 1996; Mills et al. 2004). Such direct experimental information from bioassays is not available from the regions of high inorganic N : P ratios within the Sargasso Sea. We thus performed nutrient addition bioassay experiments using trace element clean sampling to establish the nutrient(s) influencing phytoplankton physiology and limiting primary productivity on a transect across the mid-latitude North Atlantic. Biomass-independent phytoplankton physiological parameters were measured within these experiments in an attempt to circumvent weaknesses in interpretation associated with perturbation of grazing pressure (Cullen 1991; Cullen et al. 1992; Graziano et al. 1996). Such indices provide a measure of short-term physiological nutrient stress that must still be interpreted cautiously with relation to growth rate.

Here we demonstrate proximal N limitation of primary productivity and net chlorophyll accumulation consistent with results from previous bioassays elsewhere in the North Atlantic (Graziano et al. 1996; Mills et al. 2004). Data and arguments for overall N and P (hereafter NP) co-limitation of *Synechococcus*, which became the dominant component of the picophytoplankton upon relief from nutrient limitation, are also presented. It is suggested that a condition approximating NP co-limitation of some components of the autotrophic community may reconcile observations of proximate N limitation with alternative evidence for P limitation (Ammerman et al. 2003).

Methods

Eight nutrient addition bioassay experiments were performed in the central North Atlantic in March and April 2004 as part of the Meteor 60 Transient Tracers Revisited expedition (Moore et al. 2006*a*). Here we report detailed results from the five experiments initiated in waters between 21°N and 32°N where macronutrients were undetectable using standard colorimetric techniques (Fig. 1). Sampling dates and locations are presented in

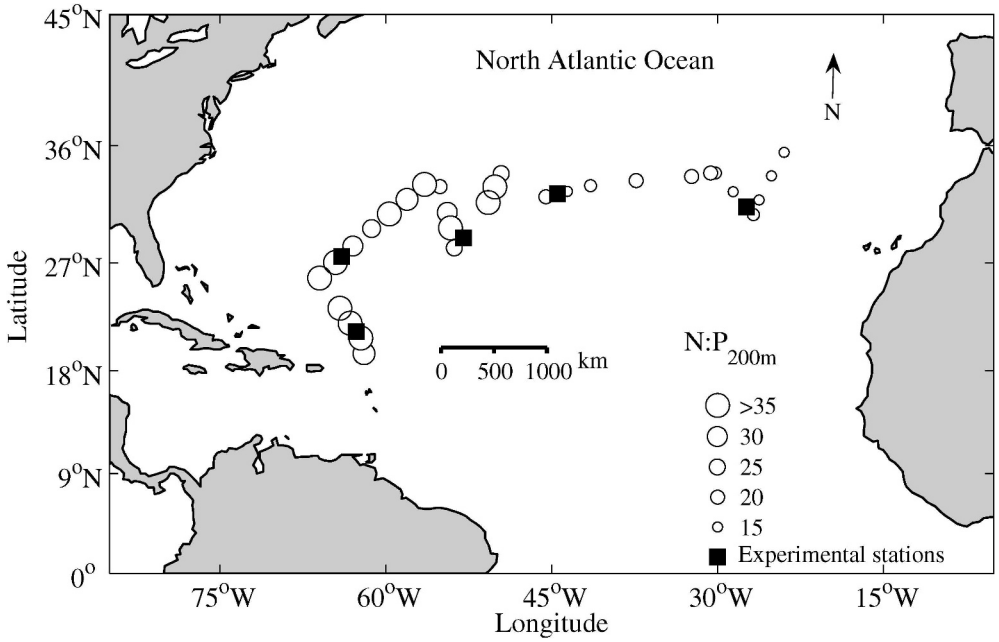

Fig. 1. Map showing the locations of nutrient enrichment bioassay experiments performed during the M60 cruise superimposed on the N : P ratio at 200 m. N : P ratios decrease from high values in the region of the Sargasso Sea to values approaching the deep-water ratio of ~14.7 : 1 in the east.

Table 1. Experiments were performed using a highly replicated fully factorial design to establish which nutrient(s) were limiting different components of the microbial community (Mills et al. 2004; Moore et al. 2006*a*).

Water sampling, bottle filling, and incubations were performed using methods described previously (Moore et al. 2006*a*). Briefly, water was collected from near surface and incubated in 1.18-liter bottles for 48 h after the addition of nutrients added alone and in combination to final concentrations of 1.0 μmol L^{-1} NH_4^+, 1.0 μmol L^{-1} NO_3^-, 0.2 μmol L^{-1} NaH_2PO_4, and 2.0 nmol L^{-1} $FeCl_3$. For the majority of treatments, 2 μmol L^{-1} N was added as 1.0 μmol L^{-1} NH_4NO_3, however, a separate treatment of 1.0 μmol L^{-1} KNO_3 added alone was also included. With the exception of the $FeCl_3$, all nutrient stocks were passed through a Chelex-100 column to remove trace metal contamination. Post-incubation measurements confirmed that the added inorganic nutrients had not been fully

Table 1. Initial conditions for bioassay experiments. Mean (±SE) of triplicate samples, except for DFe where the standard error of an individual sample analyzed four times is presented. $N : P_{200}$ indicates the N : P ratio within the thermocline at approximately 200 m below the sampling location.

	21°N 62°W	28°N 64°W	29°N 53°W	32°N 44°W	31°N 27°W
Sea surface temperature	25.4	22.7	21.4	19.6	19.7
Mixed layer depth (m)	133	67	68	129	122
NO_3((nmol L^{-1})	<30	<30	<30	<30	<30
PO_4^{3}((nmol L^{-1})	<8	<8	<8	<8	14 (3)
Total dissolved Fe (nmol L^{-1})	0.51 (0.05)	0.47 (0.05)	0.21 (0.02)	0.27 (0.01)	0.25 (0.01)
$N : P_{200}$ (mol mol^{-1})	36.2	32.3	22.6	18.6	17.6
Chlorophyll *a* (mg L^{-1})	0.067 (0.006)	0.043 (0.002)	0.045 (0.006)	0.081 (0.004)	0.09 (0.01)
Prochlorococcus (cells mL^{-1})	24,590 (5,000)	11,880 (860)	33,880 (1,220)	43,100 (2,490)	41,020 (750)
Synechococcus (cells mL^{-1})	3180 (650)	4360 (180)	8990 (580)	6840 (560)	2,970 (100)
Picoeukaryotes (cells mL^{-1})	431 (74)	325 (14)	681 (64)	392 (59)	466 (11)
Synechococcus cellular nucleic acid content (relative)	72.3 (3)	56.3 —	55.7 (0.4)	47.3 (0.2)	42.9 (0.5)

depleted. Further treatments involving the addition of Saharan aerosols and soils were also performed (Mills et al. 2004; Moore et al. 2006*a*), detailed results of which will be reported elsewhere. Trace element clean sampling and incubation techniques were strictly adhered to throughout the experimental procedure. All treatments were run in triplicate. Bottles were incubated for 48 h at 20% surface irradiance and cooled by surface seawater (Moore et al. 2006*a*). Parallel sets of triplicate incubations were run for primary production via ^{14}C incorporation and all other variables (Mills et al. 2004). Water for the initial rate measurements and state variables was collected throughout the filling of the incubation bottles.

Primary production—Phytoplankton inorganic carbon fixation was measured by the addition of 1.85 MBq ^{14}C-bicarbonate to one triplicate set of incubation bottles. Initial rates were measured on unamended bottles during the first 24 h of incubation. Carbon fixation rates in nutrient amended treatments and unamended controls were assessed during the second 24-h period. Incubations were terminated by gentle filtration onto Whatman GF/F filters. Filters were fumed with HCl for 30 minutes, then transferred to scintillation vials and 10 mL of scintillation cocktail added. Vials were left for >24 h in the dark, then counted on a Packard Tricarb liquid scintillation counter on-board ship. Total activity was assessed on 250-μL subsamples removed from initial and control bottles.

Chlorophyll a—Chlorophyll was measured in triplicate on initial water used for incubations and on sub-samples collected from all treatments at 48 h. Sub-samples of 500 mL were filtered onto GF/F filters, frozen in 1 mL of deionized water (Milli-Q, Millipore) for 3 h, then thawed with the addition of 9 mL acetone (Glover et al. 1986). After subsequent 24-h extraction in the dark, fluorescence was measured on a Turner designs 10-AU fluorometer (Welschmeyer 1994).

Analytical flow cytometry—The abundance and cellular composition of picophytoplankton was evaluated by analytical flow cytometry (AFC). Samples (2 mL) were collected and preserved in 1% gluteraldehyde, then frozen at −80°C for transport back to the laboratory (Zubkov et al. 1998). Samples were thawed at 4°C and analyzed for particle abundance, side scatter, and red (chlorophyll) and orange (phycoerytherin) auto-fluorescence using a FACSort (Becton Dickinson) flow cytometer. Data analysis was performed using WinMDI (version 2.8, Joseph Trotter). Plots of side scatter versus orange fluorescence and red fluorescence were used to discriminate and enumerate *Prochlorococcus, Synechococcus*, and picoeukaryotes. Relative changes in cellular phycoerytherin and chlorophyll for these groups were also calculated in this manner. Accurate enumeration of *Prochlorococcus* was often not possible within these oligotrophic surface waters (Zubkov et al. 1998) because of the low cellular chlorophyll as a result of acclimation to both high light and nutrient stress (*see* below). Samples were also analyzed after staining with the nucleic acid stain SYBR Green II (Molecular Probes), which binds to RNA and both single- and double-stranded DNA. Sub-samples (500 μL) were incubated for more than an hour at room temperature with 50 μL of 300 mmol L^{-1} potassium citrate and 5 μL of a 1% dilution of a commercial stock of SYBR Green II. Scatterplots of red and orange fluorescence versus side scatter and green fluorescence were used to estimate relative changes in cellular nucleic acid content (Marie et al. 1997). Particle counts and fluorescence were calibrated against a 0.5-μm bead standard (Fluoresbrite Microparticles, Polysciences).

Fast repetition rate fluorometry—Variable chlorophyll fluorescence was measured on dark adapted samples using a FASTtracka fast repetition rate fluorometer (Chelsea Scientific Instruments) using previously described protocols (Moore et al. 2006*b*). Non-linearities in instrument response were characterized using extracts of chlorophyll *a* (Chl *a*) and pigments from natural phytoplankton communities. Induction curves were averaged over 512 individual sequences to minimize error due to noise. Fluorescence transients were then fitted to a biophysical model (Kolber et al. 1998; Laney 2003; Moore et al. 2006*b*) to calculate the functional absorption cross section of photosystem II (σ_{PSII}) and the measured maximal and minimal chlorophyll fluorescence levels ($F_{m,meas}$ and $F_{o,meas}$).

Filtrates from each sample were analyzed to directly measure the background fluorescence F_b (Cullen and Davis 2003). The magnitude of background fluorescence was further estimated by regressing acetone-extracted chlorophyll from filtered samples against $F_{m,meas}$ and $F_{o,meas}$ (Fig. 2a). The calculated intercept values, indicating the background fluorescence at zero particulate chlorophyll, were highly comparable with the independent direct measurements of F_b (Fig. 2b). The background (F_b) varied little between sampling locations. For comparison, a reading of ~0.01 instrument units was obtained with Milli-Q water. Maximum (F_m) and minimum (F_o) fluorescence levels for the phytoplankton population were thus calculated as ($F_{m,meas} - F_b$) and ($F_{o,meas} - F_b$), respectively. The maximal photochemical quantum yield ($F_v : F_m$) was calculated as $(F_{m,meas} - F_{o,meas})/(F_{m,meas} - F_b)$. Failure to account for the background fluorescence, which was relatively large because of the low initial chlorophyll concentrations within the study region, would have resulted in considerable errors (40–90%) in estimates of $F_v : F_m$ (Cullen and Davis 2003).

Nutrients—Concentrations of NO_3^- and SRP were measured on-board using standard colorimetric techniques (Grasshoff et al. 1999). SRP concentrations were also measured using the MAGIC protocol (Karl and Tien 1992). For this purpose, samples (120 mL) were filtered through acid-washed 0.2-μm polycarbonate filters. then frozen and stored at −40°C. Additions of 1.0 mL of 1.0 mol L^{-1} NaOH to 100-mL subsamples induced coprecipitation of $Mg(OH)_2$ and SRP. The samples were then centrifuged (5 min at 1,000 × g) and the supernatant removed. The pellet was resuspended in 10-mL 0.1 mol L^{-1} HCl, and SRP was then determined using the standard molybdenum blue assay (Grasshoff et al 1999). Our 10-fold

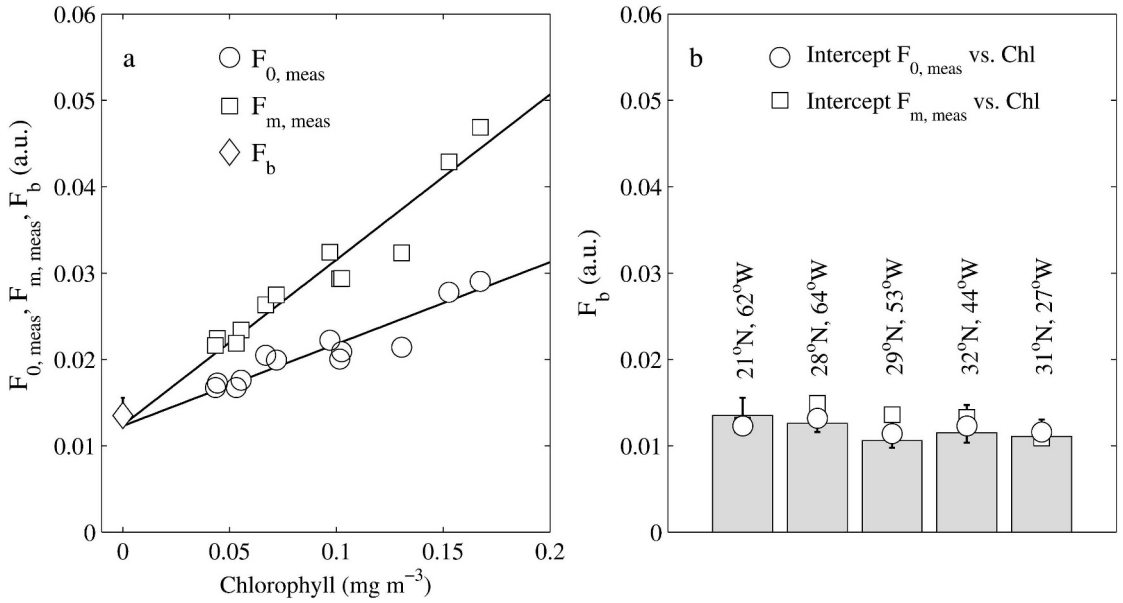

Fig. 2. Contribution of background fluorescence to measured maximal and minimal fluorescence levels. (a) $F_{o, meas}$ and $F_{m, meas}$ versus filtered chlorophyll from the experiment at 21°N, 62°W. Symbols indicate mean values ($n = 3$) from each of the treatments. Mean and standard deviation of all blank samples designated F_b ($n = 36$) also indicated. (b) Comparison of directly measured background fluorescence (bars) and estimates from regressions of $F_{m, meas}$ and $F_{o, meas}$ versus filtered chlorophyll. Error bars for measured backgrounds indicate standard deviations from all samples ($n = 36$).

concentration step resulted in a detection limit of ~8.0 nmol L^{-1}.

Total dissolved Fe (DFe) was analyzed using flow-injection chemiluminescence (Bowie et al. 1998). Samples were filtered using 25-mm-diameter Gelman syringe filters (0.2-μm pore size, polytetrafluoroethylene (PTFE) membrane). A 12-h acidification and 12-h reduction period were allowed before analysis of DFe.

Statistical analysis—Treatment means from bioassay experiments and differences between sampling locations were compared using a one-way analysis of variance (ANOVA) followed by a Tukey–Kramer means comparison test ($\alpha = 0.05$).

Results

Initial conditions—Initial nitrate concentrations were below the limit of detection (30 nmol L^{-1}) at all experimental sites (Table 1). SRP concentrations were lower than 8 nmol L^{-1} at all stations apart from the most easterly experiment (27°W, 31°N), where an initial concentration of 14 ± 3 nmol L^{-1} was measured. N : P ratios for dissolved nutrients at the thermocline ranged from >30 : 1 to <18 : 1 along a gradient from west to east (Table 1; Fig. 1). Iron concentrations were greater than 0.2 nmol L^{-1} at all locations, with highest levels (~0.5 nmol L^{-1}) observed in the Sargasso Sea to the west of the transect (Table 1). Sea surface temperature decreased from the southwest to the northeast, whereas mixed layer depths (0.5°C difference from surface) varied between 70 m and 130 m (Table 1). Initial chlorophyll concentrations (<0.1 mg Chl *a* m^{-3}) and carbon fixation rates (<0.4 mmol m^{-3} d^{-1}) were also low at all experimental sites, with chlorophyll specific production at the incubation irradiance (P*) decreasing from ~6 mol C (g Chl *a*) $^{-1}$ d^{-1} in the west to ~2–3 mol C (g Chl *a*) $^{-1}$ d^{-1} in the east. Phytoplankton abundances ranged from an estimated 1–4 × 10^4 cells mL^{-1} for the numerically dominant *Prochlorococcus* through ~3–9 × 10^3 cells mL^{-1} for *Synechococcus* to ~300–700 cells mL^{-1} for the picoeukaryotes. As mentioned above, concentrations of *Prochlorococcus* were likely to be underestimated because of a proportion of the population being indistinguishable from the baseline as a result of low cellular chlorophyll concentrations.

Analysis of climatological mixed layer depths (MLD) and ocean color data (Moore et al. 2006*a*), indicated seasonal cycles in MLD at all stations and significant seasonal cycles in surface chlorophyll at all stations excluding 21°N, 62°W (not shown). Maximum chlorophyll concentrations slightly lagged maximum MLDs in January–February. In the majority of our sampling region (Fig. 1), vertical mixing in late winter/early spring thus appears to penetrate the nutricline, resulting in the injection of nutrients into surface waters and a spring bloom. The seasonal cycle of phytoplankton pigment is thus similar to observations at the nearby Bermuda Atlantic Time-series study (BATS) (Michaels et al. 1994). Bloom magnitude increases to the north of the sampling region, presumably as a consequence of deeper mixing and, hence, enhanced nutrient input. As mentioned above, all the experiments reported here were initiated post-bloom when macronutrients were depleted and chlorophyll had decreased.

Response of the bulk phytoplankton community—The response of inorganic carbon fixation, phytoplankton

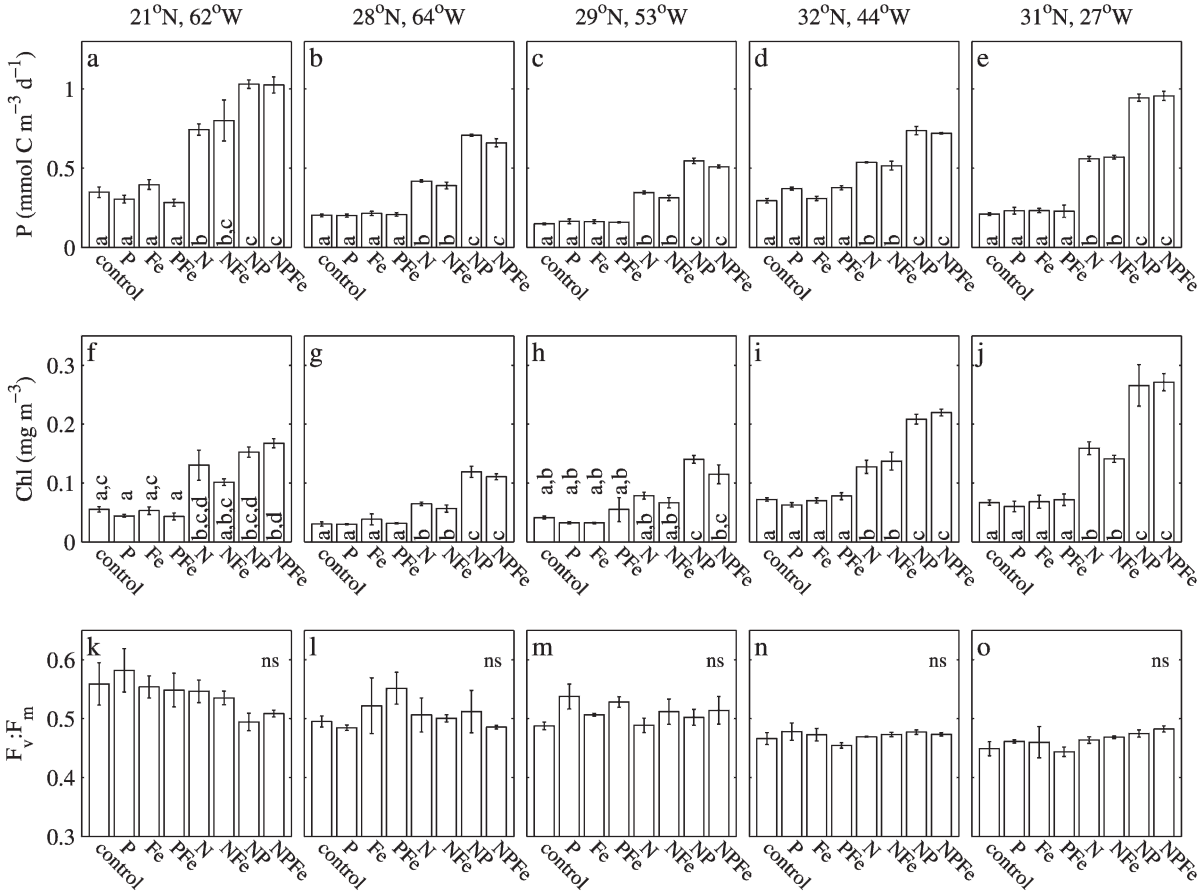

Fig. 3. Response of bulk phytoplankton community characteristics to nutrient addition. (a–e) Inorganic carbon fixation measured from 24–48 h after the addition of the indicated nutrients. (f–j) Chlorophyll concentration measured at 48 h. (k–o) Phytoplankton photochemical quantum efficiency ($F_v:F_m$) measured at 48 h. Error bars indicate standard errors. Letters indicate means that are statistically indistinguishable ($\alpha = 0.05$), with ns indicating no significant differences between treatments (ANOVA).

pigment (chlorophyll) accumulation and values of $F_v:F_m$ to the various nutrient additions were highly consistent in all the experiments (Fig. 3). No significant differences in productivity or Chl *a* were observed between control bottles and those amended with either Fe or P alone or in combination for any of the experiments (Fig. 3a–j). In contrast, addition of N alone resulted in significant (1.5–2-fold) increases in inorganic carbon fixation and Chl *a* across all experiments. Additions of P when in combination with N resulted in a further significant increase in both production and Chl *a* to levels around threefold higher than control treatments after 48 h (Fig. 3a–j). Adding Fe in combination with N or N and P did not significantly affect productivity or Chl *a*. Inorganic carbon fixation and chlorophyll concentration were highly correlated overall ($R^2 = 0.707$, $n = 50$, $p < 0.0001$).

Despite clear evidence for N limitation of phytoplankton productivity and chlorophyll concentrations, no significant differences in values of $F_v:F_m$ when corrected for blank effects were observed between treatments in any of the experiments (Fig. 3k–o). Similarly, the functional absorption cross section of photosystem II (σ_{PSII}) and both ratios of F_0 and F_m to chlorophyll ($F_0:Chl$ and $F_m:Chl$), which have also been interpreted as being indicative of nutrient stress (Olaizola et al. 1996), were insensitive to the alleviation of N limitation. Taken across experiments, these parameters describing the efficiency of PSII light absorption and energy transfer were highly correlated, with higher $F_0:Chl$ and σ_{PSII} associated with lower $F_v:F_m$ (Fig. 4). However, significant differences were only observed between experiments (ANOVA, $p < 0.05$) rather than within any single experiment (Figs. 3k–o, 4). For the current study, differences in PSII characteristics between natural communities therefore appeared to represent some characteristic of phytoplankton ecophysiology that was not directly related to physiological nutrient stress (Behrenfeld et al. 2006), with changes in community composition being one possibility (Moore et al. 2005*a*; Moore et al. 2006*b*).

Cellular and group specific responses—Cellular chlorophyll contents for *Prochlorococcus*, *Synechococcus*, and picoeukaryotes broadly reflected results based on bulk community chlorophyll concentrations and carbon fixation. No consistent changes in cellular chlorophyll were observed for any of the groups after the addition of P or Fe alone or in combination (Fig. 5). In contrast, cellular chlorophyll increases were consistently observed across all experiments for all three autotrophic groups after the

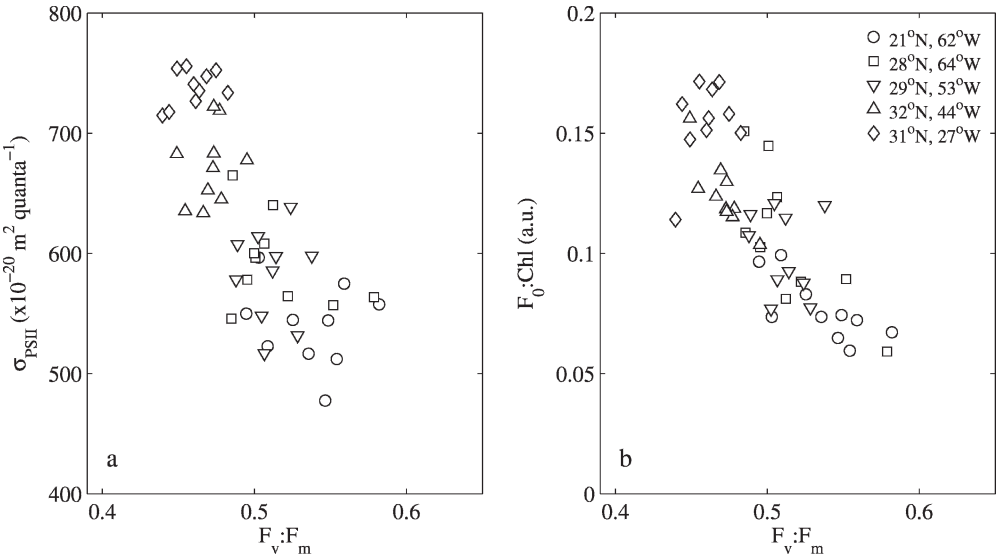

Fig. 4. Relationship between parameters describing photosystem II light absorption and photochemical efficiency taken from data collected across all treatments in all experiments. (a) Relationship of σ_{PSII} to $F_v:F_m$, $r^2 = 0.578$, $p < 0.0001$, $n = 50$. (b) Relationship of the ratio of minimal fluorescence to chlorophyll $F_0:Chl$ with $F_v:F_m$, $r^2 = 0.658$, $p < 0.0001$, $n = 50$. No significant differences ($\alpha = 0.05$) were found between initial conditions and post-incubation values regardless of the nutrient(s) added within any of the individual experiments. However, when considered across the whole data set, the ranges of parameters measured both pre- and post-incubation were statistically different between experiments, as were initial values (ANOVA, $\alpha = 0.05$).

addition of N alone or in combination with P (Fig. 5). However, differences in responses were observed between autotrophic groups.

Responses in NP treatments over that of N treatments were minor for *Prochlorococcus* with around 1.5–2-fold increases in cellular chlorophyll in both cases (Fig. 5a–e). Similarly picoeukaryote cellular chlorophyll increased by ~1.2–2-fold after the addition of N alone or in combination with P (Fig. 5k–n). The response of cellular chlorophyll was higher for *Synechococcus* with ~3–7-fold increases on the addition of N and a further significant increase to 5–15 times control values on the combined addition of N and P (Fig. 5f–j). Similarly, estimates of *Synechococcus* cellular phycoerytherin concentration in the N and NP treatments were 3–11 and 5–16 times values in the controls, respectively (Fig. 5f–j). The magnitudes of these changes were consistent with previous observations (Graziano et al. 1996).

A comparison of cellular chlorophyll concentrations between N (1 μmol L^{-1} NH_4NO_3) and NO_3^- (1 μmol L^{-1} KNO_3) treatments also indicated differences between groups. Responses of *Synechococcus* to NO_3^- additions were consistent with responses to NH_4NO_3, whereas *Prochlorococcus* cellular chlorophyll concentration showed no significant differences between controls and NO_3^- treatments (Fig. 5). Responses of picoeukaryotes to nutrient addition were generally less consistent between experiments, and differences between treatments were not as well defined as for prokaryotes (Fig. 5). This likely reflected poorer statistical confidence because of the lower number of events recorded by AFC for this numerically less abundant group and/or differences in response between taxa within the potentially more diverse assemblage represented by the picoeukaryotes. However, there was some indication that the picoeukaryotes also responded less to NO_3^- than NH_4NO_3 addition, particularly in the experiment performed at the eastern end of the transect (Fig. 5).

Low levels of chlorophyll (red) auto-fluorescence combined with leakage of SYBR Green II fluorescence into the red channel resulted in stained *Prochlorococcus* frequently being indistinguishable from heterotrophic bacteria, particularly under non-N amended conditions. However, higher levels of cellular chlorophyll and the presence of phycoerythrin enabled the separation of *Synechococcus* from heterotrophic bacteria (Marie et al. 1997). Changes in relative cellular nucleic acid content in response to the various nutrient treatments could thus be estimated. Significant increases in nucleic acid content for *Synechococcus* were typically observed within NP and NPFe treatments (Fig. 6). As SYBR Green II binds to all nucleic acids, the observed signals may have represented a combination of increased cellular DNA and/or RNA. Significant differences between experiments were also observed, with generally higher nucleic acid contents in the south and west than toward the east of the transect (Fig. 6).

Histograms of cellular nucleic acid content for *Synechococcus* only resolved single peaks for control incubations and treatments amended with N(and/or +Fe) or P(and/or Fe) alone (Fig. 6b). In contrast bimodal distributions of cellular nucleic acid content were observed in NP treatments, with peaks separated by a factor of approximately two. The combination of a relatively low number of recorded events and hence high coefficients of variation,

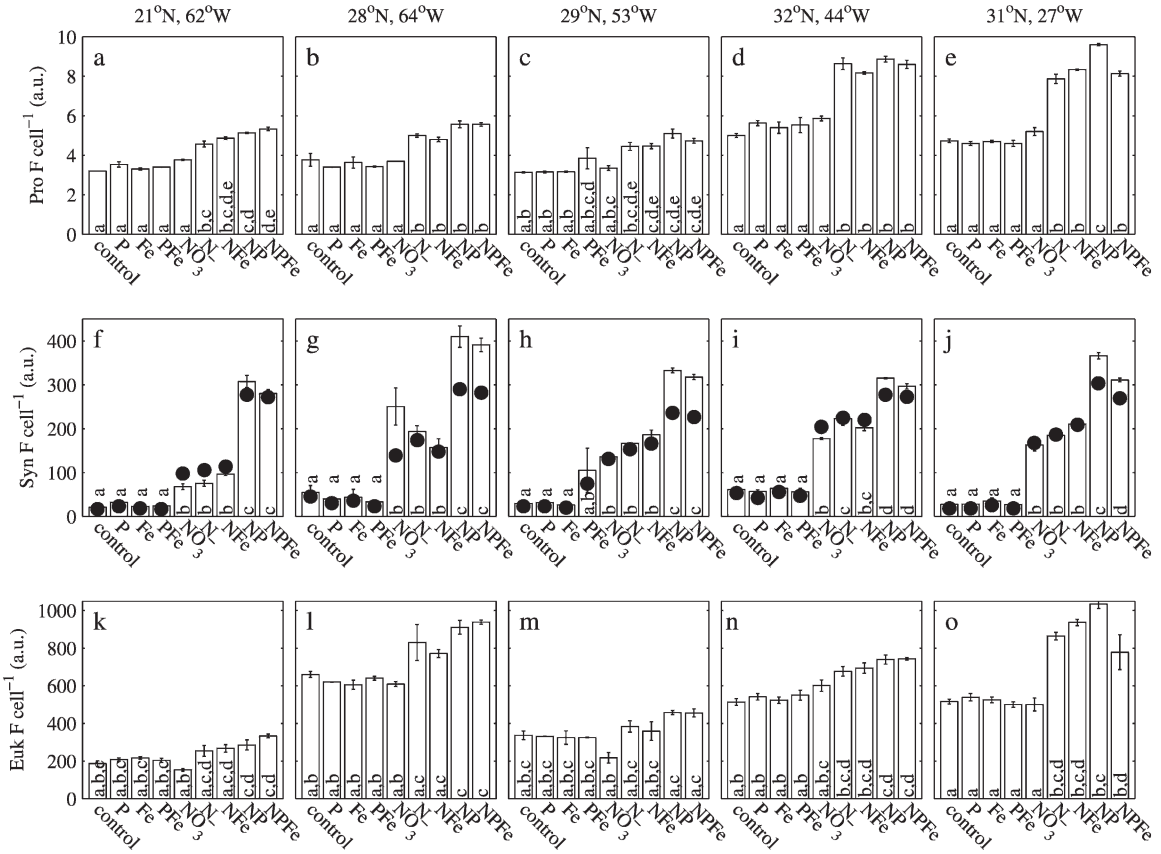

Fig. 5. Group-specific responses of fluorescence per cell as measured by AFC. (a–e) *Prochlorococcus* cellular chlorophyll fluorescence measured at 48 h after the addition of the indicated nutrients. (f–j) *Synechococcus* cellular chlorophyll fluorescence (bars) and phycoerythrin fluorescence (closed symbols). (k–o) Cellular chlorophyll fluorescence of picoeukaryotes. Error bars and letters in italics indicate standard errors and statistically indistinguishable mean values ($\alpha = 0.05$) for chlorophyll fluorescence. Statistical analysis of data for *Synechococcus* phycoerythrin fluorescence (f–j) yielded similar results (not shown). NH_4NO_3 and KNO_3 additions are labeled N and NO_3^-, respectively.

uncertainties regarding the relative contribution of RNA and DNA to the signals recorded on cells stained with SYBR Green II, and sampling only performed at a single point within the diel cycle prevented accurate cell cycle analysis (Vaulot et al. 1996; Marie et al. 1997). However, the proportion of cells in phase G_1 was estimated to have reduced from >90% under initial, control, and single additions of N(and/or Fe) and P(and/or Fe) to between 70% and 80% after NP(Fe) additions. Similar results were obtained for changes in *Synechococcus* cell cycles in the Mediterranean after the addition of P alone (Vaulot et al. 1996).

Few statistically significant changes in autotrophic cell numbers could be observed within our relatively short (48 h) experiments. As mentioned above, accurate enumeration of *Prochlorococcus* was frequently not possible under non–N-amended conditions. The addition of N, either alone or in combination with P and/or Fe, enabled more accurate counts because of the observed increase in cellular chlorophyll (Fig. 5a–e). An upper bound of at most 50% increases in *Prochlorococcus* cell abundance on N addition could thus be calculated. However, it is possible that all of this apparent increase resulted from the described artefact. No significant differences (ANOVA, $p > 0.05$) were observed between treatments for *Synechococcus* concentrations except for the experiment performed in the southwest of the transect at 21°N, 62°W. For this experiment *Synechococcus* concentrations increased around 2.7-fold from 3,170 (±650, 1 SE) cells mL^{-1} initially to 7,900 (±840) and 9,000 (±510) cells mL^{-1} for NP and NPFe treatments, respectively, compared to a range of ~4,500–5,500 cells mL^{-1} within controls and all other treatments (Fig. 7g). Some increases in picoeukaryote cell abundance were also observed within NP and NPFe treatments (Fig. 7h), however these were only significant for the 21°N, 62°W and 31°N, 27°W experiments.

Contributions of the different autotrophic groups to total community chlorophyll were calculated by multiplying cell concentrations by cellular red fluorescence (Table 2). The relative contributions of *Prochlorococcus*, *Synechococcus*, and picoeukaryotes within initial sampling water and controls indicated no tendency for dominance by any single group. In contrast, after N addition, *Synechococcus* dominated community chlorophyll (i.e., ~50% or greater) in all cases (Table 2).

Meta-analysis and comparisons of initial conditions with treatments—The gradients in initial ecosystem structure and physiology described above (Table 1) were still apparent at

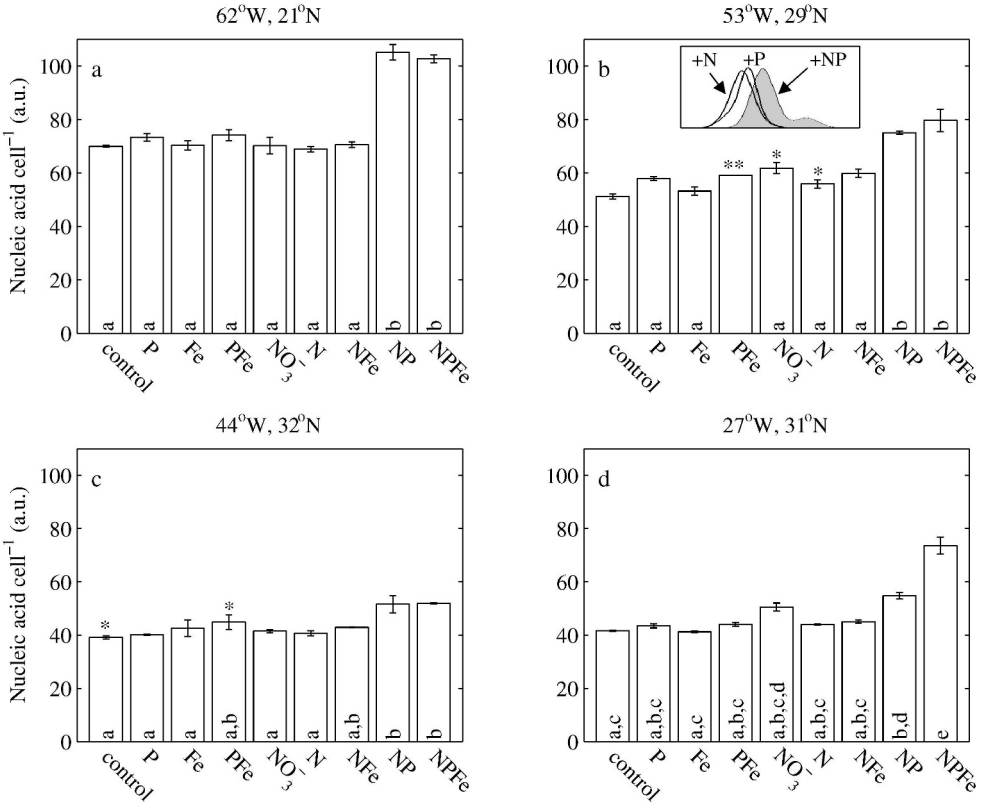

Fig. 6. Relative changes in *Synechococcus* cellular nucleic acid content. (a–d) Relative changes in nucleic acid content for four of the five experiments. Error bars and letters indicate standard errors and statistically indistinguishable mean values ($\alpha = 0.05$) respectively, $n = 3$ except for treatments indicated by * ($n = 2$) and ** ($n = 1$). (Inset in b), Smoothed histograms of *Synechococcus* cellular nucleic acid content from +N, +P, and +NP treatments as indicated.

the end of the 48-h experiments. Differences in initial chlorophyll, productivity, and community structure between sites were generally preserved within control treatments (Fig. 7; Table 2). Physiological variability including cellular chlorophyll and *Synechococcus* cellular nucleic acid content (Fig. 7), as well as PSII photophysiology (Fig. 4), was also consistent between initial conditions and control treatments. Overall, the majority of variables measured within controls were statistically indistinguishable from initial conditions. Taken together, the constancy of community structure and physiology during the short experimental duration suggests that containment effects, a potential confounding factor in the interpretation of bioassay experiments (Cullen et al. 1992), were minor. Consistent positive responses to N and NP addition in a range of variables including bulk community carbon fixation and chlorophyll (Fig. 7a,b), *Prochlorococcus* and *Synechococcus* cellular chlorophyll (Fig. 7d,e) and *Synechococcus* cellular nucleic acid (Fig. 7i) were thus observed throughout the sampling region (Fig. 1) despite variability in many of the initial values and, hence, presumably the ecosystem state.

Discussion

Limiting nutrients in the oligotrophic sub-tropical North Atlantic—No evidence for a significant effect of iron on autotrophic carbon fixation, pigment biomass, or phytoplankton physiology was found within the experiments presented here under conditions of very low macronutrients (Fig. 3). These observations contrast with the evidence obtained on the same cruise indicating periods of iron limitation during the spring bloom to the north discussed elsewhere (Moore et al. 2006*a*). For simplicity, and unless otherwise stated, in the remaining discussion the effects of macronutrient addition within our experiments are assumed to be indicative of the response both with and without further addition of Fe.

Clear evidence for macronutrient limitation was observed within every experiment. The addition of P alone resulted in no significant increases in community carbon fixation, bulk community chlorophyll concentration, or the cellular contents of chlorophyll (Figs. 3, 7). Consistent observations that the addition of N and P together resulted in larger increases in bulk chlorophyll concentration and primary productivity than N alone are open to two possible interpretations. Either these nutrients were co-limiting in situ or, during the course of our experiments, P (co-) limitation was induced (or forced) by the addition of N. The latter case implies the existence of an internal cellular P reserve or some residual bioavailable P pool in situ. Although we could not fully differentiate between all these possibilities, observations of the accumulation of cellular

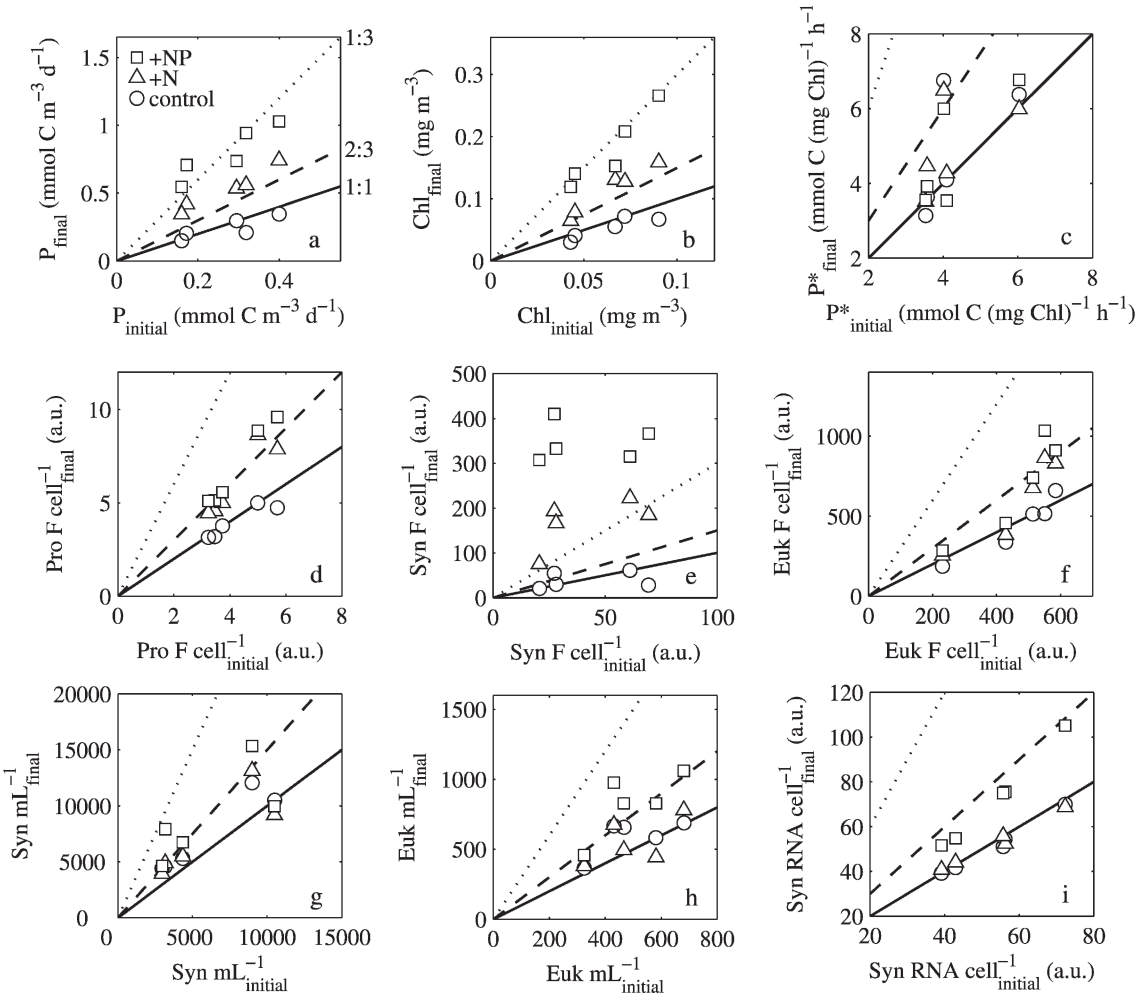

Fig. 7. Meta-analysis of experiments and comparisons of post-incubation values with initial conditions. (a) Plots of post-incubation (final) autotrophic community production measured in control, +N, and +NP treatments against initial values for all five experiments. (b) Final versus initial bulk chlorophyll concentration. (c) Final versus initial chlorophyll specific production. (d) Final versus initial *Prochlorococcus* cellular chlorophyll fluorescence. (e) Final versus initial *Synechococcus* cellular chlorophyll fluorescence. (f) Final versus initial cellular chlorophyll fluorescence for picoeukaryotes. (g) Final versus initial *Synechococcus* cell numbers. (h) Final versus initial picoeukaryote cell numbers. (i) final versus initial *Synechococcus* cellular nucleic acid content. Lines indicate ratios of post incubation values to initial conditions of 1 : 1, 2 : 3 and 1 : 3 for the indicated treatments. Symbols indicate treatment means ($n = 3$), error bars have been omitted for clarity (*see* Figs. 3, 5, and 6). All symbols and lines in (b–i) are as in (a).

pigments and nucleic acid in *Synechococcus* provided some insight.

Assuming that the observed proportionality between increases in community productivity and chlorophyll concentration (Fig. 3) were also representative of responses at the group level (Fig. 5), changes in pigmentation presumably reflected increased cellular carbon fixation. N addition alone increased the cellular contents of chlorophyll in *Prochlorococcus, Synechococcus*, and the picoeukaryote group and also increased phycoerytherin in *Synechococcus.* Such responses are consistent with the high N requirement and low P requirement for synthesis of these pigment–protein macromolecular complexes (Geider and La Roche 2002). Phycoerytherin in particular represents a significant pool of cellular N in *Synechococcus*, which has been observed to be degraded when N becomes limiting (Wyman et al. 1985). P addition with N resulted in greater increases of *Synechococcus* cellular chlorophyll and phycoerytherin content (Figs. 5, 7e). Again, this may suggest *Synechococcus* pigment synthesis was forced to P-limitation in the +N treatment. However, such limitation may not be direct because of the low P requirement for pigment–protein complexes (Geider and La Roche 2002).

For *Synechococcus,* significant increases in cellular nucleic acid content were generally only observed after the addition of N and P together (Figs. 6, 7i). Although we could not unequivocally ascribe these observations to increased DNA and/or RNA, the cellular content of both these macromolecules increases along with growth rate in *Synechococcus* (Lepp and Schmidt 1998). Further, the addition of N and P together potentially resulted in a lower proportion of *Synechococcus* cells being within G_1 at the time of sampling (Fig. 6b), suggestive of arrested cell cycles in non-NP treatments (Olson et al. 1986; Vaulot et al. 1996;

Table 2. Percent contribution of various groups to total picoautotrophic chlorophyll. Relative cellular red (chlorophyll) fluorescence multiplied by cellular abundances are expressed as percentages of the total. Values presented are mean ±SE. Groups are *Prochlorococcus* (Pro), *Synechococcus* (Syn) and picoeukaryotes (Euk).

			Treatment				
Experiment		Initial	Control	+P	+ NO_3^-	+N	+NP
21°N, 62°W	Pro	34±0.1	21±3	15±2	18±2	31±3	8±4
	Syn	26±2	34±8	47±7	67±4	47±6	83±5
	Euk	40±2	44±11	38±8	15±4	22±6	10±2
28°N, 64°W	Pro	13±1	4±2	4±1	2±1	6±0.4	2±0.2
	Syn	34±2	50±11	46±0.1	84±3	72±6	85±1
	Euk	54±2	46±13	50±1	14±2	22±6	13±1
29°N, 53°W	Pro	16±6	5±1	5±2	2±1	5±2	3±0.3
	Syn	39±5	57±6	56±5	90±7	83±4	89±1
	Euk	45±1	37±5	40±3	8±6	12±2	9±2
32°N, 44°W	Pro	26±6	23±2	25±2	15±1	17±2	10±0.4
	Syn	56±3	53±1	49±3	71±1	72±3	75±0.3
	Euk	18±4	25±1	25±2	14±2	11±1	15±1
31°N, 27°W	Pro	34±1	23±3	23±2	14±2	26±1	22±1
	Syn	30±2	20±2	20±2	53±3	47±1	52±2
	Euk	37±3	57±3	56±2	33±4	28±1	26±1

Liu et al. 1999). However, given the caveats mentioned above such a conclusion must clearly be treated with caution. Irrespectively, the cellular accumulation of at least some forms of nucleic acid was co-limited by both N and P (Fig. 6). These observations are consistent with the biochemical composition of nucleic acids, which contain significant amounts of N and P (Geider and La Roche 2002) and suggest that *Synechococcus* was co-limited by both N and P in situ.

Further, NP co-limitation of nucleic acid synthesis enables us to hypothesize indirect mechanisms for the lower cellular chlorophyll and phycoerytherin observed both in situ and after N addition alone. For example, if pigment synthesis in *Synechococcus* was transcriptionally controlled, then P-limitation may have been restricting mRNA synthesis. Alternatively, NP co-limitation of ribosomal RNA content may limit the maximum rate of protein synthesis.

In similar experiments performed in warmer (>27°C) tropical waters to the south, Davey et al. (pers. comm.) observed convincing evidence of NP co-limitation of net cell increases. For the current study the only experiment where significant changes in *Synechococcus* cell numbers were observed (21°N, 62°W) also suggested NP co-limitation of net growth. The lack of net increases in cell concentrations within our more northerly experiments (Fig. 1) may have resulted from reduced growth rates at lower temperatures (Table 1) and/or higher grazing pressure after the spring bloom. Irrespectively, in keeping with Davey et al. (pers. comm.), the data at 21°N, 62°W are again consistent with biochemical arguments as, in addition to N-rich protein and NP-rich nucleic acid synthesis, cell proliferation can require the synthesis of P-rich phospholipids (Geider and La Roche 2002), although *see* below and Van Mooy et al. (2006).

Proximal N-limitation was thus apparent in all the picophytoplankton groups measured (Fig. 5). For *Synechococcus* we further suggest that the data presented here support NP co-limitation of nucleic acid synthesis and, potentially, growth. Arrigo (2005) recently suggested a classification scheme for types of nutrient co-limitation ranging from two or more resources limiting different populations within the community to direct physiological simultaneous co-limitation. We suggest that in the central North Atlantic at the time of our study, *Synechococcus* was close to experiencing the latter type of "multi-nutrient (NP) co-limitation"(Arrigo 2005). That is, in situ concentrations of both (bio-available) N and P were depleted to levels too low for cellular uptake to maintain maximal growth rates.

Bulk community responses (Fig. 3) appeared dominated by *Synechococcus* (Fig. 5; Table 2), with the possible exception of the under-sampled larger eukaryotes (*see* below). Hence, despite proximal N limitation and no evidence for a secondary P effect on the cellular chlorophyll contents of *Prochlorococcus* and the picoeukaryotes (Fig. 5), it appears that any residual P pool in the oligotrophic sub-tropical North Atlantic during late spring is limited (Wu et al. 2000; Ammerman et al. 2003). Consequently, at the ecosystem and biogeochemical level we suggest that phytoplankton biomass (yield) was potentially restricted by a lack of both N and P (Fig. 3).

Insensitivity of $F_v : F_m$ to nutrient limitation in the oligotrophic North Atlantic—The lack of sensitivity of $F_v : F_m$ to N limitation within this study (Fig. 3k–o) is consistent with previous results from the oligotrophic North Atlantic (Graziano et al. 1996) and tropical Pacific (Behrenfeld et al. 2006). However, these results contrast with responses to alleviation of Fe stress within high-nutrient low-chlorophyll (HNLC) systems (Behrenfeld et al. 1996; Behrenfeld et al. 2006) and our observations further to the north within the spring bloom (Moore et al. 2006*a*). Behrenfeld et al. (2006) suggested that such contrasting responses of $F_v : F_m$ in different oceanographic

regions reflect fundamental differences in physiology following relief of limitation by N or Fe.

A precipitous decline in $F_v : F_m$ is typically observed in response to both N and Fe starvation in batch cultures of eukaryotes (Geider et al. 1993; Berges et al. 1996; Price 2005) and prokaryotes (Berges et al. 1996; Steglich et al. 2001). Conversely, $F_v : F_m$ is apparently less sensitive to both N (Parkhill et al. 2001) and Fe (Price 2005) limitation within steady-state cultures. Thus, the low sensitivity of $F_v : F_m$ to N limitation may indicate that in situ autotrophic populations were in a state of balanced nutrient-limited growth (Parkhill et al. 2001).

Re-supply of regenerated N and P through the microbial loop within the relatively quiescent surface waters of the macronutrient-limited oligotrophic subtropics might enable the development of balanced growth. In contrast, episodic supply of new Fe due to mixing events or atmospheric deposition may result in a greater potential for unbalanced growth within Fe-limited HNLC regions. Consequently, in addition to direct physiological arguments (Behrenfeld et al. 2006), physical and ecological processes may also contribute to observed differences in indices of nutrient stress between contrasting oceanographic regimes. Other physiological variables including σ_{PSII}, the ratio of fluorescence per unit chlorophyll, and the chlorophyll specific rate of carbon fixation, albeit at a single irradiance level, were also relatively insensitive to relief of proximal N limitation for the experimental duration (Figs. 4, 7c).

As an alternative to balanced N(P) (co-)limited growth, it could be argued that the insensitivity of $F_v : F_m$ and other variables might reflect an absence of growth rate (Blackman type) nutrient limitation. Maintenance of phytoplankton at near-maximal growth rates by efficient nutrient regeneration despite limitation of the yield of phytoplankton biomass by low nutrient supply could then be hypothesized (Goldman 1980; Cullen 1991; Cullen et al. 1992). For example, in northerly experiments, evidence for tight coupling of heterotrophic grazing to autotrophic production was provided by the lack of significant increases in autotrophic cell numbers, despite clear increases in net community carbon fixation (Figs. 3, 7). However, as discussed above, increases in cellular pigment and nucleic acid contents above in situ and control incubations on addition of N(+P) strongly suggested a degree of physiological nutrient stress.

Implications of group specific responses for community structure and function—Phytoplankton community structure can respond to changes in nutrient availability at a number of taxonomic levels. *Prochlorococcus* tends to dominate in the most oligotrophic waters with a shift to *Synechococcus*, picoeukaryotes, and larger eukaryotes as nutrient concentrations increase (Zubkov et al. 1998; Durand et al. 2001). Finer-scale genetic variation can be superimposed on these broad group-specific trends. For example, differing *Prochlorococcus* ecotypes were observed to dominate over a range of oligotrophic conditions (Johnson et al. 2006). In contrast to the majority of *Synechococcus* isolates, cultured *Prochlorococcus* strains are incapable of utilizing NO_3^- (Moore et al. 2002). The bioassay data presented here indicated that the *Prochlorococcus* ecotypes present in the studied surface waters were similarly incapable of using NO_3^- (Fig. 5).

Synechococcus demonstrated the strongest response to N addition, either as NH_4NO_3 or NO_3^- (Fig. 5). *Synechococcus* thus dominated community chlorophyll concentration after 48 h, particularly within NP or NO_3^- treatments (Table 2). Physical inputs of N from below the euphotic zone (Lewis et al. 1986; Michaels et al. 1994; McGillicuddy et al. 1998) will principally be in the form of NO_3^-. Our results are thus consistent with *Synechococcus* dominating the picoautotrophic response to such NO_3^- input (Glover et al. 1988; Durand et al. 2001). *Synechococcus* is therefore likely to contribute more to new production (Dugdale and Goering 1967) within the spring bloom than *Prochlorococcus* (Durand et al. 2001; Moore et al. 2002).

In addition to *Prochlorococcus*, picoeukaryotes also responded less in NO_3^- than in NH_4NO_3 treatments (Fig. 5). Most of the assemblage represented by the picoeukaryotes might be expected to be capable of accessing NO_3^-. Hence the lack of response may simply represent a slower induction of NO_3^- uptake or reduction compared to the rapidly responding *Synechococcus* population. The larger eukaryotes that dominate autotrophic carbon during the spring bloom in this region (Durand et al. 2001) were not evaluated during the current study. Further work investigating the response of these organisms is clearly merited.

Larger phytoplankton are expected to be at a disadvantage in nutrient-limited systems because of their lower surface area-to-volume ratio (Chisholm 1992). Consequently, the smallest organisms e.g., *Prochlorococcus*, might be expected to dominate the community. Indeed *Prochlorococcus* appears highly adapted for growth in a nutrient-impoverished environment, having a minimal genome that presumably helps to minimize both cellular N and P (Dufresne et al. 2003). Additionally *Prochlorococcus* minimizes cellular P demand further via the use of sulfolipids instead of phospholipids (Van Mooy et al. 2006). However, depending on the efficiency of recycling, it is still possible that even this likely best competitor for limiting nutrients may be growth rate limited, as the increases in *Prochlorococcus* chlorophyll fluorescence upon the addition of N alone suggest (Fig. 5); *see* also Graziano et al. (1996).

Irrespectively, larger autotrophs, including both the marginally bigger prokaryote *Synechococcus* and eukaryotes, might be expected to be physiologically limited, consistent with the data presented here (Figs. 5, 6). Additionally, when compared to *Prochlorococcus*, *Synechococcus* appears to have a reduced capacity to substitute phospholipids with sulfolipids (Van Mooy et al. 2006). In contrast, these larger organisms may be better equipped to respond rapidly under conditions where nutrients become available (Table 2), again consistent with observation (Glover et al. 1988; Zubkov et al. 1998; Durand et al. 2001). Observed differences in the degree of N or NP (co-) limitation between groups (Fig. 5) may thus have been influenced by genotypic variability in cellular N and P requirements. Differential responses of *Prochlorococcus*, *Synechococcus,* and picoeukaryotes (Fig. 5) likely contrib-

uted to the initial bulk community responses to N addition in the absence of P (Fig. 3).

Biogeochemical implications—High N : P ratios within the thermocline in the sub-tropical North Atlantic (Fig. 1) are assumed to result from high rates of N_2 fixation followed by subsequent remineralization of N-rich organic material at depth (Michaels et al. 1994; Wu et al. 2000; Hansell et al. 2004). These high rates of N_2 fixation have in turn been related to high atmospheric Fe inputs and subsequent relief of potential Fe(P) (co-)limitation of diazotrophy (Falkowski 1997; Wu et al. 2000; Mills et al. 2004). The low SRP concentrations in this region are thus suggested to be a consequence of relatively high production by diazotrophs (Wu et al. 2000). As previously pointed out (Wu et al. 2000), assuming phytoplankton N : P requirements are 16 : 1, the upward fluxes of nutrients in this region should provide N in excess of P. Such excess N should in turn result in P limitation and suppress N_2 fixation (Tyrrell 1999; Mills et al. 2004). If one accepts that the Redfield ratio of 16 : 1 is the switchover point between N and P limitation, high N_2 fixation accompanied by high dissolved and particulate N : P presents a paradox (Wu et al. 2000).

Additionally, despite the high N : P input ratios (Table 1) associated with winter convection, by the time of our study in late spring photosynthesis and chlorophyll synthesis were proximally N limited, although we cannot exclude NP co-limitation (Figs. 3, 5, 6, 7). Preferential remineralization of P over N was invoked to explain such observations (Ryther and Dunstan 1971; Wu et al. 2000). However, we suggest that plasticity within phytoplankton cellular N : P ratios (Geider and La Roche 2002) may also play a role. Comparing a theoretical model with experimental data (Klausmeier et al. 2004) suggested that higher cellular N : P ratios (>30 : 1) would be a selective advantage in oligotrophic conditions. Increased requirements for N-rich resource acquisition proteins, including nutrient transporters, combined with lower growth rates decreasing the requirement for relatively P-rich ribosomes, can thus be hypothesized to result in acclimation and/or adaptation toward high cellular N : P ratios (Geider and La Roche 2002; Klausmeier et al. 2004). Cellular elemental stoichiometries for the organisms dominating oligotrophic environments (Bertilsson et al. 2003) and further adaptations to minimize P requirements (Van Mooy et al. 2006) further support this suggestion.

It is thus possible that multi-nutrient (NP) co-limitation develops in the region of the current study as a consequence of biochemical co-limitation (sensu Arrigo, 2005). Specifically, during drawdown after nutrient inputs with high N : P ratios, as P approaches limiting concentrations phytoplankton may need to devote proportionally more N to the synthesis of nutrient acquisition proteins to access the increasingly scarce P resource, driving the system toward co-limitation. Such a mechanism could be hypothesized to operate at either a cellular or ecological (taxonomic) level and potentially represents an important characteristic of oligotrophic waters, governing the balance between N and P limitation.

In summary we conclude that N is the proximal limiting nutrient for chlorophyll synthesis and carbon fixation in the oligotrophic sub-tropical North Atlantic. However, our results also suggest that some phytoplankton groups and overall autotrophic community yield are limited by the availability of both N and P. Further comprehension of the causes and consequences of such NP co-limitation is likely to have important implications for our understanding of oceanic ecology and biogeochemistry.

References

Ammerman, J. W., R. R. Hood, D. A. Case, and J. B. Cotner. 2003. Phosphorous deficiency in the Atlantic: An emerging paradigm in oceanography. EOS **84:** 165–170.

Arrigo, K. R. 2005. Marine microorganisms and global nutrient cycles. Nature **437:** 349–355.

Behrenfeld, M. J., A. J. Bale, Z. S. Kolber, J. Aiken, and P. G. Falkowski. 1996. Confirmation of iron limitation of phytoplankton photosynthesis in the equatorial Pacific Ocean. Nature **383:** 508–511.

———, and others. 2006. Controls on tropical Pacific Ocean productivity revealed through nutrient stress diagnostics. Nature **442:** 1025–1028.

Berges, J. A., D. O. Charlebois, D. C. Mauzerall, and P. G. Falkowski. 1996. Differential effects of nitrogen limitation on photosynthetic efficiency of photosystems I and II in microalgae. Plant Physiol. **110:** 689–696.

Bertilsson, S., O. Berglund, D. M. Karl, and S. W. Chisholm. 2003. Elemental composition of marine Prochlorococcus and Synechococcus: Implications for the ecological stoichiometry of the sea. Limnol. Oceanogr. **48:** 1721–1731.

Bowie, A. R., E. P. Achterberg, R. F. C. Mantoura, and P. J. Worsfold. 1998. Determination of sub-nanomolar levels of iron in seawater using flow injection with chemiluminescence detection. Analytica Chimica Acta **361:** 189–200.

Chisholm, S. W. 1992. Phytoplankton size, p. 213–237. *In* P. G. Falkowski and A. Woodhead [eds.], Primary productivity and biogeochemical cycles in the sea. Plenum.

Cullen, J. J. 1991. Hypotheses to explain high-nutrient conditions in the open sea. Limnol. Oceanogr. **36:** 1578–1599.

———, and R. F. Davis. 2003. The blank can make a big difference in oceanographic measurements. Limnol. Oceanogr.-Bulletin **12:** 29–35.

———, X. Yang, and H. L. Macintyre. 1992. Nutrient limitation of marine photosynthesis, p. 69–88. *In* P. G. Falkowski and A. Woodhead [eds.], Primary productivity and biogeochemical cycles in the sea. Plenum.

Dufresne, A., and others. 2003. Genome sequence of the cyanobacterium Prochlorococcus marinus SS120, a nearly minimal oxyphototrophic genome. Proc. Natl. Acad. Sci. USA **100:** 10020–10025.

Dugdale, R. C., and J. J. Goering. 1967. Uptake of new and regenerated forms of nitrogen in primary production. Limnol. Oceanogr. **12:** 196–206.

Durand, M. D., R. J. Olson, and S. W. Chisholm. 2001. Phytoplankton population dynamics at the Bermuda Atlantic Time-series station in the Sargasso Sea. Deep-Sea Res. Pt II **48:** 1983–2003.

Falkowski, P. G. 1997. Evolution of the nitrogen cycle and its influence on the biological sequestration of CO2 in the ocean. Nature **387:** 272–275.

Fanning, K. A. 1992. Nutrient provinces in the sea—concentration ratios, reaction-rate ratios, and ideal covariation. J. Geophys. Res.-Oceans **97:** 5693–5712.

Geider, R. J., and J. La Roche. 2002. Redfield revisited: variability of C : N : P in marine microalgae and its biochemical basis. Eur. J. Phycol. **37:** 1–17.

———, J. Laroche, R. M. Greene, and M. Olaizola. 1993. Response of the photosynthetic apparatus of Phaeodactylum-Tricornutum (Bacillariophyceae) to nitrate, phosphate, or iron starvation. J. Phycol. **29:** 755–766.

Glover, H. E., L. Campbell, and B. B. Prezelin. 1986. Contribution of Synechococcus spp to size-fractioned primary productivity in 3 water masses in the Northwest Atlantic-Ocean. Mar. Biol. **91:** 193–203.

———, B. B. Prezelin, L. Campbell, M. Wyman, and C. Garside. 1988. A nitrate-dependent Synechococcus bloom in surface Sargasso sea-water. Nature **331:** 161–163.

Goldman, J. C. 1980. Physiological processes, nutrient availability, and the concept of relative growth rate in marine phytoplankton ecology, p. 179–194. *In* P. G. Falkowski [ed.], Primary productivity in the sea. Plenum.

Grasshoff, K., K. Kremling, and M. Ehrhardt. 1999. Methods of seawater analysis. Wiley.

Graziano, L. M., R. J. Geider, W. K. W. Li, and M. Olaizola. 1996. Nitrogen limitation of North Atlantic phytoplankton: Analysis of physiological condition in nutrient enrichment experiments. Aquat. Microb. Ecol. **11:** 53–64.

Hansell, D. A., N. R. Bates, and D. B. Olson. 2004. Excess nitrate and nitrogen fixation in the North Atlantic Ocean. Mar. Chem. **84:** 243–265.

Johnson, Z. I., E. R. Zinser, A. Coe, N. P. Mcnulty, E. M. S. Woodward, and S. W. Chisholm. 2006. Niche partitioning among Prochlorococcus ecotypes along ocean-scale environmental gradients. Science **311:** 1737–1740.

Karl, D. M., and G. Tien. 1992. Magic—a sensitive and precise method for measuring dissolved phosphorus in aquatic environments. Limnol. Oceanogr. **37:** 105–116.

Klausmeier, C. A., E. Litchman, T. Daufresne, and S. A. Levin. 2004. Optimal nitrogen-to-phosphorus stoichiometry of phytoplankton. Nature **429:** 171–174.

Kolber, Z. S., O. Prasil, and P. G. Falkowski. 1998. Measurements of variable chlorophyll fluorescence using fast repetition rate techniques: Defining methodology and experimental protocols. Biochimica Et Biophysica Acta-Bioenergetics **1367:** 88–106.

Laney, S. R. 2003. Assessing the error in photosynthetic properties determined by fast repetition rate fluorometry. Limnol. Oceanogr. **48:** 2234–2242.

Lepp, P. W., and T. M. Schmidt. 1998. Nucleic acid content of Synechococcus spp. during growth in continuous light and light/dark cycles. Archiv. Microbiol. **170:** 201–207.

Lewis, M. R., W. G. Harrison, N. S. Oakey, D. Hebert, and T. Platt. 1986. Vertical Nitrate Fluxes in the Oligotrophic Ocean. Science **234:** 870–873.

Liu, H. B., R. R. Bidigare, E. Laws, M. R. Landry, and L. Campbell. 1999. Cell cycle and physiological characteristics of Synechococcus (WH7803) in chemostat culture. Mar. Ecol.-Prog. Ser. **189:** 17–25.

Lomas, M. W., A. Swain, R. Shelton, and J. W. Ammerman. 2004. Taxonomic variability of phosphorus stress in Sargasso Sea phytoplankton. Limnol. Oceanogr. **49:** 2303–2310.

Marie, D., F. Partensky, S. Jacquet, and D. Vaulot. 1997. Enumeration and cell cycle analysis of natural populations of marine picoplankton by flow cytometry using the nucleic acid stain SYBR Green I. Appl. Environ. Microbiol. **63:** 186–193.

Martiny, A. C., M. L. Coleman, and S. W. Chisholm. 2006. Phosphate acquisition genes in Prochlorococcus ecotypes: Evidence for genome-wide adaptation. Proc. Natl. Acad. Sci. USA **103:** 12552–12557.

McGillicuddy, D. J., and others. 1998. Influence of mesoscale eddies on new production in the Sargasso Sea. Nature **394:** 263–266.

Michaels, A. F., and others. 1994. Seasonal patterns of ocean biogeochemistry at the United-States JGOFS Bermuda Atlantic time-series study site. Deep-Sea Res. Pt. I **41:** 1013–1038.

Mills, M. M., C. Ridame, M. Davey, J. La Roche, and R. J. Geider. 2004. Iron and phosphorus co-limit nitrogen fixation in the eastern tropical North Atlantic. Nature **429:** 292–294.

Moore, C. M., M. I. Lucas, R. Sanders, and R. Davidson. 2005*a*. Basin-scale variability of phytoplankton bio-optical characteristics in relation to bloom state and community structure in the Northeast Atlantic. Deep-Sea Res. Pt. I **52:** 401–419.

———, and others. 2006*a*. Iron limits primary productivity during spring bloom development in the central North Atlantic. Glob. Change Biol. **12:** 626–634.

———, and others. 2006*b*. Phytoplankton photoacclimation and photoadaptation in response to environmental gradients in a shelf sea. Limnol. Oceanogr. **51:** 936–949.

Moore, L. R., M. Ostrowski, D. J. Scanlan, K. Feren, and T. Sweetsir. 2005b. Ecotypic variation in phosphorus acquisition mechanisms within marine picocyanobacteria. Aquat. Microb. Ecol. **39:** 257–269.

———, A. F. Post, G. Rocap, and S. W. Chisholm. 2002. Utilization of different nitrogen sources by the marine cyanobacteria Prochlorococcus and Synechococcus. Limnol. Oceanogr. **47:** 989–996.

Olaizola, M., R. J. Geider, W. G. Harrison, L. M. Graziano, G. M. Ferrari, and P. M. Schlittenhardt. 1996. Synoptic study of variations in the fluorescence-based maximum quantum efficiency of photosynthesis across the North Atlantic Ocean. Limnol. Oceanogr. **41:** 755–765.

Olson, R. J., D. Vaulot, and S. W. Chisholm. 1986. Effects of environmental stresses on the cell-cycle of 2 marine-phytoplankton species. Plant Physiol. **80:** 918–925.

Parkhill, J. P., G. Maillet, and J. J. Cullen. 2001. Fluorescence-based maximal quantum yield for PSII as a diagnostic of nutrient stress. J. Phycol. **37:** 517–529.

Price, N. M. 2005. The elemental stoichiometry and composition of an iron-limited diatom. Limnol. Oceanogr. **50:** 1159–1171.

Quigg, A., and others. 2003. The evolutionary inheritance of elemental stoichiometry in marine phytoplankton. Nature **425:** 291–294.

Redfield, A. C. 1958. The biological control of chemical factors in the environment. American Scientist **46:** 205–221.

Ryther, J. H., and W. M. Dunstan. 1971. Nitrogen, phosphorus, and eutrophication in coastal marine environment. Science **171:** 1008–1013.

Scanlan, D. J., and W. H. Wilson. 1999. Application of molecular techniques to addressing the role of P as a key effector in marine ecosystems. Hydrobiologia **401:** 149–175.

Steglich, C., and others. 2001. Nitrogen deprivation strongly affects Photosystem II but not phycoerythrin level in the divinyl-chlorophyll b-containing cyanobacterium Prochlorococcus marinus. Biochimica Et Biophysica Acta-Bioenergetics **1503:** 341–349.

Tyrrell, T. 1999. The relative influences of nitrogen and phosphorus on oceanic primary production Nature **400:** 525–531.

Van Mooy, B. A. S., G. Rocap, H. F. Fredricks, C. T. Evans, and A. H. Devol. 2006. Sulfolipids dramatically decrease phosphorus demand by picocyanobacteria in oligotrophic marine environments. Proc. Natl. Acad. Sci. USA **103:** 8607–8612.

Vaulot, D., N. Lebot, D. Marie, and E. Fukai. 1996. Effect of phosphorus on the Synechococcus cell cycle in surface Mediterranean waters during summer. Appl. Environ. Microbiol. **62:** 2527–2533.

Welschmeyer, N. A. 1994. Fluorometric analysis of chlorophyll-a in the presence of chlorophyll-b and pheopigments. Limnol. Oceanogr. **39:** 1985–1992.

Wu, J. F., W. Sunda, E. A. Boyle, and D. M. Karl. 2000. Phosphate depletion in the western North Atlantic Ocean. Science **289:** 759–762.

Wyman, M., R. P. F. Gregory, and N. G. Carr. 1985. Novel role for phycoerythrin in a marine cyanobacterium, synechococcus strain Dc2. Science **230:** 818–820.

Zubkov, M. V., M. A. Sleigh, G. A. Tarran, P. H. Burkill, and R. J. G. Leakey. 1998. Picoplanktonic community structure on an Atlantic transect from 50 degrees N to 50 degrees S. Deep-Sea Res. Pt. I **45:** 1339–1355.

Received: 22 December 2006
Accepted: 28 August 2007
Amended: 24 September 2007

Paper E: *Nitrogen and phosphorus co-limitation of bacterial productivity and growth in the oligotrophic subtropical North Atlantic*

Synopsis

N and P additions caused 10-fold increases in bacterial productivity and biomass in the same nutrient addition bioassay experiments from the oligotrophic North Atlantic Ocean described in Papers C and D. DOC additions did not affect the heterotrophic bacterial community unless N and P were also added, indicating that the heterotrophic bacterial community was NP co-limited and not DOC limited as is usually presumed. These experiments took place shortly after the spring bloom where grazing and lysis may have released DOC, thus sustaining the heterotrophic population and inducing N and P limitation. There was no response with additions of iron and calculations of iron requirements for heterotrophic cells showed that the iron pool was sufficient for heterotrophic bacteria at the time of sampling. Analytical Flow Cytometry showed that a small subset of large cells with high nucleic acid content created the response. There were no changes in the numerically more dominant small low nucleic acid content heterotrophic bacteria. Although the large cells were numerically less abundant they contributed up to 80% of the RNA biomass, which may have significant implications for nutrient cycling. Analysis of clone libraries showed the presence of SAR 11 bacteria, which may make up part of the small celled population. These oligotrophic bacteria have previously been shown to grow slowly and to not respond to nutrient additions. In contrast, the large celled heterotrophs could be opportunistic bacteria with the ability to respond quickly to nutrient impulses. As shown in Paper D, the picophotoautotrophic communities in these experiments were also N limited. In other words, heterotrophic bacteria and phytoplankton were in direct competition for inorganic nutrients. In fact, the increase in bacterial productivity was greater than the increase in primary productivity. Atmospheric dust deposition, which also supplies N and P, could therefore stimulate the

large cells, increasing competition between heterotrophs and phytoplankton and thus changing the cycling of organic matter.

Contribution

C. M. Moore, M. Mills, A. Milne, E. Achterberg and I contributed equally to the success of the eight experiments performed during the Meteor 60 cruise to the North Atlantic Occean. I was in charge of organizing the bottle cleaning and filling, nutrient additions, and bottle preparations for the incubators. I also measured and analyzed the chlorophyll a data at sea and constructed and analyzed 16S rDNA clone libraries from bioassay experiment samples. M. Mills prepared the manuscript and I provided comments and suggestions.

Limnol. Oceanogr., 53(2), 2008, 824–834

Nitrogen and phosphorus co-limitation of bacterial productivity and growth in the oligotrophic subtropical North Atlantic

M. M. Mills[1,2]
Marine Biogeochemistry, IFM-Geomar, D-24105 Kiel, Germany

C. M. Moore
Department of Biological Sciences, University of Essex, Colchester CO4 3SQ, United Kingdom

R. Langlois
Marine Biogeochemistry, IFM-Geomar, D-24105 Kiel, Germany

A. Milne
School of Earth, Ocean and Environmental Sciences, University of Plymouth, Plymouth PL4 8AA, United Kingdom

E. Achterberg
School of Ocean and Earth Science, National Oceanography Centre, University of Southampton, Southampton SO14 3ZH, United Kingdom

K. Nachtigall and K. Lochte
Marine Biogeochemistry, IFM-Geomar, D-24105 Kiel, Germany

R. J. Geider
Department of Biological Sciences, University of Essex, Colchester CO4 3SQ, United Kingdom

J. La Roche
Marine Biogeochemistry, IFM-Geomar, D-24105 Kiel, Germany

Abstract

Bacterial productivity and biomass are thought to be limited by dissolved organic carbon (DOC) in much of the world's oceans. However, the mixed layer of oligotrophic oceans is often depleted in dissolved inorganic nitrogen and phosphate, raising the possibility that macronutrients may also limit heterotrophic bacterial growth. We used nutrient bioassay experiments to determine whether inorganic nutrients (N, P, Fe) and/or DOC could limit bacterial productivity and biomass in the central North Atlantic during the spring of 2004 (Mar–Apr). We observed that both heterotrophic bacterial productivity and biomass were co-limited by N and P in the oligotrophic North Atlantic, and additions of labile DOC (glucose) provided no stimulation unless N and P were also added. Flow cytometry results indicated that only a small subset of large cells high in nucleic acid content were responsible for the increased productivity in the combined NP amendments. In contrast, nutrient additions elicited no net change on the dominant component of the bacterial population, composed of small cells with relatively low nucleic acid content. In the combined NP treatments the relative increase in bacterial production was greater than that measured when phytoplankton productivity was relieved of nitrogen limitation. These results suggest that N and P co-limitation in the bacterial community results in increased competition between the heterotrophic and autotrophic components of the surface communities in the Central North Atlantic Ocean, and potentially impacts the cycling of organic matter by the bacterioplankton.

[1] Corresponding author (mmmills@stanford.edu).
[2] Present address: Department of Geophysics, Stanford University, Stanford, California 94305.

Acknowledgements

We thank the captain and crew of the *F/S Meteor* and the scientists aboard the Meteor 60 Transient Tracers Revisited cruise, especially D. Wallace, P. Fritsche, F. Malien, and M. Schütt. M. Zubkov and R. Holland assisted with the flow cytometry analysis. Comments from two anonymous reviewers considerably improved an earlier version of this manuscript. The first five authors made equal contributions to the success of the experiments at sea.

This work was supported by DFG grants WA1434/6-1 to D. Wallace and K.L., RO2138/4-2 to J.L.R., and NERC grants to R.J.G. and E.P.A.

In oligotrophic oceanic surface waters, the cycling of organic matter by the bacterial community and the subsequent nutrient uptake and production by autotrophs are tightly coupled. The bacterioplankton consume labile organic carbon released by the phytoplankton (Duarte and Cebrian 1996), which in turn depend on the inorganic nutrients mineralized through consumption of the dissolved organic matter by the bacteria (Kirchman 2004). In this way, the bacteria and the phytoplankton do not compete but are dependent on each other for production.

The assumption in this scenario is that the organic matter produced by phytoplankton is rich enough in nitrogen (N) and phosphorus (P) to sustain the bacterial requirement. Bacteria typically have lower carbon : nitrogen (C : N) and carbon : phosphorus (C : P) requirements than phytoplankton (Vadstein and Olsen 1989). Therefore, either the C : N : P stoichiometry of bacterial substrates must be relatively low in order to meet bacterial N and P demands or the bacteria must utilize supplementary N and P sources to meet these demands. In coastal systems that receive enhanced nutrient loads phytoplankton release dissolved organic matter (DOM) with a low C : N (La Roche et al. 1997). However, in oligotrophic environments where inorganic nutrients are scarce (Wu et al. 2000), phytoplankton may release nutrient-poor DOM (Obernosterer and Herndl 1995). Hence, carbon substrates for the acquisition of energy might be plentiful while available nitrogen and phosphorus for building proteins and nucleic acids may be scarce. The heterotrophic bacteria may, therefore, become limited by nitrogen and phosphorus, putting them in direct competition with phytoplankton for the same nutrients.

Nitrogen is thought to be the primary limiting nutrient for phytoplankton productivity in the oligotrophic North Atlantic Ocean (Graziano et al. 1996; Moore et al. 2006). However other studies have used geochemical evidence and enzyme activity assays to suggest that P availability plays a role in controlling autotrophic productivity and community structure in the North Atlantic Ocean (Ammerman et al. 2003; Lomas et al. 2004). In oligotrophic environments where ambient nutrient concentrations are extremely low, the paradigm of a single nutrient limiting phytoplankton may not always be valid, and the autotrophic community can be co-limited by multiple nutrients (Arrigo 2005). For example, (Mills et al. 2004) showed that the diazotrophic community of the Eastern Tropical North Atlantic was co-limited by phosphorus and iron, while Davey et al. (unpubl. data) and Moore et al. (2008) found that cell division of the picophytoplankton community in the same location required addition of both N and P. Similarly, the phytoplankton community was shown to be NP co-limited in the Eastern Mediterranean during the large-scale phosphorus enrichment experiment CYCLOPS (Thingstad et al. 2005).

Several investigations have indicated that heterotrophic bacterial populations can also experience N and/or P limitation in oligotrophic systems (Cotner et al. 1997; Rivkin and Anderson 1997; Caron et al. 2000), although limitation by carbon is thought to be more common (Cherrier et al. 1996; Church et al. 2000; Carlson et al. 2002). If heterotrophic bacterial limitation by macronutrients is an emerging pattern for the oligotrophic ocean gyres, what are the implications for the biogeochemistry of the oceans?

The micronutrient iron (Fe) is also important to both prokaryotic and eukaryotic microbial communities in the oceans. Its role in limiting phytoplankton communities in high-nutrient low-chlorophyll (HNLC) regions of the oceans is definite (Boyd et al. 2007), while in the North Atlantic Moore et al. (2006) recently showed that Fe can regulate primary productivity in deep mixed layers during the spring bloom. There is relatively little evidence, however, for proximal Fe limitation in oceanic prokaryotes, except for the expected role that iron availability may play in controlling nitrogen fixation in diazotrophic cyanobacteria (Mills et al. 2004). On the basis of regular inputs of desert dust rich in Fe over the North Atlantic Ocean it has been argued that Fe concentrations in this region should exceed the requirements of diazotrophs (Kustka et al. 2003). However, even in the oceanic region receiving the highest dust deposition, recent evidence of PFe co-limitation of diazotrophic activity (Mills et al. 2004) indicates that our understanding of diazotroph Fe demands and/or the bioavailability of dissolved Fe in the oceans is incomplete.

With few exceptions, the bulk heterotrophic bacterial community does not generally appear to suffer from Fe limitation, perhaps due to the ability of this group to produce siderophores which bind inorganic Fe(III) making it more available for uptake (Rue and Bruland 1995). A direct stimulation of bacterial activity upon Fe additions has been recorded (Pakulski et al. 1996) in the Southern Ocean, and an indirect secondary stimulation of the bacterial community has been observed when the primary DOC limitation was alleviated in the same environment Church et al. (2000).

In order to address issues of microbial nutrient limitation we focused our investigations on heterotrophic bacterial communities in the oligotrophic North Atlantic where autotrophic production has previously been directly shown to be strongly N limited (Graziano et al. 1996; Mills et al. 2004; Moore et al. 2006). We examined the changes in bacterial productivity and biomass in response to additions of inorganic nutrients (N, P, Fe), alone and in combination with a labile DOC (glucose). Our results indicate that there is significant overlap in the inorganic nutrients that limit autotrophic and heterotrophic biomass in this system and consequently potential competition for the sparse resources between these groups. As such we hypothesize that macronutrient limitation of the heterotrophic bacterial community results in increased resource competition between the autotrophic and heterotrophic portions of the microbial community and that the tightly coupled production and recycling of organic matter in this environment may be affected.

Material and methods

Study site and sample collection—We conducted our experiments aboard the Transient Tracers Revisited cruise (Meteor 60/5) between 09 Mar and 13 Apr 2004 in the tropical and central North Atlantic Ocean (Fig. 1). Eight experiments were conducted during the cruise; five of which

were in oligotrophic waters ($NO_3^- < 0.03$ μmol L^{-1}, chlorophyll *a* (Chl *a*) < 0.1 μg L^{-1}; Table 1) while the remaining three were performed in waters associated with winter mixing that contained relatively high nutrient and Chl *a* concentrations and were published elsewhere (Moore et al. 2006). The present paper discusses only those experiments in the oligotrophic environments.

Surface seawater was collected between 22 : 00 and 02 : 00 using trace-metal clean techniques. Nocturnal mixing ensured that the water samples represented a mixed water column. Water was pumped while underway (ship speed < 18 km h^{-1}, ~ 3 m depth) from a towed fish using a polytetrafluoroethylene (PTFE) diaphragm pump (A15, Almatec) into a 60-liter carboy housed in a trace-metal clean container (class 1000) where all manipulations of the water samples took place. Water was siphoned from the carboy into randomly selected 1.2-liter acid-washed polycarbonate bottles. All initial conditions were determined from three samples randomly collected during the filling period. Under a laminar flow hood (class 100), nutrients (N, P, Fe) were randomly added alone and in all possible combinations to final concentrations of 1.0 μmol L^{-1} NH_4^+ + 1.0 μmol L^{-1} NO_3^- (combined nitrogen treatment), 0.2 μmol L^{-1} NaH_2PO_4, and 2.0 nmol L^{-1} $FeCl_3$ (Fig. 2) to triplicate bottles. The nutrient concentrations were chosen so that they were comparable to concentrations measured after deep mixing in the North Atlantic and to obtain a measurable response within the relatively short 48-h experimental period. All nutrient stocks, with the exception of the $FeCl_3$, were pretreated with Chelex to remove trace metal contamination. A separate NO_3^- treatment (1.0 μmol L^{-1}) was also carried out. The bottles were capped, sealed with a strip of Parafilm, and placed into plastic ziplok bags in on-deck incubators with circulating surface seawater. In three of the experiments (53°W, 44°W, 27°W) DOC (glucose) was added to duplicate bottles at t = 24 h to a final concentration of 10 μmol glucose L^{-1}, either alone or in combination with the other nutrients. The glucose addition was similar to previously conducted experiments by Carlson and Ducklow (1996) and Carlson et al. (2002). The controls in the nonDOC experiments did not receive any nutrient additions while controls for the DOC treatments received only glucose. The bottles were incubated for 48 h before the final samples were collected. We used the shortest experimental duration possible that allowed for a detectable response to nutrient additions while also minimizing bottle effects. Light was attenuated to 20% of incident surface irradiance with blue filters (Lee Filters No. 172, Lagoon Blue). Two other sets of triplicate bottles were treated exactly the same as described above but were analyzed for $^{14}CO_2$ fixation and $^{15}N_2$ fixation. The results from the $^{14}CO_2$ fixation bottles were reported in (Moore et al. 2006), while the N_2 fixation results will be reported elsewhere. In a companion paper Moore et al. (2008) describe the phytoplankton community response in these same experiments.

Subsamples were taken from the N_2 fixation set of triplicate bottles at the end of the 48-h incubation period for inorganic nutrient analysis. Nitrate and soluble reactive phosphorus (SRP) were analyzed using a nutrient autoanalyzer with a

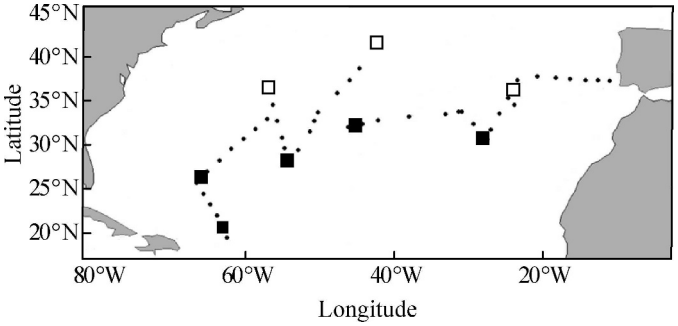

Fig. 1. Map showing the Meteor 60 cruise track. Experiments were conducted at the squares on the map and dots are stations along the cruise track. Experimental sites denoted by filled squares were oligotrophic ($NO_3^- < 0.03$ μmol L^{-1}, Chl *a* < 0.1 μg L^{-1}) and are included in this manuscript. Experimental sites denoted by open squares were spring bloom sites (NO_3^- > 0.03 μmol L^{-1}, Chl *a* > 0.1 μg L^{-1}) and are not included here.

detection limit of 0.03 μmol L^{-1} (Grasshoff et al. 1999); SRP was also determined in those treatments without added PO_4^{-3} using the MAGIC protocol described in Karl and Tien (1992) with a detection limit of 8.0 nmol L^{-1}. Ammonium was measured using the method of Holmes et al. (1999) with a detection limit of 15 nmol L^{-1}. Total dissolved Fe (DFe) was analyzed using flow-injection chemiluminescence (Bowie et al. 1998) with a detection limit of 40 pmol L^{-1}. Samples for DFe were filtered using 25-mm-diameter Gelman™ syringe filters (0.2 μm pore size, PTFE membrane). A 12-h acidification and 12-h reduction period was allowed prior to analysis of DFe, in order to ensure all DFe was converted to Fe(II).

Bacterial abundance and production—Samples for bacterial abundance measurements were collected by pipetting 1.9-mL subsamples into cryotubes containing 0.1 mL of glutaraldehyde (20%). The samples were immediately frozen at −80°C and stored frozen until flow cytometric analysis. Prior to enumeration the samples were thawed at room temperature, and analyzed on a Becton Dickinson FACSort™ flow cytometer after staining with the nucleic acid stain SYBR Green II. The heterotrophic bacterial community was distinguished from the two dominant cyanobacterial groups *Synechococcus* sp. and *Prochlorococcus* sp. based on side scatter (cell size), red (chlorophyll) and orange (phycoerytherin) fluorescence, and relative nucleic acid content (Simon et al. 1994, Marie et al. 1997). Heterotrophic bacterial abundance and estimates of their relative nucleic acid content and size were evaluated from plots of cellular side scatter versus green fluorescence using WinMDI (version 2.8, Joseph Trotter). The heterotrophic bacteria were further divided into two subgroups, small cells with low nucleic acid content, SLNA, and large cells with high nucleic acid content, LHNA (Fig. 3). Particle counts and fluorescence were calibrated against a 0.5-μm bead standard (Fluoresbrite Microparticles, Polysciences).

Bacterial productivity was measured according to Lochte et al. (1997) by incubating 10-mL of water (taken from a 100-mL subsample) with 0.185 MBq of ^{3}H-Thymidine, equivalent to an addition of 8 nmol thymidine

Table 1. Initial conditions and limiting nutrients for bioassay experiments. Mean (±SD) of triplicate samples, except for DFe where the standard error of an individual sample analyzed four times is presented.

Latitude (°N)	21°N	28°N	29°N	32°N	31°N
Longitude (°W)	62°W	64°W	53°W	44°W	27°W
Bacterial productivity	0.27	0.31	0.35	0.69	0.78
(pmol thymidine L^{-1} h^{-1})	−0.42	−0.18	−0.17	−0.17	−0.08
Bacterial abundance $\times 10^8$ L^{-1}	2.63	2.25*	3.38	2	3.99
	−0.38		−0.22	−0.06	−0.13
Chlorophyll a (μg L^{-1})	0.067	0.043	0.045	0.081	0.091
	−0.006	−0.002	−0.006	−0.004	−0.01
NH_4^+ (μmol L^{-1})	N/A	N/A	0.135	<0.025	<0.025
NO_3^- (μmol L^{-1}) †	<0.03	<0.03	<0.03	<0.03	<0.03
PO_4^{3-} (μmol L^{-1}) †	<0.010	<0.010	<0.010	<0.010	0.014
					−0.005
DFe (nmol L^{-1})	0.51	0.47	0.21	0.27	0.25
	−0.05	−0.01	−0.02	−0.03	−0.01
Limiting nutrient‡	NP	NP	NP	NP	NP

* Only one replicate was available for analysis.
† Sample concentrations below the detection limits of 0.03 μmol L^{-1} and 0.08 μmol L^{-1} for NO_3^- and PO_4^{3-}, respectively.
‡ Nutrient treatment resulting in significant increase of bacterial productivity (and abundance of the LHNA group).

L^{-1} (specific activity of 0.002 MBq $pmol^{-1}$) for approximately 6 h in the dark. At the end of the incubation, formalin (100 μL 37%) was added to stop bacterial activity. For each treatment, a poisoned control was measured to correct for nonspecific labeling. Samples were filtered onto polycarbonate filters (25-mm diameter, 0.2-μm pore size) under low vacuum (<0.2 bar) and rinsed well. Filters were placed in 10-mL scintillation vials and 4-mL scintillation cocktail was added (Lumagel Plus; Lumac SC, Groningen, The Netherlands). The samples were left for 24 h in the dark before counting on a scintillation counter. Bacterial productivity is presented here as the thymidine uptake rate. In order to compare bacterial productivity to phytoplankton productivity ($^{14}CO_2$ fixation from Moore et al. 2006) we applied a thymidine conversion factor of 1.18×10^{18} cells produced per mol thymidine incorporated (Ducklow 1983). An average cell volume of 0.04 μm^3 (Carlson and Ducklow 1996) and a carbon conversion factor of 2.5×10^{-7} μg C μm^{-3} (Fry 1988) were used to determine equivalent carbon units.

Results

Bacterial productivity and abundance—Bacterial productivity in the initial (ambient water) samples at the oligotrophic stations was highest at the two eastern-most experimental sites, decreasing by approximately 50% to the west and south (Table 1). These observations coincided with similar trends in Chl *a* concentrations. Total bacterial cell abundance was constant across the oligotrophic Central North Atlantic Ocean averaging $2.94 \times 10^8 \pm 0.35 \times 10^8$ cells L^{-1}.

Bottle effects were minimal as shown by the comparison of the initial measurements and controls measured after 48 h (Fig. 4). Across all experiments, bacterial productivity in the controls did not significantly differ from the initials (Fig. 4A, analysis of variance [ANOVA] with Tukey HSD post hoc test, $p > 0.05$). Likewise, total cell abundance of the heterotrophic bacterial community in the controls did not differ significantly from the initials (Fig. 4B; ANOVA with Tukey HSD post hoc test, $p > 0.05$). Small, though significant, differences were noted when examining bacterial groups separately. The SLNA group differed significantly in abundance between the control and initial in the experiment at 44°W, with the control having approximately 1.3-fold higher cell abundances (Fig. 4C). The abundance of the LHNA group was approximately 1.5-fold higher in the control at the 53°W site as well as the control and +DOC alone treatment at the 27°W site (Fig. 4D). These were small differences when compared to the treatment responses shown below.

At all sites, bacterial productivity was co-limited by N and P (Fig. 5A–E). Productivity was 11–35-fold greater in the +NP treatments than in the control. The combined addition of +NPFe did not significantly stimulate productivity above that of the +NP treatment. In contrast to productivity, total community abundance of heterotrophic bacteria did not significantly increase relative to the control in the +NP treatment (Fig. 5F–J).

The addition of glucose alone resulted in no significant increase in bacterial productivity, total community abundance, or group-specific abundance (Fig. 4A–D). Bacterial productivity increased 50–100-fold and bacterial abundance increased 2–3-fold compared with the control when glucose was added along with N and P. No further stimulation in productivity or abundance was recorded when labile DOC was added with NPFe, with the exception of a small increase in abundance at the 32°N station (Fig. 5I).

Bacterial productivity was also measured in the dark at two stations, with and without the combined addition of N and P, to assess if autotrophic activity resulted in enhanced bacterial production rates (Fig. 6). Unamended dark productivity was not significantly different than that measured in the control ($p > 0.05$). However, the +NP amended dark productivity was 18–60-fold higher than the control rates (natural irradiance), and equal to, or greater than in the +NP treatments with natural irradiance. At the 32°N site, the productivity in the dark +NP treatment

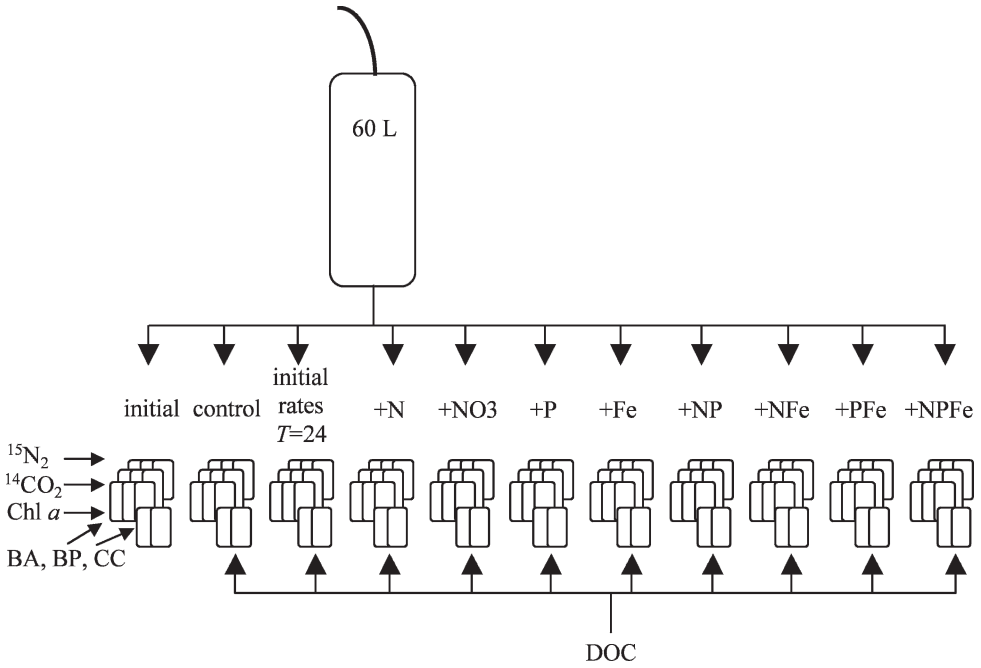

Fig. 2. Experimental design for the nutrient limitation bioassays onboard the Meteor 60 cruise. Surface seawater was collected trace-metal clean, dispensed into 1.0-liter polycarbonate bottles and nutrients (N, P, Fe) and dissolved organic carbon (DOC) were added alone and in combination. Triplicate incubations for each nutrient treatment were performed. Three full sets of triplicate bottles were carried out; one for measurements of $^{15}N_2$ fixation rates, one for $^{14}CO_2$ fixation rates, and the third for measurements of bacterial production rates (BP), bacterial abundance (BA), Chl *a* concentrations, and community composition (CC) measurements. See text for full description of design and methods.

responded approximately three times more then the +NP treatment in the light, suggesting competition between autotrophs and heterotrophs for the nutrients N and P.

At all sites the initial abundance of the LHNA group was an order of magnitude lower ($\times 10^4$) than the SLNA group ($\times 10^5$). The treatment responses in the LHNA group mirrored that of the net heterotrophic bacterial productivity changes, increasing above the control only when N and P were added together (Fig. 5K–O). No further significant increase was measured when Fe was added together with N and P. Net growth rates for the LHNA group in the +NP and +NPFe treatments averaged 0.46 d^{-1}. The SLNA heterotrophic bacterial group did not increase in biomass above the control under any nutrient amendments. In fact, the abundance in the SLNA group at times decreased below the control abundances (Fig. 5R,S,T).

The addition of labile DOC did not increase the abundance of the SLNA group. As in the −DOC treatments, the LHNA group only increased its abundance when glucose was added in combination with N and P (Fig. 5M–O). The combined NP + DOC treatment resulted in a 10–38-fold increase in cellular abundance in this group. A significant further increase in the number of LHNA cells was recorded when all nutrients (NPFe) and labile DOC were added at the 32°N site. Net growth rates of the LHNA in the NP + DOC and NPFe + DOC treatments were 2.75 and 2.97 d^{-1} respectively.

Relative changes in the heterotrophic bacterial community—The LHNA heterotrophic bacterial group comprised <20% of the initial bacterial community. This remained relatively constant in all nutrient treatments, except for the combined N and P treatments where they comprised up to 40% (Fig. 7). In the NP + DOC treatments, the LHNA group comprised 50–70% of the community.

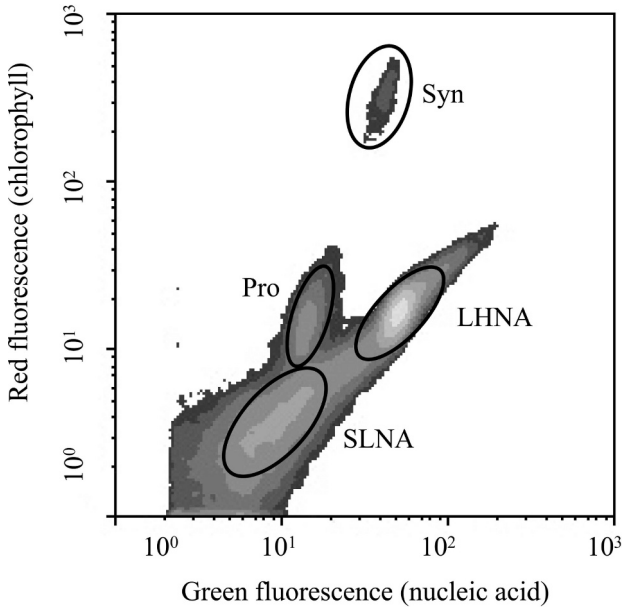

Fig. 3. Typical plot from flow cytometry analysis showing separation of the two heterotrophic bacterial groups (SLNA and LHNA), as well as the two dominant cyanobacterial groups *Prochlorococcus* and *Synechococcus*.

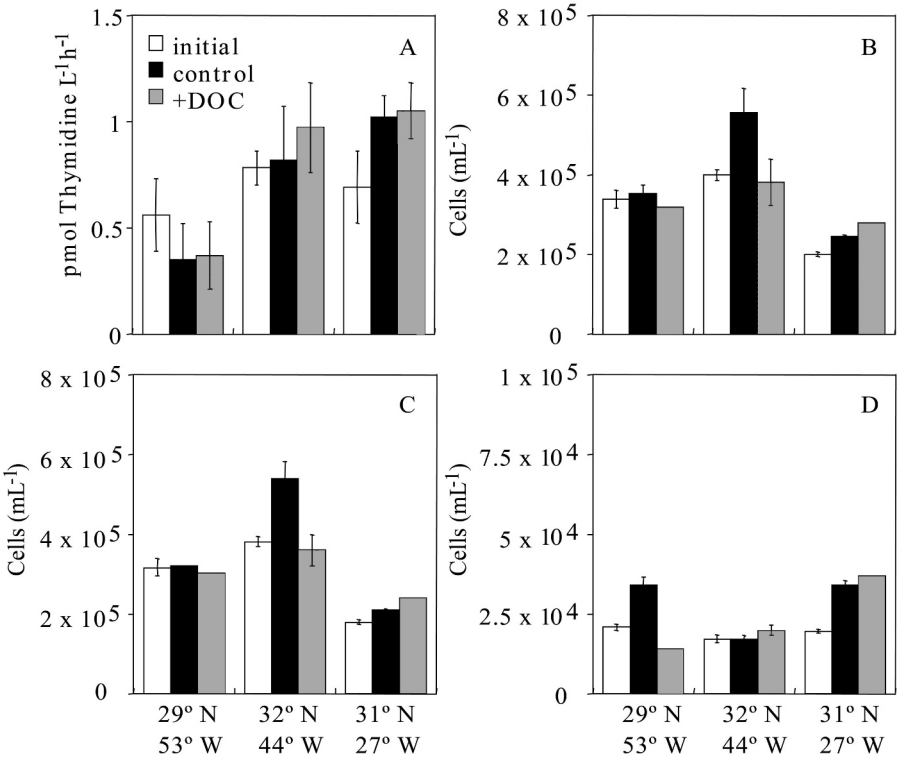

Fig. 4. Results from three experiments comparing (A) thymidine incorporation rate, (B) total heterotrophic cell abundance, (C) SLNA cell abundance, and (D) LHNA cell abundance in the initial, control, and DOC treatments. Error bars represent ±1 standard error.

Despite the low percent contribution of the LHNA group in the ambient oceanic water, it accounted for between 26–57% of the heterotrophic bacterial nucleic acid pool (Fig. 7). After 48 h, the LHNA nucleic acid pool increased by approximately 35% in the controls at the 28°N and 29°N sites, respectively, but no increase was measured at the other sites. Upon the combined addition of N and P, the LHNA nucleic acid pool ranged from 59% to 85%, a 1.5–2-fold increase. In the DOC treatments, little change was recorded in the percent composition of the nucleic acid pool relative to the −DOC treatments, with the exception of those treatments containing both N and P. In these treatments the LHNA nucleic acid pool increased to between 89–95% of the total heterotrophic bacterial nucleic acid pool.

Bacterial productivity relative to primary productivity—We estimated carbon-based bacterial production to determine the relative proportion of bacterial productivity to primary productivity. The initial rates averaged 5% ± 2% (avg. ±SE) of $^{14}CO_2$ net carbon fixation rates (Fig. 8A). This average remained statistically unchanged unless both N and P were added together. Net bacterial productivity rates then increased to 29–40% of the net CO_2 fixation rates. Assuming autotrophic productivity was not stimulated by the addition of DOC, than net bacterial productivity rates would have increased to >100% of the net CO_2 fixation rates in the NP + DOC treatments. Autotrophic fixation of CO_2 was not measured in the DOC treatments, but in vivo chlorophyll *a* fluorescence measurements were lower in the NP + DOC treatments relative to the NP treatments alone at the 31° and 32°N sites (Fig. 8B) suggesting lower Chl *a* concentrations resulted from increased competition for inorganic N and P between autotrophs and heterotrophs.

Discussion

The results of the bioassay experiments clearly demonstrated that net heterotrophic bacterial productivity and biomass in the central North Atlantic were nitrogen and phosphorus co-limited during Mar and Apr 2004. There was a greater than 10-fold increase in bacterial productivity and biomass when N and P were added together, as well as a substantial change in bacterial community composition. A further 3–10-fold increase in productivity and biomass occurred when DOC was added together with N and P, but not in any other treatment. This enhancement suggests that once NP co-limitation was relieved, net heterotrophic bacterial production became carbon (energy) limited.

The addition of Fe, alone or with N and P did not stimulate bacterial productivity or biomass. The concentrations of dissolved Fe observed during our study are consistent with the measurements of Wu and Boyle (2002), who reported surface water values for the Sargasso Sea decreasing from 0.8 nmol L^{-1} (26°N) to 0.2 nmol L^{-1} at 32°N. Additionally, dFe concentrations made near the BATS site during spring 2004, the same time and area as our study, ranged between 0.09 and 0.26 nmol L^{-1} (Sedwick et al. 2005), and are in good agreement with the values we present. If the measured initial thymidine uptake

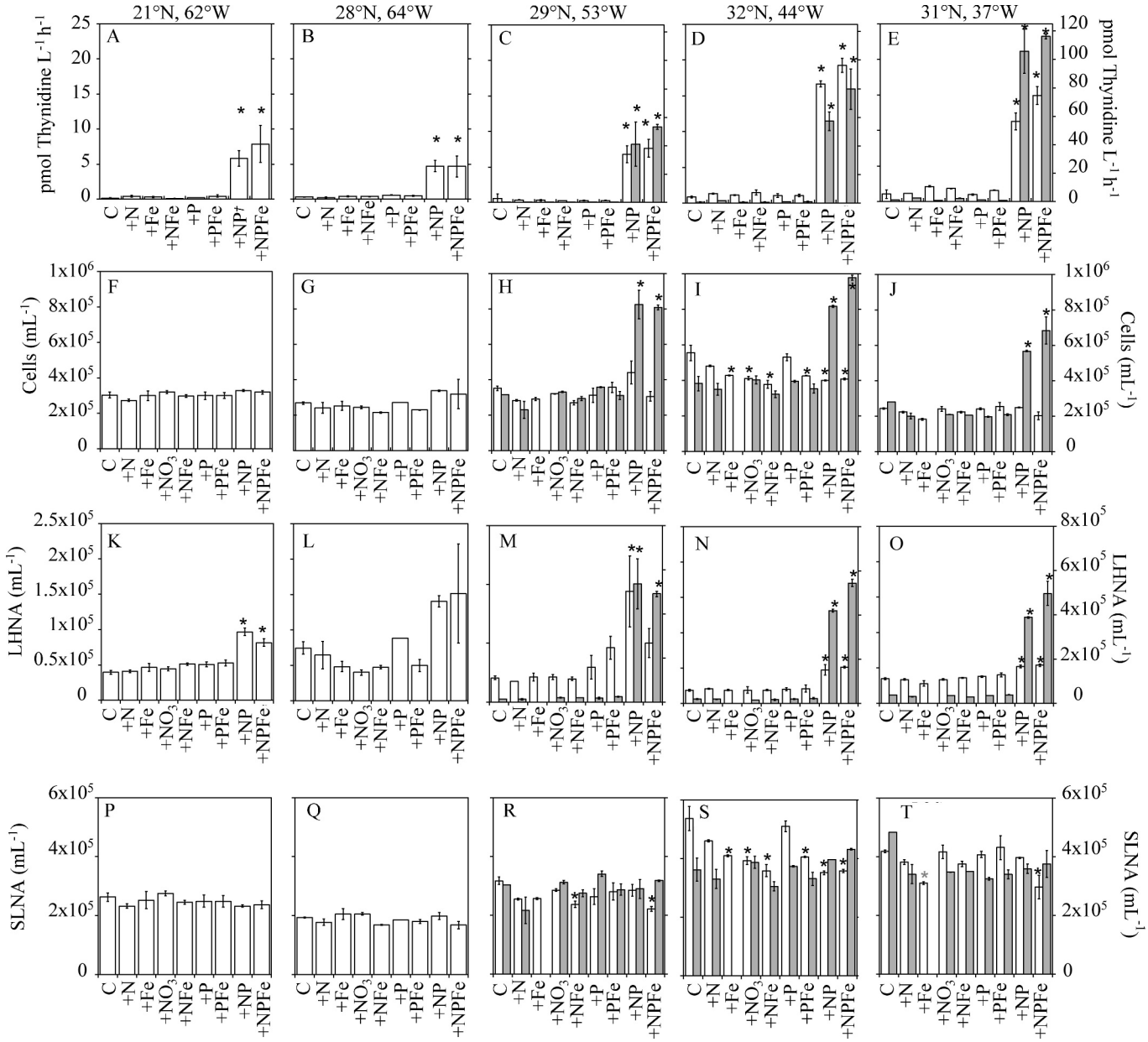

Fig. 5. Comparison of (A–E) thymidine incorporation rate, (F–J) total heterotrophic cell abundance, (K–O) LHNA cell abundance, and (P–T) SLNA cell abundance responses in the different nutrient treatments. Thymidine incorporation rates were measured between 24–48 h; all cell abundances were sampled at 48 h. Note DOC responses are shaded bars and where present correspond to the second *y*-axis. All white bars are the –DOC treatments and correspond to the primary *y*-axis. Error bars represent ±1 standard error. Asterisks (*) indicate significant difference from the control indicated ($\alpha = 0.05$).

rates are converted to equivalent carbon productivity rates (as described above) and multiplied by a Fe : C of 7.5–9.1 (pmol : μmol; Tortell et al. 1996) we calculate the Fe required to meet the initial bacterial productivity rates ranges from 0.030 to 0.130 nmol L^{-1} d^{-1}. The lowest ambient dFe concentrations measured here were approximately 0.25 nmol L^{-1}, almost 2-fold greater than needed to support heterotrophic bacterial productivity. Thus, the experimental results and simple calculation of bacterial Fe requirements suggest that Fe availability at this time of year was sufficient to meet the demand of the heterotrophic bacterial community.

The fact that both the autotrophic (Moore et al. 2008) and heterotrophic microbial communities in the present investigation were co-limited by N and P suggests there was competition for macronutrients between these two groups. Consistent with this, we recorded a noticeable decrease in the in vivo chlorophyll fluorescence between the +NP treatment and the NP + DOC treatment, presumably due to the heterotrophic bacterial community out-competing the phytoplankton community for N and P under these conditions (Fig. 8B). Our data demonstrates that the relative increase in the net heterotrophic bacterial production, when NP co-limitation was relieved, was greater than the relative

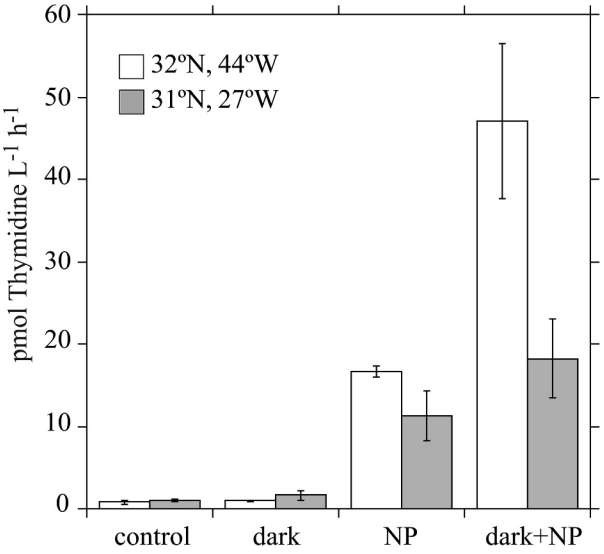

Fig. 6. Thymidine incorporation rates in the control, dark (no nutrient amendment), +NP, and dark + NP treatments at the 31°N and 32°N sites. Error bars represent ±1 standard error.

increase in phytoplankton productivity. In the present study, net heterotrophic production by bacteria as a percentage of net phytoplankton production (BP : PP) was estimated to be 5% ± 2%, similar to estimates from the BATS station in the Sargasso Sea (Steinberg et al. 2001). When only N was added, BP : PP decreased slightly as only phytoplankton productivity was stimulated. The ratio increased dramatically to 30–40% when N and P were added together. The high BP : PP under simultaneous N and P amendments are in line with the global estimate of 31% made by (Cole et al. 1998), although our bacterial production rates are net and, thus, likely underestimates. If our bacterial productivity rates are converted to bacterial carbon demand (BCD) using a bacterial growth efficiency of 14% (Carlson and Ducklow 1996), then BCD is up to four-fold higher than net primary productivity in the NP treatments.

Our results contrast with nutrient addition experiments in the Mediterranean Sea where *Synechococcus* sp. had higher maximum uptake rates and a higher affinity for inorganic phosphate than the heterotrophic bacterial community (Moutin et al. 2002). Similar to the Moutin et al. (2002) investigation, *Synechococcus* sp. responded most strongly to NP amendments in the present experiments (Moore et al. in press). However, the greater net increase in heterotrophic bacterial production relative to autotrophic production suggests that the heterotrophs were the superior competitors. One reason for this observation may have been that our experiments were conducted relatively soon after the high spring productivity period. DOC lost from the phytoplankton during the spring bloom, through exudation, grazing, and/or viral lysis, may have sustained the post–spring-bloom heterotrophic bacterial community, which was subsequently driven to NP co-limitation. These experiments support the idea that the low concentration of inorganic nutrients and proportionately higher concentration of organic matter in oligotrophic systems favors prokaryotic heterotrophs (Cotner and Biddanda 2002).

In addition, recent evidence has shown that while heterotrophic bacteria have high P demands due to membrane phospholipids, some autotrophs (e.g., *Prochlorococcus*) have high concentrations of sulpholipid membranes (Van Mooy et al. 2006) and, thus, possibly lower P demands. This would be an ecological advantage in a phosphate-depleted environment and a likely contributor to the ecological success of *Prochlorococcus* in the open ocean. However, microbes containing relatively more phospholipids, such as heterotrophic bacteria or *Synechococcus,* would likely be better at acquiring phosphate when it becomes available.

Interestingly, the separation of the heterotrophic bacterial community into two groups based on their nucleic acid content lead us to conclude that the increase in bacterial productivity after enrichment with N and P can be attributed to the response of the LHNA group, a numerically minor component of the bacterial population. The LHNA group accounted on average for <15% of the initial bacterial community and increased in abundance to >30% in response only to the +NP amendments. Thus, growth of LHNA bacteria was presumably the reason for the stimulated productivity measured in the bulk community. While the LHNA group was relatively less abundant the cells were estimated to be >5-fold larger, based on cellular side scatter and nucleic acid content, and thus formed a major proportion of the bacterial biomass. The cellular RNA content indicated that the LHNA group made up approximately 20–70% of the initial heterotrophic bacterial biomass. Under the NP amendments the RNA content rose to >50–80% of the biomass and we assume a proportionally similar amount of the productivity. Thus comparisons based on cell abundance most likely underestimate the importance of the LHNA group to the cycling of nutrients in these waters. The LHNA heterotrophic bacterial group appears adapted to maximize their growth under transient periods of high nutrient inputs, while remaining numerically a small component of the bacterial community until such a transient period arrives.

In contrast to the LHNA, net growth of the SLNA cells was not limited or co-limited by N, P, or DOC. We hypothesize that this group was a true oligotrophic prokaryote such as the SAR-11 bacterioplankton *Pelagibacter ubique* (Giovannoni et al. 2005). The SAR11 clade consistently peaks in abundance during the summer (Morris et al. 2005) when temperature and nutrient concentrations are at their seasonal highest and lowest respectively. Likewise, concentrations of inorganic N and P in the mid-latitude North Atlantic were typically low during this cruise (Table 1), but have been shown to be even lower at other times of the year (Wu et al. 2000). Members of the SAR11 clade, such as *Pelagibacter ubique,* do not respond to nutrient enrichment and are adapted to grow slowly (Giovannoni et al. 2005). Their streamlined genome and small cell size economize in P and N and the analysis of their genome indicates they are metabolically very simple. Thus, genes coding for nitrate uptake and assimilation are absent, as for *Prochlorococcus*, the main group of oligotrophic photosynthetic prokaryotes (Rocap et al. 2003). Members of the SAR-11 clade were present in the initial community at the 64°W and 27°W sites, the only

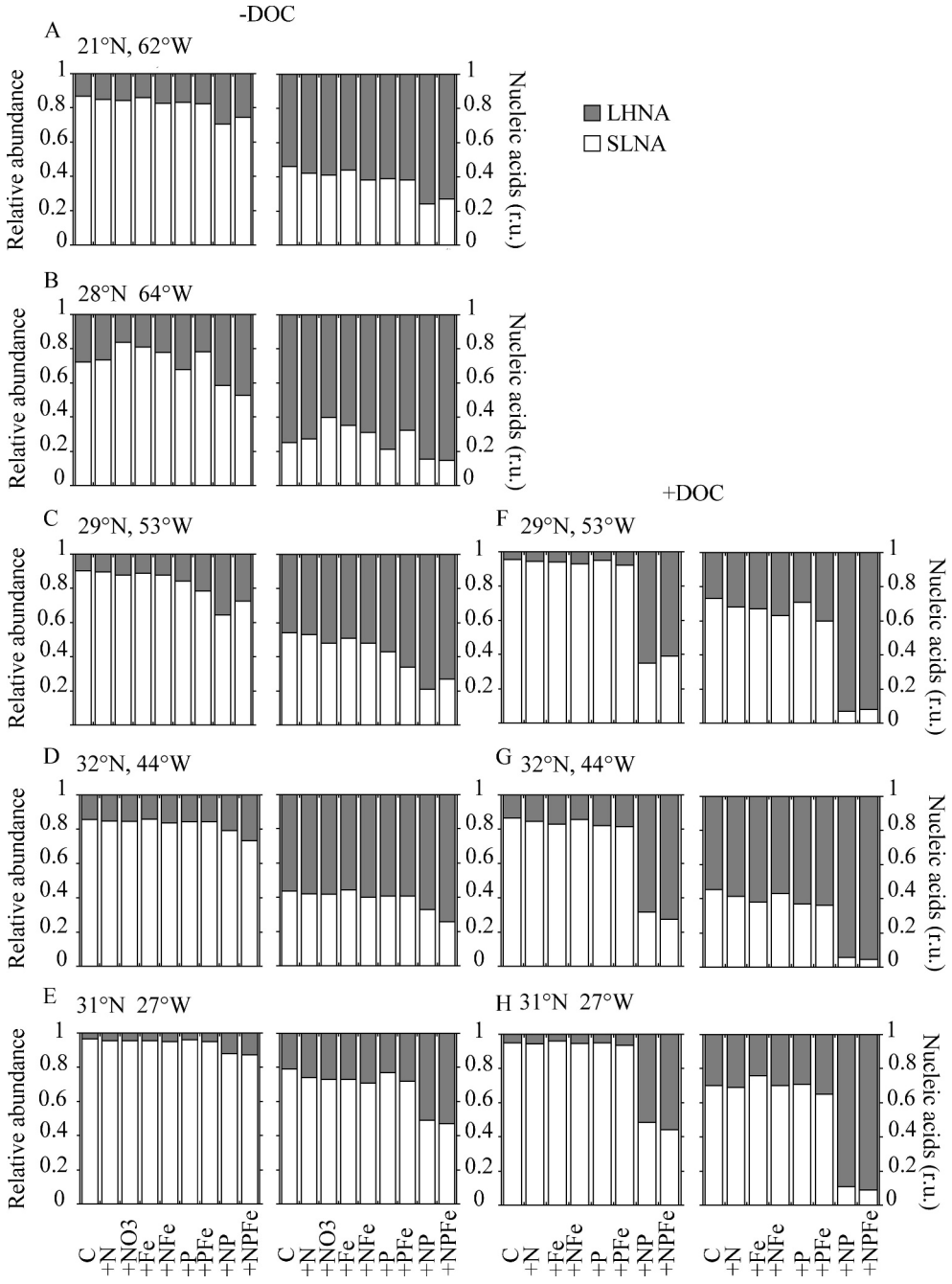

Fig. 7. Relative abundances of the two heterotrophic bacterial groups (SLNA and LHNA) and their relative contributions to the heterotrophic bacterial nucleic acid pool in the different treatments (A–E) –DOC treatments, (F–H) +DOC treatments. r.u. is relative units and is a measure of the fluorescence emitted by the stained nucleic acids. The fluorescence is proportional to the nucleic acid content per cell.

two stations for which 16S rRNA sequences are available (R. Langlois and W. Mohr pers. comm.). The lack of response by the SLNA group to nutrient addition suggests that they predominantly belong to SAR11 clade and are true oligotrophic bacteria (Giovannoni et al. 2005).

The low levels of nutrients in our study region would likely limit the largest cells most (e.g., the LHNA group) due to their lower surface-area-to-volume ratio. Moreover, the low nucleic acid content of the SLNA group implies their cellular requirement for P (and N) was low. Although we assume that the SLNA and LHNA groups in the present study are two different ecological types of bacteria, the former truly "oligotrophic" and the latter "opportunistic," we cannot rule out that these may be inactive and active components of a single group with the techniques we employed here. However, field data often indicate that different groups of bacteria account for differences in bacterial activity (Cottrell and Kirchman 2003) and that

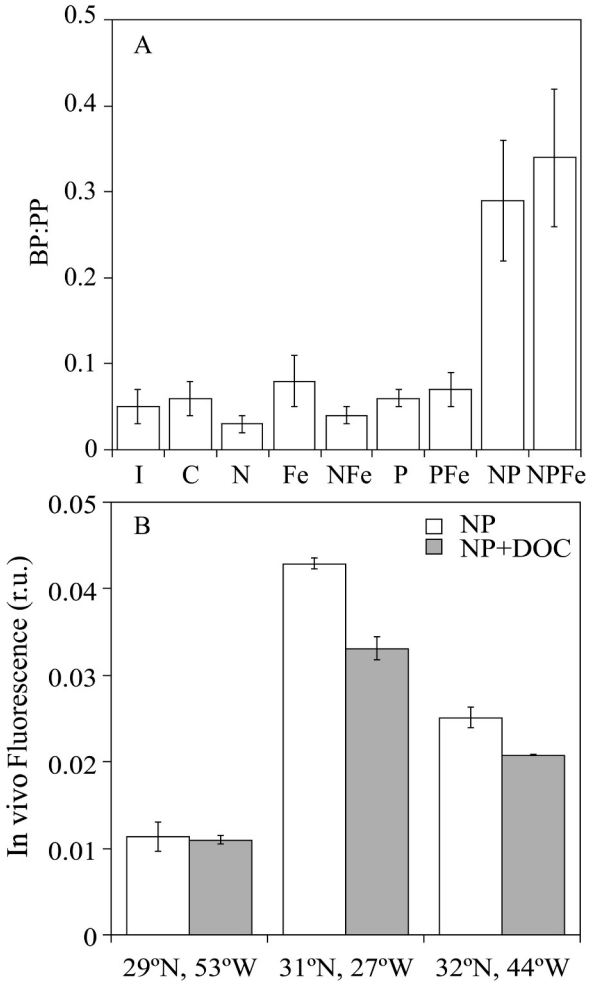

Fig. 8. A) Bacterial production (BP) as a proportion of primary production (PP). BP estimated using a thymidine conversion factor of 1.18×10^{18} cells produced per mole thymidine incorporated (Ducklow 1993). An average cell volume of 0.04 μm^3 and a carbon conversion factor of 2.5×10^{-7} μg C μm^{-3} was used to determine equivalent carbon units. PP data are from Moore et al. 2006 and Moore et al. (in press). B) Comparison of the mean (±SE) in vivo chlorophyll *a* fluorescence in the NP and NP + DOC treatments presented in relative fluorescence units (r.u.).

bacteria responding to a stimulus are clearly distinguishable from those that do not respond (Cottrell and Kirchman 2000). The presence of more opportunistic bacterial groups related to *Alteromonas, Pseudoalteromonas*, Marinobacter, Marinomonas and members of the Cytophagale clades were also detected in the initial bacterial community at these stations (R. Langlois and W. Mohr, pers. comm.). Sequenced genomes from representative members of these bacterial groups indicate that at least some have the necessary genes encoding for the assimilation of nitrate.

The consistency of the NP co-limitation across the large latitudinal (21°N–32°N) and longitudinal (62°W–27°W) gradient covered in our study suggests that net heterotrophic bacterial community productivity was NP co-limited across the oligotrophic mid-latitude waters of the North Atlantic during the period of our study. Analyses of two bacterial groups suggest that the net productivity response to inorganic nutrient addition was most likely dominated by increase in growth rate of large, nucleic-acid-rich "opportunistic" bacteria, while the smaller "oligotrophs" were unaffected. The opportunistic bacteria that were N and P co-limited are likely in direct competition with photoautotrophs for macronutrients. Such competition may interfere with the tightly coupled production and recycling of organic matter in oligotrophic oceanic surface waters (Thingstad et al. 1997). Likewise, atmospheric deposition of high N : P aerosols, a major source of new nutrients to the open ocean, would stimulate autotrophic productivity (Moore et al. 2006) and fuel the competition between autotrophs and heterotrophs for sparse nutrients. Future global warming scenarios predict increased oceanic stratification and acute nutrient limitation. Thus, understanding how nutrients constrain microbial productivity in the surface waters of oligotrophic oceans may lead to improvements in our comprehension of the role these processes play in the biogeochemistry of present and future oceans.

References

Ammerman, J. W., R. R. Hood, D. A. Case, and J. B. Cotner. 2003. Phosphorus deficiency in the Atlantic: An emerging paradigm in oceanography. EOS (Transactions, American Geophysical Union) **84:** 165–170.

Arrigo, K. R. 2005. Marine microorganisms and global nutrient cycles. Nature **437:** 349–355.

Bowie, A. R., E. P. Achterberg, R. F. C. Mantoura, and P. J. Worsfold. 1998. Determination of sub-nanomolar levels of iron in seawater using flow injection with chemiluminescence detection. Anal. Chim. Acta **361:** 189–200.

Boyd, P. W., and others. 2007. Mesoscale iron enrichment experiments 1993–2005: Synthesis and future directions. Science **315:** 612–617.

Carlson, C. A., and H. W. Ducklow. 1996. Growth of bacterioplankton and consumption of dissolved organic carbon in the Sargasso Sea. Aquat. Microb. Ecol. **10:** 69–85.

———, and others. 2002. The effect of nutrient amendments on bacterioplankton production, community structure and DOC utilization in the northwestern Sargasso Sea. Aquat. Microb. Ecol. **30:** 13–36.

Caron, D., E. L. Lim, R. W. Sanders, M. R. Dennett, and U.-G. Berninger. 2000. Responses of bacterioplankton to organic carbon and inorganic nutrient additions in two oceanic ecosystems. Aquat. Microb. Ecol. **22:** 175–184.

Cherrier, J., J. E. Bauer, and E. R. M. Druffel. 1996. Utilization and turnover of labile dissolved organic matter by bacterial heterotrophs in eastern north Pacific surface waters. Mar. Ecol. Prog. Ser. **139:** 267–279.

Church, M. J., D. A. Hutchins, and H. W. Ducklow. 2000. Limitation of bacterial growth by dissolved organic matter and iron in the Southern Ocean. Appl. Environ. Microbiol. **66:** 455–466.

Cole, J. J., S. E. G. Findlay, and M. L. Pace. 1998. Bacterial production in fresh and saltwater ecosystems: A cross-system overview. Mar. Ecol. Prog. Ser. **43:** 1–10.

Cotner, J. B., J. W. Ammerman, E. R. Peele, and E. Bentzen. 1997. Phosphorus-limited bacterioplankton growth in the Sargasso Sea. Aquat. Microb. Ecol. **13:** 141–149.

———, and B. A. Biddanda. 2002. Small players, large role: Microbial influence on biogeochemical processes in pelagic aquatic ecosystems. Ecosystems **5:** 105–121.

Cottrell, M. T., and D. L. Kirchman. 2000. Natural assemblages of marine proteobacteria and members of the Cytophaga-Flavobacter cluster consuming low- and high-molecular-weight dissolved organic matter. Appl. Environ. Microb. **66:** 1692–1697.

———. 2003. Contribution of major bacterial groups to bacterial biomass production (thymidine and leucine incorporation) in the Delaware estuary. Limnol. Oceanogr. **48:** 168–178.

Duarte, C. M., and J. Cebrian. 1996. The fate of marine autotrophic production Limnol. Oceanogr. **41:** 1758–1766.

Ducklow, H. W. 1983. Production and fate of bacteria in the oceans. Bioscience **33:** 494–501.

Fry, J. C. 1988. Determination of biomass, p. 27–72. *In* B. Austin [ed.], Methods in aquatic bacteriology. John Wiley & Sons.

Giovannoni, S. J., and others. 2005. Genome streamlining in a cosmopolitan oceanic bacterium. Science **309:** 1242–1245.

Grasshoff, K., K. Kremling, and M. Ehrhardt. 1999. Methods of seawater analysis. Wiley-VCH.

Graziano, L. M., R. J. Geider, W. K. W. Li, and M. Olaizola. 1996. Nitrogen limitation of North Atlantic phytoplankton: Analysis of physiological condition in nutrient enrichment experiments. Aquat. Microb. Ecol. **11:** 53–64.

Holmes, R. M., A. Aminot, R. Kerouel, B. A. Hooker, and B. J. Peterson. 1999. A simple and precise method for measuring ammonium in marine and freshwater ecosystems. Can. J. Fish. Aquat. Sci. **56:** 1801–1808.

Karl, D. M., and G. Tien. 1992. Magic—a sensitive and precise method for measuring dissolved phosphorus in aquatic environments. Limnol. Oceanogr. **37:** 105–116.

Kirchman, D. L. 2004. A primer on dissolved organic material and heterotrophic prokaryotes in the ocean, p. 31–63. *In* M. F. a. T. Oguz [ed.], The ocean carbon cycle and climate: Proceedings of the NATO advanced study on ocean carbon cylce and climate. Kluwer Academic.

Kustka, A., S. Sanudo-Wilhelmy, E. Carpenter, D. Capone, J. Burns, and W. Sunda. 2003. Iron requirements for dinitrogen- and ammonium-supported growth in cultures of Trichodesmium (IMS 101): Comparison with nitrogen fixation rates and iron:carbon ratios of field populations. Limnol. and Oceanogr. **48:** 1869–1884.

La Roche, J., R. Nuzzi, R. Waters, K. Wyman, P. G. Falkowski, and D. W. R. Wallce. 1997. Brown tide blooms in Long Island's coastal waters linked to interannual variability in groundwater flow. Glob. Change Biol. **3:** 397–410.

Lochte, K., P. K. Bjornsen, H. Giesenhagen, and A. Weber. 1997. Bacterial standing stock and production and their relation to phytoplankton in the Southern Ocean. Deep-Sea Res. Part II Top. Stud. Oceanogr. **44:** 321–340.

Lomas, M. W., A. Swain, R. Shelton, and J. W. Ammerman. 2004. Taxonomic variability of phosphorus stress in Sargasso Sea phytoplankton. Limnol. Oceanogr. **49:** 2303–2310.

Marie, D., F. Partensky, S. Jacquet, and D. Vaulot. 1997. Enumeration and cell cycle analysis of natural populations of marine picoplankton by flow cytometry using the nucleic acid stain SYBR Green I. Appl. Environ. Microbiol. **63:** 186–193.

Mills, M. M., C. Ridame, M. Davey, J. La Roche, and R. J. Geider. 2004. Iron and phosphorus co-limit nitrogen fixation in the eastern tropical North Atlantic. Nature **429:** 292–294.

Moore, C. M., and others. 2006. Iron limits primary productivity during spring bloom development in the central North Atlantic. Glob. Change Biol. **12:** 626–634.

———, M. M. Mills, R. Langlois, A. Milne, E. P. Achterberg, J. La Roche, and R. J. Geider. 2008. Relative influence of nitrogen and phosphorus availability on phytoplankton physiology and productivity in the oligotrophic sub-tropical North Atlantic Ocean. Limnol. Oceanogr. **53:** 291–305.

Morris, R. M., K. L. Vergin, J. C. Cho, M. S. Rappe, C. A. Carlson, and S. J. Giovannoni. 2005. Temporal and spatial response of bacterioplankton lineages to annual convective overturn at the Bermuda Atlantic time-series study site. Limnol. Oceanogr. **50:** 1687–1696.

Moutin, T., and others. 2002. Does competition for nanomolar phosphate supply explain the predominance of the cyanobacterium Synechococcus? Limnol. Oceanogr. **47:** 1562–1567.

Obernosterer, I., and G. J. Herndl. 1995. Phytoplankton extracellular release and bacterial-growth—dependence on the inorganic N-P ratio. Mar. Ecol. Prog. Ser. **116:** 247–257.

Pakulski, J. D., and others. 1996. Iron stimulation of Antarctic bacteria. Nature **383:** 133–134.

Rivkin, R. B., and M. R. Anderson. 1997. Inorganic nutrient limitation of oceanic bacterioplankton. Limnol. Oceanogr. **42:** 730–740.

Rocap, G., and others. 2003. Genome divergence in two Prochlorococcus ecotypes reflects oceanic niche differentiation. Nature **424:** 1042–1047.

Rue, E., and K. Bruland. 1995. Complexation of Fe(III) by natural ligands in the central north Pacific as determined by a new competitive ligand equilibrium/absorptive cathodic voltammetry method. Mar. Chem. **50:** 117–138.

Sedwick, P. N., and others. 2005. Iron in the Sargasso Sea (Bermuda Atlantic time-series study region) during summer: Eolian imprint, spatiotemporal variability, and ecological implications. Glob. Biogeochem. Cycles **19:** GB4006. doi: 10.1029/2004GB002445.

Simon, N., R. G. Barlow, D. Marie, F. Partensky, and D. Vaulot. 1994. Flow cytometry analysis of oceanic photosynthetic picoeucaryotes. J. Phycol. **30:** 922–935.

Steinberg, D. K., C. A. Carlson, N. R. Bates, R. J. Johnson, A. F. Michaels, and A. H. Knap. 2001. Overview of the US JGOFS Bermuda Atlantic time-series study (BATS): A decade-scale look at ocean biology and biogeochemistry. Deep-Sea Res. Part II Top. Stud. Oceanogr. **48:** 1405–1447.

Thingstad, T. F., Á. Hagström, and F. Rassoulzadegan. 1997. Accumulation of degradable DOC in surface waters: Is it caused by a malfunctioning microbial loop? Limnol. Oceanogr. **42:** 398–404.

———, and others. 2005. Nature of phosphorus limitation in the ultraoligotrophic eastern Mediterranean. Science **309:** 1068–1071.

Tortell, P. D., M. T. Maldonado, and N. M. Price. 1996. The role of heterotrophic bacteria in iron-limited ocean ecosystems. Nature **383:** 330–332.

Vadstein, O., and Y. Olsen. 1989. Chemical-composition and phosphate-uptake kinetics of limnetic bacterial communities cultured in chemostats under phosphorus limitation. Limnol. Oceanogr. **34:** 939–946.

Van Mooy, B. A. S., G. Rocap, H. F. Fredricks, C. T. Evans, and A. H. Devol. 2006. Sulfolipids dramatically decrease phosphorus demand by picocyanobacteria in oligotrophic marine environments. Proc. Natl. Acad. Sci. U. S. A. **103:** 8607–8612.

Wu, J. F., and E. Boyle. 2002. Iron in the Sargasso Sea: Implications for the processes controlling dissolved Fe distribution in the ocean. Glob. Biogeochem. Cycles **16:** 1086. doi:10.1029/2001GB001453, 2002.

Wu, J., W. Sunda, E. A. Boyle, and D. M. Karl. 2000. Phosphate depletion in the western North Atlantic ocean. Science **289:** 759–762.

Received: 9 December 2006
Accepted: 4 October 2007
Amended: 16 November 2007

Paper F: *Effects of Dust and Nutrient Additions on Diazotrophic Communities* (in preparation)

Synopsis

Samples from nutrient addition bioassay experiments were analyzed by qPCR in order to look at nutrient limitations in the diazotrophic communities of the Atlantic Ocean. Abundances of the filamentous, Groups A, B and C unicellular and Gamma A phylotypes were measured. Nitrogen fixation was co-limited by phosphorus and iron. However, diazotrophic phylotype abundances increased above the control with the addition of iron in two experiments and phosphate in one experiment. Iron concentrations in the latter experiment were much higher than in the other two experiments. Saharan dust additions caused an increase in nitrogen fixation and a massive increase in *nifH* abundances of all phylotypes. Complementary laboratory experiments of Saharan dust additions to *Trichodesmium erythraeum* cultures demonstrated that *Trichodesmium* is able to use Saharan dust to at least partially fulfill its iron requirements. The results of these experiments showed that nutrient limitation can be very complex; nitrogen fixation was clearly phosphorus and iron co-limited while the organisms that carry out nitrogen fixation increased in abundances only upon the addition of iron (or in one case phosphorus). It is apparent that more research is needed to clarify which nutrients are limiting diazotrophic growth and activity in the environment. This study showed that Saharan dust can potentially provide iron to the diazotrophic community and positively affects both diazotrophic phylotype abundances and nitrogen fixation rates.

Contribution

The Meteor 55 bioassay experiments were carried out at sea by M. Mills, M. Davey, and C. Ridame. I assisted with the experiments and collected the samples for molecular analysis. M. Mills provided the nitrogen fixation data. D. Huemmer assisted with preparation of the qPCR plates for the bioassay samples. All parts of the laboratory experiments were planned and performed by me. I analyzed all data and prepared the manuscript which is in preparation to be submitted to the Journal of Geophysical Research.

Effects of Dust and Nutrient Additions on Diazotrophic Communities

Rebecca J. Langlois[1], Matthew M. Mills[1,3], Celine Ridame[1,4], Margaret Davey[2], Richard J. Geider[2], Julie LaRoche[1]

[1]Leibniz Institute for Marine Science, Duesternbrooker Weg 20, 24105 Kiel, Germany
[2]Department of Biological Sciences, University of Essex, Colchester CO4 3SQ, UK
[3]Dept. of Geophysics, Stanford University, Stanford, CA 94305
[4]Maître de Conférences, Université Pierre et Marie Curie, LOCEAN-IPSL place Jussieu, 75252, Paris Cedex 05

Abstract

The controls on marine nitrogen fixation and diazotroph distribution and abundance are poorly understood. Nutrient addition bioassay experiments were performed to study the effects of nutrient and Saharan dust additions on natural diazotrophic communities in the Atlantic Ocean. Samples for molecular analysis were collected at the beginning and end of the 48 hour bottle incubation. Nitrogen fixation rates were measured using the ^{15}N isotope. TaqMan probes specific to the diazotrophic phylotypes filamentous cyanobacteria, unicellular Groups A, B, and C cyanobacteria and a gamma proteobacteria were used to quantify *nifH* abundances. Results showed that nitrogen fixation was co-limited by phosphorus and iron, while *nifH* abundances increased with additions of either iron or phosphorus. Saharan dust additions stimulated fixation rates and caused increases in all phylotype *nifH* abundances. Laboratory culture experiments using iron free YBCII media supported the theory that the filamentous cyanobacterium *Trichodesmium* is able to access and utilize iron from Saharan dust. These results indicate that atmospheric dust deposition may greatly influence the distribution of various diazotrophic groups by alleviating nutrient stress, particularly iron stress, in the Atlantic Ocean.

Introduction

The marine nitrogen inventory is controlled by biologically mediated gain and loss processes. Nitrogen enters the cycle through the process of biological dinitrogen fixation; the reduction of atmospheric dinitrogen gas to ammonium. Only a few specialized bacteria and archaea which contain the highly conserved protein nitrogenase are able to fix dinitrogen. Nitrogen leaves the nitrogen cycle through the processes of denitrification and anammox (anaerobic ammonium oxidation). Both of these processes are also carried out by bacteria. Global rates of nitrogen fixation, denitrification, and anammox are difficult to estimate and result in large uncertainties in balancing the marine nitrogen budgets [*La Roche and Breitbarth*, 2005; *Mulholland*, 2006]. Although nitrogen fixation was ignored in early nitrogen budgets, recent data from the field, modeling and paleooceanography indicate that nitrogen fixation is very important to the marine nitrogen cycle [*Codispoti et al.*, 2001; *Deutsch et al.*, 2007; *Mahaffey et al.*, 2005].

Due to the relatively low abundance of diazotrophs (nitrogen fixing organisms) and diel cycle of fixation, nitrogen fixation is not an easy process to study. Abundances of the common open-ocean species *Synechococcus* and *Prochlorococcus* have been reported to be 10 x 10^6 cells ml^{-1} and 125 x 10^6 cells ml^{-1}, respectively, in the Atlantic Ocean [*Davey et al.*, 2008]. In contrast to this, average total *nifH* concentrations in the sub-tropical Atlantic Ocean are reported to be 2.5 x 10^4 cells ml^{-1} [*Langlois et al.*, 2008], three orders of magnitude smaller. Though, one of the more common diazotrophs, *Trichodesmium,* can form blooms large enough to be seen by satellite [*Capone et al.*, 2005; *Subramaniam et al.*, 2002].

Two important methodological advances have contributed to our current understanding of marine nitrogen fixation. First, a sensitive technique for measuring low rates of nitrogen fixation using $^{15}N_2$ gas as a tracer of nitrogen fixation in incubations of bulk water samples [*Montoya et al.*, 1996] has provided N_2 fixation rates in areas where diazotrophs were not visually detectable in the water column [*Montoya et al.*, 2006; *Zehr et al.*, 2001]. Second, a molecular technique has also been developed using nested polymerase chain reaction (PCR) of the *nifH* gene from the iron protein of nitrogenase [*Zani et al.*, 2000]. This method has been applied to a variety of environments including

open oceans [*Langlois et al.*, 2005; *Zehr et al.*, 1998], cyanobacterial mats [*Omoregie et al.*, 2004], seagrass beds [*Lovell et al.*, 2001], and hydrothermal vents [*Mehta et al.*, 2003] and has rapidly expanded the discovery of new diazotrophic organisms and range of potential habitats where nitrogen fixation may occur. Quantitative estimates using quantitative PCR (qPCR) of *nifH* genes and transcripts from diverse phylotypes have shown that the relative abundance of unicellular versus filamentous diazotrophs vary widely within and between oceanic basins [*Church et al.*, 2008; *Langlois et al.*, 2008].

Despite recent advances, the environmental factors that control nitrogen fixation and diazotroph distribution are still poorly understood [*Langlois et al.*, 2008]. Amounts of phosphate, iron and atmospheric dust deposition have all been hypothesized to affect diazotrophic activity and nitrogen fixation. While diazotrophs should not be limited by low fixed nitrogen concentrations, surface waters of oligotrophic oceans are also depleted in phosphate and iron. Phosphate is considered the ultimate limiting nutrient because there are no sources of phosphate to the oceans other than remineralization, where as aeolian dust supplies iron to oligotrophic oceans [*Jickells et al.*, 2005] and biological dinitrogen fixation can provide fixed nitrogen [*Karl et al.*, 2002]. Large areas of some oligotrophic oceans exist which have high nitrate and low chlorophyll concentrations (HNLC regions), most likely due to low iron concentrations [*Behrenfeld et al.*, 1996]. Diazotrophs are also theorized to be limited by iron [*Karl et al.*, 2002] due to a higher iron requirement for the iron-rich nitrogenase enzyme [*Kustka et al.*, 2003]. Diazotrophic phototrophs are further exacerbated by iron limitation because the photosynthetic apparatus also requires iron. The tropical North Atlantic Ocean is subjected to dust deposition from seasonal Saharan dust storms and *Trichodesmium* is abundant throughout this region [*Capone et al.*, 2005; *Langlois et al.*, 2008]. The abundance of *nifH* genes appear to be related to the amount of atmospheric dust deposition [*Langlois et al.*, 2008]. However, nitrogen fixation has been shown to be phosphate limited [*Sanudo-Wilhelmy et al.*, 2001], while a combination of iron and phosphate limited nitrogen fixation in another study [*Mills et al.*, 2004].

Three nutrient addition bioassay experiments were conducted in the sub-tropical North Atlantic Ocean to look at the effects of nitrate, phosphate, iron, all combinations of these and Saharan dust additions on natural diazotrophic phylotype abundances using

qPCR. Primary production in a sub-set of the same bioassay experiments was shown to be nitrogen limited [*Davey et al.*, 2008], while dinitrogen fixation was iron and phosphate co-limited [*Mills et al.*, 2004]. Abundances of five diazotrophic phylotypes were estimated, including filamentous cyanobacteria (*Trichodesmium*), Group A unicellular cyanobacteria, Group B unicellular cyanobacteria (*Crocosphaera*), Group C unicellular cyanobacteria (*Cyanothece*), and gamma protoebacteria. Results showed a very large increase in phylotype abundances in incubations amended with Saharan dust. To further investigate the effects of dust additions, laboratory experiments were conducted using cultures of *Trichodesmium erythraeum* IMS101. Increases in *Trichodesmium nifH* abundances were also induced with dust additions in the lab experiment.

Materials and Methods

Bioassay Experiments

Samples for molecular analysis were collected at the start and conclusion of three bioassay experiments performed during the Meteor 55 research cruise (experiments A-C) [*Davey et al.*, 2008; *Mills et al.*, 2004]. Station locations and initial conditions are given in Table 1. Experiments were conducted using trace metal clean techniques. Surface seawater was pumped on-board using a diaphragm pump into a trace metal clean container. Seawater was collected in 60 l carboys and then siphoned into acid cleaned and seawater rinsed 1 l polycarbonate Nalgene bottles. Nutrients additions of 1.0 µm ammonium nitrate (+N), 0.2 µm phosphate (+P), and 2.0 nM iron chloride (+Fe), and all combinations thereof were made to triplicate bottles under a laminar flow hood. Saharan dust was added alone at final concentrations of 0.5 mg l^{-1} (D1) and 2.0 mg l^{-1} (D2). Bottles were then placed in incubators shaded to 20% light with blue filters. Incubator water temperature was maintained with constant flowing seawater. Parallel sets of triplicate bottles were initiated for ^{15}N fixation, ^{14}C fixation, and chlorophyll measurements. Results of nitrogen fixation, carbon fixation, chlorophyll, and flow cytometry can be found elsewhere [*Davey et al.*, 2008; *Mills et al.*, 2004]. 1.5 l of seawater collected during the experiment set up were filtered as described below for

characterizing the initial diazotrophic community. At the end of the 48 hour incubation, 300-800 ml of water was combined from the set of triplicate chlorophyll bottles and filtered under low vacuum pressure (0.2 bar) onto 25 mm diameter, 0.2 μm Durapore filters (Millipore). After filtration, filters were immediately frozen at -80°C until extraction in the lab.

DNA/RNA Extraction, *nifH* Amplification and Cloning

DNA from the bioassay experiments was extracted using the Qiagen DNeasy Plant extraction kit. Filters were broken up by holding the cryo-tube containing the filter in liquid nitrogen for 30 sec and then using a sterile pipette tip as a pestle. Lysis buffer was applied directly to the filter pieces and extraction followed according to the manufacturer's instructions. DNA was eluted into 50 μl PCR grade water. Amplification and cloning of *nifH* was performed as described in Langlois et al [*Langlois et al.*, 2005], using the nested PCR protocol and *nifH* primers described by Zani et al [*Zani et al.*, 2000]. Bands of the correct size (354 b) from the control, +PFe and dust samples were inserted into the Topo TA vector and into Top 10 chemically competent *E. coli* cells according to the manufacturer's instructions (Invitrogen). Clones were screened for inserts using T3 and T7 primers. Screened inserts of the correct size were sequenced. *nifH* sequences from the initial microbial populations have already been published [*Langlois et al.*, 2005].

Culture Manipulations

Non-axenic cultures of *Trichodesmium erythraeum* ISM101 were grown in YBCII media [*Chen et al.*, 1996]. Cultures were inoculated in sterile plastic tissue flasks under a laminar flow hood to limit bacterial and iron contamination, and grown under a 12:12 hr light:dark cycle with an irradiance of 150 μE m^{-2} sec^{-1}. Growth and relative abundance was estimated daily using a PHYTO-PAM phytoplankton analyzer (Walz Mess und Regeltechnik. Cultures were also gently shaken to re-suspend settled filaments and visually inspected daily. At the start of the experiment, 4 ml stock culture was

transferred into 40 ml iron-free YBCII media for each treatment and replicate during late exponential growth phase. YBCII media was modified to contain normal amounts of iron (0.41 μM), 2x amount of iron (0.82 μM), and unmodified (iron free) in triplicate. 9 mg of Saharan dust from a ≤ 90 μm sifted soil fraction collected 20 km north-west of Agadir in Morocco (courtesy of Dr. A. Baker) was added to triplicate bottles of YBCII media with normal iron amounts and iron free. Three sets of triplicate bottles for each treatment (i.e. nine bottles total) were inoculated; one set for Phyto-Pam measurements, another for filtration on day 3 (60 hrs) and the last set for filtration on day 7 (168 hrs). Starting inoculation amounts (4 ml of stock culture) were filtered in triplicate for T=0 measurements of *nifH* abundances. All Phyto-Pam measurements and filtration occurred at the same time each day (3 hours into the light cycle) to avoid diel variations in the data set. The experiment was repeated three times. PHYTO-PAM analysis and visual observation was always done, but samples for molecular extraction and qPCR analysis were collected only once. Samples were processed as above using the Qiagen All-Prep DNA/RNA extraction kit.

cDNA Synthesis and qPCR

DNA and RNA concentrations were measured using the Picogreen DNA and Ribogreen RNA quantitation kits (Molecular Probes), respectively. RNA samples from the culture experiment were transcribed to cDNA using the Quanti-Teq cDNA synthesis kit and DNase digest step (Qiagen) according to the manufacturer's instructions. Abundances of filamentous (*Trichodesmium*), Group A unicellular, Group B unicellular, Group C unicellular, and Gamma A proteobacterial *nifH* were estimated in the bioassay samples using the specific TaqMan probe and primer sets described in Langlois et al [*Langlois et al.*, 2008] (Table 2). Plasmid standards for each primer/probe set Langlois et al [*Langlois et al.*, 2008] were used, and the same standard dilutions were used to measure all samples. TaqMan master mix (Applied Biosystems) was used and samples were run in an ABI Prism 7000 Real-Time PCR cycler, using the default program and increasing the number of cycles to 45. All bioassay samples were run in triplicate, while standards and no template controls (NTCs) were run in duplicate. Abundances of

Trichodesmium erythraeum nifH in culture experiment samples were estimated using the primer set *T.erythraeum nifH* (Table 2). All culture experiment DNA, cDNA, and RNA samples were run in triplicate using SYBRgreen master mix (Invitrogen) and the default thermocycler program was modified as follows: the activation time was reduced to 2 min. and the annealing time to 30 sec. The filamentous standard was used to quantify the number of copies in these reactions (primer efficiency= 97%, R2= 0.998). No amplification was observed in NTC and RNA reactions after 40 cycles indicating that all reagents were clean and that there was no contaminating DNA in cDNA reactions. Quantities of *nifH* phylotypes in the qPCR reactions were calculated using the ABI Sequence Detection Software (v. 1.2.3) with RQ application.

Results

Diazotrophic Community Composition in Bioassay Experiments

Diazotroph diversity decreased from west to east as seen by the number of phylotypes detected by qPCR; all five were quantifiable in experiment A, while only two were quantifiable in experiment C. Analysis of the clone libraries showed that no new phylotypes were stimulated by the nutrient additions and that the qPCR probes targeted all dominant diazotrophic phylotypes. The filamentous and unicellular Group A phylotypes were detected in all experiments and were most abundant. Unicellular Groups B and C were quantifiable only in experiment A. The Gamma A phylotype was detected in experiments A-C, but not quantifiable in experiment C. Despite the variation in diazotroph composition of each experiment, trends were observed in both total *nifH* abundances and nitrogen fixation (Fig. 1). Nitrogen fixation was co-limited by P and Fe in all three experiments. Despite this clear association in nitrogen fixation rates, the +PFe addition caused an increase in total *nifH* copy numbers above the control only in experiment C. Dust additions also caused an increase in nitrogen fixation above the control; however the higher dust concentration did not cause an additional increase in fixation rates and the observed increase was not as large as in the +PFe treatment. Saharan dust induced a very large increase in average total *nifH* copies detected above the

control (Fig. 1). This increase almost tripled with additions of higher dust concentrations. The largest increases in Saharan dust treatments occurred in experiment B, and the smallest in experiment C (Fig. 2).

While the increase in *nifH* abundance with dust additions held for all phylotypes in at least one experiment, the effect of nutrient additions was more complex (Figs. 2). In experiment A, the only experiment where Group B, Group C, and Gamma A phylotypes were quantifiable, only additions of dust and Fe caused increases in *nifH* abundances above the control (Fig. 2a-b). Additions of +PFe caused no further increases in *nifH* abundances indicating that these groups were Fe-limited. Interestingly, increasing the concentration of Saharan dust caused a decrease in Group C *nifH* concentrations. The filamentous phylotype was detected in the +PFe treatment in all three experiments, though more abundant than the control in experiment B only (Fig.2c). This phylotype was also quite abundant in +P and +Fe treatments, though not in all three experiments. This is in contrast to all +N treatments where the filamentous phylotype was rarely detected and never at concentrations above the control. Additions of N seemed to suppress filamentous *nifH* DNA abundances. In contrast, additions of +NP caused increases in Group A *nifH* equal to or higher than that of the control (Fig 2b-d). Group A was rarely detected in +P treatments, but always detected in +Fe and +PFe treatments. Of these treatments, a reduction in Group A *nifH* was observed in the +Fe treatment in experiment C. In contrast to the other experiments, *nifH* abundances appeared to be stimulated by P additions in experiment C as opposed to +Fe or +PFe in the other experiments. In general, diazotroph diversity was highest in the +Fe, +PFe, and dust treatments in all experiments. In most cases, *nifH* concentrations were reduced to undetectable in treatments where N was added, with the exception of Group A in +NP treatments.

Effects of Saharan Dust on *Trichodesmium* Cultures

Culture experiments where *Trichodesmium erythraeum* was grown in media without Fe (-Fe), normal media concentrations of Fe (+Fe, 0.41 μM), Saharan dust (Dust-Fe and Dust+Fe), and twice the normal amount of Fe (2x Fe, 0.82 μM) showed that the

effect of dust observed in field samples can also be partially replicated in cultures. The absence of Fe in the culture medium had a dramatic effect on the *Trichodesmium* colonies. No colonies were observed in –Fe media after day 3 and within 48 hours of transferring the culture colonies became very short, thick, and darkly red colored. However, some colonies were observed in all Dust-Fe bottles at the end of the experiment. Large radial colonies were observed in all bottles amended with Saharan dust. This change in morphology occurred within 24 hours of adding the dust. Long, thin filaments, characteristic of healthy *Trichodesmium*, were observed in the +Fe and 2x +Fe bottles. Some single filaments were observed in the Dust+Fe bottles, while all biomass appeared to be in radial colonies in the Dust-Fe bottles.

Quantities of *nifH* increased with time in all treatments where Fe was added to the media throughout the experiment and contained roughly the same amount of *nifH* at the end of the seven days (Fig 3a). There was no change in amount of *nifH* over the seven days in the –Fe, +Dust treatment and *nifH* decreased in –Fe media. The amount of cDNA was more variable. Quantities of *nifH* cDNA decreased in all treatments on day 3 (60 hours), with the smallest reduction observed in the 2x Fe treatment, followed by the Dust-Fe treatment (Fig 3b). By day seven (130 hours), all +Fe treatments had similar amounts of cDNA. Although the Dust-Fe treatment had relatively high cDNA *nifH* concentrations on day three, cDNA concentrations on day seven were almost two orders of magnitude smaller than +Fe treatments. Amounts of cDNA in the –Fe bottles decreased by nearly three orders of magnitude on day three to undetectable in some bottles on day seven. Even though all +Fe treatments reached the same *nifH* concentration by day seven, variations could be seen on day three (Fig 3 and 4). Concentrations of *nifH* DNA were higher with higher concentrations of Fe, whether from Saharan dust or media or both, while *nifH* cDNA was much higher in 2x Fe only (Fig 4). Although the Dust+Fe response was not much different from the other +Fe treatments, the –Fe and Dust-Fe responses were clearly different. These results clearly show that *Trichodesmium erythraeum* is able to access and utilize Fe from Saharan dust.

Discussion

Importance of Fe for Nitrogen Fixation

Fe appeared to be the nutrient limiting the abundance of diazotrophic phylotypes in all experiments except for experiment C, where only P additions caused increases in *nifH* concentrations and dust had a minor effect. As in the experiments A and B, primary productivity was N limited in experiment C [*Davey et al.*, 2008]. Experiment C was located close to the African coast, an area of high aeolian dust deposition. Fe concentrations measured during the same cruise increased eastwardly across the Atlantic Ocean [*Croot et al.*, 2004] indicating that diazotrophs in this area may not have been as Fe-stressed as in the more westerly stations. Although P additions caused increases in *nifH* concentrations at this site, nitrogen fixation rates were enhanced by the addition of +PFe. P and Fe are both important elements for nitrogen fixation and, thus, diazotrophic organisms. Based on the increases in all diazotrophic phylotypes with additions of Saharan dust, it appears that dust is very efficient at providing diazotrophs with nutrients, especially the Fe that they require.

Saharan dust contains many elements and trace metals, the most biologically important being P and Fe [*Baker et al.*, 2006], though some N can adsorb to dust particles [*Mills et al.*, 2004]. The amount of P and Fe released during the above described bioassay experiments was at the nmol level [*Mills et al.*, 2004], however the diazotrophic community was able to respond to this low level influx of nutrients. Even though the largest increase in nitrogen fixation rates occurred with additions of dissolved P and Fe solutions, fixation was also elevated in dust treatments indicating that the Saharan dust stimulated the diazotrophic community. Quantification of the *nifH* gene, which codes for an iron-rich structural gene in the nitrogenase enzyme, revealed that the diazotrophic community was indeed stimulated at the genetic level by Saharan dust additions. Additions of Saharan dust were the only manipulations that resulted in large increases in *nifH* gene concentrations above the control. There was also a secondary effect of dust concentration; the larger dust addition resulted in a further increase in *nifH* copy numbers.

Patterns in *Trichodesmium* abundance have been previously correlated to dust deposition [*Lenes et al.*, 2001; *Orcutt et al.*, 2001]. At BATS, *Trichodesmium* colony abundance varied according to the amount of dust deposition; however fixation rates did not increase with increasing dust deposition [*Orcutt et al.*, 2001]. This is similar to the results of the bioassay experiments. One reason why diazotrophic organisms increase without an increase in fixation rates may be due to N, along with P and Fe, being released from the dust. Although diazotrophic organisms are capable of producing fixed N from N_2, they are also able to utilize both ammonium and nitrate [*Holl and Montoya*, 2005]. In fact, a laboratory experiment with *Trichodesmium* showed that iron-limited cultures were able to grow on NO_3 better than by fixing nitrogen [*Reuter et al.*, 1990].

The reason for this may be that nitrogen fixation is an expensive process for cells to perform, in respect to both energy and trace metal requirements. The nitrogenase enzyme alone requires 19 to 24 Fe atoms [*Shi et al.*, 2007], which raises the susceptibility of diazotrophs, especially open ocean diazotrophs, to Fe-limitation. Cyanobacteria, such as the unicellular and filamentous phylotypes studied in these experiments, also need iron for the photosynthetic machinery, which is another 23-24 Fe atoms [*Shi et al.*, 2007]. During nitrogen fixation, an organism uses 16 ATP molecules provided by photosynthesis per N_2 molecule. Saharan dust may have provided enough Fe and P to support production of photosynthetic pigments which provided energy for either diazotrophic growth or genome multiplication, but was not large enough to support further increases in nitrogen fixation. It has been shown that iron stressed *Trichodesmium* cultures do preferentially down-regulate nitrogen fixation to conserve Fe for photosynthesis [*Küpper et al.*, 2008; *Shi et al.*, 2007]. Under severe Fe limitation, which resulted in N-starvation, *Trichodesmium* resorted back to nitrogen fixation [*Küpper et al.*, 2008]. It is possible that open-ocean diazotrophs are in a permanent state of severe Fe limitation where a balance between nitrogen fixation and photosynthesis must be reached.

Aeolian dust deposition has long been suspected to provide Fe to *Trichodesmium* colonies in the Atlantic Ocean [*Carpenter et al.*, 1991]. A *Trichodesmium* bloom off western Florida, large enough to draw-down P, occurred after a large deposition event [*Lenes et al.*, 2001]. Results of the bioassay experiments showed that dust additions

clearly affected not only *Trichodesmium*, but the other diazotrophic phylotypes as well. *Trichodesmium* appears to have several mechanisms for effectively scavenging Fe from dust particles [*Carpenter et al.*, 1991]. It is possible that other diazotrophs may also use some of these mechanisms. For instance, *Trichodesmium* colonies adsorb iron very quickly and secrete a material that increases the dissolution of Fe from dust [*Carpenter et al.*, 1991]. Colonies of *Trichodesmium* collected in the field rapidly attached to dust particles and scanning electron microscopy revealed dust particles among bundles of *Trichodesmium* filaments [*Carpenter et al.*, 1991]. Changes in *Trichodesmium* morphology, from single filaments to large colonies upon dust addition, were observed in our culture experiments.

The culture experiments also showed that *Trichodesmium* is able to utilize Fe from atmospheric dust to, at least partially, fulfill its iron requirements. Increases in *nifH* copy numbers were not higher with dust as an iron source than that of dissolved Fe in the culture experiments as in the field experiments, but cultured *Trichodesmium* which is accustomed to high nutrient and Fe concentrations may have been in a different physiological state than the oceanic diazotrophs. It is also possible that increases in *nifH* gene copy numbers were not observed in the –Fe, +Dust treatment because Fe was being relegated to photosynthesis as opposed to nitrogen fixation as explained above. Another concern is that the amount of iron estimated to be released from the dust was probably actually much lower than expected. Nevertheless, when placed in media with atmospheric dust as the sole Fe source, the culture did not immediately die as in the -Fe control indicating that *Trichodesmium* was able to use Fe from the dust.

Although atmospheric dust deposition has long been observed to be correlated with diazotroph distribution, especially of *Trichodesmium* [*Mahaffey et al.*, 2005], until now no studies have looked at whether or not diazotrophs are directly affected by and able to use dust. Bioassay experiments demonstrated that the abundance of diazotrophic organisms increases with Fe additions, while nitrogen fixation is PFe co-limited. Saharan dust additions caused large increases in *nifH* concentrations and increased nitrogen fixation rates. Culture experiments with *Trichodesmium* grown in Fe-free media and Saharan dust showed that at least one diazotrophic organism is able to access and use Fe from dust. Experiments with other cultured open-ocean diazotrophs need to be

performed to see if this is a characteristic of all diazotrophs. A correlation between modeled annual aeolian dust deposition and *nifH* phylotype abundance has been observed in the Atlantic Ocean [*Langlois et al.*, 2008] supporting the results of the experiments presented here. Saharan dust deposition appears to play a major role in the distribution of diazotrophic organisms, and thus nitrogen fixation in the Atlantic Ocean.

References:

Baker, A.R., T.D. Jickells, M. Witt, and K.L. Linge, Trends in the solubility of iron, aluminium, manganese, and phosphorus in aerosol collected over the Atlantic Ocean, *Marine Chemistry*, *98*, 43-58, 2006.

Behrenfeld, M.J., A.J. Bale, Z.S. Kolber, J. Aiken, and P.G. Falowski, Confirmation of iron limitation of phytoplankton photosynthesis in the equatorial Pacific Ocean, *Nature*, *383*, 508-510, 1996.

Capone, D., J. Burns, J.P. Montoya, A. Subramaniam, C. Mahaffey, T. Gunderson, A.F. Michaels, and E.J. Carpenter, Nitrogen fixation by Trichodesmium spp.: An important source of new nitrogen to the tropical and subtropical North Atlantic Ocean, *Global Biogeochemical Cycles*, *19* (GB2024), doi:10.1029/2004GB002331, 2005.

Carpenter, E.J., D.G. Capone, and J.G. Rueter, *Marine Pelagic Cyanobacteria: Trichodesmium and other Diazotrophs*, 357 pp., 1991.

Chen, Y.-B., J.P. Zehr, and M. Mellon, Growth and nitrogen fixation of the diazotrophic filamentous nonheterocystous cyanobacterium *Trichodesmium* sp. IMS 101 in defined media: Evidence for a circadian rhythm, *J. Phycol.*, *32*, 916-923, 1996.

Church, M.J., K.M. Bjoerkman, D.M. Karl, M.A. Saito, and J.P. Zehr, Regional distribution of nitrogen-fixing bacteria in the Pacific Ocean, *Limnol. Oceanogr.*, *53* (1), 63-77, 2008.

Codispoti, L.A., J.A. Brandes, J.P. Christensen, A.H. Devol, S.W.A. Naqvi, H.W. Paerl, and T. Yoshinari, The oceanic fixed nitrogen and nitrous oxide budgets: Moving targets as we enter the anthropocene?, *Sci. Mar.*, *62*, 85-105, 2001.

Croot, P., P. Streu, and A. Baker, Short residence time for iron in surface seawater impacted by atmospheric dry deposition from Saharan dust events, *Geophysical Research Letters*, *31* (23), doi:10.1029/2004GL020153, 2004.

Davey, M., G.A. Tarran, M.M. Mills, C. Ridame, R.J. Geider, and J. La Roche, Nutrient limitation of picophytoplankton photosynthesis and growth in the tropical North Atlantic, *Limnology and Oceanography*, *53* (5), 1722-1733, 2008.

Deutsch, C., J. Sarmiento, D.M. Sigman, N. Gruber, and J.P. Dunne, Spatial coupling of nitrogen inputs and losses in the ocean, *Nature*, *445*, 163-167, 2007.

Holl, C.M., and J.P. Montoya, Interactions between nitrate uptake and nitrogen fixation in continuous cultures of the marine diazotroph *Trichodesmium* (Cyanobacteria), *J. Phycol.*, *41*, 1178-1183, 2005.

Jickells, T.D., Z.S. An, K.K. Andersen, A. Baker, G. Bergametti, N. Brooks, J.J. Cao, P.W. Boyd, R.A. Duce, K.A. Hunter, H. Kawahata, N. Kubilay, J. La Roche, P.S. Liss, N. Mahowald, J.M. Prospero, A.J. Ridgwell, I. Tegen, and O. Torres, Global Iron Connections Between Desert Dust, Ocean Biogeochemistry, and Climate, *Science*, *308*, 67-71, 2005.

Karl, D., A. Michaels, B. Bergman, D. Capone, E. Carpenter, R. Letelier, F. Lipschultz, H. Paerl, D. Sigman, and L. Stal, Dinitrogen fixation in the world's oceans, *Biogeochemistry*, *57*, 47-98, 2002.

Küpper, H., I. Setlik, S. Seibert, O. Prasil, E. Setlikova, M. Strittmatter, O. Levitan, J. Lohscheider, I. Adamska, and I. Berman-Frank, Iron limitation in the marine

cyanobacterium *Trichodesmium* reveals new insights into regulation of photosynthesis and nitrogen fixation, *New Phytologist*, 1-15, 2008.

Kustka, A., S. Sanudo-Wilhelmy, E.J. Carpenter, D.G. Capone, and J.A. Raven, A revised estimate of the iron use efficiency of nitrogen fixation, with special reference to the marine cyanobacterium Trichodesmium spp. (Cyanophyta), *J. Phycol.*, *39* (1), 12-25, 2003.

La Roche, J., and E. Breitbarth, Importance of the diazotrophs as a source of new nitrogen in the ocean, *Journal of SEA Research*, *53*, 67-91, 2005.

Langlois, R.J., D. Huemmer, and J. La Roche, Abundances and Distributions of the Dominant *nifH* Phylotypes in the Northern Atlantic Ocean, *Appl. Envir. Microbiol.*, *74* (6), 1922-1931, 2008.

Langlois, R.J., J. La Roche, and P.A. Raab, Diazotrophic Diversity and Distribution in the Tropical and Subtropical Atlantic Ocean, *Appl. Envir. Microbiol.*, *71* (12), 7910-7919, 2005.

Lenes, J.M., B.P. Darrow, C.l. Cattrall, C.A. Heil, M. Callahan, G.A. Vargo, R.H. Byrne, J.M. Prospero, D.E. Bates, K.A. Fanning, and J.J. Walsh, Iron fertilization and the *Trichodesmium* response on the West Florida shelf, *Limnology and Oceanography*, *46* (6), 1261-1277, 2001.

Lovell, C.R., M.J. Friez, J.W. Longshore, and C.E. Bagwell, Recovery and phylogenetic analysis of nifH sequences from diazotrophic bacteria associated with dead aboveground biomass of Spartina alterniflora, *Appl. Envir. Microbiol.*, *67* (11), 5308-5314, 2001.

Mahaffey, C., A.F. Michaels, and D. Capone, The Conundrum of Marine N_2 Fixation, *American Journal of Science*, *305*, 546-595, 2005.

Mehta, M.P., D.A. Butterfield, and J.A. Baross, Phylogenetic diversity of nitrogenase (nifH) genes in deep-sea and hydrothermal vent environments of the Juan de Fuca ridge, *Appl. Envir. Microbiol.*, *69* (2), 960-970, 2003.

Mills, M.M., C. Ridame, M. Davey, J. La Roche, and R.J. Geider, Iron and phosphorus co-limit nitrogen fixation in the eastern tropical North Atlantic, *Nature*, *429* (6989), 292-294, 2004.

Montoya, J.P., M. Voss, and D. Capone, Spatial variation in N_2-fixation rate and diazotroph activity in the Tropical Atlantic, *Biogeosciences Discussions*, *3*, 1739-1761, 2006.

Montoya, J.P., M. Voss, P. Kähler, and D.G. Capone, A simple, high-precision, high-sensitivity tracer assay for N_2 fixation, *Applied and Environmental Microbiology*, *62* (3), 986-993, 1996.

Mulholland, M.R., The fate of new production from N_2 fixation, *Biogeosciences Discussions*, *3*, 1049-1080, 2006.

Omoregie, E.O., L.L. Crumbliss, B.M. Bebout, and J.P. Zehr, Determination of Nitrogen-Fixing Phylotypes in Lyngbya sp. and Microcoleus chthonoplastes Cyanobacterial Mats from Guerrero Negro, Baja California, Mexico, *Appl. Environ. Microbiol.*, *70* (4), 2119-2128, 2004.

Orcutt, K.M., F. Lipschulz, K. Gundersen, R. Arimoto, A.F. Michaels, A.H. Knap, and J.R. Gallon, A seasonal study of the significance of N_2 fixation by *Trichodesmium spp.* at the Bermuda Atlantic Time-series Study (BATS) site, *DSR II*, *48*, 1583-1608, 2001.

Reuter, J.G., K. Ohki, and Y. Fujita, The effect of iron nutrition on photosynthesis and nitrogen fixation in cultures of Trichodesmium (Cyanophyceae), *j Phycol*, *26*, 30-35, 1990.

Sanudo-Wilhelmy, S.A., A.B. Kustka, C.J. Gobler, D.A. Hutchins, M. Yang, K. Lwiza, J. Burns, D.C. Capone, J.A. Raven, and E.J. Carpenter, Phosphorus limitation of nitrogen fixation by Trichodesmium in the central Atlantic Ocean, *Nature*, *411* (66-69), 2001.

Shi, T., Y. Sun, and P. Falkowski, Effects of iron limitation on the expression of metabolic genes in the marine cyanobacterium *Trichodesmium erythraeum* IMS101, *Environ Microbiol*, *9* (12), 2945-2956, 2007.

Subramaniam, A., C.W. Brown, R.R. Hood, E.J. Carpenter, and D.G. Capone, Detecting Trichodesmium blooms in SeaWiFS imagery, *Deep-Sea Research Part II-Topical Studies in Oceanography*, *49* (1-3), 107-121, 2002.

Zani, S., M.T. Mellon, J.L. Collier, and J.P. Zehr, Expression of nifH Genes in Natural Microbial Assemblages in Lake George, New York, Detected by Reverse Transcriptase PCR, *Appl. Envir. Microbiol.*, *66*, 3119-3124, 2000.

Zehr, J.P., M.T. Mellon, and S. Zani, New Nitrogen-Fixing Microorganisms Detected in Oligotrophic Oceans by Amplification of Nitrogenase (nifH) Genes, *Appl. Envir. Microbiol.*, *64* (9), 3444-3450, 1998.

Zehr, J.P., J. Waterbury, P.J. Turner, J.P. Montoya, E. Omoregie, G. Steward, A. Hansen, and D.M. Karl, Unicellular cyanobacteria fix N2 in the subtropical North Pacific Ocean, *Nature*, *412* (9 August), 635-638, 2001.

Table 1. Summary of bioassay experiments. Nutrient(s) limiting primary production, nitrogen fixation and chlorophyll a are shown. Initial nitrate and phosphate concentrations are given. The detection limits are 0.3 µM and 0.03 µM for NO_3 and PO_4 respectively. The *nifH* enrichment was calculated by normalizing the *nifH* concentration in the D2 treatment to that of the control.

	A[a]	B[a]	C[b]
Location	4°N 24°W	11°N 18°W	6°N 15°W
Date	Oct 2002	Nov 2002	Nov 2002
Primary Productivity	N	N	N
Nitrogen fixation	PFe	PFe	PFe
Chlorophyll a	N	N	N
NO_3	nd	nd	nd
PO_4	≤0.03 µM	≤0.03 µM	nd
Fe	1.12 nM	0.98 nM	20.9 nM
nifH enrichment	6.8	54.0	0.4

[a] [*Mills et al.*, 2004]
[b] [*Davey et al.*, 2008]

Table 2. TaqMan primers and probes and SYBRgreen primers

	Forward	Reverse	Probe
Filamentous[a]	TGGCCGTGGTATTATTACTGCTATC	GCAAATCCACCGCAAACAAC	AAGGAGCTTATACAGATCTA
Group A[a]	TAGCTGCAGAAAGAGGAACTGTAGAAG	TCAGGACCACCGGACTCAAC	TAATTCCTGGCTATAACAAC
Group B[a]	TGCTGAAATGGGTTCTGTTGAA	TCAGGACCACCAGATTCTACACACT	CGAAGACGTAATGCTC
Group C[a]	TCTACCCGTTTGATGCTACACACTAA	GGTATCCTTCAAGTAGTACTTCGTCTAGCT	AAACTACCATTCTTCACTTAGCAG
Gamma A[a]	TTATGATGTTCTAGGTGATGTG	AACAATGTAGATTTCCTGAGCCTTATTC	TTGCAATGCCTATTCG
T.erythraeum nifH	GGTCCTGAGCCTGGTGTAGG	GATAGCAGTAATAATACCACGGCCA	-

[a] [*Langlois et al.*, 2008]

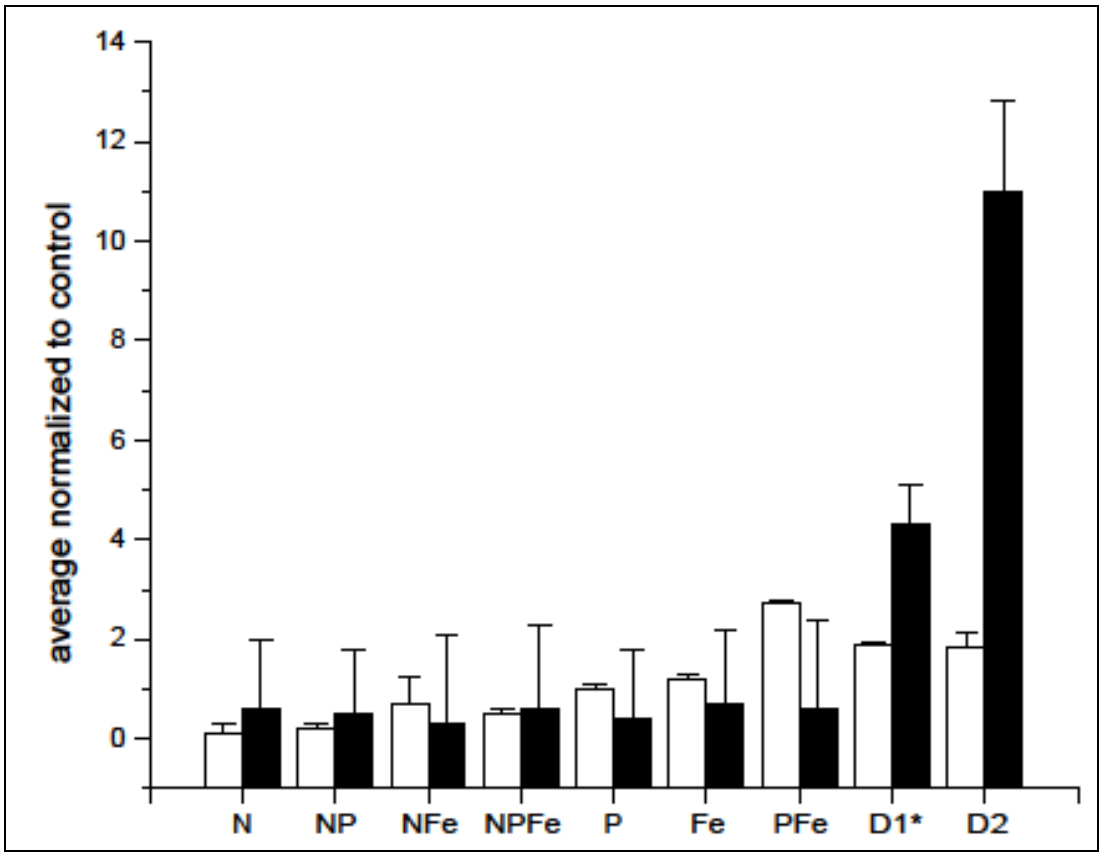

Figure 1. Results of bioassay experiments Average nitrogen fixation rates (nmol N l^{-1} d^{-1}), normalized to the fixation rate of the control (white bars) and average total *nifH* copies l^{-1} normalized to the average *nifH* abundance in the control (black bars) are shown. Error bars indicate the standard error.

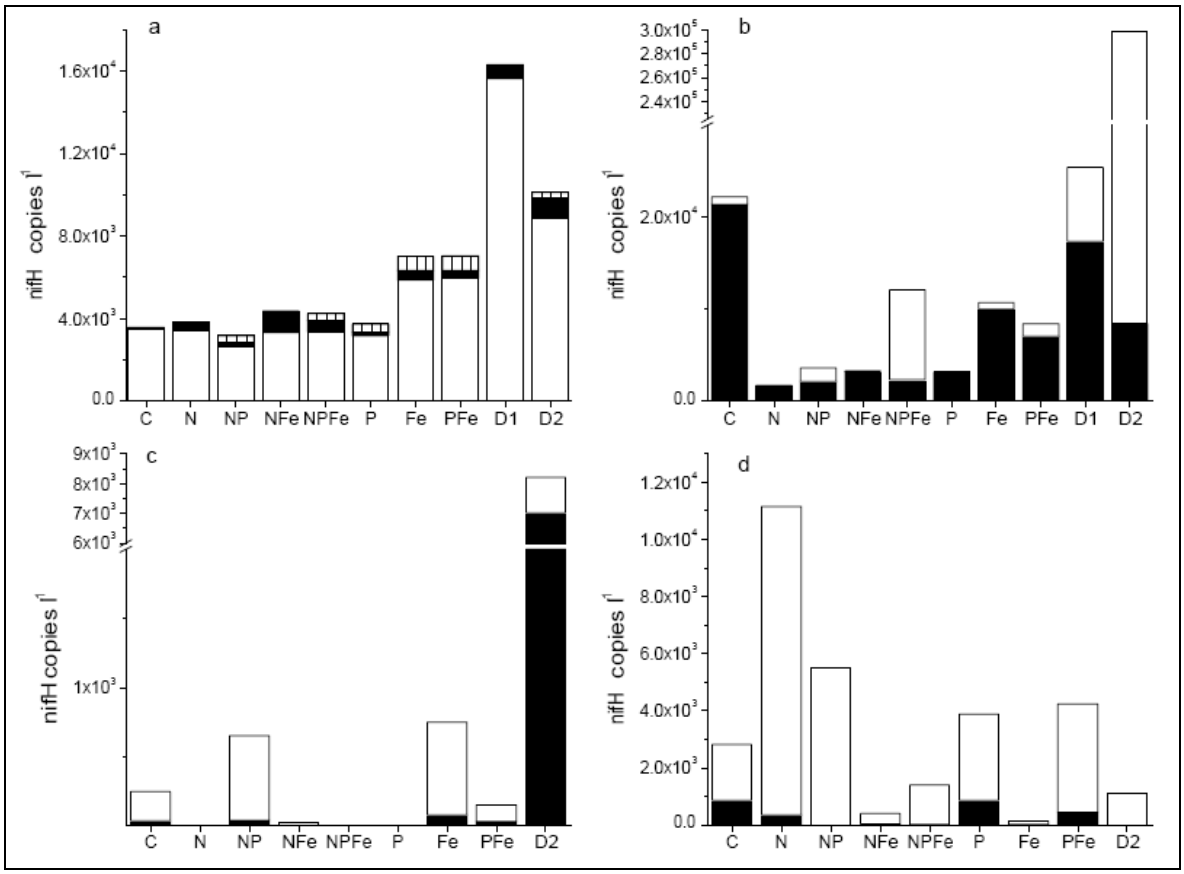

Figure 2. Abundances of phylotypes in experiments A-C. In a, concentrations (*nifH* copies l^{-1}) of Group C (white bars), Group B (black bars) and Gamma A (striped bars) are given. Filamentous (black bars) and Group A concentrations (*nifH* copies l^{-1}) in experiments A, B and C are shown in panels b, c, and d, respectively.

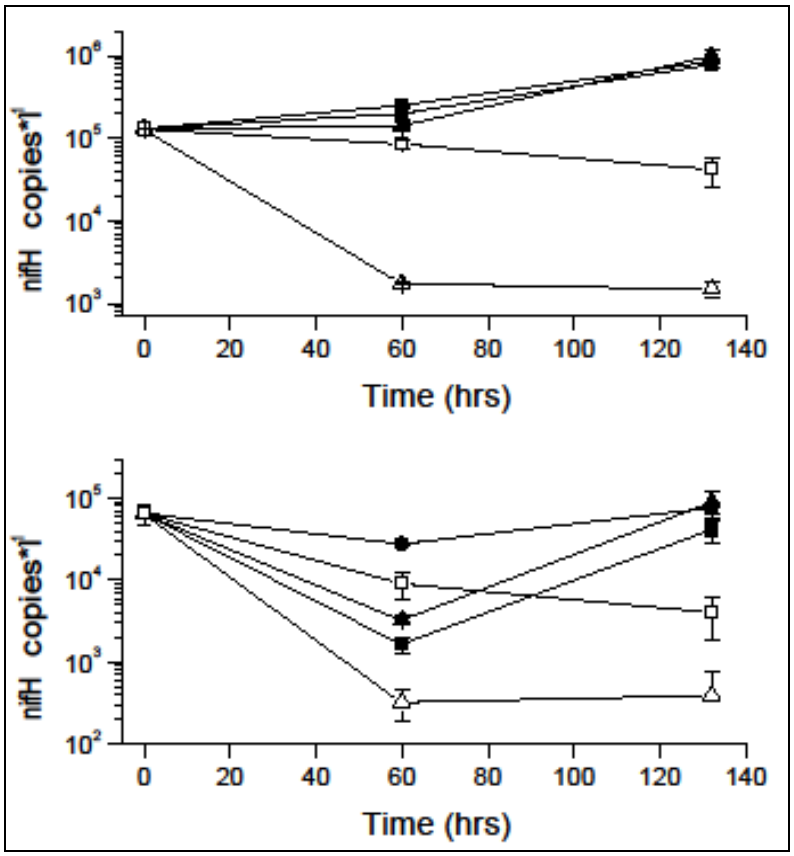

Figure 3. Effects of dust and/or iron on *nifH* DNA and cDNA. Average abundances of *nifH* DNA (a) and cDNA (b) (*nifH* copies l^{-1}) during the culture experiment. Error bars indicate standard error. Symbols refer to the treatments as follows: 2x Fe-black circles, +Fe-black triangles, Dust+Fe-black squares, -Fe-white triangles, and Dust-Fe-white squares.

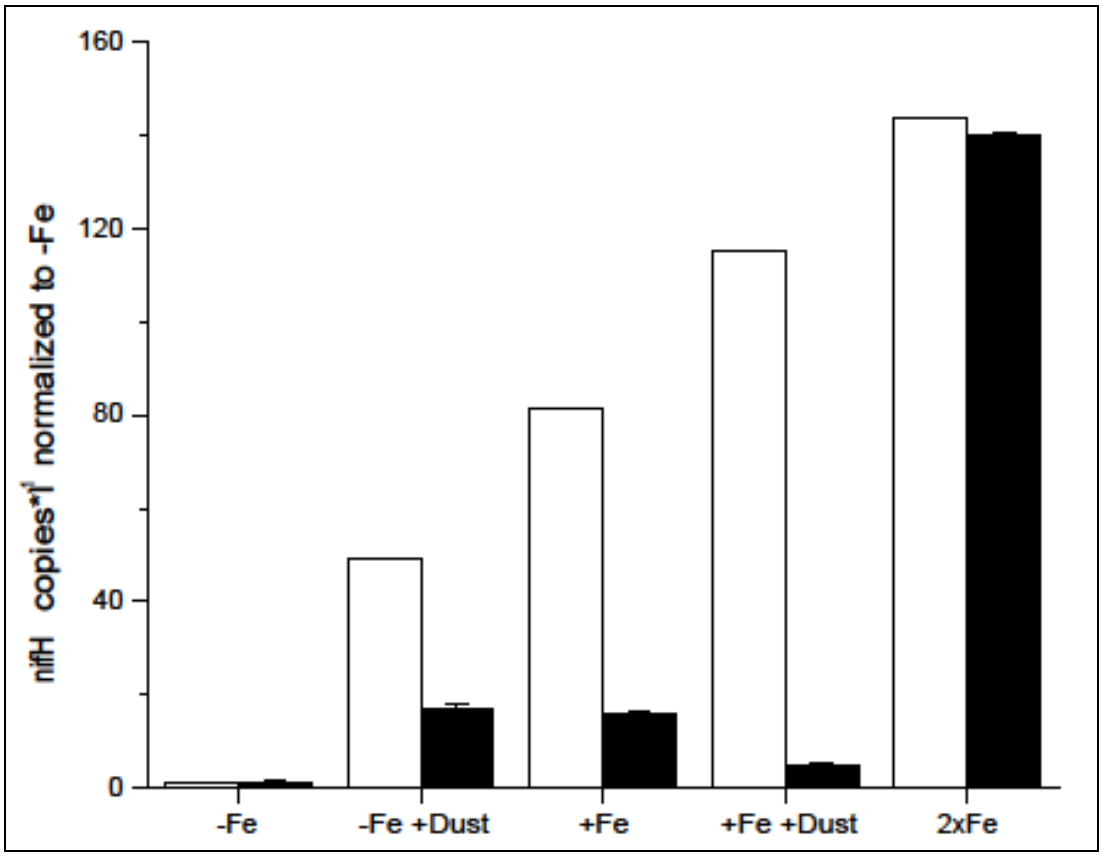

Figure 4. Differences in *Trichodesmium nifH* abundances after 3 Days (60 hours). Average DNA (white bars) and cDNA (black bars) abundances (*nifH* copies l^{-1}) were normalized to the –Fe control. Standard error bars are shown.

Paper G: *Impacts of Atmospheric Anthropogenic Nitrogen on the Open Ocean*

Synopsis

This manuscript explored effects of atmospheric anthropogenic N (AAN) in the open oceans. Amounts of anthropogenic N have increased in the atmosphere and these human perturbations reach the open ocean. Predicting exactly how AAN affects the open ocean is difficult because there are many unknowns. Despite this, the influx of fixed nitrogen to the open oceans from AAN is of increasing importance as amounts of AAN deposition are approaching estimated amounts of fixed N produced by biological dinitrogen fixation. AAN comes from fossil fuel emissions and production and use of fertilizers. As demand of these is expected to increase, AAN deposition is expected to increase further. The fraction of AAN of total N deposited in the oceans has already increased to 80% since 1860. Deposition is especially high near land masses with dense populations such as Asia, India, North and South America, Europe, and western Africa. It has been estimated that nearly all surface oceans are affected. AAN is composed of oxidized N species, NH_3, and of a poorly characterized organic N fraction. This means that AAN deposited on N-limited regions would have a greater effect on primary production than in areas where N concentrations are already high, however most AAN falls on waters with low N concentrations. Diazotrophs are probably not affected by direct AAN deposition, as the resulting concentrations in surface waters are too dilute to affect nitrogenase. As phytoplankton are generally N-limited, increases in surface ocean N could make P-limitation, especially of dinitrogen fixation, worse. It should be noted that the controls on dinitrogen fixation are not completely understood. AAN deposition is therefore similar to a 'long term low level fertilization.' The amount of anthropogenic carbon is also increasing. Using Redfield ratios it was estimated that up to 10% of oceanic uptake of anthropogenic carbon could be due to AAN deposition. The interaction between these N and C sources is an important consideration for constructing accurate models. Another biological consideration of AAN is that species composition

could be changed, leading to a change in N and C export. About 3% of the global annual new production could be attributed to AAN. This could be counter-acted by predicted increases in N_2O, a green house gas, from AAN. In conclusion, the amount of AAN deposition to the open oceans is increasing; however, the effects of this are not completely understood and very complex.

Contribution

I was invited, along with two other doctorate students to participate in a 3 day workshop on effects of anthropogenic nitrogen on the open ocean. This manuscript, prepared by R. A. Duce, was the result of discussions and writing sessions held during and after the workshop.

Impacts of Atmospheric Anthropogenic Nitrogen on the Open Ocean

R. A. Duce,[1*] J. LaRoche,[2] K. Altieri,[3] K. R. Arrigo,[4] A. R. Baker,[5] D. G. Capone,[6] S. Cornell,[7] F. Dentener,[8] J. Galloway,[9] R. S. Ganeshram,[10] R. J. Geider,[11] T. Jickells,[5] M. M. Kuypers,[12] R. Langlois,[2] P. S. Liss,[5] S. M. Liu,[13] J. J. Middelburg,[14] C. M. Moore,[11] S. Nickovic,[15] A. Oschlies,[2] T. Pedersen,[16] J. Prospero,[17] R. Schlitzer,[18] S. Seitzinger,[3] L. L. Sorensen,[19] M. Uematsu,[20] O. Ulloa,[21] M. Voss,[22] B. Ward,[23] L. Zamora[17]

Increasing quantities of atmospheric anthropogenic fixed nitrogen entering the open ocean could account for up to about a third of the ocean's external (nonrecycled) nitrogen supply and up to ~3% of the annual new marine biological production, ~0.3 petagram of carbon per year. This input could account for the production of up to ~1.6 teragrams of nitrous oxide (N_2O) per year. Although ~10% of the ocean's drawdown of atmospheric anthropogenic carbon dioxide may result from this atmospheric nitrogen fertilization, leading to a decrease in radiative forcing, up to about two-thirds of this amount may be offset by the increase in N_2O emissions. The effects of increasing atmospheric nitrogen deposition are expected to continue to grow in the future.

Nitrogen is an essential nutrient in terrestrial and marine ecosystems. Most nitrogen in the atmosphere and ocean is present as N_2 and is available only to diazotrophs, a restricted group of microorganisms that can fix N_2. Most organisms can only assimilate forms of reactive nitrogen (fixed nitrogen, N_r), including oxidized and reduced inorganic and organic forms. The availability of N_r limits primary production, the conversion of inorganic carbon to organic carbon (*1*), in much of the ocean. Reactive nitrogen enters the ocean via rivers, N_2 fixation, and atmospheric deposition. It is removed via N_2 formation by denitrification and anaerobic ammonium oxidation (anammox), nitrous oxide (N_2O) and ammonia emissions, and burial of organic matter in sediments. Human activities have severely altered many coastal ecosystems by increasing the input of anthropogenic nitrogen through rivers and groundwater, direct discharges from wastewater treatment, atmospheric deposition, and so forth, resulting in increasing eutrophication. Human activities have also added large quantities of atmospheric N_r to central ocean regions.

Riverine input of N_r to the oceans is estimated as 50 to 80 Tg N year^{-1} (*2*–*4*). However, much is either lost to the atmosphere after N_2 conversion or buried in coastal sediments, never reaching oceanic regions (*5*). We assume that riverine N_r has a negligible impact on the open ocean nitrogen inventory, and we do not consider it further. Estimates of global ocean N_2 fixation range from 60 to 200 Tg N year^{-1} (*2*, *6*–*8*). Although impacts of the amplified nitrogen inputs to terrestrial systems are being continuously evaluated (*3*, *9*), here we show that atmospheric transport and deposition is an increasingly important pathway for N_r entering the open ocean, often poorly represented in analyses of open ocean anthropogenic impacts (*10*–*16*). Atmospheric N_r input is rapidly approaching global oceanic estimates for N_2 fixation and is predicted to increase further due to emissions from combustion of fossil fuels and production and use of fertilizers. Our objective is to highlight the growing importance of anthropogenic atmospheric N_r (AAN) deposition to the oceans and evaluate its impact on oceanic productivity and biogeochemistry.

Atmospheric Emission and Deposition of Nitrogen Species

Atmospheric emissions of N_r are primarily oxidized nitrogen species, NO_x (NO + NO_2) and NH_3. Recent studies suggest that atmospheric water-soluble organic nitrogen is far more abundant than conventionally thought, constituting ~30% of total N_r deposition (*13*, *17*–*20*). Given the uncertain origins and complex composition of this material, the importance of direct emissions and secondary formation of organic nitrogen is unclear. However, measurements suggest that an important fraction is anthropogenic (*13*, *17*). We therefore assume that in 1860, the relationship between organic and inorganic nitrogen deposition was the same as it is today and increase our 1860 estimate so that organic nitrogen represents 30% of total N_r deposition. The uncertainties associated with this assumption emphasize the need for further research on atmospheric organic nitrogen.

Estimated total N_r and AAN emissions in 1860, 2000, and 2030 (Table 1) show that anthropogenic emissions have significantly increased since the mid-1800s and future increases are expected (*21*). Over the next 20 to 25 years, the proportion of NH_3 emissions will likely increase due to enhanced atmospheric emission controls predicted to be more effective for NO_x than NH_3 (Table 1) (*21*). An important fraction of atmospheric N_r emissions is deposited on the ocean (Table 1). In 1860, this amounted to ~20 Tg N year^{-1}, of which ~29% was anthropogenic. By 2000, the total N_r deposition to the ocean had more than tripled to ~67 Tg N year^{-1}, with ~80% being anthropogenic. This is greater than the 39 Tg N year^{-1} reported by (*14*), in part because our estimate includes water-soluble organic nitrogen. Estimates of anthropogenic emissions for 2030 indicate a ~4-fold increase in total atmospheric N_r deposition to the ocean and an ~11-fold increase in AAN deposition compared with 1860 (*22*).

The spatial distribution of atmospheric deposition has also changed greatly (Fig. 1, A and B). Deposition to most of the ocean was <50 mg N m^{-2} year^{-1} in 1860, with very few areas >200 mg N m^{-2} year^{-1}. Most oceanic deposition was from natural sources; anthropogenic sources impacted only a few coastal regions. By 2000, deposition over large ocean areas exceeded 200 mg N m^{-2} year^{-1}, reaching >700 mg N m^{-2} year^{-1} in many areas. Intense deposition plumes extend far downwind of major population centers in Asia, India, North and South America, around Europe, and west of Africa (Fig. 1B). A direct comparison of deposition in 1860 and 2000 shows almost all ocean surface areas now being affected by AAN deposition (Fig. 1, A and B). Predictions for 2030 (fig. S1) indicate similar patterns, but with

[1]Departments of Oceanography and Atmospheric Sciences, Texas A&M University, College Station, TX 77843, USA. [2]Leibniz-Institut fuer Meereswissenschaften, 24105 Kiel, Germany. [3]Institute of Marine and Coastal Sciences, Rutgers University, Rutgers/NOAA CMER Program, New Brunswick, NJ 08901, USA. [4]Department of Environmental Earth System Science, Stanford University, Stanford, CA 94305, USA. [5]School of Environmental Sciences, University of East Anglia, Norwich NR4 7TJ, UK. [6]Department of Biological Sciences, University of Southern California, Los Angeles, CA 90089, USA. [7]QUEST–Earth Sciences, University of Bristol, Bristol BS8 1RJ, UK. [8]European Commission, Joint Research Centre, Institute for Environment and Sustainability, TP290, I-21020, Ispra (Va), Italy. [9]Department of Environmental Sciences, University of Virginia, Charlottesville, VA 22904, USA. [10]John Murray Laboratories, The King's Buildings, Edinburgh EH9 3JW, UK. [11]Department of Biological Sciences, University of Essex, Colchester CO4 3SQ, UK, and National Oceanography Centre, University of Southampton, Southampton SO14 3ZH, UK. [12]Max Planck Institute for Marine Microbiology, Celsiusstrasse 1, D-28359 Bremen, Germany. [13]Key Laboratory of Marine Chemistry Theory and Technology Ministry of Education, College of Chemistry and Chemical Engineering, Ocean University of China, Qingdao 266100, Peoples Republic of China. [14]Netherlands Institute of Ecology, Korringaweg 7, 4401 NT Yerseke, Netherlands. [15]Atmospheric Research and Environment Programme, World Meteorological Organization, BP2300, 1211 Geneva 2, Switzerland. [16]University of Victoria, Post Office Box 3055 STN CSC, Victoria, BC V8W 3P6, Canada. [17]Rosenstiel School of Marine and Atmospheric Sciences, University of Miami, Miami, FL 33149, USA. [18]Alfred Wegener Institute for Polar and Marine Research, 27568 Bremerhaven, Germany. [19]National Environmental Research Institute, Aarhus University, Denmark. [20]Ocean Research Institute, University of Tokyo, Tokyo 164-8639, Japan. [21]Departamento de Oceanografía, Centro de Investigación Oceanográfica, COPAS, and Nucleo Milenio EMBA, Universidad de Concepción, Casilla 160-C, Concepción, Chile. [22]Leibnitz Institute for Baltic Sea Research, Warnemünde, 18119 Rostock, Germany. [23]Department of Geosciences, Princeton University, Princeton, NJ 08544, USA.

*To whom correspondence should be addressed. E-mail: rduce@ocean.tamu.edu

increased deposition further into open ocean regions (*21*, *22*). The ratio of 2030-to-2000 deposition rates (Fig. 1C) shows up to a factor of 2 increase in Southeast Asia, the Bay of Bengal, and the Arabian Sea; up to a 50% increase off western Africa; and up to 30% across essentially all the mid-latitude North Atlantic and North Pacific. As Galloway *et al*. (*9*) conclude, controlling NO_x emissions using maximum feasible reductions could substantially decrease future emissions, so the increases we predict on deposition rates (Fig. 1C) may represent upper limits.

Impact on New Primary Production and the Biological Pump

Present global open ocean primary production is estimated at ~50 Pg C $year^{-1}$ (*23*), equivalent to ~8800 Tg N $year^{-1}$, assuming Redfield stoichiometry (Table 2). Because ~78% of this production is driven by regeneration of N_r within surface waters (*24*) (*a* in Fig. 2), it is more relevant to evaluate the impact of AAN deposition on oceanic productivity and biogeochemistry by comparing AAN with global new production, estimated at ~11 Pg C $year^{-1}$ (*24*–*26*). New production (*b* in Fig. 2 and Table 2) is dominated by nitrate regenerated at depth from sinking organic matter and subsequently returned to the euphotic zone via physical transport (*b′* in Fig. 2) (*27*). Over sufficiently large space and time scales

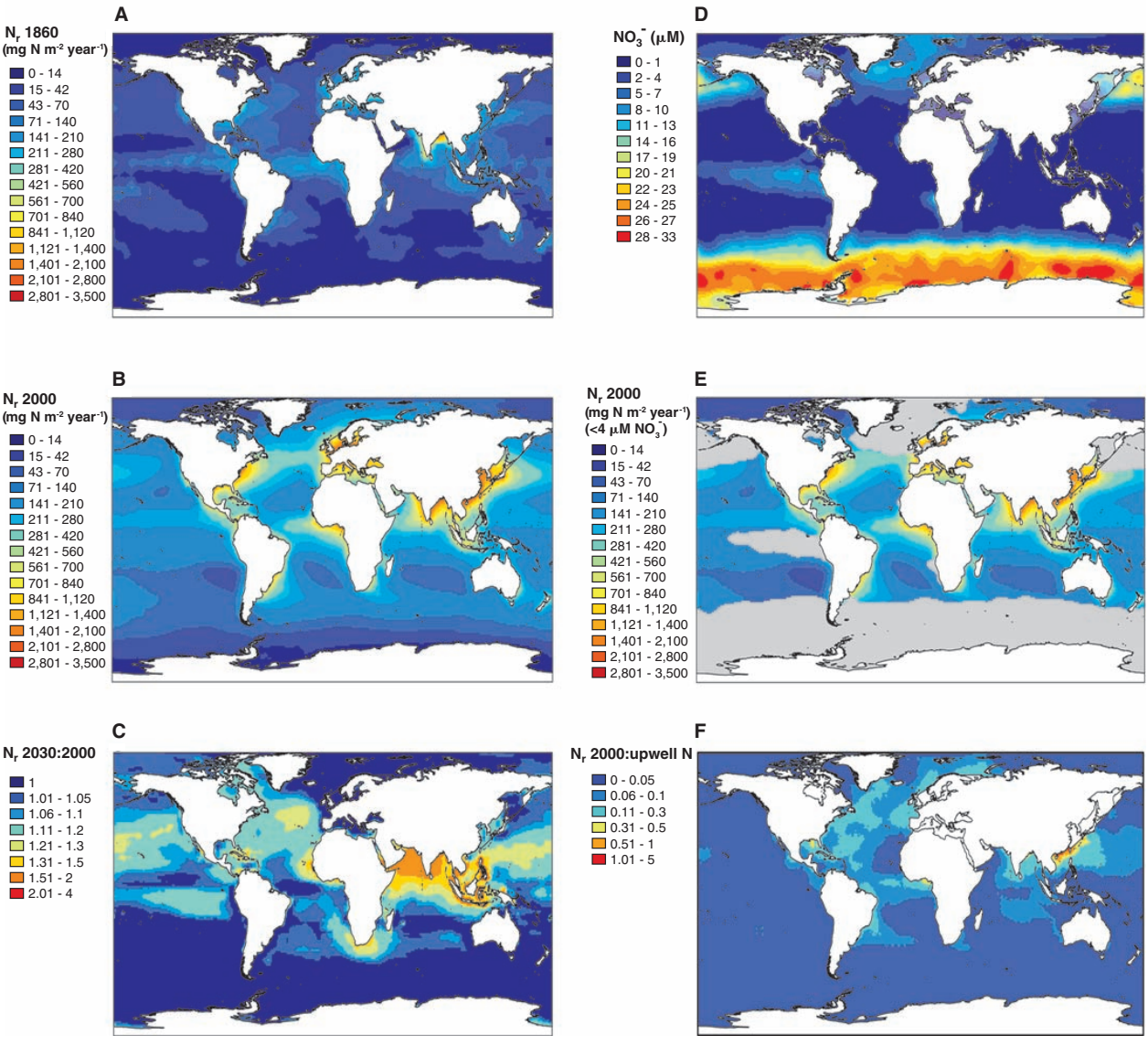

Fig. 1. (**A**) Total atmospheric reactive nitrogen (N_r) deposition in 1860 in mg m^{-2} $year^{-1}$ [NH_x and NO_y are derived from (*3*), with the addition of 30% of the total nitrogen as organic nitrogen]. Total atmospheric N_r deposition in 1860 was ~20 Tg N $year^{-1}$, AAN was ~5.7 Tg N $year^{-1}$. (**B**) Total atmospheric reactive nitrogen (N_r) deposition in 2000 in mg m^{-2} $year^{-1}$ [derived from (*21*) with the addition of 30% of the total nitrogen as organic nitrogen]. Total atmospheric N_r deposition in 2000 was ~67 Tg N $year^{-1}$, AAN was ~54 Tg N $year^{-1}$. (**C**) Ratio of the projected flux of N_r to the ocean in 2030 to that in 2000. (**D**) Nitrate concentrations (μM) in the surface (0 to 1 m) waters of the ocean (*43*). (**E**) Similar to (B), but with regions where surface nitrate >4 μM has been masked out. Total atmospheric N_r deposition in 2000 to the nonmasked areas was ~51 Tg N $year^{-1}$, AAN was ~41 Tg N $year^{-1}$. (**F**) Ratio of total N_r deposition to dissolved inorganic nitrogen (DIN) supply into the upper 130 m as diagnosed from a model fitted to oceanic tracer observations (*44*). To reduce noise, computation of the ratio has been limited to areas with DIN supply exceeding 0.05 mol m^{-2} $year^{-1}$.

(1 to ~1000 years), nitrate-driven new production is balanced by the biologically mediated export of particulate and dissolved organic matter from the surface layer (*b″* in Fig. 2). On a similar time scale, this component of new production is almost neutral in terms of carbon assimilation (*28*) because degradation processes release N_r and CO_2 in stoichiometric amounts equivalent to the initial elemental composition of the organic matter. In the absence of denitrification and other fixed nitrogen losses in the ocean interior, nitrate-based new production can be considered a closed loop within which the biologically mediated carbon export (*b″*) is balanced by a return flux of dissolved inorganic carbon (*b′*), resulting in near-zero net air-sea CO_2 exchange.

Only external (to the ocean) sources of N_r that reach the surface mixed layer can affect the steady-state balance of the biologically mediated flux of CO_2 across the air-sea interface. The two known open ocean sources of external N_r are biological N_2 fixation (*c* in Fig. 2) and atmospheric deposition (*d*). Together these contribute a net oceanic input of N_r that can support "completely new production" and hence influence global oceanic N_r and the net atmosphere-to-ocean exchange of CO_2, assuming an adequate supply of other nutrients (P, Fe). Although N_2 fixation must have dominated the flux of external new nitrogen in the preindustrial world, atmospheric N_r deposition is now approaching N_2 fixation as a result of the dramatic increase in the anthropogenic component (Table 2).

Can this atmospheric N_r deposition be rapidly assimilated into primary production? It will impact the biogeochemistry of oceanic areas that are either perennially or seasonally depleted in surface nitrate, but will have little effect in high-nutrient, low-chlorophyll (HNLC) regions where the concentration of surface nitrate is always high. Comparing surface nitrate concentrations (Fig. 1D) and total N_r deposition (Fig. 1B) shows the relatively small overlap between high N_r deposition and significant surface nitrate concentrations. In regions where surface nitrate is seasonally depleted (i.e., where productivity is nitrogen limited), atmospheric deposition would likely be assimilated during the year. Although N_r generally is seasonally exhausted in regions where mean annual nitrate is <7 μM, a more conservative value of <4 μM is used to calculate the distribution of the atmospheric N_r deposition in present-day nitrogen-depleted waters (Fig. 1E). The calculated global N_r deposition to regions with mean nitrate <4 μM is ~51 Tg N $year^{-1}$, or ~76% of the total atmospheric N_r deposited in the ocean, compared to ~56 Tg N $year^{-1}$ (~84% of total deposition) if <7 μM is used as a threshold. Corresponding values for AAN are ~41 and ~45 Tg N $year^{-1}$. Using the areas delineated by the <4 μM and <7 μM nitrate concentrations above, we calculate that ~67 to 75% of oceanic surface waters are potentially seasonally nitrogen limited, although some of these areas may not be exclusively nitrogen limited but rather colimited (*1*). It has recently been assumed that only 40% of the ocean is nitrogen limited (*14*), although this estimate did not allow for N/P colimitation such as seen in the North Atlantic and other areas designated P-limited in (*14*). These are likely underestimates because much of the N_r is deposited upstream of N_r-depleted regions (e.g., HNLC Southern Ocean) and will eventually be advected into thermocline waters of nitrogen-limited regions of the Southern Hemisphere and North Atlantic and thus are important to future (decades to centuries) productivity and biogeochemistry (*29*).

The total atmospheric deposition plus N_2-fixation flux to the ocean is ~167 Tg N $year^{-1}$ (Table 2). Assuming complete assimilation, these external N_r sources can support a maximum biologically mediated flux of ~1.0 Pg C $year^{-1}$, of which ~0.4 Pg C $year^{-1}$ is from atmospheric deposition. Deposition of AAN alone could support up to ~0.3 Pg C $year^{-1}$, or ~3% of all new production, including that from nutrients upwelled from deep waters, and ~32% of the productivity derived from external N_r supply (Table 2). In 1860, AAN supported a biologically mediated carbon flux of only ~0.03 Pg C $year^{-1}$, so from 1860 to the present the potential impact of AAN on net primary productivity has increased ~10-fold. An earlier lower estimate (0.16 Pg C $year^{-1}$) of new (export) production generated by AAN deposition (*14*) assumed a different nitrogen-limited area, lower atmospheric fluxes, and the assumption that N enhancement will result in the replacement of diazotrophs by other phytoplankton.

Increased new production due to AAN fertilization coincides with the anthropogenic perturbation of the global carbon cycle and penetration of anthropogenic carbon in the ocean. The current anthropogenic CO_2 uptake by the ocean is ~2.2 ± 0.5 Pg C $year^{-1}$ (*30*), primarily attributed to physical-chemical processes (the "solubility pump"). Assuming that new production draws down atmospheric CO_2 according to Redfieldian stoichiometry, up to ~10% of the present anthropogenic carbon uptake could be attributed to anthropogenic nitrogen fertilization This potentially significant enhancement of the oceanic uptake of anthropogenic carbon indicates the need to incorporate this factor in future Earth system assessments and models, as has already been done for terrestrial ecosystems (*31*). This estimate may be lower if the dissolved organic carbon or particulate organic carbon produced is regenerated at shallow depths (*32*). The efficiency and longevity of this anthropogenic nitrogen fertilization effect depend on temporal uncoupling of the new N_r inputs (N_2 fixation and atmospheric deposition) from N_r removal (e.g., denitrification/anammox and burial). Assuming that all other essential nutrients are in adequate supply, it will be operational as long as the

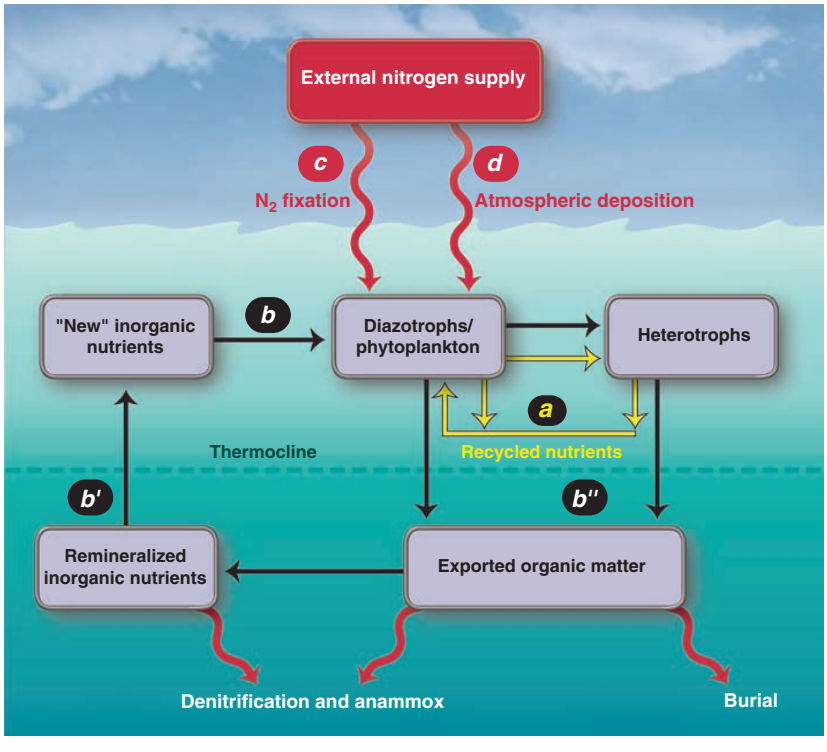

Fig. 2. Schematic of the processes supplying nutrients for surface primary production. See text for detailed description.

increase in new N_r (and associated additional CO_2 uptake) is not balanced by increased regeneration of N_2 and CO_2 and release at the ocean-air interface. Eventually, if AAN deposition levels off, the ocean may reach a new steady state with respect to nitrogen gains and losses that is neutral with respect to CO_2 uptake over time scales similar to the oceanic N residence time (~1000 years).

The future impact of AAN on productivity must be evaluated in the context of predicted changes in productivity caused by other variables. For instance, elevated concentrations of atmospheric CO_2 may have resulted in excess carbon consumption and export because of shifting C:N stoichiometry (*33*), and it is unclear whether projected AAN and high CO_2 concentrations have synergy or compensate. El Niño–Southern Oscillation (ENSO)–induced higher water temperatures and the associated increased stratification in low-latitude oceans may have reduced productivity by 60% in some regions (*34*). Thus, in a warmer climate, decreases in productivity due to restricted injection of nutrient-rich deep water would only accentuate the importance of AAN contributions to new production in low-latitude oligotrophic oceanic areas where AAN already has a strong effect. Assuming that all N_r deposition is assimilated into primary production, this N_r-driven new production could contribute as much as 20% of the total new (or export) production in such regions where upwelling is limited, e.g., the North Atlantic gyre (Fig. 1F). The contribution of N_r deposition to new production is higher in the Atlantic than the Pacific and can reach magnitudes comparable to export production along some continental areas.

Table 1. Atmospheric nitrogen emissions and deposition to the ocean. Assumed uncertainties—emissions: 1860: ±50%; 2000: NO_x ±30%, NH_3 ±50%; 2030: see text and (*20*). Deposition: 1860: ±50%; 2000: NO_y/NH_x ±40%, organic N ±50%; 2030: see text and (*20*).

	1860* (Tg N year^{-1})	2000† (Tg N year^{-1})	2030† (Tg N year^{-1})
Emission to the atmosphere			
Total NO_x	13 (7–20)	52 (36–68)	54‡
Anthropogenic NO_x	2.6 (1.3–4)	38 (27–49)	43
Total NH_3	21 (11–32)	64 (32–96)	78‡
Anthropogenic NH_3	7.4 (3.7–11)	53 (27–80)	70
Total atmospheric N emissions	34 (18–52)	116 (68–164)	132
Total anthropogenic N_r (AAN)	10 (5–15)	91 (54–129)	113
Deposition to the ocean			
Total NO_y	6.2 (3.1–9.3)	23 (14–32)	25
Anthropogenic NO_y	1.2 (0.6–1.8)	17 (10–24)	18
Total NH_x	8 (4–12)	24 (14–34)	29
Anthropogenic NH_x	2.4 (1.2–3.6)	21 (13–29)	25
Total organic N_r	6.1 (3.0–9.1)	20 (10–30)	23
Anthropogenic organic N_r	2.1 (1.0–3.1)	16 (8–24)	19
Total N_r deposition	20 (10–30)	67 (38–96)	77
Total anthropogenic N_r (AAN)	5.7 (2.8–8.5)	54 (31–77)	62

*From (*3*). †Derived from (*21*); see text and (*26*). ‡NO_x and NH_3 based on ~80% and ~90% anthropogenic, respectively [from (*3*)].

Table 2. Atmospheric nitrogen deposition to the ocean in 2000 and its impact on productivity. Global-scale estimates of total primary production (*23*); new production (*24–26*); N_2 fixation (*2*, *6–8*). Most letters in italics refer to flux pathways in Fig. 2.

		Global ocean nitrogen (Tg N year^{-1})	Resultant global ocean productivity (Pg C year^{-1})
Total primary production (*a*+*b*+*c*+*d*)		~8800 (7000–10,500)	~50 (40–60)
New production (NP) (*b*)		~1900 (1400–2600)	~11 (8–15)
Marine N_2 fixation (*c*)		~100 (60–200)	~0.57 (0.3–1.1)
Total net N_r deposition (*d*) (NO_y+NH_x+Org. N_r)		~67 (38–96)	~0.38 (0.22–0.55)
Total external nitrogen supply (*c*+*d*)		~167 (98–296)	~0.95 (0.56–1.7)
Anthropogenic N_r deposition (AAN) (*e*)		~54 (31–77)	~0.31 (0.18–0.44)
Marine N_2 fixation as % NP N_r	= *c*/*b*		~5.3% (2.3–14.3%)
Total N_r deposition as % NP N_r	= *d*/*b*		~3.5% (1.5–6.9%)
AAN as % NP N_r	= *e*/*b*		~2.8% (1.2–5.5%)
Total N_r deposition as % external N supply	= *d*/(*c*+*d*)		~40% (13–98%)
AAN as % external N supply	= *e*/(*c*+*d*)		~32% (10–79%)

On the basis of future scenarios for anthropogenic emissions, AAN contribution to primary production could approach current estimates of global N_2 fixation by 2030. Fertilization of the surface layer by atmospheric deposition, primarily AAN, could even lead to a decrease in N_2 fixation due to biological competition (*14*). However, atmospheric N_r deposition has a very small effect on the surface seawater ambient N_r concentrations, too little to inhibit nitrogenase activity directly [e.g., we estimate that an extremely rare and large atmospheric deposition event distributed over a 25-m mixed-layer depth could increase the N_r concentration by only ~ 45 nM (*35*), which is too small to suppress N_2 fixation (*36*)]. Atmospheric N_r deposition more likely represents a long-term low-level fertilization of the ocean that has consequences for the natural biogeochemical cycles of nitrogen and carbon and their ongoing anthropogenic perturbations. Biological evidence suggests that phytoplankton communities in oceanic gyres are presently nitrogen limited (*1*). Atmospheric N_r deposition, in the absence of significant atmospheric deposition of phosphorus, may exacerbate phosphorus limitation of N_2 fixation. The long-term effect of AAN deposition on N_2 fixation depends on whether P or Fe limits N_2 fixation and on the supply ratio of bioavailable N:P:Fe derived from atmospheric deposition (*37*). Atmospheric deposition of phosphorus is much less perturbed by human activity than N_r (*13*, *37*). Hence, the overall impact of atmospheric deposition is likely to be a shift in the N/P balance of surface waters. Some marine diazotrophs can exploit dissolved organic phosphorus pools and may obtain an adequate P supply by degrading compounds such as phosphonates (*38*).

Changes in species composition and productivity can lead to changes in the export of nitrogen and carbon to deep ocean water, resulting in a shift of deep ocean N/P ratios away from Redfield stoichiometry, which could then influence the chemistry of upwelled waters remote from the loci of atmospheric depositions. Remineralization of this extra organic carbon flux in deep waters may reduce the deepwater O_2 concentration, and the resultant microbial N_2 production will act to restore the N/P ratio toward the Redfield value, as suggested to have happened in the past (*39*). (See Supporting Online Material, including fig. S2).

Impact on N_2O Emissions from the Ocean

Another important issue is whether increasing atmospheric N_r inputs to the ocean can alter marine emissions of nitrous oxide (N_2O), a major greenhouse gas. Estimates of global sea-to-air N_2O fluxes vary considerably. Two recent estimates are the Intergovernmental Panel on Climate Change (IPCC) assessment (*30*) (3.8 Tg N year^{-1} as N_2O) and the calculation by Bange of the mean from data in (*40*) (6.2 Tg N year^{-1}). Using the mean (5.0 Tg N year^{-1}) and the range of these two estimates, and assuming that the nitrogen in

this "recent" N_2O flux originally entered the oceans from N_2 fixation (100 Tg N $year^{-1}$) and atmospheric deposition (67 Tg N $year^{-1}$), then the emission of 5.0 Tg N $year^{-1}$ as N_2O results from nitrification and denitrification of part of this 167 Tg N $year^{-1}$ entering the surface ocean. This assumes that N_2O production in the near-surface ocean is at steady state and there are no significant time lags between atmospheric input and N_2O formation. Normalizing the N_2O flux to the atmosphere by the "completely new" nitrogen input (5.0:167) can then be used to estimate that AAN deposition has resulted in the production of up to ~1.6 Tg N_2O-N $year^{-1}$, or about a third of total oceanic N_2O emissions. This approach suggests that in 1860, only ~0.2 Tg N $year^{-1}$ (~5%) of the sea-to-air flux of N_2O was driven by atmospheric anthropogenic inputs, assuming simplistically that N_2O production is linearly related to N supply. [We use linear scaling due to the lack of experimental and modeling studies that address the spatial and nonlinear response of N_2O emissions to N deposition, although important regional variations are likely (*41*).] This suggests that from 1860 to the present, the increase in AAN has led to nearly an order of magnitude increase in anthropogenic N_2O emission from the oceans. Calculations and estimates of increases for 2030 are in table S1.

While oceanic AAN deposition may result in increased N_2O emissions, increasing radiative forcing, AAN also increases primary production (up to ~0.3 Pg C $year^{-1}$ detailed above) and export production to the deep ocean, removing CO_2 from the atmosphere and therefore decreasing radiative forcing. With a Global Warming Potential of 298 for N_2O (*42*), the net balance suggests that about two-thirds of the decrease in radiative forcing from CO_2 uptake could be offset by the increase due to N_2O emissions. The uncertainty in our estimates is considerable; however, the estimates suggest the potential importance of AAN to N_2O emissions and therefore the need for future research in regions such as oceanic Oxygen Minimum Zones (OMZs), which, although small in area, are potentially important for N_2O emissions. The future role of OMZs will be influenced not only by AAN but also by climate and other global changes.

Conclusions

This analysis emphasizes the potential importance of the growing quantity of atmospheric reactive (fixed) nitrogen that enters the open ocean as a result of human activities and its impact on the present marine nitrogen cycle. Considering the increasing demand for energy and fertilizers, the emissions of AAN are expected to grow over the coming decades. Atmospheric deposition of anthropogenic nitrogen to the ocean may account for up to ~3% of the annual new oceanic primary productivity, but about a third of the primary productivity generated as a result of the external input of nitrogen to the ocean. The input of AAN is approaching that of N_2 fixation as a source of marine reactive nitrogen. Although local AAN deposition seems unlikely to alter significantly local phytoplankton species composition, the phytoplankton community could be affected by the slow long-term fertilization of surface waters by AAN. Moreover, AAN inputs to the ocean have potentially important climatic implications. Up to about a tenth of the anthropogenic atmospheric carbon uptake by the ocean (as CO_2) may result from this fertilization. In addition, AAN inputs may stimulate N_2O emissions, with possibly about two-thirds of the decrease in radiative forcing from increased CO_2 uptake by the ocean being offset by the increase in radiative forcing from increased N_2O emissions.

There is clearly much we do not know about the extent and time scale of the impacts of AAN deposition on the oceans and the feedbacks to the climate system. The issues are complex and interactive, and they must be considered in climate scenarios. Areas of particular importance include understanding more fully the sources, chemical speciation, reactivity, and availability of atmospheric organic nitrogen; developing more realistic models of N_r deposition to the ocean, coupled with measuring N_r deposition over extended periods of time in open ocean regions; understanding the relationships between, and impacts of, the atmospheric deposition of bioavailable N, P, and Fe; and understanding the mechanisms and time scales involved in the oceanic response to N_r deposition, coupled with a new generation of Earth system models that take into account long-term low-level nitrogen fertilization of the ocean and evaluate the effect on N_2O emissions and the duration of the enhanced (anthropogenic) CO_2 uptake.

References and Notes

1. M. M. Mills, C. Ridame, M. Davey, J. La Roche, R. J. Geider, *Nature* **429**, 292 (2004).
2. N. Gruber, J. Sarmiento, in *The Sea: Biological-Physical Interactions*, A. R. Robinson, J. F. McCarthy, B. Rothschild, Eds. (Wiley, New York, 2002), vol. 12, pp. 337–399.
3. J. N. Galloway *et al.*, *Biogeochemistry* **35**, 3 (1996).
4. S. P. Seitzinger, J. A. Harrison, E. Dumont, A. H. W. Beusen, A. F. Bouwman, *Global Biogeochem. Cycles* **19**, GB4S01 (2005).
5. S. Seitzinger *et al.*, *Ecol. Appl.* **16**, 2064 (2006).
6. C. Mahaffey, A. F. Michaels, D. G. Capone, *Am. J. Sci.* **305**, 546 (2005).
7. J. K. Moore, S. C. Doney, K. Lindsay, N. Mahowald, A. F. Michaels, *Tellus* **58B**, 560 (2006).
8. C. Deutsch, J. L. Sarmiento, D. M. Sigman, N. Gruber, J. P. Dunne, *Nature* **445**, 163 (2007).
9. J. N. Galloway *et al.*, *Science* **320**, 889 (2008).
10. R. A. Duce *et al.*, *Global Biogeochem. Cycles* **5**, 193 (1991).
11. J. M. Prospero *et al.*, *Biogeochemistry* **35**, 27 (1996).
12. C. M. Duarte *et al.*, *J. Geophys. Res.* **111**, G04006 (2006).
13. T. Jickells, *Biogeosciences* **3**, 271 (2006).
14. A. Krishnamurthy, J. K. Moore, C. S. Zender, C. Luo, *J. Geophys. Res.* **112**, G02019 (2007).
15. H. W. Paerl, *Nature* **315**, 747 (1985).
16. S. C. Doney *et al.*, *Proc. Natl. Acad. Sci. U.S.A.* **104**, 14580 (2007).
17. S. E. Cornell, T. D. Jickells, J. N. Cape, A. P. Rowland, R. A. Duce, *Atmos. Environ.* **37**, 2173 (2003).
18. K. A. Mace, R. A. Duce, N. W. Tindale, *J. Geophys. Res.* **108**, 4338 (2003).
19. T. Nakamura, H. Ogawa, D. K. Maripi, M. Uematsu, *Atmos. Environ.* **40**, 7259 (2006).
20. If the assumption that in 1860 the relationship between organic and inorganic N in deposition was the same as today, i.e., that organic nitrogen is ~30% of the total N_r, is in error, then it is likely that both the total and the anthropogenic nitrogen deposition in 1860 would have been less than indicated in Table 1.
21. F. Dentener *et al.*, *Global Biogeochem. Cycles* **20**, GB4003 (2006).
22. The deposition estimates for 2030 are based on the S2 simulation of NO_x and NH_3 emissions to the atmosphere presented in (*21*), which uses an IIASA CLE 2030 current emission regulation scenario, termed "likely" in that paper. We estimate that the atmospheric emission and deposition values shown in Table 1 for 2030 have uncertainties of ~40 to 50%. Dentener *et al.* (*21*) also discuss results using the "optimistic" IIASA Maximum Feasible Reduction (MFR) scenario and the "pessimistic" IPCC SRES A2 scenario. Depending on the regional development path of N_r emissions, N_r depositions may be lower by 10 to 70% (MFR) or higher by 30 to 200%.
23. M. E. Carr *et al.*, *Deep-Sea Res. Part II* **53**, 741 (2006).
24. E. A. Laws, P. G. Falkowski, W. O. Smith, H. Ducklow, J. J. McCarthy, *Global Biogeochem. Cycles* **14**, 1231 (2000).
25. A. Oschlies, *Deep-Sea Res. Part II* **48**, 2173 (2001).
26. H. W. Ducklow, *Rev. Geophys.* **33**, 1271 (1995).
27. R. C. Dugdale, J. J. Goering, *Limnol. Oceanogr.* **12**, 196 (1967).
28. W. S. Broecker, *Global Biogeochem. Cycles* **5**, 191 (1991).
29. J. L. Sarmiento, N. Gruber, M. A. Brzezinski, J. P. Dunne, *Nature* **427**, 56 (2004).
30. K. Denman *et al.*, in *Climate Change 2007: The Physical Science Basis*, S. Solomon *et al.*, Eds. (Cambridge Univ. Press, Cambridge, 2007), pp. 544–547.
31. F. Magnani *et al.*, *Nature* **447**, 849 (2007).
32. A. Gnanadesikan, J. L. Sarmiento, R. D. Slater, *Global Biogeochem. Cycles* **17**, 1050 (2003).
33. U. Riebesell *et al.*, *Nature* **450**, 545 (2007).
34. M. J. Behrenfeld *et al.*, *Nature* **444**, 752 (2006).
35. A. F. Michaels, D. A. Siegel, R. J. Johnson, A. H. Knap, J. N. Galloway, *Global Biogeochem. Cycles* **7**, 339 (1993).
36. C. M. Holl, J. P. Montoya, *J. Phycol.* **41**, 1178 (2005).
37. A. R. Baker, S. D. Kelly, K. F. Biswas, M. Witt, T. D. Jickells, *Geophys. Res. Lett.* **30**, 2296 (2003).
38. S. T. Dyhrman *et al.*, *Nature* **439**, 68 (2006).
39. R. S. Ganeshram, T. F. Pedersen, S. E. Calvert, G. W. McNeill, M. R. Fontugne, *Paleoceanography* **15**, 361 (2000).
40. H. W. Bange, *Atmos. Environ.* **40**, 198 (2006).
41. X. Jin, N. Gruber, *Geophys. Res. Lett.* **30**, GL18458 (2003).
42. S. Solomon *et al.*, in *Climate Change 2007: The Physical Science Basis,* S. Solomon *et al.*, Eds. (Cambridge Univ. Press, Cambridge, 2007).
43. M. E. Conkright *et al.*, *World Ocean Atlas 2001,* vol. 4, *Nutrients*, S. Levitus, Ed., NOAA Atlas NESDros. Inf. Serv. 52 (U.S. Government Printing Office, Washington, DC, 2002).
44. R. Schlitzer, *J. Phys. Oceanogr.* **37**, 259 (2007).

45. We acknowledge the leadership of the Surface Ocean–Lower Atmosphere Study (SOLAS) project (www.solas-int.org) and the International Nitrogen Initiative (www.initrogen.org) of SCOPE and the International Geosphere-Biosphere Programme (IGBP; www.igbp.kva.se) for conceiving this synthesis. We thank the Scientific Committee on Oceanic Research, IGBP, the U.S. National Oceanic and Atmospheric Administration, and the European Science Foundation for partial support of the work. We thank J. Hare of the SOLAS International Project Office for help in organizing the workshop and E. Breviere of that office for help in making the Nitrogen Workshop in Norwich, UK, a success. We acknowledge two anonymous reviewers for constructive feedback.

Supporting Online Material

www.sciencemag.org/cgi/content/full/320/5878/893/DC1
SOM Text
Figs. S1 and S2
Table S1
References

10.1126/science.1150369

IV. Discussion

Nutrient Limitation in the North Atlantic Ocean

Primary production is, in general, nitrogen limited in the North Atlantic Ocean. A total of twelve nutrient addition bioassay experiments were conducted across the northern Atlantic Ocean and all but one experiment showed nitrogen limitation of primary productivity (Papers C and D [*Davey et al.*, 2008; *Mills et al.*, 2004; *Moore et al.*, 2008; *Moore et al.*, 2006a]). The one exception to this trend showed iron limitation of primary productivity during the spring bloom (Paper C [*Moore et al.*, 2006a]). This is most likely a transient limitation, but still a significant finding. The Atlantic Ocean is usually not considered iron limited due to the aeolian dust supply from the Saharan Desert, however the variability in dust supply could affect the timing and size of the spring bloom (Paper C [*Moore et al.*, 2006a]). In all other bioassay experiments performed in the framework of this thesis, bulk chlorophyll a and picophytoplankton chlorophyll concentrations increased with additions of nitrogen, which indicates that nitrogen is the proximal nutrient limiting phytoplankton growth.

Analytical flow cytometry of the bioassay experiment samples showed that picophytoplankton abundances generally increased with additions of nitrogen and further increases were seen with simultaneous additions of nitrogen and phosphorus (Paper D [*Davey et al.*, 2008; *Moore et al.*, 2008]). In two bioassay experiments a subgroup of *Synechococcus* sized cells with dim fluorescence, called dim *Synechococcus*, increased in abundance with simultaneous additions of phosphorus and iron instead of nitrogen [*Davey et al.*, 2008]. This response is expected for diazotrophic organisms. Unfortunately, only a subset of samples were available for qPCR analysis from these two experiments but *nifH* abundances of the unicellular Group C (*Cyanothece*-like) phylotype correlated well ($R^2 = 0.97$) with dim *Synechococcus* abundances (Figure IV-1). The correlation fell slightly ($R^2 = 0.92$) when all available Group C phylotypes abundances were compared with dim *Synechococcus* abundances. The identification of unicellular

Group C by flow cytometry could be useful in determining abundances of this diazotroph in the field.

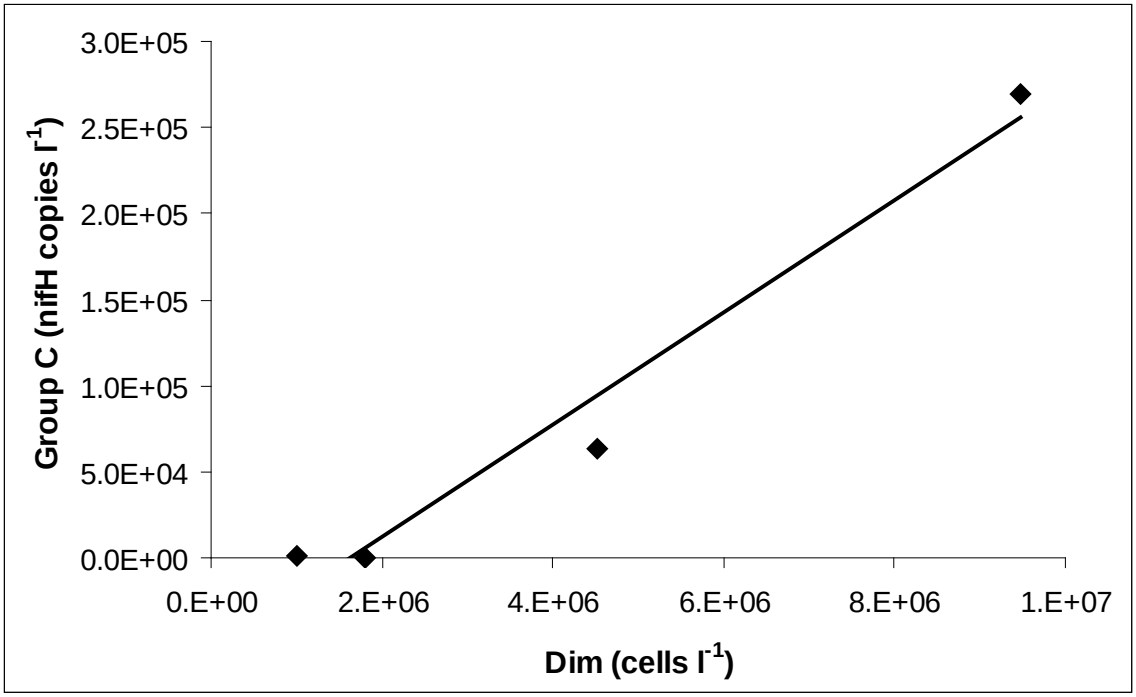

Figure IV-1: Correlation of Group C with Dim *Synechococcus* Abundances Group C abundances were estimated by qPCR and are reported as *nifH* copies l^{-1}. Dim Synechococcus cell abundances (cells l^{-1}) were determined by analytical flow cytometry.

The results of the bioassay experiments also showed that heterotrophic bacteria in the North Atlantic Ocean are co-limited by nitrogen and phosphorus (Paper E [*Mills et al.*, 2008]). Heterotrophic and photoautotrophic oceanic communities are not traditionally considered to be competitors for nutrient resources [*Duarte and Cebrian*, 1996; *Kirchman*, 2004]. It is assumed that phytoplankton growth is limited by the availability of dissolved inorganic nutrients, while heterotrophic bacteria are limited by the availability of dissolved organic carbon. However in the bioassay experiments, bacterial growth and productivity were stimulated by simultaneous additions of nitrogen and phosphorus rather than the addition of dissolved organic carbon. These findings suggest that heterotrophic bacteria are in direct competition with the nitrogen limited phytoplankton community (Paper E [*Mills et al.*, 2008]). As both primary and bacterial production are nitrogen or nitrogen co-limited limited in the Atlantic Ocean, biological

dinitrogen fixation is a key pathway that can increase the amount of fixed nitrogen available to the photoautotrophic and heterotrophic communities.

Bioassay experiments showed that in contrast to the phytoplankton and heterotrophic bacteria, dinitrogen fixation is co-limited by phosphorus and iron. In most experiments, small increases in the dinitrogen fixation rates were observed with additions of either phosphate or iron, but rates almost tripled with the simultaneous addition of phosphate and iron (Paper F [Langlois et al. in prep.] [*Mills et al.*, 2004]). Abundances of diazotrophic phylotypes increased with additions of Saharan dust (Paper F [Langlois et al. in prep.]). Saharan dust can supply both iron and phosphorus to diazotrophic communities [*Baker et al.*, 2006]. Both available phosphorus and iron appear to influence dinitrogen fixation rates in the Atlantic Ocean, while Saharan dust seems to influence diazotroph phylotype abundances (Papers B and F [*Langlois et al.*, 2008] [Langlois et al. in prep.]). Though the factors that control diazotroph distribution and dinitrogen fixation are not yet fully understood, both iron and phosphorus are important for diazotrophs in the North Atlantic [*Mills et al.*, 2004]. The results of this thesis indicate that Saharan Dust had the greatest effect in stimulating the abundance of *nifH* phylotypes in the bioassay incubations. Given the consistent pattern in all of the experiments, it is surprising that dust stimulates large increases in diazotrophic phylotypes while the highest rates of nitrogen fixation are in the phosphorus plus iron treatment. The reason for this is not yet understood, but it is possible that nitrate is also released from the dust thus providing a fixed nitrogen source. Phosphorus and iron from Saharan dust are most likely vital limiting resources to nutrient cycling in the Atlantic Ocean.

Changes in Nitrogen Fixation Paradigms

Many views and assumptions about marine diazotrophs and nitrogen fixation have shifted in the past 20 years. One of the primary changes is the acknowledgement that *Trichodesmium* and the diatom-diazotroph associations are not the only marine diazotrophs and that they may not be the most important dinitrogen fixers. Results from work during this thesis and others show that *Trichodesmium* is undoubtedly a major

contributor to global marine biological dinitrogen fixation, as it is very abundant throughout the tropical and sub-tropical Atlantic Ocean (Paper B [*Davis and McGillicuddy Jr.*, 2006; *Langlois et al.*, 2008]). Though no diatom-diazotroph associations were detected in the Atlantic Ocean during this thesis, a recent study looking at the effects of the Amazon River plume on dinitrogen fixation found that this system's highest fixation rates occurred in mesohaline waters and were attributed to the diatom-diazotroph associations [*Subramaniam et al.*, 2008]. In addition to these diazotrophs, new unicellular cyanobacterial and γ–proteobacterial diazotrophs were described and were shown to be widely distributed throughout the Atlantic and Pacific Oceans (Papers A and B [*Church et al.*, 2008; *Church et al.*, 2005; *Langlois et al.*, 2008; *Langlois et al.*, 2005]). Due to their large distributions, these diazotrophs have the potential to also supply a significant amount of fixed nitrogen to the nitrogen inventory.

In addition to increasing the number of described diazotrophic phylotypes, results from this thesis indicate that the importance of the various diazotrophic phylotypes may be different in the Atlantic and Pacific Oceans. *Trichodesmium* was by far the most abundant phylotype detected in the Atlantic Ocean, followed by the uncultured unicellular Group A phylotype (Paper B [*Langlois et al.*, 2008]). In contrast, the Group A phylotype was the most widely distributed and commonly detected phylotype in a long north-south transect through the Pacific Ocean [*Church et al.*, 2008]. Phosphorus and iron availability differ between the two oceanic basins and perhaps this influences the preponderance of *Trichodesmium* versus Group A.

Aeolian dust from Africa's Sahara Desert supplies the Atlantic Ocean with iron and possibly phosphorus while there is no equivalent source of iron to the Pacific subtropical gyres. The Atlantic iron supply may stimulate the diazotrophic community and cause a depletion of phosphate. Phosphate concentrations are indeed low in the North Atlantic Ocean [*Wu et al.*, 2000] and in one study *Trichodesmium* dinitrogen fixation was shown to be limited by phosphorus [*Sanudo-Wilhelmy et al.*, 2001]. Bioassay experiments conducted in parallel to the work presented in this thesis showed that bulk dinitrogen fixation was co-limited by phosphorus and iron [*Mills et al.*, 2004]. Saharan dust additions stimulated dinitrogen fixation and nucleic acid samples from the dust treatments showed that diazotrophic phylotype abundances increased many fold

(Paper F [Langlois et al. in prep]). In contrast, soluble reactive phosphate has been measured to be at least as high as 100 nmol l^{-1} in both the North and South Pacific subtropical gyres suggesting that iron limitation may prevail in these locations [*Church et al.*, 2008]. Two separate sets of experiments have shown that phosphate and simultaneous phosphate and iron additions had no effect on phylotype abundances or dinitrogen fixation rates in the Pacific Ocean [*Needoba et al.*, 2007; *Zehr et al.*, 2007]. Assuming that *Trichodesmium* is dominant in the Atlantic Ocean and Group A in the Pacific, the cellular physiology of the two may allow one to be adapted to low phosphorus concentrations and the other to low iron. This, however, is highly speculative and until the Group A is in culture or its genome fully analyzed we can only make rough conjectures about its cellular physiology.

Of the sequenced marine cyanobacterial genomes, only *Trichodesmium erythraeum* contains genes for organic phosphate (phosphonate) utilization [*Dyhrman et al.*, 2006]. This could give it a significant advantage over other diazotrophs and marine microbes in the low phosphorus Atlantic Ocean. *Crocosphaera watsonii*, antoher diazotroph whose genome is also sequenced, does not contain genes for phosphonate utilization, but has been shown to scavenge phosphorus by using a high-affinity phosphate transporter (*pstS* gene) [*Dyhrman and Haley*, 2006]. Presently it is unknown how other diazotrophs may have adapted to low phosphorus environments.

Results from this thesis also showed that biological dinitrogen fixation is not constrained to the warm, oceanic subtropical gyres. The Cluster III diazotrophic phylotype was detected as far as 40°N in North Atlantic in waters as cool as 18°C (Paper B [*Langlois et al.*, 2008]). Whether or not this phylotype fixes dinitrogen remains to be determined, but *nifH* transcripts of the same phylotype were recovered at station ALOHA in the Pacific Ocean [*Church et al.*, 2005]. Low nitrogen fixation rates have been measured off the coast of California in 19°C water [*Needoba et al.*, 2007]. Although the rates were low compared to rates measured in the subtropical gyres, the amount of nitrogen fixed could account for 10% of the new production [*Needoba et al.*, 2007]; indicating that fixation outside of the assumed 20-25°C range may not be globally significant, but it can impact the local nitrogen cycle greatly. Dinitrogen fixation can also occur at temperatures much warmer than previously thought. An archaeal anaerobic

methanogen isolated from a deep sea vent has been shown to fix nitrogen at temperatures of 92°C, 28° warmer than dinitrogen fixation was previously shown to occur [*Mehta and Baross*, 2006].

Although the highest diazotrophic abundances estimated in the Pacific and Atlantic Oceans were associated with low nitrate concentrations (Paper B [*Church et al.*, 2008; *Langlois et al.*, 2008]), the Cluster III phylotype was detected at relatively high nitrate concentrations (>0.5 μM) in the Atlantic Ocean (Paper B [*Langlois et al.*, 2008]). The presence of diazotrophs in waters with high nitrate concentrations is a bit puzzling, as it is assumed that diazotrophs, which have slow growth rates, should be outcompeted by other microbes when nitrate is available. Laboratory culture experiments have shown that although concentrations of nitrate as low as 0.5 μM inhibit dinitrogen fixation, *Trichodesmium* is able to use nitrate for growth [*Holl and Montoya*, 2005]. These results imply that higher nitrate concentrations should not automatically connote an absence of diazotrophic organisms. Diazotrophs may be metabolically flexible with respect to nitrogen uptake, but until all diazotrophic phylotypes are in culture or their genomes sequenced this remains unknown.

While molecular biological techniques have substantially improved our knowledge on the diversity of diazotrophic organisms and their distributions, the factors that control diazotroph distributions and their activity are still uncertain. Understanding the factors that influence dinitrogen fixation and diazotroph distribution will improve estimates of present and predictions of future biological dinitrogen fixation.

Potential Consequences of Anthropogenic Perturbations on the Marine Nitrogen Cycle

The nitrogen and carbon biogeochemical cycles are inherently connected. Organic material is produced by photosynthesis, which is the process of converting carbon dioxide, fixed nitrogen, phosphate and water into a six-carbon sugar using sunlight. This process not only links the nitrogen and carbon cycles, but the phosphorus cycle as well. Global effects of increases in anthropogenic carbon dioxide and nitrogenous gases will also affect the global nitrogen cycle; however there are still large

uncertainties as to exactly how the nitrogen cycle will be affected [*Gruber and Galloway*, 2008].

Amounts of atmospheric anthropogenic nitrogen due to fossil fuel burning and fertilizer production have also been increasing (Paper G [*Duce et al.*, 2008]). About 10% of the oceans' absorption of anthropogenic carbon and 3% of the global annual new production have been attributed to deposition of anthropogenic nitrogen over the open oceans (Paper G [*Duce et al.*, 2008]). Although increasing primary production through anthropogenic nitrogen deposition causes a negative feedback for global warming, this may be counter-acted by an increase in N_2O production (Paper G [*Duce et al.*, 2008]). Another tentative negative feedback has been proposed where increases in carbon dioxide increase the carbon to nitrogen uptake ratio of marine phytoplankton, causing an increase in carbon fixation and draw-down of carbon dioxide [*Gruber and Galloway*, 2008].

In addition to direct perturbations of the nitrogen cycle through increased anthropogenic nitrogen deposition and carbon dioxide concentrations, climate change will also have an effect. The International Panel on Climate Change predicts that air temperatures will continue to increase, as will ocean water temperatures. Increasing oceanic water temperatures are associated with an increase in ocean stratification which may cause an increase in areas limited by fixed nitrogen, thus potentially giving diazotrophic organisms more niches to inhabit. An increase in ocean temperatures will also directly affect diazotrophic physiology and potentially change the areas where a diazotroph can fix dinitrogen. Laboratory experiments showed that *Trichodesmium erythraeum* grew optimally at 24-30°C and a predicted increase in ocean temperatures could cause a 16% decrease in area with optimum temperatures for Trichodesmium growth and dinitrogen fixation [*Breitbarth et al.*, 2006].

The International Panel on Climate Change also predicts that arid areas will become drier, which may cause an increase in dust deposition. A modeling study showed dust deposition to high nitrogen low chlorophyll areas caused a direct and short term increase in carbon dioxide drawdown due to stimulation of the phytoplankton [*Moore et al.*, 2006b]. Over longer (decadal) timescales, the increase in dust deposition stimulated dinitrogen fixation causing a greater absorption of carbon dioxide by the oceans than direct stimulation of dust over high nitrogen low chlorophyll areas [*Moore et al.*, 2006b].

In contrast to the International Panel on Climate Change's prediction, the model predicted that dust deposition would decrease in the future resulting in reduced carbon dioxide uptake by the oceans and a positive feedback to global warming [*Moore et al.*, 2006b]. However, the exact effects of dust deposition on dinitrogen fixation are not known and at least one cyanobacterial diazotroph fixes dinitrogen uncoupled to carbon fixation [*Zehr et al.*, 2008], thus introducing large uncertainties into the model and its predictions.

Anthropogenic nitrogen loading of rivers causes eutrophication of coastal systems, though this is assumed not to affect the open ocean (Paper G [*Duce et al.*, 2008; *Gruber and Galloway*, 2008]). However, large river systems, such as the Amazon and Congo, do discharge water and nutrients far away from coastal systems and into oceanic systems. In the case of the Amazon, excess phosphorus, silica and iron have been shown to stimulate diatom-diazotroph associations, dinitrogen fixation and carbon drawdown [*Subramaniam et al.*, 2008]. Changes in the hydrological cycle, which are predicted to occur with global warming, fertilizer use and land use could all affect the nutrient cycling of such systems [*Subramaniam et al.*, 2008].

There are a lot of uncertainties in predicting the future status of the global ecosystem which make it difficult to foresee changes in the marine nitrogen cycle. Some predicted changes, such as increasing ocean temperature may or may not increase dinitrogen fixation. The fate of dust deposition in future scenarios is uncertain and it is vague whether or not dust deposition will increase in future scenarios, therefore the effects of changes in dust deposition on nitrogen fixation are unknown. Better understanding of how temperature changes and dust deposition affect dinitrogen fixation and diazotroph abundances would improve model predictions. Though the actual changes and magnitude of anthropogenic perturbations cycle are not known, human activities will cause changes in the marine nitrogen cycle and dinitrogen fixation.

References:

Baker, A.R., T.D. Jickells, M. Witt, and K.L. Linge, Trends in the solubility of iron, aluminium, manganese, and phosphorus in aerosol collected over the Atlantic Ocean, *Marine Chemistry*, *98*, 43-58, 2006.

Breitbarth, E., A. Oschlies, and J. LaRoche, Physiological constraints on the global distribution of Trichodesmium- effect of temperature on diazotrophy, *Biogeosciences*, *3*, 1-10, 2006.

Church, M.J., K.M. Bjoerkman, D.M. Karl, M.A. Saito, and J.P. Zehr, Regional distribution of nitrogen-fixing bacteria in the Pacific Ocean, *Limnol. Oceanogr.*, *53* (1), 63-77, 2008.

Church, M.J., B.D. Jenkins, D.M. Karl, and J.P. Zehr, Vertical distributions of nitrogen-fixing phylotypes at Stn ALOHA in the oligotrophic North Pacific Ocean, *Aquatic Microbial Ecology*, *38*, 3-14, 2005.

Davey, M., G.A. Tarran, M.M. Mills, C. Ridame, R.J. Geider, and J. La Roche, Nutrient limitation of picophytoplankton photosynthesis and growth in the tropical North Atlantic, *Limnology and Oceanography*, *53* (5), 1722-1733, 2008.

Davis, C.S., and D.J. McGillicuddy Jr., Transatlantic Abundance of the N2-Fixing Colonial Cyanobacterium Trichodesmium, *Science*, *312*, 1517-1520, 2006.

Duarte, C.M., and J. Cebrian, The fate of marine autotrophic production, *Limnol. Oceanogr.*, *41*, 1758-1766, 1996.

Duce, R.A., J. La Roche, K. Altieri, K.R. Arrigo, A.R. Baker, D.G. Capone, S. Cornell, F. Dentener, J. Galloway, R.S. Ganeshram, R.J. Geider, T.D. Jickells, M.M. Kuypers, R.J. Langlois, P.S. Liss, S.M. Liu, J.J. Middelburg, C.M. Moore, S. Nickovic, A. Oschlies, T. Pedersen, J.M. Prospero, R. Schlitzer, S. Seitzinger, L.L. Sorensen, M. Uematsu, O. Ulloa, M. Voss, B.B. Ward, and L. Zamora, Impacts of Atmospheric Anthropogenic Nitrogen on the Open Ocean, *Science*, *320*, 893-897, 2008.

Dyhrman, S.T., P.D. Chappell, S.T. Haley, J.W. Moffett, E.D. Orchard, J.B. Waterbury, and E.A. Webb, Phosphonate utilization by the globally important marine diazotroph *Trichodesmium*, *Nature*, *439*, 68-71, 2006.

Dyhrman, S.T., and S.T. Haley, Phosphorus Scavenging in the Unicellular Marine Diazotroph *Crocosphaera watsonii*, *Appl. Envir. Microbiol.*, *72* (2), 1452-1458, 2006.

Gruber, N., and J.N. Galloway, An Earth-system perspective of the global nitrogen cycle, *Nature*, *451*, 293-296, 2008.

Holl, C.M., and J.P. Montoya, Interactions between nitrate uptake and nitrogen fixation in continuous cultures of the marine diazotroph *Trichodesmium* (Cyanobacteria), *J. Phycol.*, *41*, 1178-1183, 2005.

Kirchman, D.L., A primer on dissolved organic material and heterotrophic prokaryotes in the ocean, in *The ocean carbon cycle and climate*, edited by M.F.a.T. Oguz, pp. 31-61, Kluwer Academic, 2004.

Langlois, R.J., D. Huemmer, and J. La Roche, Abundances and Distributions of the Dominant *nifH* Phylotypes in the Northern Atlantic Ocean, *Appl. Envir. Microbiol.*, *74* (6), 1922-1931, 2008.

Langlois, R.J., J. La Roche, and P.A. Raab, Diazotrophic Diversity and Distribution in the Tropical and Subtropical Atlantic Ocean, *Appl. Envir. Microbiol.*, *71* (12), 7910-7919, 2005.

Mehta, M.P., and J.A. Baross, Nitrogen Fixation at 92^{o}C by a Hydrothermal Vent Archaeon, *Science*, *314*, 1783-1786, 2006.

Mills, M.M., C.M. Moore, R.J. Langlois, A. Milne, E.P. Achterberg, K. Nachtigall, K. Lochte, R. Geider, and J. La Roche, Nitrogen and phosphorus co-limitation of bacterial productivity and growth in the oligotrophic subtropical North Atlantic, *Limnology and Oceanography*, *53* (2), 824-834, 2008.

Mills, M.M., C. Ridame, M. Davey, J. La Roche, and R.J. Geider, Iron and phosphorus co-limit nitrogen fixation in the eastern tropical North Atlantic, *Nature*, *429* (6989), 292-294, 2004.

Moore, C.M., M. Mills, R.J. Langlois, A. Milne, E.P. Achterberg, J. La Roche, and R. Geider, Relative influence of nitrogen and phosphorus availability on phytoplankton physiology and productivity in the oligotrphic sub-tropical North Atlantic Ocean, *Limnology and Oceanography*, *53* (1), 291-305, 2008.

Moore, C.M., M. Mills, A. Milne, R.J. Langlois, E.P. Achterberg, K. Lochte, R. Geider, and J. La Roche, Iron limits primary productivity during spring bloom development in the central North Atlantic, *Global Change Biology*, *12*, 626-634, 2006a.

Moore, K., S.C. Doney, K. Lindsay, N. Mahowald, and A.F. Michaels, Nitrogen fixation amplifies the ocean biogeochemical response to decadal timescale variations in mineral dust deposition, *Tellus*, *58B*, 560-572, 2006b.

Needoba, J.A., R.A. Foster, C. Sakamoto, J.P. Zehr, and K.S. Johnson, Nitrogen fixation by unicellular diazotrophic cyanobacteria in the temperate oligotrophic North Pacific Ocean, *Limnol. Oceanogr.*, *52* (4), 1317-1327, 2007.

Sanudo-Wilhelmy, S.A., A.B. Kustka, C.J. Gobler, D.A. Hutchins, M. Yang, K. Lwiza, J. Burns, D.C. Capone, J.A. Raven, and E.J. Carpenter, Phosphorus limitation of nitrogen fixation by Trichodesmium in the central Atlantic Ocean, *Nature*, *411* (66-69), 2001.

Subramaniam, A., P.L. Yager, E.J. Carpenter, C. Mahaffey, K. Bjoerkman, S. Cooley, A.B. Kustka, J.P. Montoya, S.A. Sanudo-Wilhelmy, R. Shipe, and D.G. Capone, Amazon River enhances diazotrophy and carbon sequestration in the tropical North Atlantic Ocean, *PNAS*, *105* (30), 10460-10465, 2008.

Wu, J., W. Sunda, E.A. Boyle, and D.M. Karl, Phosphate depletion in the western North Atlantic Ocean, *Science*, *289* (4 August 2000), 759-762, 2000.

Zehr, J.P., S.R. Bench, B.J. Carter, I. Hewson, F. Niazi, T. Shi, H.J. Tripp, and J.P. Affourtit, Globally Distributed Uncultivated Oceanic N_2-fixing Cyanobacteria Lack Oxygenic Photosystem II, *Science*, *322*, 1110-1112, 2008.

Zehr, J.P., J.P. Montoya, B.D. Jenkins, I. Hewson, E. Mondragon, C.M. Short, M.J. Church, A. Hansen, and D.M. Karl, Experiments linking nitrogenase gene expression to nitrogen fixation in the North Pacific subtropical gyre, *Limnol. Oceanogr.*, *52* (1), 169-183, 2007.

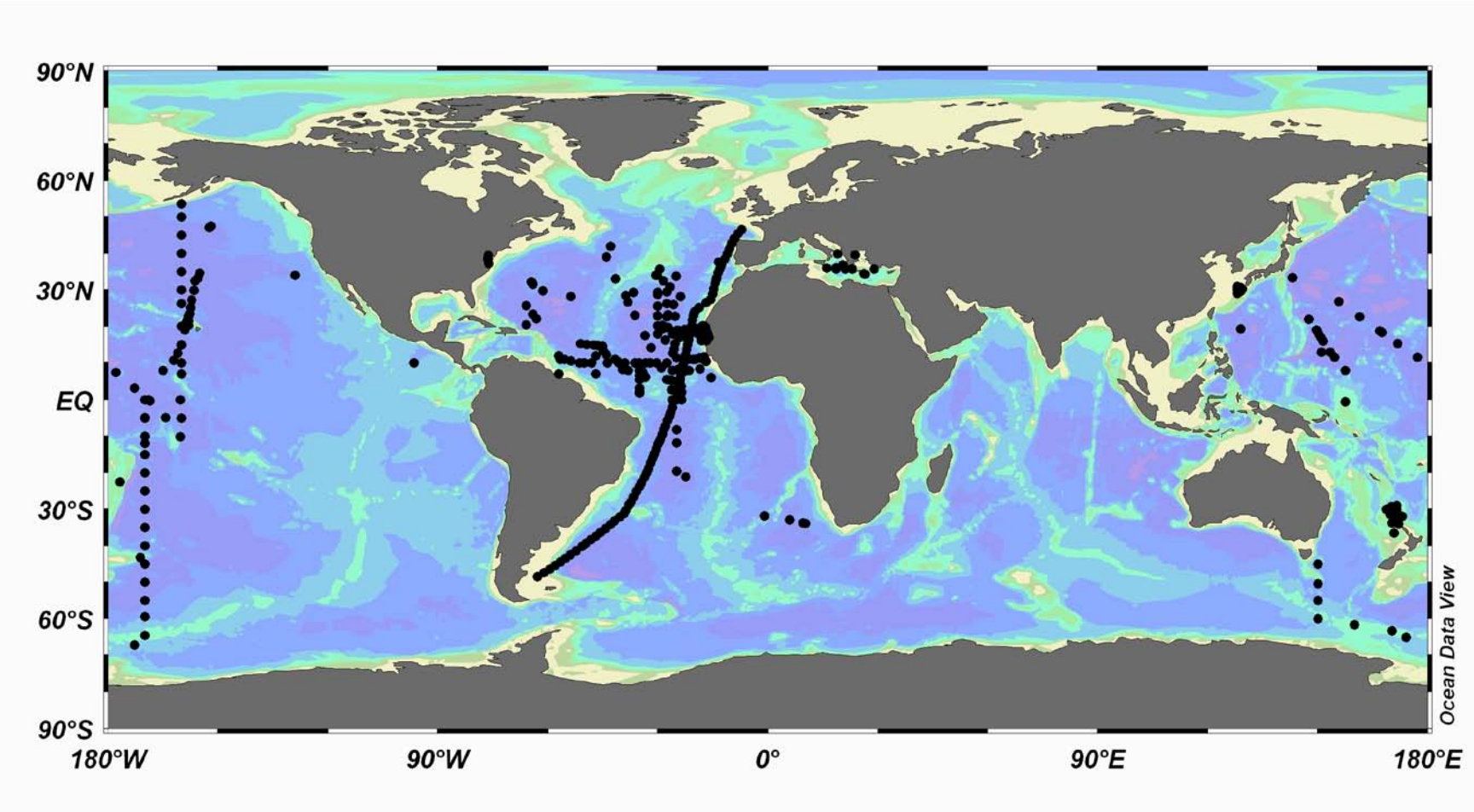

Figure V-1: Global Distribution of Sites Where Diazotroph Abundances Were Determined by qPCR (Sources: Langlois unpublished data [*Church et al.*, 2008; *Church et al.*, 2005; *Foster et al.*, 2007; *Hewson et al.*, 2007; *Langlois et al.*, 2008; *Needoba et al.*, 2007; *Short et al.*, 2004])

V. Conclusions and Outlook

The data presented in this thesis have advanced knowledge on diazotrophic organisms and nutrient limitations in the Atlantic Ocean (see boxed text). The presence of new diazotrophic phylotypes, including unicellular Group C and Gamma A was documented and the Cluster III phylotype was identified in the Atlantic Ocean for the first time (Paper A [*Langlois et al.*, 2005]). A qPCR method was developed and used to estimate diazotrophic abundances in the Atlantic Ocean on an unprecedented basin wide scale (Paper B [*Langlois et al.*, 2008]). Despite the progress made, there is still much to be determined. Many of the phylotypes identified in this and other similar studies are uncultured and their cellular physiology is unknown. Until the uncultured diazotrophs are in culture or their genomes sequenced, inferring how the organisms function in different environments will remain speculative.

The abundances of diazotrophic phylotypes have been estimated at several sites in both the Pacific and Atlantic Oceans using qPCR (Figure V-1). This coverage is much better than at the start of work on this thesis (see Figure I-2). However, the oceanic basins are large and still under sampled with respect to diazotroph abundances. This is especially true for the southern Atlantic and Pacific Oceans. P* values indicate that the Pacific oxygen minimum zones are potential hot spots of dinitrogen fixation [*Deutsch et al.*, 2007], but so far no data has been published on either dinitrogen fixation rates or diazotroph abundances for this area. In addition to poor sample coverage, temporal coverage of diazotroph abundances is also lacking. This type of sampling does not provide information patterns in the seasonal variability of the various diazotrophs. Marine diazotroph abundances may vary seasonally as does *Trichodesmium* in the Atlantic Ocean [*Orcutt et al.*, 2001]. To date there have been very few studies which monitor the abundances of diazotrophs throughout an entire year at a single location. This information could reveal seasonal variations in dinitrogen fixation rates and greatly improve estimates of global biological dinitrogen fixation.

The data delivered by qPCR are very informative about relative distributions and abundances of diazotrophs, but it is still not yet known how this data corresponds to cellular abundances and whether they could ultimately be used to estimate dinitrogen

fixation rates. One study which focused on this issue determined that unicellular Group B abundances could be determined quite well from *nifH* qPCR data and that *nifH* transcripts may be an indicator of dinitrogen fixation rates per cell [*Zehr et al.*, 2007]. Laboratory experiments with cultured diazotrophs may help to clear this concern.

Major Findings

Paper A

- Unicellular Group C and Gamma A diazotrophs described
- Cluster III described in the Atlantic Ocean for the first time
- **Improved sampling of all diazotrophs across the Atlantic Ocean, especially the eastern and northern Atlantic**

Paper B

- **First report of diazotrophic phylotype abundances on a large scale in the Atlantic Ocean**
- Identified potential optimal temperatures for seven diazotrophic phylotypes
- Identified a relationship between annual Saharan Dust deposition and phylotype abundances

Paper C

- **Iron limitation of primary productivity during the spring bloom was shown**
- Variability in Saharan dust deposition implicated as a factor in determining the on-set and duration of the Atlantic spring bloom

Paper D

- **Nitrogen limitation of primary productivity shown at seven sites in the North Atlantic**
- Indication of a possible nitrogen and phosphorus co-limitation in *Synechococcus*

Paper E

- **Nitrogen and phosphorus co-limitation of bacterial productivity and growth shown**
- Competition between phytoplankton and heterotrophic communities for dissolved inorganic nutrients shown

Paper F

- **Saharan dust potentially important in determining diazotroph abundances**
- Phosphorus and iron co-limitation of dinitrogen fixation shown
- Saharan dust stimulation of dinitrogen fixation and phylotype abundances shown
- Iron untilization from Saharan dust by *Trichodesmium erythraeum* cultures shown

Paper G

- Atmospheric anthropogenic nitrogen (AAN) deposition increasing over open ocean
- AAN deposition could account for up to 3% of global primary productivity
- **AAN inputs reaching estimates of biological dinitrogen fixation**

Reverse transcriptase-qPCR (RT-qPCR) also provides very useful information about the expression of the target genes. However, this method is difficult to apply to field samples as *nifH* is expressed at different times of the day by different organisms. For example, *Trichodesmium* fixes dinitrogen during the day and *nifH* transcripts are observed in the morning hours [*Berman-Frank et al.*, 2003], while *Crocosphaera* and *Cyanothece* fix dinitrogen during the night and *nifH* transcripts are observed in the early evening hours [*Colon-Lopez and Sherman*, 1998; *Zehr et al.*, 2007]. Some samples were tested by RT-qPCR during this thesis and *nifH* transcripts correlated well with trends in dinitrogen fixation rates (Figure V-2), but due to water limitations in the bioassay experiments only one time period and thus only part of the potentially active diazotrophic community could be sampled. Samples need to be collected throughout an entire day-light cycle in order to account for all possible *nifH* transcripts, which is sometimes not feasible during research cruises.

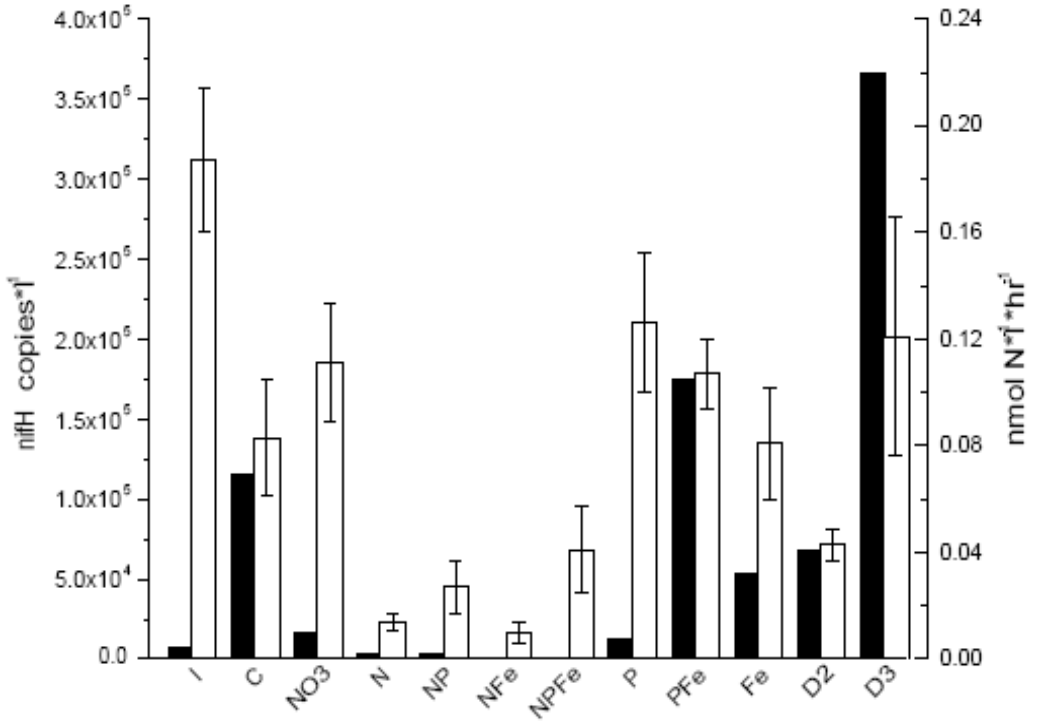

Figure V-2: Results of a Bioassay Experiment in the Sargasso Sea Filamentous *nifH* transcripts (black bars) are given as *nifH* copies l^{-1}. Dinitrogen fixation rates (white bars) and standard error are given as nmol N l^{-1} hr^{-1}. Nutrient additions are on the x-axis.

Results of nutrient addition bioassay experiments showed that nitrogen is the limiting nutrient of phytoplankton and heterotrophic bacterial communities (Papers D and E [*Mills et al.*, 2008; *Moore et al.*, 2008]). This indicates that diazotrophs have an important ecological niche in the North Atlantic Ocean. Saharan dust deposition has been implicated as factor that determines the distribution of diazotrophic organisms (Paper B [*Langlois et al.*, 2008]), perhaps by providing much needed iron and phosphorus and additions of Saharan dust to bulk water caused a large increase in *nifH* copies of all phylotypes (Paper F [Langlois et al. in prep]). However, other factors such as temperature, light, phosphorus availability or fixed nitrogen concentrations may also affect diazotroph distributions. Although there are still topics that need more research (see following boxed text), this thesis has improved understanding of diazotrophic organisms and their importance in the North Atlantic Ocean.

Future Research Directions

Diazotrophs

- Isolate and bring uncultured diazotrophic phylotypes into culture
- Conduct experiments that compare *nifH* abundances, transcripts, dinitrogen fixation rates and cellular abundances to better interpret qPCR data
- Determine ability of diazotrophs to utilize nutrients from aeolian dust dissolution organic phosphorus and fixed nitrogen

Environmental Sampling

- Improve sampling in southern Pacific and Atlantic Oceans
- Improve sampling temporally

References:

Berman-Frank, I., P. Lundgren, and P. Falkowski, Nitrogen fixation and photosynthetic oxygen evolution in cyanobacteria, *Research in Microbiology*, *154* (3), 157-164, 2003.

Church, M.J., K.M. Bjoerkman, D.M. Karl, M.A. Saito, and J.P. Zehr, Regional distribution of nitrogen-fixing bacteria in the Pacific Ocean, *Limnol. Oceanogr.*, *53* (1), 63-77, 2008.

Church, M.J., B.D. Jenkins, D.M. Karl, and J.P. Zehr, Vertical distributions of nitrogen-fixing phylotypes at Stn ALOHA in the oligotrophic North Pacific Ocean, *Aquatic Microbial Ecology*, *38*, 3-14, 2005.

Colon-Lopez, M.S., and L.A. Sherman, Transcriptional and Translational Regulation of Photosystem I and II Genes in Light-Dark- and Continuous-Light-Grown Cultures of the Unicellular Cyanobacterium Cyanothece sp. Strain ATCC 51142, *J. Bacteriol.*, *180* (3), 519-526, 1998.

Deutsch, C., J. Sarmiento, D.M. Sigman, N. Gruber, and J.P. Dunne, Spatial coupling of nitrogen inputs and losses in the ocean, *Nature*, *445*, 163-167, 2007.

Foster, R.A., A. Subramaniam, C. Mahaffey, E.J. Carpenter, D. Capone, and J.P. Zehr, Influence of the Amazon River plume on distributions of free-living and symbiotic cyanobacteria in the western tropical north Atlantic Ocean, *Limnology and Oceanography*, *52* (2), 517-532, 2007.

Hewson, I., P.H. Moisander, K.M. Achilles, C.A. Carlson, B.D. Jenkins, E. Mondragon, A.E. Morrison, and J.P. Zehr, Characteristics of diazotrophs in surface to abyssopelagic waters of the Sargasso Sea, *Aquatic Microbial Ecology*, *46*, 15-30, 2007.

Langlois, R.J., D. Huemmer, and J. La Roche, Abundances and Distributions of the Dominant *nifH* Phylotypes in the Northern Atlantic Ocean, *Appl. Envir. Microbiol.*, *74* (6), 1922-1931, 2008.

Langlois, R.J., J. La Roche, and P.A. Raab, Diazotrophic Diversity and Distribution in the Tropical and Subtropical Atlantic Ocean, *Appl. Envir. Microbiol.*, *71* (12), 7910-7919, 2005.

Mills, M.M., C.M. Moore, R.J. Langlois, A. Milne, E.P. Achterberg, K. Nachtigall, K. Lochte, R. Geider, and J. La Roche, Nitrogen and phosphorus co-limitation of bacterial productivity and growth in the oligotrophic subtropical North Atlantic, *Limnology and Oceanography*, *53* (2), 824-834, 2008.

Moore, C.M., M. Mills, R.J. Langlois, A. Milne, E.P. Achterberg, J. La Roche, and R. Geider, Relative influence of nitrogen and phosphorus availability on phytoplankton physiology and productivity in the oligotrphic sub-tropical North Atlantic Ocean, *Limnology and Oceanography*, *53* (1), 291-305, 2008.

Needoba, J.A., R.A. Foster, C. Sakamoto, J.P. Zehr, and K.S. Johnson, Nitrogen fixation by unicellular diazotrophic cyanobacteria in the temperate oligotrophic North Pacific Ocean, *Limnol. Oceanogr.*, *52* (4), 1317-1327, 2007.

Orcutt, K.M., F. Lipschulz, K. Gundersen, R. Arimoto, A.F. Michaels, A.H. Knap, and J.R. Gallon, A seasonal study of the significance of N_2 fixation by *Trichodesmium*

spp. at the Bermuda Atlantic Time-series Study (BATS) site, *DSR II*, *48*, 1583-1608, 2001.

Short, S.M., B.D. Jenkins, and J.P. Zehr, Spatial and Temporal Distribution of Two Diazotrophic Bacteria in the Chesapeake Bay, *Appl. Environ. Microbiol.*, *70* (4), 2186-2192, 2004.

Zehr, J.P., J.P. Montoya, B.D. Jenkins, I. Hewson, E. Mondragon, C.M. Short, M.J. Church, A. Hansen, and D.M. Karl, Experiments linking nitrogenase gene expression to nitrogen fixation in the North Pacific subtropical gyre, *Limnol. Oceanogr.*, *52* (1), 169-183, 2007.

VI. Acknowledgements

I received assistance and advice from many friends and colleagues during work on this thesis. In particular I would like to acknowledge the following people.

Most importantly, I thank my advisor and mentor Dr. Julie La Roche for her guidance and many creative ideas to make this thesis better. I also thank her for pushing me to strive for highest standards possible in my scientific work, which greatly improved the quality of work in this thesis and made me a better scientist.

I thank Diana Huemmer for the many hours she spent assisting me with setting up hundreds of plates for qPCR analysis and for preparing the plasmids for the qPCR standards. Collection of the qPCR data would have taken much longer without her help.

I thank Dr. Matthew Mills and Dr. C. Mark Moore for the great collaboration and fascinating conversations during the bioassay experiments at sea, which greatly influenced the focus of my thesis and my own ideas about nutrient limitations.

I thank Kerstin Nachtigall and Peter Fritsche for all of their help with getting the materials and instruments needed ready for the research cruises. I would also like to acknowledge the patience they had and help they provided in explaining the customs, dangerous goods and proforma invoice forms.

The bioassay experiments would not have been possible without the effort of many people. I recognize and thank the following groups of people: M55- Dr. Matthew Mills, Dr. Celine Ridame, and Dr. Margaret Davey; M60- Dr. Matthew Mills, Dr. C. Mark Moore, Dr. Eric Achterberg, Angela Milne, and Kerstin Nachtigall; M68- Stefanie Sudhaus, Orly Levitan, Christian Schlosser, and Dr. Peter Croot; M71- Dr. C. Mark Moore, Wiebke Mohr, Stefanie Sudhaus, Maija Heller and Julie Mosseri.

I also thank the La Roche lab group, especially Tania Kluever for teaching me molecular and culturing techniques, Stefanie Sudhaus for help with translation, and Wiebke Mohr for the several hours spent in helping me to use the ARB *nifH* database and for proof reading this thesis.

Erklärung

Hermit erkläre ich, Rebecca Judith Langlois-Warnat, dass ich die von mir eingereichte Arbeit „Distribution and Abundances of Diazotrophs and Microbial Nutrient Limitations in the North Atlantic Ocean“ selbstständig und nur unter Verwendung der angegebenen Quellen und Hilfsmittel angefertigt habe. Weiterhin wurde diese Arbeit noch nie an eine andere Universität eingereicht.

Flintbek, den 12 December 2008

(Rebecca Judith Langlois-Warnat)